# Intrinsic and synaptic adaptations in neuronal ensembles following recall of appetitive associative memories: Investigations in the striatum and prefrontal cortex with the *Fos-GFP* mouse

Joseph Ziminski

Thesis submitted to the University of Sussex for the degree of Doctor of Philosophy

July 2017

The work presented in this thesis is entirely my own except where due acknowledgement and reference was made.

Signature:.....

# Acknowledgments

All experimental work included in the present thesis was undertaken by Joseph Ziminski, with the exception of:

Electrophysiological recordings from the orbitofrontal cortex (OFC, Chapter 3): Sabine Hessler (Koya lab) (Data analysed by Joseph Ziminski).

Pavlovian approach behaviour and histological staining from *in situ hybridisation* studies (Chapter 3): Gabriella Margetts-Smith (Koya lab). Imaging of the OFC by was undertaken by Sabine Hessler. (Imaging of the NAc and all data analysis by Joseph Ziminski).

I would like to thank the school of Psychology for their support and funding of my PhD position and the research herein. Additionally, I would like to thank the Biotechnology and Biological Sciences Research Council (BBSRC, grant code BB/M0009017/1) their financial contribution to Pavlovian approach experiments (Chapters 3 and 4).

I would also like to thank Eisuke Koya for his guidance and support throughout my PhD, for his tireless support and tuition, and for making the entire process enjoyable. I would also like to give my thanks to the other members of the Koya lab who have provided unquantifiable support and made the lab a very enjoyable place to work. Similarly, I would also like to thank Hans Crombag and Sarah King for their support and advice over the last 7 years. I would also like to extend my appreciation to those who trained me in the techniques used in the present thesis, including David Mawer, Tom Macpherson, Laura Contu, Maria Meringolo, Ricardo Avvisati, Maxine Borton, Claire Dixon, Sophie Walker and Sandra Sanchez. I would also like to thank these people and the many others for support and advice, especially those members of the Badiani, King and Hall labs. Finally, I would like to thank my family, friends, and Sally Connellan for their continued help and support.

I would also like to extended thanks to the many members of the ancillary unit who supported myself and the present work, especially Collette Street and Stephanie Fisher. It is of consideration that hundreds of animals were used in the experiments that make up this thesis, and they endeavoured to ensure that high welfare standards were maintained.

# Abstract

Learned associations between rewarding stimuli and environmental cues which predict their availability play an important role in guiding behaviour. These learned associations are thought to be encoded by neuroadaptations in disperse sets of strongly activated neurons, termed neuronal ensembles, located throughout motivationally-relevant brain areas. However to date, the nature of the adaptations which occur selectively on neuronal ensembles encoding appetitive associative memories remain largely unknown. Using the *Fos-GFP* mouse, which expresses green fluorescent protein (GFP) in recently activated neurons, we investigated the intrinsic and synaptic excitability of neurons activated following exposure to stimuli associated with food (sucrose) or drug (cocaine) exposure.

We observed that in the nucleus accumbens (NAc) shell, but not orbitofrontal cortex, neurons activated following exposure to a food-associated stimulus were more intrinsically excitable than surrounding, non-activated neurons. These neurons also demonstrated increased spontaneous excitatory transmission suggestive of potentiated synaptic strength. Following extinction of the food-cue association, NAc shell neurons activated following cue exposure were no longer more excitable than surrounding neurons. This suggests that the intrinsic excitability of striatal neurons activated by a food-associated cue is dynamically modulated by changes in associative strength.

We also examined the intrinsic excitability of striatal neurons (including neurons in the NAc shell, core and dorsal striatum) activated by cocaine-associated stimuli. Interestingly, NAc shell neurons activated by cocaine-associated stimuli were not more excitable compared to the surrounding neurons regardless of extinction learning experience, possibly indicating differences between drug and food conditioning. Similar results were obtained for dorsal striatal neurons. However, NAc core neurons activated by cocaine-associated stimuli displayed an enhanced excitability which persisted following extinction, indicating that core and shell neuronal ensembles differentially encode the cocaine associative memories.

Overall, by selectively recording from stimuli-activated neurons, this work reveals novel adaptations at the intrinsic and synaptic levels on neuronal ensembles following appetitive learning with both food and drug rewards.

# Abbreviations

5-HT: 5-hydroxytryptamine

AC: adenylyl cyclase

ACg: anterior cingulate

AMPA: α-amino-3-hydroxy-5-methyl-4-isoxazolepropionic acid

AMPAR: AMPA receptor

AP: action potential

BG: basal ganglia

BLA: basolateral amygdala

Ca: calcium

CaMKII: calmodulin/ Ca2+ -dependent protein kinase II

cAMP: cyclic adenosine monophosphate

CeA: central nucleus of the amygdala

Cl: chloride

CR: conditioned response

CRE: cAMP response element

CREB: cAMP response element-binding protein

CS: conditioned stimulus

D1R: dopamine-1 receptor

D2R: dopamine-2 receptor

DAG: diacylglycerol

DS: dorsal striatum

EC: entorhinal cortex

eEPSC: evoked excitatory postsynaptic current

EGFP: enhanced green fluorescent protein

$E_K$: equilibrium potential

EPSC: excitatory postsynaptic current

ERK: extracellular signal–regulated kinase

EXT: Extinction

fAHP: fast afterhyperpolarisation

GABA: gamma-aminobutyric acid

GFP: green fluorescent protein

GPCR: G-coupled protein receptors

GPe: globus pallidus externus (globus pallidus in the rodent)

GPi: Globus pallidus internus (entopeduncular nucleus in rodents)

HP: hippocampus

IKDR: inward delayed rectifier potassium current (non-inactivating outward potassium current)

IL: infralimbic

IPSC: inhibitory postsynaptic current

K: potassium

$K_{IR}$: inwardly rectifying potassium channel

LTP: long-term potentiation

mAHP: medium afterhyperpolarisation

MAPK: mitogen-activated protein kinase

mPFC: medial prefrontal cortex

mRNA: messenger RNA

MSN: medium spiny neuron

Na: sodium

NAc: nucleus accumbens

NMDA: *N*-methyl-D-aspartate

NMDAR: NMDA receptor

OFC: orbitofrontal cortex

PA: Pavlovian approach

PBS: phosphate buffered saline

PCR: Polymerase chain reaction

PFC: prefrontal cortex

$PIP_2$: phosphatidylinositol 4,5-bisphosphate

PIT: Pavlovian-instrumental transfer

PKA: protein kinase A

PKC: protein kinase C

$p_r$: presynaptic release probability

PTLS: prolonged plateau, low threshold interneuron

Ri: input resistance;

SD: standard deviation

SEM: standard error of the mean

sEPSC: spontaneous excitatory postsynaptic current

sIPSC: spontaneous inhibitory postsynaptic current

SNc: substantia nigra pars compacta

SNr: substantia nigra pars reticulata

SR: spontaneous recovery

SRE: serum response element

SRF: serum response factor

STN: subthalamic nuclei

TRE: tetracycline response element

tTA: tetracycline transactivator

UR: unconditioned response

US: unconditioned stimulus

Vm: Resting membrane potential

VP: ventral pallidum

VS: ventral striatum

# Table of contents

behaviours

*Early studies into the functional role of the ventral striatum*

*Functional distinction between the NAc shell and core, and distinct NAc afferents*

1.2.2.1. Evidence for the role of the dorsal striatum in motivated behaviours

**1.2.3. Physiology and molecular characteristics of the striatum**

1.2.3.1. Striatal cell types and intrastriatal connectivity

*Striatal cell types*

*Intrastriatal connectivity of MSNs*

1.2.3.2. *Intrinsic physiology of MSNs*

*Ionic membrane currents in MSNs*

1.2.3.3. *Synaptic physiology of MSNs*

1.2.3.3.1 Ionotropic receptors

*Glutamate receptors*

*GABA receptors*

*Integration of ionic synaptic transmission in MSNs*

1.2.3.3.2. Metabotropic receptors

*Metabotropic glutamate and GABA receptors*

*Dopamine metabotropic receptors*

*1.2.3.3.3.* Receptor transduction pathways

*cAMP pathway*

*Calcium-activated transduction pathways*

*$PIP_2$ pathway*

**1.2.4. Anatomy, physiology and function of additional motivational system areas**

1.2.4.1. The basal ganglia

*Connectivity of the basal ganglia*

*Physiology and function of the basal ganglia*

1.2.4.2. The prefrontal cortex (PFC)

*Connectivity of the PFC*

*Physiology and function of the PFC*

1.2.4.3 The hippocampus

1.2.4.4. The amygdala

## 1.3. Neuroadaptations involved in the encoding of associative memory: selectivity for behaviourally relevant ensembles

**1.3.1. Neuroadaptations associated with the encoding of associative memory**

1.3.1.1. Early theories of learning-induced neuroadaptations and their experimental support

1.3.1.2. Synaptic adaptations following associative learning

*A role for NMDA and GPCRs in conditioned responding*

*Synaptic neuroadaptations observed following conditioned responding.*

1.3.1.3. Intrinsic adaptations following associative learning

**1.3.2. The role of neuronal ensembles in memory encoding and associative learning**

1.3.2.1. Early demonstrations of neuronal ensembles activated during appetitive

# Chapter 2.

# Materials and Methods

## 2.1. Animals

## 2.2. Behavioural Experiments

### 2.2.1. Pavlovian Approach Experiments (Chapters 3 and 4)

*Apparatus*
*Procedures*

### 2.2.2. Cocaine Conditioned Locomotion Experiments (Chapter 5)

*Apparatus*
*Procedures*

## 2.3. Histological Experiments

### 2.3.1. GFP immunofluorescence histochemistry (Chapter 3)
### 2.3.2. In situ hybridisation (Chapter 3)
### 2.3.3. Fos immunohistochemistry (Chapter 5)

## 2.4. Electrophysiological Experiments

### 2.4.1. Slice preparation and recording solutions

*Chapter 3*
*Chapter 4*

### 2.4.2. Slice imaging (All Chapters)
### 2.4.3. Current Clamp Recordings (Chapter 3 and 5)
### 2.4.4. Voltage Clamp Recordings (Chapter 4)

*Experiment 1 - AMPA receptor (AMPAR) and GABA receptor (GABAR) –mediated currents following Pavlovian approach responding*

## 6.1. Summary of Results

### 6.1.1. Differences in NAc shell ensemble neuroadaptations between Pavlovian Approach and conditioned locomotion experiments

*Following exposure to a food-associated CS*
*Following exposure drug-associated stimuli*
*Impact Summary*

## 6.2 Methodological considerations

### 6.2.1. Differences in NAc shell ensemble neuroadaptations between Pavlovian Approach and conditioned locomotion experiments

*No change in the excitability of NAc shell neurons following conditioning with cocaine*
*Persistent increases in excitability following cocaine-environment extinction, but not sucrose-CS conditioning*
*Issues with assessing the affective state of animal models*
*Future recommendations*

### 6.2.2. Further subdivision of the neurocircuitry underlying conditioned responses

*The Striatum*
*The PFC*

### 6.2.3. It is not clear what the activated neurons we are recording from are actually encoding

## 6.3. Mechanisms and function of increased ensemble excitability

### 6.3.1 Increased input resistance in GFP+ neurons

*Inward rectifiers and leak (KIR, KCNK) channels*
*Voltage-gated potassium channels*
*Why do GFP+ change excitability through $R_{in}$?*

### 6.3.2. Generalised changes to the AHP and input resistance of GFP– neurons.

*LTD– concurrent decreases in excitability?*
*In the striatum, LTD is triggered by mGluR1 and Dopamine*

## 6.4. Under what conditions might GFP+ neurons become more excitable?

*GFP+ neurons are recruited to ensembles due to enhanced baseline excitability*
*GFP+ neurons are increased in excitability following the test session*
*The enhanced excitability is a result of repeated activation of cue-activated GFP+ neurons (food and cocaine) by CS and US during learning*

## 6.5. Conclusions and future studies

*Manipulations of relevant cell populations*
*Targeted reversal of observed neuroadaptations*
*Conclusion*

## Appendix A

Animal numbers and outlier analysis

## Appendix B.

Data presented as individual data points

# Chapter 1.

# Introduction

# 1.1. Behavioural Analysis of Associative Learning

## 1.1.1 History of the behavioural analysis of associative learning

### *Pavlov and the conditioned reflex*

The theoretical outlook of early researchers of associative learning was strongly influenced by prior studies of simple motor reflexes. René Descartes first sought to characterise complex behaviour as a collection of coordinated reflex arcs (Descartes, 1975), and this set the tone of later experimental investigations into motor reflexes by pioneering physiologists such as Charles Sherrington and Rudolf Magnus (Magnus, 1924; Sherrington, 1906). In the mid 1880's, Ivan Pavlov, working at the University of St Petersburg in Russia, began his work on learnt, or conditioned reflexes. Pavlov's primary work focused on the gastric system of the dogs (for which he would later win a Nobel prize (1904)). He had noticed that the salivary response of the dog could be evoked merely by the visual appearance of food (an unconditioned stimulus, US), presented at a distance (Pavlov, 1927; Windholz, 1986). Pavlov investigated this observation experimentally and found that a neutral stimulus (or conditioned stimulus, CS) could elicit responses such as salivation if paired with delivery of the food US. Thus Pavlov, who spent almost 40 years conducting experiments detailing the nature of CS-US associations, had demonstrated for the first time that simple motor reflexes could be conditioned to environmental stimuli (Pavlov, 1927).

### *Behaviourism and modern learning theory*

Shortly after Pavlov observed the conditioned reflex, the American researcher Edward Thorndike formulated the "Law of Effect", which postulated that positively reinforced behaviours would be repeated, based on his observations that cats would quickly learn

to press a lever to escape a box for a food reward (Thorndike, 1905). This instrumental type of learning, in which a contingency between a certain response and outcome is learnt, is in contrast to Pavlovian learning in which a contingency between a stimulus and an outcome is learnt (Mackintosh, 1974). Soon after, John Watson formalised the study of behaviour into the Psychological discipline of “Behaviourism”, while also demonstrating that classical conditioning occurs in humans (Skinner, 1938). The field of Behaviourism became strongly associated with the researcher B.F. Skinner, who contributed significantly to behavioural theory and radically improved experimental data collection through the automatic measurement of behaviour using the “Skinner box” (an automated experimental chamber allowing presentation of environmental cues, operant stimuli for instrumental conditioning and reward delivery which is still widely used today) (Skinner, 1969).

Other researchers such as Clark Hull, Robert Bush and Frederick Mosteller began to formalise learning theory, creating mathematical models which attempted to predict the associative strength between a CS and US (Bush and Mosteller, 1951; Hull, 1940). The most influential model of reinforcement learning is the Rescorla-Wanger model, which built upon the work of Bush and Mosteller (Rescorla and Wagner, 1972). This model was found to have great predictive utility, and was, many years later, supported by the direct observations of the neuronal populations which encode reinforcement learning (Glimcher, 2011; Schultz *et al*, 1997). The detailed mechanisms of many associative learning processes have been elucidated by a multitude of influential behavioural researchers over the 20$^{th}$ century. In the modern era, many behavioural studies into associative learning are usually also focused on understanding the underlying biological mechanisms.

## 1.1.2. Major concepts in associative learning, with focus on Pavlovian conditioning

### 1.1.2.1. Features of the conditioned stimulus (CS), unconditioned stimulus (US) and unconditioned and conditioned response (CR)

*The US*

The unconditioned stimulus is an external stimulus which elicits an innate reflexive motor response (the unconditioned response, UR) (Pavlov, 1927). Additionally, a US usually induces a positive or negative affective response and so can be directly reinforcing. For example, and appetitive US such as food may elicit both a reflexive salivary response alongside behavioural excitation and approach behaviours. Conditioned responses such as these are thought to play an evolutionary role, allowing animals to successfully navigate their environment requiring a minimal amount of learning (Pavlov, 1927). Common appetitive USs used in laboratory investigations include rewarding food with high sugar or fat content, water following water deprivation, and access to a mate, while aversive CSs typically involve application of caustic chemical such as a mild acid, electrical shocks or puffs of air to sensitive areas of the body (Mackintosh, 1974).

*The CS*

The conditioned stimulus (originally a mistranslation of Pavlov's "conditionable stimulus" (Pavlov, 1927)) is a stimulus which, following repeated CS-US pairings, may elicit a conditioned response similar to the unconditioned response elicited by the US. An experimental CS may be discrete (located at a distinct point in the environment) or contextual (consisting of the entire environment) and be visual, auditory, olfactory or somatosensory (Antonov *et al*, 2003; Pavlov, 1927). The CS may predict the delivery of reward (a CS+) or alternatively have no relationship to delivery of the reward or predict the omission of reward (a CS-).

CSs used in behavioural experiments are typically neutral prior to conditioning, as previous exposure to the CS can influence the rate of conditioning. For example, pre-habituation to a stimulus can retard the rate of acquisition when it is used as a CS (called “latent inhibition” (Lubow, 1973)) while re-conditioning a CS to a US of opposing valence may also slow conditioning; for example, an appetitive CS+ for food is conditioned much more slowly to an aversive shock than does a CS- for food (Konorski and Scwejkowska, 1956). This suggests that following conditioning, a CS may not remain a neutral predictor of the availability of the US but comes to acquire motivational properties of its own. In support of this are experiments demonstrating that presentation of a CS can elicit CS-directed behaviours and be directly rewarding. Brown and Jenkins (1968) observed approach behaviours to a CS in pigeons, who would peck repeatedly at an illuminated “key” which was conditioned to the delivery of a food reward; pigeons would continue to peck at this food-associated CS even if this behaviour blocked food delivery (Williams and Williams, 1969). Interestingly, some individual animals appear predisposed to find the CS appealing (“sign trackers”) while others are more likely to interact with the US or site of reward delivery (“goal trackers”) (Boakes, 1977; Robinson and Flagel, 2009).

A discrete CS can be associated with a US in isolation, or presented as a compound CS consisting of two separate discrete stimuli, such as a light and a tone. Similarly, conditioning with a discrete CS can, at least initially, be considered as conditioning to a compound CS formed by the CS and the environmental context (Bouton, 2004). However, the role of context in Pavlovian conditioning may become less important as training progresses. For example, Sheffield (1965) observed that during Pavlovian salivary conditioning in dogs, salivation initially increases both during presentation of the CS and during the inter-trial interval (in which the environment is presented in the absence of the CS). However, salivation in the inter-trial interval decreases over multiple conditioning trials, as repeated exposure to the conditioning environment

remains unreinforced (Sheffield, 1965 in Mackintosh, 1974). In support of this, a context switch does not disrupt the expression of conditioned head-jerking to the presentation of a discrete CS conditioned with food (Bouton and Peck, 1989). Thus, following extended conditioning of discrete CS to an appetitive US, the role that environmental context plays may be minimal.

### *The UR and CR*

Conditioned responses are the reflexes elicited by the CS following conditioning, and are usually smaller in magnitude than the response elicited directly by the US (the unconditioned response). Observation of a conditioned response is used as an indirect behavioural measure of the strength of the CS-US association; for example, early in conditioning of the salivary reflex in the dog an unreinforced CS may elicit only minimal salivation, but salivation to the CS increases following multiple conditioning trials (Pavlov, 1927). The magnitude of the CR may also be influenced by the intensity of both the CS and US (Mackintosh, 1974) and number of distinct CS which are presented - the magnitude of conditioned responding summates when two distinct CS conditioned to the same US are presented together (Levitan, 1975). Thus, the CR is not a binary response indicating the successful recall of a CS-US association but is adaptive and varies depending on conditioning procedures used.

While most behavioural experiments typically measure only a single CR, a CS may elicit multiple CRs which may compete for expression. Konorski (1967) proposed a distinction between generalised “preparatory” responses which elicit motivation system activation prior to US delivery (e.g. behavioural excitation, increased heart rate) and “consummatory” responses which are directly related to the specific US (e.g. salivation, freezing behaviour). The behavioural excitation elicited by presentation of a CS may be of such magnitude to interfere with the expression of a CR, especially in goal-directed behaviours such as conditioned approach responses. As such, it is important to

consider a CR of interest as one of many possible, potentially competing, behavioural responses to the presentation of a CS.

### *Factors governing the formation and strength of CS-US associations*

The strength of a CS-US association is determined by the parameters of conditioning, including the order of CS/US presentation and delay between their presentation. Effective conditioning is typically observed using a *delayed conditioning* procedure, in which presentation of the CS is both a *predictor* of the US and overlaps with its delivery. Conditioning in which presentation of the CS and US overlaps exactly (simultaneous conditioning) or when the US precedes the CS (backwards conditioning) is generally ineffective (Pavlov, 1927). Furthermore, trace conditioning, in which the CS predicts the US but the CS and US do not overlap, is also less effective than delay conditioning (Balsam, 1984). The optimum delay between CS onset and US delivery differs between conditioning procedures; for example, conditioning of the nictitating membrane in the rabbit is best conditioned following a delay of only ~500 ms, while the optimum delay for Pavlovian conditioning in the dog is approximately 5-10 seconds (Mazur, 2012; Pavlov, 1927; Solomon and Groccia-Ellison, 1996).

## 1.1.2.2. Experimental methods of weakening the CS-US association

### *Extinction*

Repeated presentation of the CS in the absence of the US leads to a loss of the conditioned response, in a process known as extinction. Pavlov observed that repeated unreinforced presentations of the CS across a single day resulted in extinction of conditioned salivation. However, following an overnight break, upon testing the next morning the CS slightly regained the ability to elicit a CR (Pavlov, 1927). This “spontaneous recovery” was suggested by Pavlov to indicate that the original CS-US

association is not forgotten during extinction learning, but becomes inhibited. An extinction memory appears to be more unstable than the original CS-US association, with conditioned responses recoverable even after prolonged extinction training (Bouton and Swartzentruber, 1991). Additionally, conditioned responses can be recovered following extinction by presentation of novel stimuli, a phenomenon Pavlov termed “disinhibition” (Pavlov, 1927), as well as being reinstated by presentation of the US in isolation (Cifani *et al*, 2012).

In Pavlovian conditioning, an extinction memory is context-dependent, in contrast to the CS-US association (Sheffield, 1965 in Mackintosh, 1974; Bouton *et al*, 1989). If extinction learning occurs in a distinct environment to training, conditioned responding may be recovered by exposure to the CS in the original conditioning environment, a phenomenon termed “renewal” (Bouton and Bolles, 1979). Thus extinction likely represents a reduction of the CS-US association with reference to a specific environment, and is susceptible to disruption through a range of experimental interventions.

### *Devaluation and stimulus-stimulus/stimulus-response behaviour*

The ability of a CS to elicit a CR can also be reduced by devaluation of the US. Holland and Rescorla (1975) observed that increased locomotor activity during presentation of a food-associated CS could be reduced following devaluation of the food, either with satiation or pairing of the food with illness (through rotation). Devaluation is an effective tool in distinguishing between two putative types of classically conditioned association, stimulus-stimulus (S-S) and stimulus-response (S-R) associations. It has been suggested either that an association between a representation of the CS and US is formed during conditioning (S-S), or that conditioning between the CS and the unconditioned response occurs (S-R) (Mackintosh, 1974). These are similar to goal

driven action-outcome (A-O) learning and habituation stimulus-response behaviours in instrumental conditioning.

Devaluation of the US in the absence of the CS should disrupt S-S, but not S-R learning. The early stages of acquisition appear to be dependent on the formation of S-S associations, as they may be disrupted by US devaluation (Dickinson, 1985). However, extended training or training on a second order schedule of reinforcement (in which a CS is associated directly to second CS following conditioning) are not affected by devaluation (Dickinson, 1985; Holland *et al*, 1975), suggesting they are driven by S-R behaviours. Thus different types of conditioning paradigms result in the formation of distinct types of associations.

### 1.1.3. Drugs of Abuse as unconditioned stimuli

*Drugs of abuse as reinforcers*

Drugs of abuse are powerful reinforcers which may be used to condition both Pavlovian and instrumental behaviours (Di Chiara, 1999; Everitt and Robbins, 2013; Grimm *et al*, 2001; Koob and Volkow, 2010). Drugs of abuse function as a typical US, eliciting a range of unconditioned responses (such as changes to heart rate) and are positively reinforcing - drugs of abuse will be reliably self-administered while contexts associated with drug administration are readily approached (Koob *et al*, 2010). The URs elicited by psychoactive drugs vary as a function of their underlying pharmacology (Badiani *et al*, 2011), though most drugs of abuse increase locomotor activity in rodents (Leri *et al*, 2003). Interestingly, animals show a general preference for food rewards over drug rewards however drug associated cues are more powerful motivators (Caprioli *et al*, 2017; Lenoir *et al*, 2007; Tunstall and Kearns, 2016).

*Experimental procedures using drug US: similarities and differences to food US*

Exposure to a drug-associated CS can induce behavioural excitation and approach behaviours (Hotsenpiller *et al*, 2002), similar to a food associated CS (Holland *et al*, 1975). One example of this is drug conditioned hyperlocomotor activity or 'conditioned locomotion' in which animals show an increase in locomotor activity when exposure to a drug-associated context (Tilson and Rech, 1973).

A number of novel behavioural phenomena were first discovered when using drugs as reinforcers. Behavioural sensitisation is a phenomenon in which locomotor activation in response to drug administration is augmented following repeated administration (Tilson *et al*, 1973). This effect is context-specific, as testing in a distinct environment to conditioning does not yield behavioural sensitisation (Anagnostaras *et al*, 2002; Whitaker *et al*, 2016). Behavioural sensitisation to food rewards, in which mice will consume more food in a context associated with prior food administration, has also been observed (Le Merrer and Stephens, 2006). Another phenomenon which was first observed using psychostimulant drugs was the "incubation" effect. Following cessation of cocaine self-administration, cocaine craving, as defined by instrumental responding on a lever formerly associated with drug delivery, is potentiated or 'incubates' at a magnitude related to the duration of drug withdrawal (Grimm *et al*, 2001). This phenomenon was later demonstrated to also occur for other drugs of abuse and food reinforcers, albeit less robustly compared to drugs of abuse (Grimm *et al*, 2005; Pickens *et al*, 2011)**.**

Thus while there are similarities in the way in which food and drugs may be conditioned, the magnitude of conditioned responses are usually larger when drug reinforcers are used (Tunstall *et al*, 2016; Zombeck *et al*, 2008).

# 1.2. The Motivational System of the Brain: Anatomy, Physiology and Function

Pavlov originally hypothesised that the afferent activity caused by presentation of the CS travels through the auditory nerve, to the brain where it elicits activation of the secretory nerves, stimulating the salivary gland (Pavlov, 1927). While the basic assumptions of Pavlov appear correct, for many years the precise brain areas involved in behavioural conditioning were largely unknown. Since then, a complex network of brain regions involved in the encoding of conditioned behaviours has been elucidated. These include the basal ganglia network (BG), including its input nucleus, the striatum, as well as other forebrain regions such as the prefrontal cortex (PFC), hippocampus (HP) and amygdala alongside midbrain neuromodulatory regions such as the ventral tegmental area (VTA) and substantia nigra pars compacta (SNc) (Groenewegen *et al*, 1993; Haber, 2011; Voorn *et al*, 2004). Below, the anatomy, physiology, biochemistry and function of these areas will be explored, with special reference to the striatum, a brain region thought to have a particularly important role in encoding conditioned responses (Everitt *et al*, 2013).

## 1.2.1. Anatomy of the striatum

The striatum is an evolutionarily ancient subcortical forebrain area present in birds, reptiles, and is particularly developed in mammals (Reiner *et al*, 1998) (Figure 1). The molecular, physiological and anatomically characteristics of the striatum are comparable across mammal species (Calipari *et al*, 2012; Reiner *et al*, 1998), in which it is involved in the encoding of appetitive associations. The striatum is considered to be the primary input of the basal ganglia, a set of forebrain nuclei important for both limbic and motor processing (Haber, 2011) (Figure 2). As such, the striatum receives

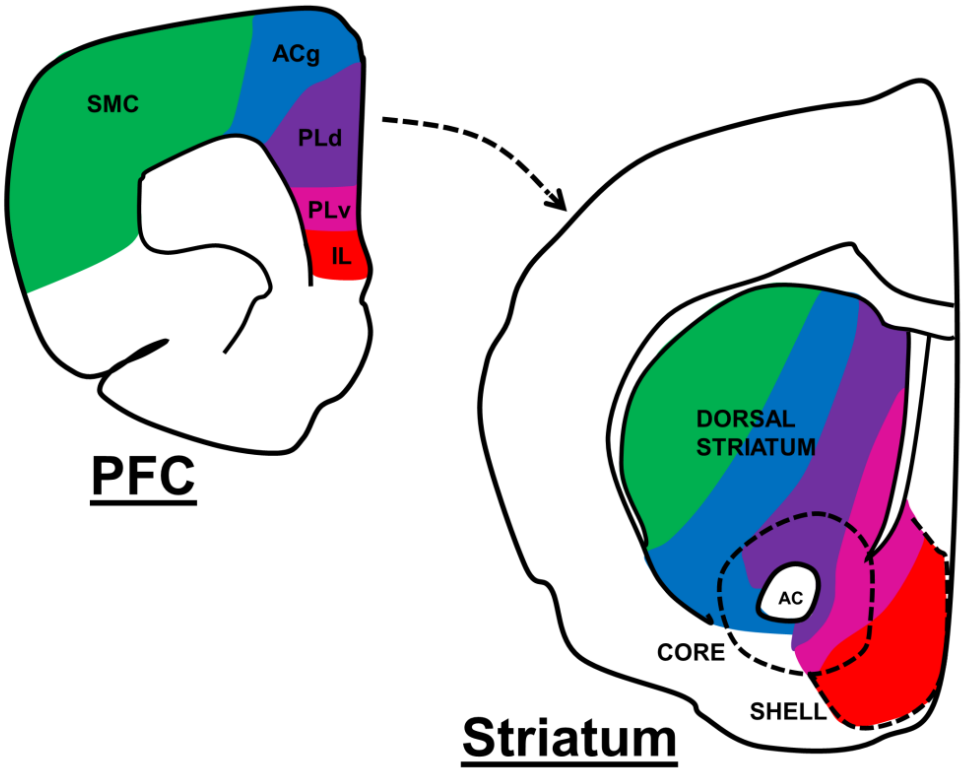


**Figure 1.** Anatomy of the striatum and its afferent projections from the prefrontal cortex (PFC). Adapted from Voorn *et al* (2004). The striatum consists of the nucleus accumbens (NAc) shell (SHELL), NAc core (CORE) and dorsal striatum (broadly defined as the region dorsal to the NAc core). The NAc shell is innervated by the infralimbic (IL) prefrontal cortex (PFC) and parts of the ventral prelimbic cortex (PLv), while the NAc core receives input from the ventral prelimbic, dorsal prelimbic (PLd) and the anterior cingulate cortex (ACg). The dorsal striatum receives projections largely from the PLd, ACg and somatosensory cortex (SMC). These projections are not strictly segregated to specific striatal sub-regions but form a continuum along the ventral-dorsal axis of the striatum. AC: anterior commissure.

input from multiple brain areas including the prefrontal cortex, hippocampus, amygdala, thalamus and midbrain dopaminergic areas while in contrast its outputs are primarily limited to a select group of basal ganglia nuclei. Thus, the striatum functions to converge a broad set of inputs from across the brain to its downstream basal ganglia targets.

#### 1.2.1.1. Anatomy of the ventral striatum

The striatum can be broadly divided into ventral and dorsal subdivisions (Heimer *et al*, 1985). The ventral striatum (VS) consists of elements of the olfactory tubercle, the

ventral section of the caudate/putamen and the nucleus accumbens (NAc), which can be further subdivided into core and shell regions (Basar *et al*, 2010; Heimer *et al*, 1991; Voorn *et al*, 2004). The core/shell distinction becomes less clear at the rostral end of the striatum, in which both regions are combined into the “rostral pole” (Salgado and Kaplitt, 2015). The NAc shell and core are related yet distinct areas distinguishable by structure, connectivity, physiology and function (Ghitza *et al*, 2004; Haber, 2011; Heimer *et al*, 1991; Kourrich and Thomas, 2009; Voorn *et al*, 2004) and have received particular attention as important structures of the motivational system (Day and Carelli, 2007).

The dorsal striatum (DS) consists of the caudate/putamen subdivisions; in humans these are separated into the distinct caudate and putamen while in the rodent they form a continuous structure (Hagan *et al*, 2011). The dorsal striatum can be subdivided into dorsolateral and dorsomedial subdivisions, based on structure, connectivity and function (Murray *et al*, 2012; Parent and Hazrati, 1995; Voorn *et al*, 2004). The dorsal striatum has received less attention for its role in associative learning than the ventral striatum, though it appears to play a crucial role in certain types of conditioned responses (Everitt *et al*, 2013).

#### 1.2.1.1.1. Afferent connections of the ventral striatum

The afferent connections of the striatum are organised across its ventromedial-dorsolateral axis and do not strictly adhere to the boundaries of striatal subregions; thus neighbouring striatal regions typically display some overlap in afferent connectivity, with remote regions of the striatum sharing very few afferents (Haber, 2011; Voorn *et al*, 2004). In general, the ventral striatum receives input from limbic brain areas while the dorsal striatum receives significant input from areas involved in sensorimotor processing.

### *Glutamatergic afferents*

Projections of the prefrontal cortex to the ventral striatum are organised along the ventral to dorsal axis of the PFC. The NAc shell receives projections which originate from the ventral orbitofrontal, ventral agranular insula and infralimbic cortex, while the core receives distinct projections from the dorsal prelimbic, anterior cingulate and dorsal agranular insula regions (Brog *et al*, 1993; Haber, 2011; Salgado *et al*, 2015; Voorn *et al*, 2004). The projections of the PFC to the striatum primarily consist of dense focal connections, however the PFC also projects diffusely, extending widely and targeting striatal subregions in a less defined manner (Haber, 2011).

The basolateral amygdala (BLA) and hippocampus both project to the NAc shell and core, sending convergent afferents with overlapping terminal fields. The shell receives input preferentially from the ventral subiculum, while parahippocampal gyrus projects preferentially to the core (Haber, 2011; Ito and Hayen, 2011). The hippocampal projection to the NAc shell is significant, accounting for approximately 30% of the asymmetric spines of the shell (Britt *et al*, 2012; Sesack and Pickel, 1990). The ventral striatum additionally receives significant glutamatergic input from the thalamus, with thalamic subnuclei differentially projecting to the shell and core (Brog *et al*, 1993; Haber, 2011; Voorn *et al*, 2004). Furthermore, the paraventricular thalamus projects to both the NAc shell and core, and in addition to glutamate may release neuromodulators such as enkephalin and substance P (Kirouac, 2015).

### *GABAergic afferents*

Inhibitory gamma-aminobutyric acid (GABA) projections to the striatum are less numerous than glutamatergic projections, however basal ganglia nuclei, which are predominantly GABAergic, send significant projections to the ventral striatum. The globus pallidus/ventral pallidum forms distinct reciprocal connections to the NAc shell and core, with the shell preferentially receiving from medial ventral pallidum and the

core from the dorsolateral ventral pallidum and globus pallidus (Brog *et al*, 1993). This is of note, as the more ventral pallidal areas are associated with limbic processing, while its more dorsal regions are involved preferentially in motor processing.

The prefrontal cortex and hippocampus also send a small number of inhibitory projections to the ventral striatum (Lee *et al*, 2014; Sesack *et al*, 1990), while the VTA (which provides a significant dopaminergic input to the ventral striatum) has been demonstrated to co-release GABA (Van Bockstaele and Pickel, 1995).

### *Additional afferents*

Dopamine is a neurotransmitter known to play a crucial role in reward learning and motivated behaviour (Di Chiara and Imperato, 1988). Dopaminergic projections to the ventral striatum originate in the midbrain ventral tegmental area and substantia nigra pars compacta. The VTA primarily innervates the NAc shell and the NAc core (Haber *et al*, 2000; Ikemoto, 2007), although some sparse projections to the core from the SNc have been reported (Salgado et al, 2015; Ikemoto, 2007). While noradrenergic (NA) projections to the NAc core are extremely sparse, the caudal NAc shell receives NA projections originating primarily in the A2 region of the nucleus tract solitaries (Delfs *et al,* 1998).

The caudal most region of the NAc shell, named the “septal pole” and adjacent medial-shell areas receive a somewhat unique pattern of innervation compared to other areas of the ventral striatum, receiving afferents from the bed nucleus of stria terminalis, medial amygdala, lateral habenula and neuromodulatory inputs from the hypothalamus (Brog *et al*, 1993).

#### 1.2.1.1.2. Efferent connections of the ventral striatum

The ventral striatum converges its many inputs to downstream basal ganglia areas. Both the NAc shell and core innervate the ventral pallidum, the entopeduncular nucleus (analogous to the globus pallidus internus in the human), globus pallidus (globus pallidus externus in the human) and the substantia nigra pars reticular (SNr) (Heimer *et al*, 1991; Kelley, 2004; Voorn *et al*, 2004). Ventral striatal outputs mirror the topography of their inputs, with the NAc shell projecting preferentially to the medial ventral pallidum and the NAc core projecting to dorsolateral VP (Heimer *et al*, 1991). The outputs of NAc core are similar to those of the dorsal striatum, projecting primarily to BG areas, while the NAc shell has unique projections to subcortical limbic regions (Heimer *et al*, 1991; Voorn *et al*, 2004). The NAc shell projects to the lateral hypothalamus, extended amygdala (EA; sublenticular extended amygdala, central amygdala and stria terminalis) (Heimer *et al*, 1991; Usuda *et al*, 1998) and basal forebrain cholinergic projections (BFCP). The BFCP is an aggregate of cholinergic neurons located throughout the basal forebrain, including in the extended amygdala and ventral pallidum, which provides direct cholinergic innervation to the amygdala and PFC. Thus the NAc shell may be able to directly influence cholinergic projections to the cortex in a manner independent of the basal ganglia system (Zaborszky and Cullinan, 1992).

Similar to their input, both the NAc shell and core shell project to the VTA (Heimer *et al*, 1991; Watabe-Uchida *et al,* 2012) however Heimer *et al* (1991) also observed projections from the core to the SNc. Optogenetic stimulation of the NAc to VTA pathway demonstrates that NAc efferents preferentially target non-dopaminergic GABA interneurons in the VTA. Thus the NAc has the ability to regulate its own dopamine input, with increased firing to the VTA potentiating accumbens dopamine release (Xia *et al*, 2011).

### 1.2.1.2. Anatomy of the Dorsal Striatum

*Afferent Connections of the dorsal striatum*

The afferents of the dorsal striatum, which are less widespread than the ventral striatum, originate primarily in the sensorimotor cortices and the thalamus. The cortical projections to the dorsal striatum are organised in a ventromedial-dorsolateral topography, with the anterior cingulate projecting to the more ventral regions of the dorsal striatum and sensorimotor cortex areas projecting at the most dorsolateral region (Dube *et al*, 1988; Kemp and Powell, 1971a; Somogyi *et al*, 1981). The cortical projections to the dorsal striatum are significant, with ~30-40% of asymmetrical synapses in the dorsal striatum formed by cortical afferents (Kemp *et al*, 1971a). Projections from the sensorimotor cortex are glutamatergic and convey cutaneous receptive fields for the body, including trunk, limbs and head (Kemp *et al*, 1971a; Voorn *et al*, 2004) which project in diffuse manner, rather than in focal point-to-point body maps (Brown *et al*, 1998).

The dorsal striatum also receives glutamatergic input from the thalamus, which contribute an additional ~20-25% of the asymmetrical synapses. The intralaminar nucleus of the thalamus (consisting of the parafascicular nucleus, paracentral thalamic nucleus and central lateral thalamic nucleus) strongly innervates the dorsal striatum (Kemp *et al*, 1971a); these thalamic areas play an important role in motor function (Dube *et al*, 1988; Van der Werf *et al*, 2002; Voorn *et al*, 2004). Thus the dorsal striatum primarily receives input from brain areas involved in sensorimotor processing, in contrast to the ventral striatum which preferentially receives afferent connections from limbic brain areas.

Dopaminergic input to the dorsal striatum is exclusively provided by the SNc (Beckstead *et al*, 1979). Additionally, dorsal raphe nuclei also send serotoninergic projections to the caudate/putamen (van der Kooy and Kuypers, 1979). In contrast, NA

projections to the dorsal striatum are extremely sparse and are in many cases undetectable (Delfs et al, 1998; Schwarz and Lou, 2015).

*Efferent connections of the dorsal striatum*

The dorsal striatum, similar to the nucleus accumbens core, projects almost exclusively to downstream basal ganglia regions associated with motor output (Groenewegen, 2003). The dorsal striatum sends dense projections to the substantia nigra (Maurin *et al*, 1999) and the dorsal pallidum, including both the entopeduncular nucleus and globus pallidus (Maurin *et al*, 1999; Nagy *et al*, 1978). Mirroring its afferent connectivity from dopaminergic regions, the dorsal striatum innervates the dopaminergic SNc, but not the VTA (Maurin *et al*, 1999).

### 1.2.1.3. Striatal anatomy: functional considerations

Thus the striatum receives both limbic and motor input organised topographically along its ventromedial to dorsolateral axis (Voorn *et al*, 2004), with the ventral striatum receiving projections from predominantly limbic areas, and the dorsal striatum from motor-processing areas. The NAc shell receives significant afferents from the infralimbic PFC and ventral agranular insula, the lateral hypothalamus, ventral subiculum, basolateral amygdala and ventral portion of the ventral pallidum (Haber, 2011; Ito *et al*, 2011; Sesack *et al*, 1990), all regions associated with limbic processing. The afferent connections of the NAc shell from the most ventral portions of the PFC, lateral hypothalamus and ventral pallidum, are entirely distinct from the core, along with its unique efferent connections outside of the basal ganglia (Brog *et al*, 1993; Heimer *et al*, 1991).

The NAc core receives inputs from the amygdala, hippocampus, prelimbic prefrontal cortex and ventral anterior cingulate cortex (Haber, 2011; Ito *et al*, 2011; Sesack *et al*,

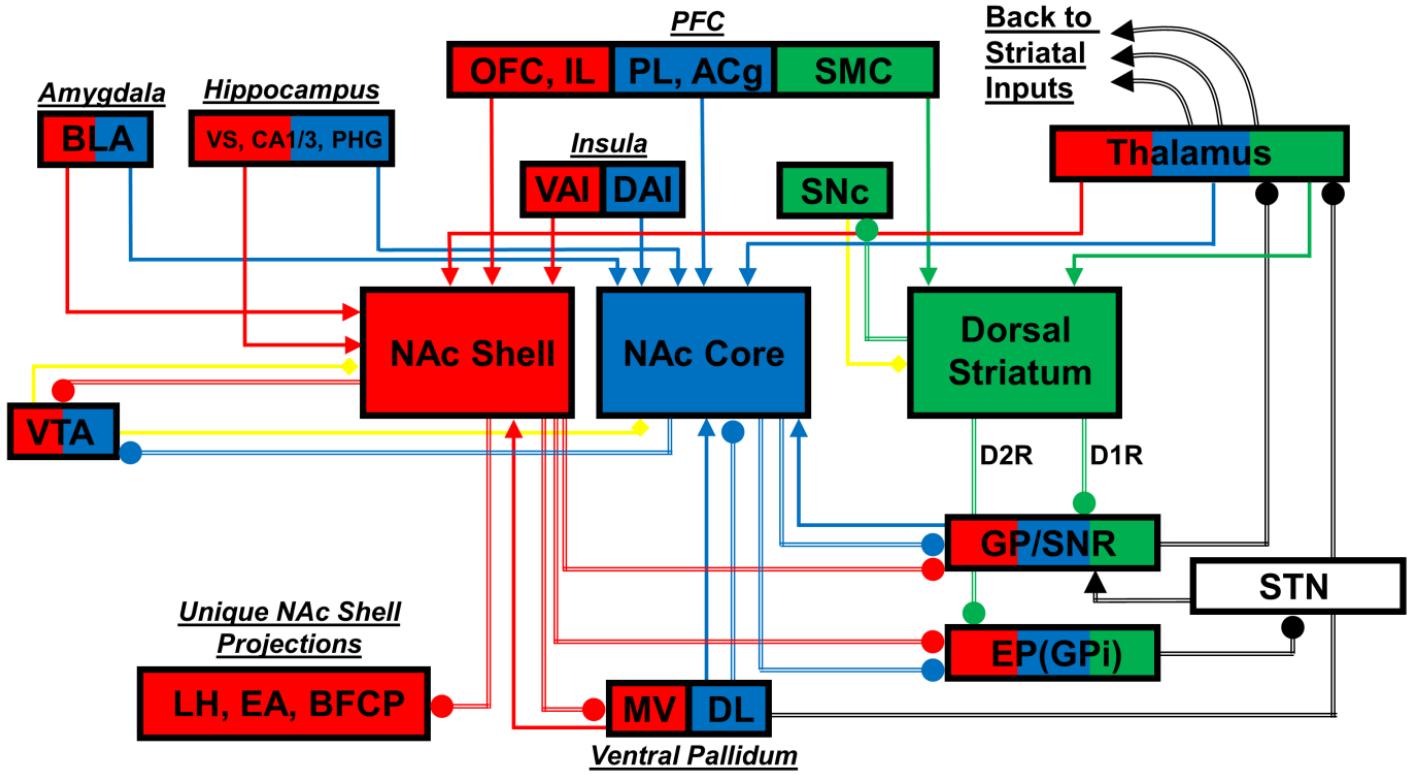


**Figure 2.** Afferent and efferent connections of the striatum. Glutamatergic, GABAergic and dopaminergic are shown with pointed, round and diamond arrowheads, respectively. With the exception of the nucleus accumbens (NAc) shell, the striatum projects primarily to basal ganglia nuclei. The primarily output of the basal ganglia is the thalamus, which in turn projects back to the brain areas providing innervation to the striatum, forming the classical loops of the basal ganglia (Alexander *et al*, 1986) (Projections of basal ganglia nuclei downstream of the striatum are shown double-lined, black). The afferent connections to the NAc shell (red, solid), core (blue, solid) and dorsal striatum (green, solid) originating from the amygdala, hippocampus, prefrontal cortex (PFC), thalamus, ventral pallidum are shown. The striatum also receives dopaminergic projections from the ventral tegmental area (VTA) and substantia nigra pars compacta (SNc) (in yellow). The efferent connections of the striatum are distinct between the NAc shell, core and dorsal striatum (double-lined, red, blue and green respectively). **Abbreviations:** *Amygdala* - BLA: basolateral nucleus of the amygdala, *Hippocampus* – VS: ventral subiculum, PHG: parahippocampal gyrus, CA1/3: *Cornu Ammonis* 1/3, PFC – OFC: orbitofrontal cortex, IL: infralimbic, PL: prelimbic, ACg: anterior cingulate cortex, SMC: sensorimotor cortex, *Insula* – VAI: ventral agranular insula, DAI: dorsal agranular insula, *Ventral pallidum* – MV: medioventral, DL: dorsolateral, *Unique NAc Shell Projections* – LH: lateral hypothalamus, EA: extended amygdala, BFCP: basal forebrain cholinergic projections. *Other*- GP/SNR: globus pallidus (globus pallidus externus in humans)/ substantia nigra pars reticula, EP(GPi): entopeduncular nucleus (globus pallidus internus in humans), STN: subthalamic nucleus. D1R – dopamine 1 receptor, D2R – dopamine 2 receptor.

1990); and makes reciprocal connections to the dorsomedial ventral pallidum (Brog *et al*, 1993; Maurin *et al*, 1999; Nagy *et al*, 1978). Thus while the core receives similar inputs to the NAc shell, these more commonly from adjacent portions of afferent regions which play a more pronounced role in motor processing. At its most dorsal regions the striatum receives inputs which are almost exclusively related to

sensorimotor processing. For example, the dorsal striatum does not receive afferents from the hippocampus or amygdala, instead receiving input from frontal sensorimotor cortices and thalamic nuclei associated with motor processing. Thus the striatum can be characterised as a unique input area to the basal ganglia which processes limbic and motor information in a gradated manner along its ventromedial to dorsolateral axis.

## 1.2.2. Evidence for the role of the striatum in motivated behaviour

### 1.2.2.1. Evidence for the role of the ventral striatum in motivated behaviour

*Early studies into the functional role of the ventral striatum*

Early studies characterising the function of discrete brain regions were typically exploratory in nature, observing the effect of simple electrical or chemical stimulation of cortical and subcortical brain regions, guided by a rich understanding of the underlying anatomy (Mogenson *et al*, 1980). Amongst the first demonstrations that the midbrain dopamine system and ventral striatum was involved in appetitive responses was the observation that electrical stimulation to the medial forebrain bundle (containing midbrain-to-forebrain dopaminergic axons) elicits ingestive behaviours in rats; the relevant dopaminergic projections were later found to originate in the VTA (Huang and Mogenson, 1972). At the time, the functional dopaminergic connections from the VTA to the NAc were well known (Mogenson *et al*, 1980), and increasing dopamine or opioid transmission in the NAc itself were shown to facilitate feeding behaviour (Colle and Wise, 1988; Mucha and Iversen, 1986). Thus attention was drawn to the dopaminergic projections to the NAc and the ventral striatum as a possible system involved in the expression of appetitive behaviours.

Direct evidence for the NAc's role in reinforcement came from observations that rodents would self-administer electrical stimulation to the NAc, in a manner regulated by dopamine (Phillips and Fibiger, 1978). While animals will self-stimulate many areas

of the brain (such as the PFC) (Phillips *et al*, 1978), the VTA and NAc appear particularly important to the expression of dopamine-mediated motivated responses. For example, lesions of the NAc and VTA, but not medial prefrontal cortex (mPFC), disrupt cocaine self-administration (Martin-Iverson *et al*, 1986; Roberts and Koob, 1982; Roberts *et al*, 1980), while intra-accumbens, but not dorsal striatum, infusions of amphetamine in a particular environmental context lead to conditioned place preference (Carr and White, 1983).

The NAc is not only involved in the processing of directly reinforcing unconditioned stimuli, it also plays an important role in the encoding of reward-associated CSs. For example, amphetamine infusion to the NAc facilitates conditioned responding for a water-associated CS in water-deprived rats, an effect blocked by 6-OHDA lesions of the NAc (which selectively target dopaminergic projections) (Taylor and Robbins, 1984, 1986). Furthermore, dopamine depletion in the NAc inhibits both the acquisition and expression of Pavlovian approach behaviours (Parkinson *et al*, 2002). These findings suggest that the ventral striatum plays a particularly important role in appetitive conditioning and the encoding of reward-associated CS, in a manner regulated by dopamine.

### *Functional distinction between the NAc shell and core, and distinct NAc afferents*

A functional distinction between the NAc shell and core subregions has been revealed through selective manipulations of these areas. Such studies typically implicate the NAc shell in encoding the motivating properties of reinforcers, while the NAc core appears to be important for the processing of classically conditioned CSs. For example, lesions of the NAc core, but not shell, disrupt the acquisition of Pavlovian approach responses (Parkinson *et al*, 2000b), suggesting the core is crucial for the formation of Pavlovian conditioned reflexes between a CS and US. However, expression of Pavlovian approach is reduced following infusion of GABA agonists muscimol and

baclofen to either the core or shell (Blaiss and Janak, 2009). Thus, the core appears important for the acquisition and retention of a CS-US relationship while the NAc shell may be important to the expression of classically conditioned behaviours - interestingly, Blaiss *et al* (2009) observed that shell inactivation increased responding to a CS-, suggesting the shell may play a role in inhibiting inappropriate responses during the expression of conditioned behaviours. Similar findings have been reported using drug reinforcers, Ito *et al* (2004) made NAc core and shell lesions to rats responding on a second-order reinforcement schedule for cocaine. In this paradigm, animals are taught to self-administer cocaine on a fixed-ratio schedule, before a second-order training schedule is used, in which animals must press the lever multiple times only for the presentation of a light CS; after a certain number of CS presentations have occurred, animals received an infusion of cocaine. Lesions to the NAc core did not affect cocaine self-administration, but disrupted the formation and expression of self-administration under the second-order schedule of reinforcement. NAc shell lesions, however, had no effect on the acquisition or expression of second-order responding but significantly affected cocaine-potentiated responding. Together these studies suggest that the core is important for the encoding of CS-US associations while the NAc shell may mediate directly reinforcing effects of a US and inhibition of behaviour unrelated to the acquisition of reward.

Researchers have also sought to characterise the function of the distinct afferent connections of the NAc. Serial disconnection studies permit functional dissection of the connectivity between two brain areas; in this paradigm, a pair of target brain area are each unilaterally lesioned on opposing hemispheres, leaving functioning in the remaining regions spared but all connectivity between both target regions lost. Ito *et al* (2008) observed the effect of disconnecting the hippocampus and NAc shell on an appetitive contextual discrimination task and conditioned place preference to food. They found that destruction of the hippocampus-NAc connection significantly perturbed

context-dependent CS-US conditioning (in which the CS only predicted the US in a specific context) as well as conditioned place preference to a food reward. However, the lesions had no effect on conditioning to a discrete CS. Lesions to the amygdala-NAc pathway, however cause disruption of discrete CS encoding as assayed through Pavlovian to instrumental transfer (Shiflett and Balleine, 2010), as well as conditioned place preference for a food reinforcer (Everitt *et al*, 1991). Hence, serial disconnection studies suggest that while some pathways may show a selectivity for processing particular information (such as the hippocampus-NAcs role in contextual learning) other afferent pathways may encode multiple distinct processes involved in Pavlovian conditioning.

More recently, technologies permitting the selective expression of light-gated ion channels (channelrhodopsins) in mammalian brain tissue allow precise control over specific neuronal circuits in real time (Boyden *et al*, 2005). Over 40 years since the VTA-NAc pathway was first implicated in motivated responding, Steinberg *et al* (2014) demonstrated that rats will self-stimulate optogenetic activation of the VTA-NAc pathway in a manner antagonised by blockage of NAc D1/D2 receptors, conclusively demonstrating that dopamine release through the VTA-NAc pathway is intrinsically motivating. Selective modulation of NAc afferent pathways using optogenetics has also demonstrated a role for specific glutamatergic projections in appetitive conditioning; for example, Stuber *et al* (2011) demonstrated that transient optogenetic inhibition of the BLA-NAc pathway reduces CS-induced sucrose-seeking . Similarly, inhibition of this pathway also reduces cue-induced reinstatement of cocaine (Stefanik and Kalivas, 2013). Thus optogenetic dissection supports experimental evidence gained using the disconnection method, demonstrating the role of the amygdala-NAc pathway in the encoding of discrete CSs.

#### 1.2.2.1. Evidence for the role of the dorsal striatum in motivated behaviours

Early observations into the function of the dorsal striatum suggested the region played a role in inhibiting appetitive responses. For example, stimulation of the caudate putamen, in contrast to the NAc, reduces feeding behaviour (Gravante *et al*, 1985) while other studies demonstrated that lesions to the caudate/putamen disrupts differential reinforcement of lower rates (DRL; in which animals are rewarded for withholding responses) (Hansing *et al*, 1968). Furthermore, manipulations which in the NAc blocked appetitive conditioning, appeared to have no effect when undertaken the DS. For example, lesions to the dorsal striatum did not reliably block amphetamine facilitated conditioned responding (Taylor *et al*, 1986), while intra NAc, but not DS amphetamine injections were observed to elicit conditioned place reference (Carr *et al*, 1983). These studies suggested that the DS likely plays a less significant role in appetitive conditioning that the ventral striatum.

However, a selective role of the dorsolateral striatum has been observed in the encoding of stimulus-response behaviours following appetitive conditioning. Yin *et al* (2004) lesioned the dorsolateral striatum of rats prior to instrumental training for a sucrose reward on an interval schedule (which rapidly leads to S-R responding, due to the weak relationship between response and reinforcement (Dickinson, 2010). They next tested the effect of devaluation on responding in lesioned and sham-lesioned animals, and observed that although all rats learnt to respond for food, only lesioned rats were affected following US devaluation. As reinforcer devaluation selectively disrupts action-outcome but not stimulus response behaviours, this suggests that dorsolateral striatum encodes S-R responding, while A-O behaviours are encoded elsewhere. Later studies suggest that the transition from A-O to S-R responding is underpinned by encoding along the ventromedial-dorsolateral axis of the stratum. In an elegant serial disconnection study, Belin and Everitt (2008) unilaterally lesioned the

NAc core (thus blocking serial ventral-dorsal striatum connectivity in the lesioned hemisphere), then trained animals under a second-order schedule of reinforcement, which is known to lead to S-R responding (Holland *et al*, 1975). At test, they infused the dopamine antagonist α-flupenthixol into the DS contralateral to the NAc core lesion, and observed deficits in instrumental responding on the second order schedule of reinforcement. This suggests the intact DS, despite functioning normally, was not able to encode stimulus-response responding due to its functional disconnection from the ventral striatum. Thus, these studies suggest an important role not only for the DS in motivated behaviour, but suggest how both the ventral and dorsal striatum may interact during conditioning.

## 1.2.2. Physiology and molecular characteristics of the striatum

The function of the striatum and the expression of learning-induced changes is dependent on complex array of neuronal cell types with distinct physiological and molecular profiles. In order to understand how the striatum encodes learned associations, its structure must be explored. As such, the physiology and molecular biochemistry of the striatum will be discussed below.

### 1.2.2.1. Striatal cell types and intrastriatal connectivity

*Striatal cell types*

The primary output neurons of the striatum are GABAergic medium spiny neurons (MSNs). MSNs make up ~90-95% of striatal neurons, and are characterised by their medium size, branching dendrites with a significant number of dendritic spines, and collaterals to surrounding MSNs (Kemp and Powell, 1971b; Lobo, 2009; Tepper *et al*, 2010). The wide branching dendritic arborisations with many spines function to converge the significant number of inputs the striatum receives from across the brain.

In additional to MSNs, the striatum contains giant aspiny cholinergic interneurons (Durieux *et al*, 2011) and an array of GABAergic interneurons, which may be identified using a number of exclusively expressed molecular markers. These include parvalbumin (fast spiking interneurons), neuropeptide Y and nitric oxide (prolonged plateau, low threshold (PTLS) class interneurons), or calretinin expressing interneurons (of which the physiology is yet unknown) (Kawaguchi, 1993; Tepper *et al*, 2010). A class of striatal interneuron co-expressing TH and GABA has been identified and were once thought to release dopamine, however recent optogenetic studies suggest they release only GABA (Xenias *et al*, 2015).

### *Intrastriatal connectivity of MSNs*

Early visualisation of horseradish peroxidase-filled MSNs suggested their axons made significant collateral connections contacting surrounding neurons. However, early physiological investigations using paired recordings between MSNs failed to observe direct MSN-MSN connectivity (Jaeger *et al*, 1994; Tepper and Plenz, 2006). However, more recent studies have demonstrated physiological evidence for a widespread but weak network of MSN collateral connections (Czubayko and Plenz, 2002; Tepper *et al*, 2006). Inhibitory tone onto MSNs is also provided by GABAergic interneurons. A single fast-spiking GABAergic interneuron synapses onto approximately 300-500 neuron striatal MSNs, which are approximately 4-5 times stronger than MSN-MSN synapses, demonstrating low vesicle release failure rates (Koos and Tepper, 1999, 2002; Tepper *et al*, 2006). Recent investigations utilising optogenetic stimulation of MSNs, rather than paired recordings, demonstrate that though individual MSN-MSN synapses are weak, convergent inputs of multiple MSNs onto single neurons may parallel the inhibitory influence of GABAergic interneurons, which are divergently connected to multiple MSNs (Chuhma *et al*, 2011). MSNs make direct connections also to

cholinergic interneurons but not to fast-spiking GABAergic interneurons (Chuhma *et al*, 2011).

The neuroanatomy of the striatum can thus be characterised by the convergence of glutamatergic input through a single-neuron layer of MSNs, which inhibit each other through lateral connections (Tepper *et al*, 2006). These experimental observations support theoretical models of striatal function in which competing sets of medium spiny neurons function to filter afferent information and bias striatal output to basal ganglia targets (Wickens *et al*, 1991).

### *1.2.3.2. Intrinsic Physiology of MSNs*

MSNs are distinguishable based on their hyperpolarised resting potential (~-80mV), pronounced inward rectification and slow depolarising ramp at near-threshold potentials (Mermelstein et al, 1998). MSNs exhibit pronounced up-state/down-state fluctuations in vivo, determined by synaptic drive and stabilised by potassium channel function (Wilson and Kawaguchi, 1996); however these state transitions are not observed in slice preparations due to removal of glutamatergic afferent cell bodies.

#### *Ionic membrane currents in MSNs*

At hyperpolarised potentials, MSNs display pronounced inward rectification determined by a number of rectifying potassium ion channels, with the Kv1.2 channel playing a major role (Hibino et al, 2010; Nisenbaum and Wilson, 1995; Shen et al, 2004). Inwardly rectifying potassium channels ($K_{IR}$) preferentially pass inward currents due to polyamine-dependent block of outward currents at potentials above the potassium equilibrium potential ($E_K$, approximately -90 mV) (Hibino et al, 2010; Lopatin et al, 1995). $K_{IR}$ channels in MSNs are open at rest and play a primary role in setting the hyperpolarised resting membrane potential of MSNs close to the potassium equilibrium potential (John and Manchanda, 2011; Nisenbaum et al, 1995). $K_{IR}$ currents stabilise

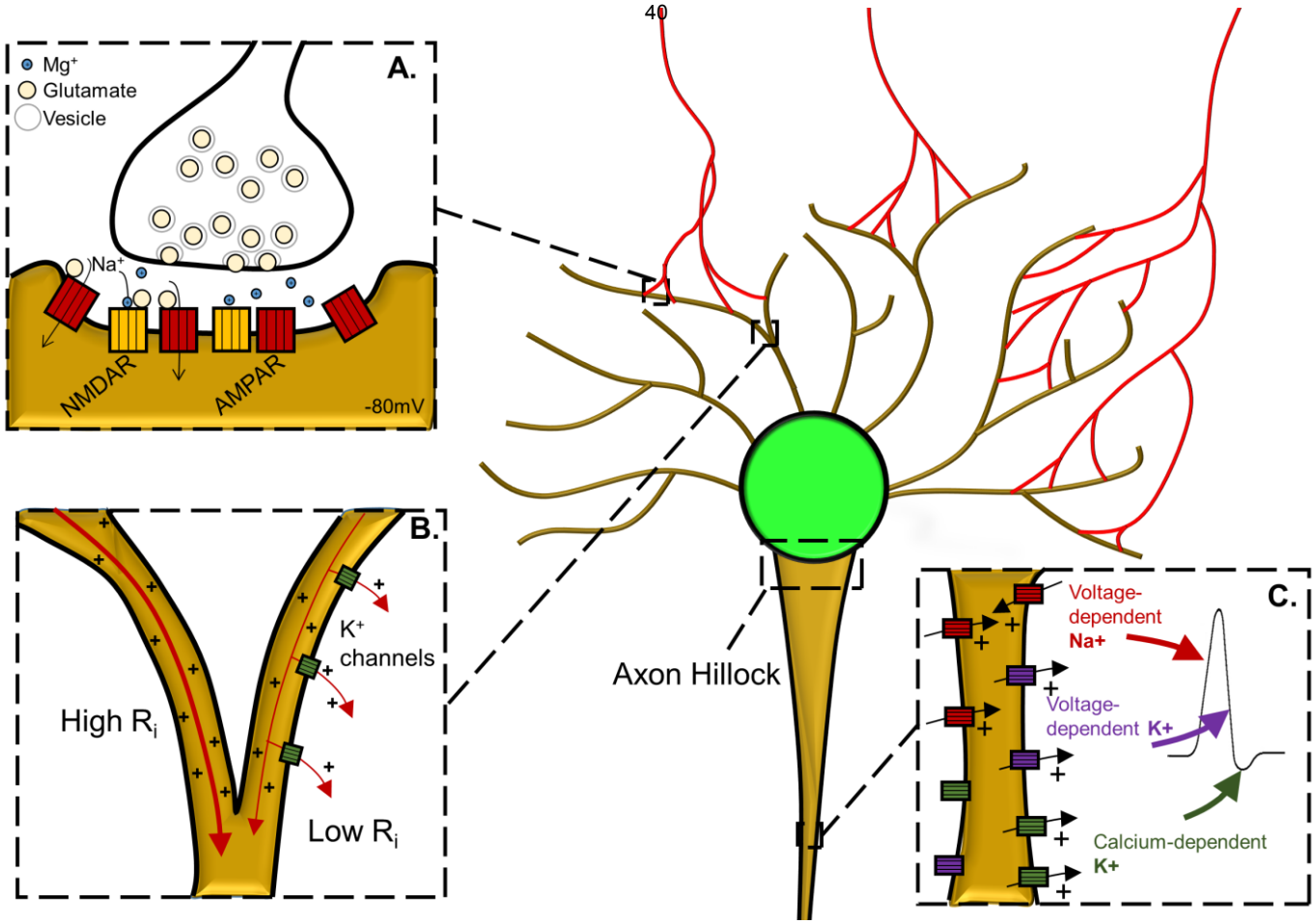


**Figure 3.** Intrinsic and synaptic physiology of the neuron. **A.** Glutamatergic synaptic transmission. Glutamate is packaged in vesicles and released from the presynaptic bouton into the synaptic cleft. The binding of glutamate to AMPA receptors (AMPARs) on the postsynaptic membrane results in positive sodium ($Na^+$) current (Glur2-lacking AMPARs may also carry a calcium current). At resting membrane potentials (e.g. -80mV in the nucleus accumbens), NMDA receptors (NMDARs) are blocked by positively charged extracellular magnesium. This block is removed following depolarisation of the membrane permitting a sodium *and* calcium current to flow though the NMDARs. Thus concurrent stimulation of AMPAR receptors (which depolarise the membrane) and NMDAR receptors (which are highly permeable to calcium) permit activation of calcium-dependent signalling pathways involved in regulation of neuronal plasticity.

**B.** Intrinsic excitability in the dendrite. Positive sodium or calcium currents flow from the synapse through the dendrite, towards the cell soma and axon hillock. In the dendrite and soma, potassium ($K^+$) channels permit the flow of potassium along its electrostatic gradient (outwards, due to the high intracellular concentration of potassium). Following excitatory synaptic input, currents activated by voltage-gated and leak $K^+$ channels carry an outward $K^+$ current, reducing the membrane voltage. This reduces the length constant of the dendrite and so limits the distance synaptic input can travel (low input resistance ($R_i$), right). If $K^+$ channels are closed or internalised, the resistance (and so length constant) of the membrane is increased (high input resistance, left).

**C.** Action potential (AP) kinetics are regulated by axonal ion channel function and expression. An action potential is generated when the activation threshold of voltage-gated sodium channels is reached at the axon hillock. Activation of voltage-gated sodium channels (red) lead the depolarisation phase of the AP (red arrow) and propagate the AP along the axon. Delayed voltage-dependent $K^+$ channels result in $K^+$ efflux and cause the repolarisation phase (purple arrow). Calcium -dependent $K^+$ channels underlie the hyperpolarisation phase in which $K^+$ efflux transiently brings the resting membrane potential close to the $K^+$ reversal potential (slightly more hyperpolarised than the resting membrane potential). Thus, the kinetics of all phases of the AP may be regulated by ion channel function and expression.

the resting membrane potential to the MSN downstate; following hyperpolarising current injection they pass an inward positive current, drawing the membrane potential towards $E_K$ and producing the MSNs characteristic inward rectification (John et al, 2011; Nisenbaum et al, 1995). Following depolarising current injections from rest (which is close to $E_k$), $K_{IR}$ channels do still pass outward current, stabilising the resting membrane potential (John et al, 2011; Nisenbaum et al, 1995; Shen et al, 2007) as such, inhibiting $K_{IR}$ has the effect of increasing MSN excitability (Luscher and Slesinger, 2010) (Figure 3B).

At depolarised potentials, $K_{IR}$ channels become effectively inactivated and potassium currents mediated through alternate channels dominate (Hibino et al, 2010). Outwardly-rectifying potassium currents are primarily carried by two types of channel, the family of A-type potassium currents and a relatively non-inactivating outward current (IKDR) (Hammond, 2014; Nisenbaum et al, 1995). At depolarised potentials these channels hyperpolarise the membrane in opposition of depolarising synaptic inputs and activation of voltage-gated $Na^+$ and $Ca^{2+}$ currents ($E_{Na}$: +40 mV, $E_{Ca,}$ +134 mV) (Bean, 2007; Nisenbaum et al, 1995). The opposition between these currents is the cause of the slow depolarizing ramp which is characteristic of MSNs (Nisenbaum et al, 1995). Additionally, the non-inactivating IKDR and fast-inactivating A-type currents contribute to the firing properties of MSNs and may play a role in their rhythmic, non-bursting firing pattern (Hammond, 2014).

The threshold of MSNs is regulated primarily by expression of voltage sensitive $Na^+$ currents at the axon initial segment (Cantrell, 2001, Zhang et al, 1998) while $Na^+$ and $K^+$ channels at the axonal nodes of Ranvier underlie spike firing kinetics. The afterhyperpolarisation (AHP) (both fast AHP (fAHP) and medium AHP (mAHP)) is regulated by a class of voltage-dependent calcium-activated $K^+$ currents (Volchis et al, 1999; Ishikawa et al, 2009) (Figure 3C).

### 1.2.3.3. Synaptic physiology of the striatum

#### *1.2.3.3.1. Ionotropic receptors*

##### *Glutamate receptors*

The α-amino-3-hydroxy-5-methyl-4-isoxazolepropionic acid (AMPA) and *N*-methyl-D-aspartate receptor (NMDA) receptors are tetrameric transmembrane proteins which mediate glutamate transmission across the brain (Figure 3A). The subunit families of AMPA (GluR 1-4) and NMDA receptors (GluN1-2) form heteromeric configurations and are subject to alternative splicing, conferring a high level of receptor diversity; as such excitatory transmission in the striatum is underlied by an complex array of receptor isoforms (Gotz *et al*, 1997; Kessels and Malinow, 2009; Nakanishi, 1992; Paoletti and Neyton, 2007). While both AMPA and NMDA receptors are predominately located postsynaptically, presynaptic and extrasynaptic receptors of each variant have been observed in the striatum (Bouvier *et al*, 2015; Ferrario *et al*, 2011; Fujiyama *et al*, 2004; Garcia-Munoz *et al*, 2015). Both AMPA and NMDA receptors are non-selective cation channels which pass $Na^+$ and $K^+$ with similar efficiency, reversing at approximately 0 mV, however the NMDA receptor is additionally permeable to $Ca^{2+}$ and also requires co-activation with glycine (Brog *et al*, 1993; Maki and Popescu, 2014). The most common AMPA receptor isoform contains the GluR2 subunit and are permeable only $K^+$ and $Na^+$, however GluR2-lacking AMPA receptors additionally pass $Ca^{2+}$ ( Voglis and Tavernarakis, 2006;  Man, 2011). Thus alterations in AMPA receptor subunit isoform expression and NMDA receptor function can confer significant changes in neuronal function and susceptibility to long-term plasticity through increased $Ca^{2+}$ permeability.

AMPA receptors mediate fast synaptic transmission, demonstrating rapid activation and desensitisation kinetics. AMPA receptor kinetics are dependent on subunit configuration, which varies widely across neuron types and subregions of the basal ganglia (for example, GluR2-lacking AMPA receptors posses increased single chancel

conductance (Man, 2011)), though deactivation kinetics are typically in the range of 1-10 ms (Gotz *et al*, 1997; Kleppe and Robinson, 1999). NMDA receptors exhibit a comparatively prolonged desensitisation, with time constants of >100 ms commonly observed (Kleppe *et al*, 1999). Additionally, NMDA receptors demonstrate a voltage-dependent activation due to block by extracellular $Mg^{2+}$ ions at hyperpolarised potentials; this ionic block dissociates with a time constant long enough to require prolonged depolarisation to activate the NMDA receptor (Blanke and VanDongen, 2009; Zhu and Auerbach, 2001). Thus, NMDARs are thought to be important co-incident detectors gating calcium entry events (Blanke *et al*, 2009).

Excitatory glutamate transmission is also carried by the tetrameric Kainate receptor, which is located both pre- and postsynaptically, though primarily mediates presynaptic transmission (Contractor *et al*, 2011). Kainate receptors demonstrate slower activation and deactivation kinetics than AMPA receptors, and are widely expressed in the striatum (Chergui *et al*, 2000). Kainate receptors regulate presynaptic transmission at both excitatory and inhibitory synapses, and are through to play an important role in stabilizing network function and in the facilitation of short and long-term potentiation (Contractor *et al*, 2011).

### *GABA receptors*

GABA ionotropic receptors ($GABA_A$ class) are transmembrane heteromeric pentamers, in their most common configuration consisting of 2 α, 2 β and a single γ or ϵ /δ subunit. Similar to glutamate receptors, $GABA_A$ receptors are also subject to alternative slicing and RNA editing, permitting a large variation of receptor configurations; indeed, single neurons containing up to 8 isoforms of $GABA_A$ receptor have been observed (Sigel and Steinmann, 2012). GABA receptors are selectively permeable to $Cl^-$ anions, reversing close to the $Cl^-$ reversal potential ($E_{Cl}$ = ~ -60mV) (Czubayko *et al*, 2002). In contrast to glutamatergic receptors, the reversal potential of $GABA_A$ receptors is highly dynamic

and can be modulated following learning, profoundly altering receptor function (Staley and Smith, 2001).

Synaptic GABAergic transmission is mediated by γ -containing receptors; in the striatum, the primary configuration of synaptic GABA receptor is $\alpha_2$, β, and $\gamma_2$ (Pirker *et al*, 2000). In contrast, δ subunit containing receptors are located peri- or extrasynaptically and mediate tonic inhibition. Synaptic $GABA_A$ receptors show faster intrinsic kinetics than extrasynaptic receptors, desensitizing rapidly following GABA application (Mtchedlishvili and Kapur, 2006). Extrasynaptic receptors desensitize slowly and are sensitive to low GABA concentrations (Liang *et al*, 2008). Thus extrasynaptic $GABA_A$ receptors are sensitive to ambient GABA in the extracellular space (Brickley and Mody, 2012). Both synaptic and extrasynaptic $GABA_A$ receptors are present in the striatum, thus providing both tonic inhibitory tone alongside fast synaptic inhibition.

Glycine receptors are pentameric receptors which also mediate fast synaptic chloride transmission and are sensitive to the amino acid neurotransmitter glycine (Cascio, 2004). They are present in striatal MSNs and cholinergic interneurons (Sergeeva *et al*, 2002) and have been shown to mediate synaptic depression (Chen *et al*, 2011). This means that the amino acid glycine is important for both the regulation of long-term potentiation (LTP) through action at the NMDA receptor, as well as synaptic depression through its activation of endogenous glycine receptors.

### *Integration of ionic synaptic transmission in MSNs*

In addition to intrinsic factors and synaptic receptor physiology and expression, synaptic integration in MSN dendrites is regulated by dendritic neurotransmitter receptor dynamics and shunting inhibition from tonically active GABAergic currents. Tonically active extrasynaptic GABA α4 receptors function to shunt positive current at the dendritic level, modulating synaptic gain (Prescott and De Koninck, 2003) and providing compartmentalisation of calcium signals between dendritic spines, which

reduces the summation of asynchronous excitatory postsynaptic currents (EPSCs) (Carter *et al*, 2007; Higley, 2014). Thus the physiology of MSN dendrites is such that synchronous excitatory activity is potentiated, with synchronous activity at multiple MSN spines summating supralinearly due to activation of NMDA receptors and L-type calcium channels. In contrast, repetitive activity at a single spine, or asynchronous activity across multiple spines, summate sublinearly or linearly respectively, due to AMPA receptor desensitisation and dendritic compartmentalisation of calcium signals (Carter *et al*, 2007). Thus transmission through striatal MSNs may bias concurrent inputs and filter out non-synchronous activity.

#### *1.2.3.3.2. Metabotropic receptors*

##### *Metabotropic glutamate and GABA receptors*

Metabotropic receptors are a class of receptor impermeable to ions but which modulate neuronal responses through intracellular second messenger systems (Pin and Duvoisin, 1995). G-coupled protein receptors (GPCRs) are the largest class of metabotropic receptor, characterised by a 7 transmembrane domain structure and functional coupling to guanine nucleotide-binding effector proteins (G proteins) (Kobilka, 2007). G-proteins form heteromeric complexes of α, β and γ subunits with function dictated by the binding profile of the α isoform; $G_{\alpha s}$ leads to phosphorylation of cyclic adenosine monophosphate (cAMP) through activation of adenylyl cyclase (AC), $G_{\alpha i}$ reduces phosphorylation of cAMP through AC, and activation of a $G_q$ isoform leads to activation of the phosphatidylinositol 4,5-bisphosphate ($PIP_2$) pathway (Kobilka, 2007; Ralevic and Burnstock, 1998). Through these pathways, GPCRs can regulate function and expression of ionic channels through phosphorylation and endo/exocytosis, including of both potassium and sodium channels and ionic receptors (Pin *et al*, 1995) .

Metabotropic glutamate receptors (groups mGluR1-3) are pre-, post- and extrasynaptically located and mediate excitatory $G_{\alpha s}$ signalling in medium spiny neurons. Similar to ionic receptors, metabotropic glutamate receptors exist in many genetically encoded and alternatively sliced isoforms and as such confer significant heterogeneity to the mechanisms of excitatory transmission. mGluR activation is usually associated with decreases in synaptic excitability; for example mGluR1 activation may result in the replacement of GluR2-lacking AMPA receptors with GluR2-containing receptors, decreasing synaptic strength (Bellone and Luscher, 2005). Interestingly, GABAergic metabotropic receptors ($GABA_B$) do not display such variation in receptor subtypes and consist of only three isoforms ($GABA_{B1(a)/(b)}$ and $GABA_{B2}$) which form functional $GABA_{B1}$/$GABA_{B2}$ heteromers; $GABA_{B1a}$-contaning receptors are expressed significantly in the striatum. $GABA_B$ receptors are $G_{\alpha i}$ coupled and as such function to reduce excitation by inhibiting the adenylyl cyclase/cAMP pathway (Ulrich and Bettler, 2007).

In addition to these primary neurotransmitter systems of the striatum, neuromodulators such as dopamine, 5-hydroxytryptamine (5-HT) and acetylcholine also act on distinct GPCR, their function determined by subunit isoform (Barnes and Sharp, 1999; Levey *et al*, 1991; Ward and Dorsa, 1996).

### *Dopamine Metabotropic Receptors*

Dopamine acts exclusively upon metabotropic receptors. A primary distinction is made between dopamine D1 and D2 receptor isoforms (D1R and D2R, respectively). While D1 are $G_{\alpha s}$-coupled and located postsynaptically, D2 receptors are $G_{\alpha i}$ coupled and may be pre- or postsynaptically located (Beaulieu and Gainetdinov, 2011). Both D1 and D2 receptors are expressed in the striatum, however their expression is generally exclusive to two different subtypes of MSNs, which show additional differences in physiology and efferent projection patterns (Gertler *et al*, 2008; Smith *et al*, 2013).

D1R-expressing neurons stain positive for dynorphin and substance P, while D2 neurons stain positive for enkephalin and neurotensin. Physiologically, D2 neurons are intrinsically more excitable than D1 neurons in both the ventral and dorsal striatum (Francis *et al*, 2015; Gertler *et al*, 2008; Smith *et al*, 2013). As dynorphin and enkephalin both act upon opioid receptors, these two neuron subtypes can differentially mediate intra-accumbens opiate transmission. In the dorsal striatum, but not ventral striatum, these two neuronal populations also differ in their basal ganglia connections (Smith *et al*, 2013).

#### *1.2.3.3.3. Receptor transduction pathways*

Activation of G-protein coupled receptors (GPCRs), or calcium influx through ionotropic receptors and ion channels, can modulate neuronal physiology through interactions with complex intracellular signalling cascades. These include the cAMP pathway (activated by $G_{\alpha s}$ and $G_{\alpha i}$ transduction pathways), the calmodulin/ Ca2+ -dependent protein kinase II (CaMKII) pathway (activated by increases in intracellular calcium), and the $PIP_2$ pathway (activated by $G_{\alpha}$ subunits) (Kandel, 2012; Nestler, 2001; Wong *et al*, 2005). While these molecular pathways are usually presented as distinct, there is significant cross-talk between them with important functional consequences (Impey *et al*, 1998).

##### *cAMP pathway*

GPCRs mediate neuronal physiology by regulation of the protein adenylyl cyclase through $G_{\alpha s}$/$G_{\alpha i}$ proteins, which activate and inhibit AC respectively (Pin *et al*, 1995). AC functions to phosphorylate the second messenger cAMP, which is an effector of many signalling proteins, including protein kinase A (PKA). While PKA may phosphorylate voltage and ligand-gated ion channels directly affecting their function, it

is also a kinase of the transcription factor cAMP response element-binding protein (CREB), which once phosphorylated, binds specific cAMP response elements (CRE) of target genes leading to their expression (Esteban *et al*, 2003; Kandel, 2012; Nestler, 2001; Pin *et al*, 1995; Sassone-Corsi, 2012). CRE binding sites lay upstream of an array of genes involved in the regulation of cell physiology, including expression of membrane channels and proteins involved in the formation of new synaptic connections. Thus through direct phosphorylation of membrane receptors and ion channels as well as phosphorylation of CREB, the cAMP pathway is well placed to play an important role in learning and memory (Dong *et al*, 2006; Kandel, 2012; Nestler, 2001).

### *Calcium-activated transduction pathways*

Transient increases in intracellular calcium can be achieved through activation of NMDA receptors, GluR2 lacking AMPA receptors, release of buffered calcium from intracellular stores and through voltage-gated calcium channels (Voglis *et al*, 2006; Warren *et al*, 2010; Wong *et al*, 2005). Increases in intracellular calcium levels are detected by the calmodulin protein, which gates the autophosphorylation of CaMKII. When sufficient $Ca^{2+}$/calmodulin levels are reached, CaMKII phosphorylates itself in a manner which allows it to remain active even when intracellular calcium levels are decreased to baseline (Giese and Mizuno, 2013). CaMKII is a protein kinase with diverse functional roles, and is able to both regulate voltage and neurotransmitter-gated ion channels directly, and additionally activate CREB through calcium-dependent ribosomal s6 kinase **(**RSK), which phosphorylates CREB at a separate site to PKA (Cruz *et al*, 2013; Kandel, 2012). Additionally, calmodulin can also activate the extracellular signal–regulated kinase (ERK)/ mitogen-activated protein kinases (MAPKs) pathway, which can also regulate CREB activity (Giese *et al*, 2013). Thus activation of NMDA receptors or calcium permeable AMPA receptors may influence

learning and memory-dependent processes through permitting increases in intracellular calcium levels (Giese *et al*, 2013; Voglis *et al*, 2006).

*$PIP_2$ pathway*

Many GPCRs are coupled to $G_q$ receptors, which do not mediate their effects through adenylyl cyclase but rather affect the phospholipid signalling molecule $PIP_2$ (Simonyi *et al*, 2005; Wong *et al*, 2005). $PIP_2$ hydrolysis is mediated by $G_q$ through phospholipase C, and leads to the production of diacylglycerol (DAG) and triphosphoinositol **(**$IP_3$). DAG is a signalling molecule which can activate protein kinase C (PKC), which has important roles in learning and memory, while $IP_3$ can lead to transient increases in calcium level by binding the $IP_3$ receptor releasing intracellular calcium stores (Wong *et al*, 2005). Additionally, $PIP_2$ may directly influence cell excitability through modulation of voltage-gated potassium channels (Loussouarn *et al*, 2003). Thus $G_q$ receptors are able to regulate cell physiology though the $PIP_2$ pathway (Simonyi *et al*, 2005).

## 1.2.4. Anatomy, physiology and function of additional motivational system areas

### 1.2.4.1. The basal ganglia

The basal ganglia are an interconnected set of subcortical nuclei consisting of the striatum, the ventral pallidum (VP), globus pallidus (GPi (entopeduncular nucleus in rodents), globus pallidus externus (GPe) (globus pallidus in rodents), substantia nigra pars reticula and the subthalamic nucleus (Alexander *et al*, 1986; Smith *et al*, 2009). The thalamus, though not a BG structure, is the primary output relay of the network. The BG receives significant inputs from a number of limbic and motor regions, which are converged through parallel looping circuits maintained throughout the entire basal ganglia and its efferent connections (Voorn *et al*, 2004).

### *Connectivity of the basal ganglia*

The striatum is considered the input nucleus of the basal ganglia (Alexander *et al*, 1986; Lanciego *et al*, 2012) and projects in a subregion-specifc manner to downstream BG areas. A primary BG target of the ventral striatum is the ventral pallidum. The VP also receives direct projections from many limbic brain areas, including the medial prefrontal cortex, amygdala, lateral hypothalamus and ventral tegmental area, to which it forms reciprocal connections (Perry and McNally, 2013; Smith *et al*, 2009). In turn, the VP projects to the thalamus, the primary output of the basal ganglia, which projects back to the areas providing the original striatal afferents, thus maintaining the classic BG loops (Alexander *et al*, 1986; Groenewegen *et al*, 1993; Lazarus *et al*, 2012).

GABAergic neurons in the BG may be distinguished based on their expression of D1- or D2-receptors. In the dorsal striatum, D1R neurons project to the globus pallidus internus and SNr, while D2R MSNs project first to the globus pallidus externus, which in turn targets the GPi/SNR through the STN. The GPi/SNR sends GABAergic efferents to the thalamus (which relays BG output through glutamatergic projections directed across the brain). As such, activation of the D1 pathway leads to disinhibition of the thalamus from the GPi/SNr, while activation of the D2 pathway leads to inhibition of the thalamus through the “indirect” GPe-STN-GPi/SNR pathway (Alexander *et al*, 1986; Smith *et al*, 2013; Smith *et al*, 1998). Thus, D1R activation leads to an increase in the excitatory output of the BG, while D2R activation leads to a decrease. In contrast, D1R and D2R-expressing MSNs of the ventral striatum do not differentially project to downstream BG targets (Kupchik *et al*, 2015; Smith *et al*, 2013).

### *Physiology and function of the basal ganglia*

Basal ganglia projection neurons are primarily GABAergic, with the exception of the glutamatergic projections of the thalamus and subthalamic nuclei. The physiology of GABAergic projection neurons and ratio of primary to interneuron cell type is highly

variable through the basal ganglia. For example, the VP consists of approximately 20% cholinergic interneurons (compared to ~5% in the striatum) with GABAergic projection neurons that are characterised by high-frequency firing compared to striatal MSNs (Bengtson and Osborne, 2000; Smith *et al*, 2009). The SNr however, functions to constitutively inhibit the thalamus, as such its GABAergic neurons are tonically active (MacLeod *et al*, 1980; Zhou and Lee, 2011).

Similar to the striatum, basal ganglia nuclei are involved in encoding both motor and limbic processes. Everitt *et al* (1987) demonstrated that lesions to both the VP and globus pallidus disrupt acquisition and expression of a conditioned discrimination task, in which a specific cue signalled the position of an active lever. The globus pallidus also sends projections to the lateral habenula which fire in a manner based on the expectation of reward size gained from presentations of reward-predicting or reward-omission predicting cues (Hong and Hikosaka, 2008).

The SNr appears also to play a role in appetitive learning; infusion of dopamine antagonists to the SNr disrupt psychostimulant sensitisation, while neurons of the SNr selectively alter firing rates during reward delivery and response execution during instrumental responding for food rewards (Gulley *et al*, 2002; Stewart and Vezina, 1989). BG nuclei which receive preferential inputs from the ventral striatum appear to play a particularly important role in motivated behaviours and reward learning. The ventral pallidum for example, is particularly unique as a BG nucleus in that is has been shown to contain “hotspots” which differentially encode either the hedonically or incentivising properties of reinforcing stimuli (Smith *et al*, 2009).

### 1.2.4.2. Prefrontal cortex (PFC)

*Connectivity of the PFC*

The prefrontal cortex can be broadly divided into the medial anterior cingulate (ACg) and ventral prelimbic and infralimbic cortices, the lateral insular regions (dorsal and ventral agranular), and the ventrolateral and ventromedial medial orbital cortices (OFC) (Dalley *et al*, 2004; Ongur and Price, 2000). The prefrontal cortex makes significant projections across the brain, including to the premotor cortices, sensory cortices (including somatosensory, auditory, visual and olfactory areas) as well as subcortical areas such as the hippocampus, amygdala, striatum, and the neuromodulatory VTA, basal forebrain cholinergic projection, raphe nucleus and locus coeruleus. The PFC projections to the striatum are of note as they are not reciprocal, but instead the PFC receives input from the BG though its thalamic output, forming cortico-striatal-thalamic loops, as discussed above (Carr and Sesack, 2000; Conde *et al*, 1995; Dalley *et al*, 2004; Kolb, 1984; Sesack *et al*, 1989).

Prefrontal subregions are distinguishable based on their efferent and afferent connections, with more dorsomedial prefrontal areas (including the anterior cingulate and dorsal prelimbic areas) projecting preferentially to sensory and motor cortices, with ventral areas (orbital, infralimbic, ventral prelimbic cortices) projecting to limbic areas, including the hippocampus, amygdala and ventral striatum. Additionally, more dorsal and ventral areas are more significantly interconnected to their neighbouring areas than they are to more distal PFC areas (Heidbreder and Groenewegen, 2003; Uylings *et al*, 2003).

*Physiology and function of the PFC*

The primary output neurons of the PFC are glutamatergic pyramidal cells, which are characterised by their depolarised resting membrane potential (~ -60 mV) and

reception of significant axon collaterals from surrounding pyramidal neurons. These characteristics make cortical pyramidal neurons more excitable than other neuron types, such as striatal MSNs. PFC pyramidal neurons are organised in a laminar fashion with different connectivity patterns across layers. Layer I does not contain many cell bodies but consists mainly of the dendritic projections of deeper cortical layers. Layers II and III project mainly to other cortical areas while layer V projects primarily to the striatum and VI to the thalamus (Gabbott *et al*, 2005; Kawaguchi and Kubota, 1997). Unlike medium spiny neurons, pyramidal neurons demonstrate a significant heterogeneity in morphology and firing patterns (van Aerde and Feldmeyer, 2015). Additionally, a wide variety of GABAergic interneurons are present in the PFC, making significant axonal arborisations to many surrounding pyramidal neurons permitting tight regulation of network function (Kawaguchi *et al*, 1997).

Lesions to the prefrontal cortex cause dysfunction in behavioural planning and sequencing, response inhibition, learning and memory and social behaviours (Kolb, 1984; Uylings *et al*, 2003). Thus, the PFC is well positioned to play an important role in the regulation of motivated behaviours and reward learning. The OFC is a prefrontal brain area particularly important in the encoding of food and drug rewards and associated cues. Specifically, the OFC appears to play a particularly important role in outcome representation and updating reward expectancy. As such, lesions of the OFC retard acquisition of Pavlovian approach behaviours (in which the reward outcome associated with cue presentation is increased) but has no effect on the expression of approach behaviours to cue presentations (when outcome values are unchanged) (Chudasama and Robbins, 2003). Studies from reversal learning paradigms, in which CS+ and CS- contingencies are reversed (so that CS- comes to predict reward delivery), suggest OFC neurons responding to the CS track associated outcomes (Stalnaker *et al*, 2015). In line with these observations, lesions of the OFC inhibit both reversal learning and the effects of outcome devaluation (Chudasama *et al*, 2003;

Pickens *et al*, 2005; Schoenbaum *et al*, 2003). Thus the PFC including the OFC subregion appears to play an important role in appetitive associative learning.

### 1.2.4.3. The hippocampus

The anatomy of the hippocampus is highly specialised, forming a characteristic looping cytoarchitecture in which the entorhinal cortex region functions as both the primary input and output. The entorhinal cortex (EC) sends axons through the mossy fibre tract to the dentate gyrus, which projects to the CA3 region of Ammon's horn (or CA: *Cornu Ammonis)*. CA3 in turn sends axons through the Schaffer collateral pathway to the CA1 region, which itself projects back out to the entorhinal cortex via the subiculum (Amaral and Witter, 1989). However, the hippocampus is not a closed loop system and its subregions project individually across the brain. The hippocampus is connected to a number of limbic and sensory brain regions, including the striatum, prefrontal cortex, amygdala, hypothalamus as well as from sensory, especially visual, cortices (Fanselow and Dong, 2010; Lavenex and Amaral, 2000) and is modulated by serotonin, dopamine, acetylcholine and noradrenaline (Freund and Buzsaki, 1996). The hippocampus can be anatomically and functionally divided along it's posterior/anterior axis (or homologous dorsal/ventral axis in rodents) (Fanselow *et al*, 2010).

The primary cell types of the hippocampus are glutamatergic and include: the stellate cells of the EC, granule cells in the dentate gyrus and pyramidal neurons of the CA1 and CA3. These primary neurons are characterised by high degree recurrent connectivity (Amaral, 1978) and are regulated by GABAergic interneurons such as the chandelier and basket-type cells (Freund *et al*, 1996). Functionally, the hippocampus is known to pay an important role in associative conditioning for both food and drug rewards. Lesion studies suggest that while Pavlovian conditioning to a discrete cue is independent of the hippocampus, the hippocampus mediates contextual associative learning processes underlying Pavlovian and instrumental behaviours (Honey and

Good, 1993; Ito *et al*, 2006; Ito *et al*, 2008). The hippocampus sends significant glutamatergic projections to the nucleus accumbens (Britt *et al*, 2012) and may gate the up-state/down-state of medium spiny neurons (Wilson *et al*, 1996). Thus hippocampal gating of inputs to MSNs from other brain areas may act as an “occasion setter” during associative and conditioned behaviours (Holland, 1992). The hippocampus is also necessary for drug-context dependent conditioned behaviours such as context-dependent reinstatement and drug-place preference (Atkins *et al*, 2008; Raybuck and Lattal, 2014).

### 1.2.4.4. The amygdala

The amygdala is comprised of six separate nuclei, two of which are thought to be particularly important in learning processes: the central amygdala (CeA) and the BLA (Cardinal *et al*, 2003). The BLA is highly interconnected with other limbic brain areas, sending efferent connections to the nucleus accumbens and CeA while being reciprocally connected to the medial PFC, anterior cingulate cortex and hippocampus (Janak and Tye, 2015; Ottersen, 1982; Sripanidkulchai *et al*, 1984). The BLA consists of primary glutamatergic pyramidal neurons while the CeA projection neurons are GABAergic (Janak *et al*, 2015). The CeA projects to mid-brain regions including the central medial nucleus of the thalamus, the hypothalamus and locus coeruleus and raphe nuclei, and the dopaminergic SNc and VTA (Ito *et al*, 2008; Janak *et al*, 2015; Lee *et al*, 2010; Ottersen, 1982).

While the BLA is widely involved in a number of important appetitive behaviours, lesion studies suggest the CeA appears to be specifically involved in Pavlovian approach conditioning. BLA lesions however appear to have no effect on approach conditioning, and may be more important in instrumental appetitive procedures (Everitt *et al*, 2000; Ito *et al*, 2008; Parkinson *et al*, 2000a). The functioning of the BLA is also important in the expression of drug-reinforced behaviours; lesions to the basolateral amygdala

impair second-order schedule of cocaine reinforcement and reduce cue-induced reinstatement (Meil and See, 1997; Whitelaw *et al*, 1996).

*VTA/SNc*

Dopaminergic transmission throughout the entire brain originates primarily from two midbrain nuclei, the ventral tegmental area and substantia nigra pars compacta. Dopaminergic projections to the cortex and limbic structures originate in the VTA; the mesolimbic pathway projects from the VTA to the NAc shell/core, amygdala and hippocampus while the mesocortical pathway projects from the VTA to the prefrontal cortex. The nigrostriatal pathway however originates in the SNc and projects sparsely to the NAc core (Ikemoto, 2007) and more significantly to the dorsal striatum (Arias-Carrion *et al*, 2010). The dopamine system contains only a small number of neurons, but these neurons make extensive projections with extensive axonal arborisations, with some DA neurons observed to contain up to 500,000 release sites (Andén *et al*, 1966). Interestingly, some DA projections to the striatum have been observed to co-release glutamate or GABA (Stuber *et al*, 2010; Tritsch *et al*, 2012).

Dopamine neurons fire tonically, however phasic firing is induced by synaptic drive in response to presentation of appetitive US, while tonic rates of firing may decrease following exposure to an aversive reinforcer (Tsai *et al*, 2009; Ungless *et al*, 2004). Thus dopaminergic neurons may directly encode the valence of a US (McCutcheon *et al*, 2012). Similarly, dopamine is thought to encode an error prediction signal – *in* vivo electrophysiological recordings have demonstrated that while DA neurons initially increase their firing rate to a reward, following conditioning this increase in firing shifts to the CS (Schultz *et al*, 1997). If a CS conditioned to predict a reward is followed by omission of the reward, a decrease in basal firing is observed. As such, the VTA and SNc have been implicated in a wide range of conditioned behaviours to both drugs of

abuse and natural rewards (Arias-Carrion *et al*, 2010; Berridge and Robinson, 1998; Oliva and Wanat, 2016; Stuber *et al*, 2010).

# 1.3. Neuroadaptations involved in the encoding of associative memory: selectivity for behaviourally relevant ensembles

## 1.3.1. Neuroadaptations associated with the encoding of associative memory

### 1.3.1.1. Early theories of learning-induced neuroadaptations and their experimental support

The idea that experience-induced alterations to the structure of the brain could occur during adulthood was not well accepted for most of the 20$^{th}$ century, despite its current ubiquity (Kolb *et al*, 2003). However, an early proponent of this notion was Karl Lashley, who lesioned the cortex of rats and noted the effect on reinforced maze learning. Lashley observed that the size (but not location) of the lesion was crucial to the extent of any behavioural deficits and the ability to retain future learning. His assertion that memories were not located in distinct brain regions but were distributed across the cortex, and could be regained following injury, was in contrast to the prevailing “reflex theory” of the period. This posited that cerebral functioning was similar to that of spinal reflexes, making use of pre-existing neuronal connections (Lashley, 1930). Other theorists such as the Polish psychologist Jerzy Konorski, who trained under Ivan Pavlov and coined the term “neuronal plasticity”, suggested that discrete changes in connectivity between specific neurons may underlie conditioned

responses (Konorski, 1948). Similarly, Donald Hebb (Hebb, 1949) posited that learning experiences may be accompanied by changes in the weighting between specific sets of relevant neurons. However, despite the foresight of these early theorists, conclusive experimental support would not be available for the next few decades.

The first explicit evidence that associative learning could strengthen the connections between behaviourally relevant neurons came from invertebrate preparations. The accessible nature and limited anatomical complexity of many invertebrates permits identification and measurement of neuronal circuits directly underlying conditioned behaviours (Krasne and Glanzman, 1995). For example, in the sea slug *Aplysia,* a light physical tap to the siphon (CS) elicits slow withdrawal of the siphon and gill, whereas an electric shock to the tail (US) evokes rapid gill withdrawal. Pairing the CS with the US leads to the CS later eliciting a conditioned rapid gill withdrawal which may be retained for days, while unpaired CS-US presentations have no such effect (Carew *et al*, 1972). This conditioned response is encoded by a relatively simple neuronal circuit in which activation of sensory neurons in the tail (US) is able to facilitate presynaptic transmission from the siphon-sensory neuron (CS) onto the motor neurons underlying the gill withdrawal reflex (CR) (Hawkins *et al*, 1983).

The facilitation of presynaptic transmission from the CS pathway onto the gill withdrawal motorneurons requires concurrent neural activity through the CS and US pathways. Adenylyl cyclase appears crucial for co-incidence detection in the presynaptic bouton of the CS pathway. AC is activated by $Ca^{2+}$ entry during CS-activated spiking, as well as $G_{\alpha s}$-pathway activation by a neuromodulatory neuron along the US-activated pathway. When CS-US signalling occurs concurrently, AC is activated sufficiently to elicit cAMP production to levels permitting long-term presynaptic adaptations. These lead to increased neurotransmitter release, through mechanisms such as the phosphorylation of proteins involved in vesicle exocytosis (Kandel, 2012). Furthermore, activation of NMDA receptors in the postsynaptic

membrane, dependent on presynaptic stimulation alongside postsynaptic depolarisation, leads to signalling through the CaMKII pathway. This results in the insertion of functional AMPA receptors into the postsynaptic membrane, facilitating CS transmission onto CR motorneurons (Hawkins and Byrne, 2015; Kandel, 2012).

These studies give a detailed insight into the complex neurobiological processes underlying associative conditioning. Invertebrate preparations have also been used to investigate the neuroadaptations which occur following appetitive learning. For example, single-trial appetitive conditioning in the freshwater snail *Lymnaea stagnalis* can be used to associate a neutral chemical (CS) with sucrose (US), eliciting fictive feeding (CR) following CS presentation. Persistent depolarisation in the resting membrane potential of modulatory 5-HT neurons which facilitate the CR result in axonal depolarisation and increased presynaptic calcium levels, facilitating action-potential dependent release of serotonin. These intrinsic changes are delayed following conditioning and appear over a time course suitable to the encoding of long-term memory (Kemenes *et al*, 2006). This suggests that the intrinsic excitability of neurons can be persistently regulated by appetitive conditioning in a manner which facilitates the expression of conditioned responses.

Thus, over 80 years since Pavlov discovered appetitive conditioned reflexes in the dog, direct observation of neuron to neuron facilitation in circuits *directly* underlying conditioned responses have been observed in invertebrate preparations.

### 1.3.1.2. Synaptic adaptations following associative learning in mammals

Activity-dependent potentiation of neuron to neuron transmission in mammals was first observed at hippocampal synapses by Bliss and Lomo (1973). Using *ex vivo* extracellular recording in the hippocampus of the rabbit, they stimulated the perforant pathway of the hippocampus while recording the target neuronal population in the

dentate gyrus. They observed that a high-frequency stimulation of the perforant pathway potentiated dentate gyrus EPSCs above baseline levels, for up to 10-12 hours. Since this observation, LTP at the perforant pathway has been extensively characterised, and is thought to be dependent on $Ca^{2+}$ entry through NMDA receptors and the downstream activation of CaMKII (Malenka and Nicoll, 1999). Activation of CaMKII leads to AMPA receptor insertion into the postsynaptic membrane, potentiating synaptic transmission. LTP has also been demonstrated in many other brain areas, including the striatum (Schotanus and Chergui, 2008b; Xu *et al*, 2010). These alternate forms of LTP may also be dependent upon activation of metabotropic receptors; in the nucleus accumbens, induction of LTP is also sensitive to dopamine receptor activity (Schotanus and Chergui, 2008a). While the LTP induction protocol is a useful model for studying *in vitro* neuronal plasticity, it is difficult to observe directly as a consequence of learning in living animals. As such, investigations into LTP following in associative learning in mammals have typically searched for specific alterations associated with the expression of LTP following learning, rather than measuring it directly.

### *A role for NMDARs and GPCRs in conditioned responding*

Activation of both NMDA and G-coupled protein receptors has been shown to be important for the acquisition and expression of conditioned responses. Parker *et al* (2011) observed perturbed acquisition of Pavlovian approach behaviours in transgenic mice exhibiting NMDAR knockout selective for D1R-expressing MSNs (Parker *et al*, 2011). Dalley *et al* (2005) demonstrated that infusion of NMDAR and D1R antagonists in the NAc immediately following acquisition of Pavlovian approach behaviours disrupted consolidation of the memory, retarding learning. While both the acquisition and consolidation of these Pavlovian responses appear dependent on D1R/NMDAR transmission in the NAc, consolidation of instrumental responding appears unaffected by antagonist application (Hernandez *et al*, 2005), suggesting that different learning

processes may be modulated distinctly by intracellular signalling cascades. NMDA and metabotropic receptors are also important for the expression of conditioned responses to drug reinforcers, such as cue-induced reinstatement of drug seeking (Backstrom and Hyytia, 2007; Kumaresan *et al*, 2009) and conditioned place reference (Huang *et al*, 2016; Ma *et al*, 2006).

Supporting a role for NMDAR/GPCRs in associative learning, their downstream targets also play a functional role in the encoding of associative memories. The signalling cascades ERK (NMDA/calcium-pathway mediated) and PKA (GPCR/ cAMP-pathway mediated) are both necessary for the expression of conditioned responses to both natural and drug rewards (Baldwin *et al*, 2002; Shiflett and Balleine, 2011; Sutton *et al*, 2000; Tropea *et al*, 2008). These pathways are known to modulate synaptic function through the expression of new proteins; in line with this, protein synthesis in the NAc is necessary for both consolidation of appetitive instrumental learning (Hernandez *et al*, 2002) and reconsolidation of a cocaine-context association (Bernardi *et al*, 2007). These studies suggest that both NMDA and metabotropic receptor activation following learning elicits downstream target activation and protein synthesis necessary for the expression of conditioned behaviours.

### *Synaptic neuroadaptations observed following conditioned responding.*

A functional consequence of NMDAR/GPCR activation associated with LTP is increased synaptic transmission. Synaptic strength may be increased through postsynaptic modifications (e.g. endocytosis of AMPA receptors) as well as presynaptic modifications (increased probability of neurotransmitter release).

Synaptic strength can be assayed at excitatory synapses by measuring the AMPA receptor (AMPAR) to NMDA receptor (NMDAR) ratio within a given neuron (Ungless *et al*, 2001); an increase in the AMPAR/NMDAR ratio is taken to suggests an increase in

synaptic strength. Changes in AMPAR/NMDAR ratios have been observed in dopamine neurons following appetitive Pavlovian conditioning with food reinforcers (Stuber *et al*, 2008) and in the NAc following drug sensitisation regimes (Thomas *et al*, 2001). Interestingly, AMPAR/NMDAR ratios in the VTA and NAc are differentially regulated by drug exposure. A single cocaine injection transiently increases the AMPAR/NMDAR ratio of VTA dopamine neurons for approximately 1 week, while in the NAc a decrease in AMPAR/NMDAR ratio of MSNs is observed further into the withdrawal period (approximately 10-14 days). Prolonged drug administration may cause long-lasting increases and decreases in the synaptic strength of VTA and NAc neurons, respectively (Thomas, 2001; Ungless et al, 2001; Kourrich, 2007; Luscher and Malenka, 2011). Brown *et al* (2010) observed that optogenetic stimulation of dopamine neurons alone can lead to increased AMPA receptor expression in the VTA through a D1R-dependent mechanism (Brown *et al*, 2010). Similarly, D1R receptor stimulation leads to an increase in membrane-bound AMPA receptors in NAc neurons through a PKA-dependent mechanism (Mangiavacchi and Wolf, 2004). These findings suggest that appetitive conditioning may lead to complex regulation of synaptic strength due to changes in functional AMPA receptor expression in the postsynaptic membrane, possibly through a dopamine-dependent mechanism.

In addition to insertion of AMPA receptors from the synaptic membrane, synaptic strength can also be regulated by direct phosphorylation of AMPA receptors. Crombag *et al* (2008b) generated a transgenic mouse line in which CaMKII ($ser^{831}$) and/or PKA ($ser^{845}$) phosphorylation sites on GluR1 subunits were disrupted. While phosphorylation at these sites was not necessary for the acquisition of Pavlovian approach behaviours, CaMKII but not PKA phosphorylation of GluR1 was necessary for the expression of instrumental responding for presentation of the sucrose-associated CS (conditioned reinforcement). Phosphorylation of GluR1 at $ser^{831}$ selectively increases the conductance of GluR2-lacking, GluR1 homomeric AMPA receptors (Guire *et al*, 2008),

suggesting precise modulation of excitatory synapses in a manner which potentiates $Ca^{2+}$ entry may be required for the expression of some conditioned behaviours.

The formation of new synapses has been observed following drug administration and sensitisation, food ingestion and appetitive conditioning (Crombag *et al*, 2008a; Geinisman *et al*, 2001; Li *et al*, 2004; Liu *et al*, 2016). Increasing the number of synaptic connections between specific sets of neurons is a potential mechanism by which synaptic transmission may be facilitated. Johnson *et al* (2016) visualised synaptic bouton turnover in the axons of OFC neurons projecting to the medial prefrontal cortex using *in vivo* 2-photon (2P) microscopy (using viral expression of enhanced green fluorescent protein (EGFP) in the orbitofrontal cortex (OFC) while imaging in the mPFC through a cranial window). They observed that the turnover rate of synaptic boutons in this projection was increased following training in an odour discrimination instrumental task, but not by reward ingestion alone, suggesting learning transiently increases synaptic remodelling in motivationally relevant brain areas.

Together, these studies suggest that associative learning is accompanied by alterations of synaptic strength between neuronal populations in brain areas involved in encoding conditioned responses.

### 1.3.1.3. Intrinsic adaptations following associative learning

One of the first demonstrations of changes to intrinsic excitability following associative learning in mammals was observed in sensorimotor cortex of the cat. Brons and Woody (1980) conditioned an auditory CS with a tap to the forehead (which evoked an unconditioned eye blink response). *In vivo* recordings in awake cats demonstrated a significant decrease in the required current injection to elicit spiking in the sensorimotor cortex, persisting for at least 28 days, and even following extinction learning (Brons *et al*, 1980; Zhang and Linden, 2003). Since this early observation, changes to the

intrinsic excitability of both principal neurons and interneurons has been widely demonstrated following associative learning using aversive reinforcers (McKay *et al*, 2009; McKay *et al*, 2013; Moyer *et al*, 1996; Oh and Disterhoft, 2015; Song *et al*, 2015), however fewer studies have focused on such changes following appetitive learning.

A number of studies suggest that intrinsic excitability may be important for associative learning and responses to appetitive reinforcers. Obesity prone-rats, which show dopamine system hypersensitivity, also demonstrate a significant increase in NAc core MSN excitability, compared to non-obesity prone controls (Oginsky *et al*, 2016). Hayton *et al* (2011) observed that appetitive learning can actively regulate intrinsic excitability in the prefrontal cortex of rats. Following training in which instrumental responses for food were required to be withheld before responding was cued by presentation of a CS, the excitability of prelimbic cortex pyramidal neurons was significantly depressed. Interestingly, following a similar task in which inhibition of responding was not required, but exposure to the CS and ability to instrumentally respond for food was immediate, neurons of the *infralimbic* cortex became more excitable. This suggests that distinct types of appetitive learning necessitating different behavioural responses can dynamically modulate the excitability of PFC subregions.

While the regulation of NAc intrinsic excitability following conditioning with drug reinforcers has not been extensively explored, it has been widely shown that drug administration may dynamically regulate NAc excitability. Long-term depression of accumbens neurons has been frequently observed following repeated drug administration (Kourrich *et al*, 2015; Kourrich *et al*, 2009; Zhang *et al*, 1998) while re-exposure to cocaine following withdrawal transiently increases excitability back to baseline (Mu *et al*, 2010). Dong *et al* (2006) decreased the excitability of NAc shell neurons by overexpression of the inwardly rectifying $K_{ir}2.1$ channel and observed that this potentiated psychostimulant induced increases in locomotor activity. Thus

excitability changes appear to play a functional role in the response of the motivational system to appetitive reinforcers.

### 1.3.2. The role of neuronal ensembles in memory encoding and associative learning

Thus it is clear that appetitive learning induces a number of neuroadaptations in motivation system brain areas which may function to facilitate transmission between neurons, and appear dependent on the activation of NMDAR and/or GPCRs. The majority of studies which investigate these learning-induced neuroadaptations select from the target neuronal populations randomly, largely due to technical limitations. However, neuronal populations in select brain areas do not respond uniformly to environmental stimuli, and different sets of neurons may encode different features of the learning experience (Day *et al*, 2006). Amongst the early experimental observations that distinct sets of neurons could respond selectively to environmental stimuli came from Hubel and Wiesel's single-unit recording in the visual cortex of the cat. They demonstrated that individual neurons responded preferentially, and reliability, to slits of light when presented in specific orientations (Hubel and Wiesel, 1959). Later work in the motor cortex of monkeys demonstrated that the direction of limb movement could be predicted based on the sum of single-unit responses (Georgopoulos *et al*, 1986), suggesting the population vector of neuronal activity may be used to encode certain behaviours. These studies demonstrate that distinct populations of neurons responding preferentially to environmental stimuli exist in the brain and are sufficient to encode behaviour.

### 1.3.2. Early demonstrations of neuronal ensembles activated during appetitive learning

*In vivo* electrophysiological recording in behaving animals demonstrated that the neurons of limbic brain areas do not respond uniformly during the presentation of reward-associated cues or during Pavlovian and instrumental responding. For example, early single-unit recordings in behaving primates demonstrated that ventral PFC neurons encode many distinct features of a conditioning task. Rosenkilde *et al* (1981) trained their subjects in a colour discrimination task, in which pressing a button matching the colour of a presented cue (red vs. green) was rewarded with sucrose. They observed that a large percentage of neurons (85%) fired to presentation of the coloured cues, and the firing of approximately half of these neurons discriminated between the red and green cue. Additionally, subsets of neurons fired depending on whether the trial was completed successfully and reinforced, or completed unsuccessfully and not reinforced. Thus subsets, or ensembles, of neurons in motivational system brain areas appear to encode in a reliable fashion multiple features of the conditioning experience.

Similar observations have been made in the ventral striatum, where neurons selectively encoding the valence of a reinforcer have been identified (Williams, 1989, Apicella *et al*, 1991 in Pennartz et al, 1994). Lavoie and Mizumori (1994) found that approximately 31% of NAc neurons fire when a reward is encountered along a radial arm maze, and that these activated neurons increased their firing rates for larger rewards. Thus, MSN may adapt their firing rates based on reward value (such as the amount or intensity of the US). Similarly, if the valuation of a US is reduced using a devaluation procedure, the number of NAc shell neurons which are selectively activated following exposure to the food-associated CS is significantly reduced (West and Carelli, 2016). Thus ventral striatal neurons appear to encode the nature and value of both CS and US.

Ensemble encoding of behaviours reinforced with drug US has also been observed. Sets of neurons active in the ventral striatum during learning with drug reinforcers may selectively respond during drug delivery, CS presentation, and the conditioned response (Carelli and Wightman, 2004; Janak *et al*, 1999). Carelli and Deadwyler (1994) identified sets of accumbens neurons which responded to incredibly precise features of instrumental responding during drug self-administration, with some neurons increasing firing rate selectively before the response, some after the response, with other neurons decreasing their firing rate following the response. This suggests that not only do ventral striatum neurons encode conditioned responding with incredible specificity, but they may do so by increasing or decreasing their firing rate.

#### 1.3.2.2. Neuronal ensembles: dawn of the neuronal activity marker

##### *Immediate early genes (IEGs)*

*In vivo* electrophysiology is a valuable tool for the identification and measurement of neuronal subsets activated during specific behavioural epochs of appetitive conditioning. However, it does not permit the large-scale visualisation of activated neurons in multiple brain areas. Immediate early genes (IEGs) are rapidly regulated by neuronal activity and their mRNA transcripts and protein products can be utilised as a marker for neuronal activity. Thus, as a complement to *in vivo* electrophysiology tools, many researchers since the early 1990's have visualised activated neurons using histological methods such as *in situ* hybridisation and immunohistochemistry. More recently, researchers have taken advantage of the promotor regions of IEGs such the *Fos* to express proteins allowing identification and manipulation of IEG-expressing neurons following associative learning (Kawashima *et al*, 2014). Below, the most commonly used IEG activity markers and their mechanism of induction, and transgenic tools that allow activated neurons to be identified and manipulated are reviewed.

*Fos*

The immediate early gene *c-fos* was the first activity marker successfully used to identify discretely activated neuronal populations (Hunt *et al,* 1987; Campeau *et al*, 1991; Kawashima *et al*, 2014). The protein product Fos is a transcription factor involved in diverse cellular functions and expressed only in the cell nucleus. The *c-fos* promoter regions contains cAMP response elements (CRE) and serum response elements (SRE) which are activated by CREB and serum response factor (SRF) respectively (Chaudhuri, 1997; Cruz *et al*, 2013) (Figure 4).

Activation of either response element through CREB or SRF activity may be sufficient to induce Fos expression (Wang and Prywes, 2000). Induction of Fos is dependent on ERK/MAPK mediated-phosphorylation of SRF or RSK-mediated phosphorylation of CREB (Cruz *et al*, 2013). Interestingly, Fos expression does not appear to be induced by activation of the cAMP pathway, despite its promotor region containing CRE sites; infusion of PKA inhibitors does not affect induction of striatal Fos following cocaine administration (Mattson *et al*, 2005) and cAMP cannot induce Fos in the absence of $Ca^{2+}$ entry (Zhang *et al*, 2012). Application of NMDAR antagonists prior to Fos induction suggest that inhibiting NMDAR transmission alone is sufficient to attenuate striatal Fos induced by amphetamine administration (Konradi *et al*, 1996). Thus Fos expression requires the sustained increases in intracellular calcium level associated with following prolonged synaptic activity (Cruz *et al*, 2013,) but is not a correlate of spiking activity (Luckman *et al*, 1994).

Fos messenger RNA (mRNA) expression following CRE or SRE activation peaks at approximately 30 minutes, while levels return to baseline at 120 minutes. Protein expression peaks at approximately 120 minutes and returns to baseline within 4-6 hours (Gao and Ji, 2009; Zangenehpour and Chaudhuri, 2002). The activation time course of Fos, its low basal expression and comparatively high activation threshold (Hughes *et al*, 1992; Kawashima *et al*, 2014), make it an effective reporter of neural

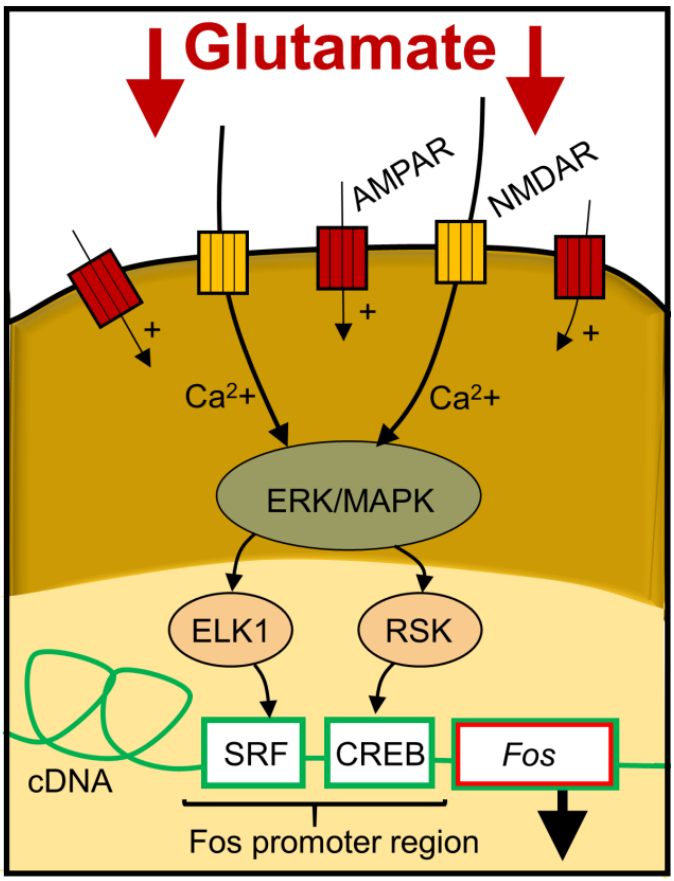


**Figure 4.** Mechanisms of *Fos* expression in the striatum. Adapted from Cruz *et al* (2013). *Fos* expression may be induced following calcium ($Ca^{2+}$) entry through NMDA receptors (NMDARs), which requires concurrent AMPA receptor (AMPAR) stimulation (see Figure 3). $Ca^{2+}$ entry leads to the phosphorylation of the extracellular signal-regulated kinase (ERK)/ mitogen-activated protein kinase (MAPK) pathway. This in turn leads to ELK-1 dependent phosphorylation of serum response factor (SRF), or ribosomal S6 kinase (RSK)-dependent phosphorylation of cAMP response element-binding protein (CREB). Activation of the transcription factors SRF or CREB results in their binding to sites in the *Fos* promotor region (serum response element (SRE) and cAMP response element (CRE), respectively). Activation of either SRE or CRE is sufficient to lead to *Fos* expression and translation. cDNA: chromosomal deoxyribonucleic acid.

activity during short to medium length behavioural tests. Fos is a relatively simple and reliable protein to visualise using immunohistochemistry (Chatterjee *et al*, 2015; Perrin-Terrin *et al*, 2016). Additionally, insertion of transgenes downstream of the *Fos* promotor sequence permits activity-dependent expression of these transgenes such as green fluorescent protein (GFP) (discussed in detail in the following section). For these reasons, Fos and/or transgene products that are coupled to the *Fos* promotor are widely used as a marker of neuron activation.

### *Zif268 & Arc*

Zif268 (also known as early growth response protein 1 (EGR-1) and nerve growth factor-induced protein A (NGFI-A) is an immediate early gene and transcription factor

also used as a marker of neuronal activation. The zif268 promoter region also contains CRE and SRE binding elements, however in different number compared to Fos, which conferring a lower threshold and higher basal levels in protein expression (Chaudhuri, 1997). In some brain areas, such as the striatum, use of zif268 as an activity marker may be problematic due to high levels of basal expression (Nguyen *et al*, 1992). While induction times of mRNA and protein levels are similar to Fos (zif268 mRNA is expressed within 30 minutes of activation while zif268 protein is expressed at 120 minutes), they remain expressed for over 6 hours (Zangenehpour *et al*, 2002).

Arc is another immediately early gene widely used as a neuronal activity marker. Unlike Fos and zif268, Arc is not a transcription factor but is a protein directly involved in cellular function; Arc mRNA is trafficked out of the nucleus to the soma and dendritic spines, where it is translated in an *ad-hoc* manner following neuronal activity and is involved in regulation of a number of experience-induced neuroadaptations (Korb and Finkbeiner, 2011; Mikkelsen and Larsen, 2006). Arc may be activated by either the ERK/MAPK pathway or the cAMP-PKA pathway (Bloomer *et al*, 2008; Waltereit *et al*, 2001). Arc mRNA peaks after 15 minutes and returns to baseline by 90 minutes while protein expression peaks at 60 minutes and returns to baseline by 5 hours. In the striatum, basal Arc expression is higher than Fos, while basal Fos expression is higher in the thalamus (Kawashima *et al*, 2014). Thus choice of activity markers varies across studies and may be tailored to the specific requirements of an experiment.

#### *1.3.2.2.2. Activity marker expression following appetitive conditioning*

*Fos immunostaining*

Quantification of Fos-expressing neurons in the rodent brain following appetitive conditioning permits visualisation of actived neuronal ensembles with single-cell resolution. Such studies typically measure the number of Fos-expressing (Fos+) “activated” neurons following a conditioning procedure in “Paired mice”, as compared

to an “Unpaired” group in which presentation of the CS and US is unpaired. However, this approach can lead to issues in interpretation of Fos data. For example, Igelstrom *et al* (2010) assayed the number of Fos-expressing neurons across the brain following a single trial of Pavlovian conditioning between a discrete auditory CS and water (US). They observed activation of paraventricular thalamus and superior colliculus, but not areas such as the striatum or anterior cingulate PFC known to be involved in appetitive conditioning. Similarly, Nordquist *et al* (2003) measured Fos expression following 1 or 4 Pavlovian approach conditioning trials in which sucrose delivery was paired with a discrete CS, but did not observe significant activation of neurons in any measured PFC subregion. These findings are surprising, considering the role of the ventral striatum and PFC in motivated behaviours, and highlight a limitation of the Fos procedure. While *in vivo* electrophysiology is able to identify subsets of activated neurons which fire during specific behaviour epochs, due to its slow time course (e.g. 90 min since behavioural test onset to detect Fos expression), IEG expression only measures the cumulative number of activated neurons over an entire behavioural test session. Hence, its expression cannot ascertain *when* a particular neuron was activated by *what* stimuli and/or behaviour (e.g. activation from the cues, stress, locomotor activity). Exposure to novel stimuli or appetitive reinforcers such as sucrose have been shown to robustly activate regions such as the NAc and PFC (Hajnal *et al*, 2009; Struthers *et al*, 2005). Thus non-specific activation in the Unpaired group can make detection of learning-related changes difficult in Paired mice. Suto *et al* (2016) have demonstrated that while two distinct CS signalling presentation or omission of a reward activate a similar number of neurons in the infralimbic cortex, selective knockout of these populations has opposing effects on behaviour. Thus it appears that it may not be the number of activated neurons which is important for the expression of conditioned behaviours, but rather than nature of the neurons activated.

Nonetheless, activation of neuronal ensembles in a number of motivation system brain areas has been observed following exposure to food-associated cues. Flagel *et al* (2011) conditioned a discrete compound CS (light illumination and lever insertion) to sucrose delivery in Paired rats over a 7 day training procedure, while Unpaired rats received random CS and US presentations; at test, all animals were exposed to the CS under extinction conditions. This procedure has the benefit of reducing baseline Fos expression in both groups due to habituation to the testing apparatus and absence of sucrose ingestion at test. They observed increased *Fos* expression in rats across several motivation-relevant brain areas, including the NAc, DS, orbitofrontal cortex and paraventricular thalamus. Interestingly, these findings were observed only in rats which sign-tracked (interacting with the CS) rather than goal-tracking animals. Furthermore, Schroeder *et al* (2001) observed increases in the medial prefrontal cortex and orbitofrontal cortex following exposure to a chocolate-associated environment. Together, these findings suggest that Fos can be used to identify neuronal populations activated following appetitive conditioning.

Fos expression has also been used to identify brain areas activated following the expression of drug-conditioned behaviours. Fos expression following drug administration is typically more robust than when using a food US (Kelley *et al*, 2005; Zombeck *et al*, 2008). However, there are significant discrepancies in studies of Fos expression following even simple conditioned behaviours using drug reinforcers, such as locomotor conditioning to a drug-associated environment (conditioned locomotion). Exposure to a psychostimulant-associated context has been shown to lead to activation of the NAc core but not the NAc shell (Hotsenpiller *et al*, 2002), the NAc shell but not NAc core (Chauvet *et al*, 2011; Rhodes *et al*, 2005) as well as both the NAc shell and NAc core (Brown *et al*, 1992; Franklin and Druhan, 2000). These data suggest that striatal ensemble recruitment is highly sensitive to experimental procedure

and may be influenced by the number and spacing of cocaine injections, habituation to novelty and drug dose (Ryabinin *et al*, 1997; Uslaner *et al*, 2003).

#### *1.3.2.2.3. Creation of transgenic animals with transgene expression controlled via the Fos promotor*

Although Fos expression can be used to visualise neurons activated following appetitive conditioning, this method has some limitations for further characterising the biochemistry and electrophysiology of these neurons. Also, Fos expression alone does not indicate whether these neurons play a causal role in learned behaviours. In order to overcome these limitations, in the last 20 years, researchers have generated innovative genetic technologies that permit the expression of transgenes in Fos-expressing, recently activated neurons. These can be used to identify recently activated neurons *in vivo* and *ex vivo*, allowing investigation into their physiological and molecular properties, as well as more direct manipulations.

##### *Fos-LacZ*

The *Fos-LacZ* mouse was originally created to permit reliable identification of Fos expressing neurons, due to issues with high-variability and poor replication in Fos-expression studies using antibody staining methods (Kawashima *et al*, 2014; Smeyne *et al*, 1992). Nearly 20 years following the creation of the *Fos-LacZ* mouse, a novel use was developed permitting the selective lesioning of Fos-expressing neurons. In *Fos-LacZ* transgenic animals, Daun02 infused into target brain regions may be converted to the toxic daunomycin only in recently activated, Fos-expressing neurons. Koya *et al* (2009) first used the Daun02 technique to selectively lesion neurons in the NAc activated during a cocaine sensitisation regime. Ablation of neurons activated on the final pairing of cocaine with a locomotor chamber attenuated the expression of locomotor sensitisation at a later test. Crucially, cocaine sensitisation did not occur if

neurons activated following cocaine administration in a separate, novel context were lesioned. This highlights the specificity of ensemble encoding, as the destruction of neurons activated only by the relevant CS-US association were involved in the expression of sensitisation**.** Thus, the Daun02 method is a valuable tool permitting selective lesioning of Fos-expressing neurons.

*Fos-GFP*

The *Fos-GFP* mouse, which expresses a *Fos-GFP* fusion protein, was engineered by Alison Barth working at the Carnegie Mellon Institute, USA (Barth *et al*, 2004). The *Fos-GFP* mouse expresses a Fos-GFP fusion protein in recently activated neurons, permitting visualisation of neuronal ensembles both *in vivo* or in *ex-vivo* slice preparations. This allows investigation into the physiological and molecular profiles of neurons activated following associative learning.

Koya *et al* (2012) utilized the *Fos-GFP* mouse to investigate the synaptic physiology of neurons activated in the NAc shell following the expression of cocaine sensitisation. They observed that neurons activated following cocaine sensitisation, but not acute cocaine administration, demonstrated a decrease in AMPAR/NMDAR ratio in recently activated, GFP+ neurons. This apparent decease in synaptic strength was due to an increase in the number of silent synapses, which contain only functional NMDA receptors. Later studies demonstrated that this finding was context specific; when animals are tested with a cocaine administration in a different context to which the sensitisation regime took place, no locomotor sensitisation occurs and the neurons activated do not show increases in silent synapses (Whitaker *et al*, 2016). These studies extend previous findings observing changes in synaptic physiology following associative learning but demonstrate that such changes may occur selectively in behaviourally relevant neurons. This draws experimental evidence even closer to the

theories of Konorski and Hebb, who hypothesised such changes may occur specifically in the neurons playing a functional role in learning (Hebb, 1949; Konorski, 1948).

The *Fos-GFP* mouse has also been used to permit electrophysiological examination of the neurons activated during conditioning with a food US. Cifani *et al* (2012) trained *Fos-GFP* rats to lever press for a food reward, then following extinction reinstated food-seeking behaviour using the pharmacological stressor yohimbine. Similarly, to Koya *et al* (2012), they observed a reduction in AMPAR/NMDAR ratios selectively in GFP+ neurons. This suggests that the neurons activated following the expression of drug or food-associated behaviours may undergo similar synaptic adaptations.

## 1.4. Aims and Hypotheses

The encoding of Pavlovian associations appears to be dependent on the regulation the intrinsic and synaptic properties of neurons in motivationally-relevant brain areas. However due to technical limitations, previous studies investigating such adaptations have largely sampled neuronal populations without distinguishing their activation history. However, i*n vivo* electrophysiology and immediate-early gene studies suggest that associative memories are encoded in sparsely activated neuronal ensembles. As such, identifying the nature of neuroadaptations occurring selectively on neuronal ensembles activated by reward-associated cues may provide novel insight into the mechanisms of associative memory encoding. Thus, we aim to identify neuronal populations activated following exposure to reward-associative stimuli and investigate potential changes in their intrinsic and synaptic excitability.

The activity marker *Fos* may be used to identify neuronal ensembles activated following exposure to reward-associated stimuli. *Fos* can be visualised in histochemical preparations or in the *Fos-GFP* mouse, which permits electrophysiological investigation. Using a simple Pavlovian approach paradigm, in with a CS is paired with

a sucrose reward, we aim use such techniques to identify the brain areas activated following exposure to the appetitive CS and assay their electrophysiological properties. Furthermore, a deeper understanding of the functional relevance of such potential adaptations may be gained by observing their regulation following changes in associative strength. As such, we will investigate how ensemble-selective adaptations may be regulated following extinction learning.

Finally, if adaptations in the neurons activated by food-associated cues are observed, it would be of interest to investigate whether such adaptations are also observed following learning with drugs such as cocaine. Such comparisons may yield insight into general mechanisms of associative memory regulation or demonstrate unique features of conditioning to drugs of abuse.

Overall, we hypothesise that changes in intrinsic and synaptic excitability may be selectively observed on neuronal ensembles activated following exposure to reward-associated stimuli.

## References


Alexander GE, DeLong MR, Strick PL (1986). Parallel organization of functionally segregated circuits linking basal ganglia and cortex. *Annu Rev Neurosci* **9**: 357-381.

Amaral DG (1978). A Golgi study of cell types in the hilar region of the hippocampus in the rat. *J Comp Neurol* **182**(4 Pt 2): 851-914.

Amaral DG, Witter MP (1989). The three-dimensional organization of the hippocampal formation: a review of anatomical data. *Neuroscience* **31**(3): 571-591.

Anagnostaras SG, Schallert T, Robinson TE (2002). Memory processes governing amphetamine-induced psychomotor sensitization. *Neuropsychopharmacology* **26**(6): 703-715.

Andén NE, Fuxe K, Hamberoer B, Hökfelt T (1966). A Quantitative Study on the Nigro-Neostriatal Dopamine Neuron System in the Rat. *Acta Physiologica* **67**(3-4): 6.

Antonov I, Antonova I, Kandel ER, Hawkins RD (2003). Activity-dependent presynaptic facilitation and hebbian LTP are both required and interact during classical conditioning in Aplysia. *Neuron* **37**(1): 135-147.

Arias-Carrion O, Stamelou M, Murillo-Rodriguez E, Menendez-Gonzalez M, Poppel E (2010). Dopaminergic reward system: a short integrative review. *Int Arch Med* **3**: 24.

Atkins AL, Mashhoon Y, Kantak KM (2008). Hippocampal regulation of contextual cue-induced reinstatement of cocaine-seeking behavior. *Pharmacol Biochem Behav* **90**(3): 481-491.

Backstrom P, Hyytia P (2007). Involvement of AMPA/kainate, NMDA, and mGlu5 receptors in the nucleus accumbens core in cue-induced reinstatement of cocaine seeking in rats. *Psychopharmacology (Berl)* **192**(4): 571-580.

Badiani A, Belin D, Epstein D, Calu D, Shaham Y (2011). Opiate versus psychostimulant addiction: the differences do matter. *Nat Rev Neurosci* **12**(11): 685-700.

Baldwin AE, Sadeghian K, Holahan MR, Kelley AE (2002). Appetitive instrumental learning is impaired by inhibition of cAMP-dependent protein kinase within the nucleus accumbens. *Neurobiol Learn Mem* **77**(1): 44-62.

Balsam P (1984). Relative time in trace conditioning. *Ann N Y Acad Sci* **423**: 211-227.

Barnes NM, Sharp T (1999). A review of central 5-HT receptors and their function. *Neuropharmacology* **38**(8): 1083-1152.

Barth AL, Gerkin RC, Dean KL (2004). Alteration of neuronal firing properties after in vivo experience in a FosGFP transgenic mouse. *J Neurosci* **24**(29): 6466-6475.

Basar K, Sesia T, Groenewegen H, Steinbusch HW, Visser-Vandewalle V, Temel Y (2010). Nucleus accumbens and impulsivity. *Prog Neurobiol* **92**(4): 533-557.

Bean BP (2007). The action potential in mammalian central neurons. *Nat Rev Neurosci* **8**(6): 451-465.

Beaulieu JM, Gainetdinov RR (2011). The physiology, signaling, and pharmacology of dopamine receptors. *Pharmacol Rev* **63**(1): 182-217.

Beckstead RM, Domesick VB, Nauta WJ (1979). Efferent connections of the substantia nigra and ventral tegmental area in the rat. *Brain Res* **175**(2): 191-217.

Belin D, Everitt BJ (2008). Cocaine seeking habits depend upon dopamine-dependent serial connectivity linking the ventral with the dorsal striatum. *Neuron* **57**(3): 432-441.

Bellone C, Luscher C. (2005). mGluRs induce a long-term depression in the ventral tegmental area that involves a switch of the subunit composition of AMPA receptors. *Eur J Neurosci,* **21**(5): 1280–1288.

Bengtson CP, Osborne PB (2000). Electrophysiological properties of cholinergic and noncholinergic neurons in the ventral pallidal region of the nucleus basalis in rat brain slices. *J Neurophysiol* **83**(5): 2649-2660.

Bernardi RE, Lattal KM, Berger SP (2007). Anisomycin disrupts a contextual memory following reactivation in a cocaine-induced locomotor activity paradigm. *Behav Neurosci* **121**(1): 156-163.

Berridge KC, Robinson TE (1998). What is the role of dopamine in reward: hedonic impact, reward learning, or incentive salience? *Brain Res Brain Res Rev* **28**(3): 309-369.

Blaiss CA, Janak PH (2009). The nucleus accumbens core and shell are critical for the expression, but not the consolidation, of Pavlovian conditioned approach. *Behav Brain Res* **200**(1): 22-32.

Blanke ML, VanDongen AMJ (2009). Activation Mechanisms of the NMDA Receptor. In: Van Dongen AM (ed). *Biology of the NMDA Receptor*: Boca Raton (FL).

Bliss TV, Lomo T (1973). Long-lasting potentiation of synaptic transmission in the dentate area of the anaesthetized rabbit following stimulation of the perforant path. *J Physiol* **232**(2): 331-356.

Bloomer WA, VanDongen HM, VanDongen AM (2008). Arc/Arg3.1 translation is controlled by convergent N-methyl-D-aspartate and Gs-coupled receptor signaling pathways. *J Biol Chem* **283**(1): 582-592.

Boakes RA (1977). Performance on learning to associate a stimulus with positive reinforcement. In: Hurwitz DH (ed). *Performance on learning to associate a stimulus with positive reinforcement*. Lawrence Erlbaum Associates: New Jersey.

Bouton ME (2004). Context and behavioral processes in extinction. *Learn Mem* **11**(5): 485-494.

Bouton ME, Bolles RC (1979). Contextual control of the extinction of conditioned fear. *Learning and Motivation* **10**(4): 21.

Bouton ME, Peck CA (1989). Context effects on conditioning, extinction, and reinstatement in an appetitive conditioning preparation. *Animal Learning & Behavior* **17**(2): 10.

Bouton ME, Swartzentruber D (1991). Sources of relapse after extinction in Pavlovian and instrumental learning. *Clinical Psychology Review* **11**(2): 17.

Bouvier G, Bidoret C, Casado M, Paoletti P (2015). Presynaptic NMDA receptors: Roles and rules. *Neuroscience* **311**: 322-340.

Boyden ES, Zhang F, Bamberg E, Nagel G, Deisseroth K (2005). Millisecond-timescale, genetically targeted optical control of neural activity. *Nat Neurosci* **8**(9): 1263-1268.

Brickley SG, Mody I (2012). Extrasynaptic GABA(A) receptors: their function in the CNS and implications for disease. *Neuron* **73**(1): 23-34.

Britt JP, Benaliouad F, McDevitt RA, Stuber GD, Wise RA, Bonci A (2012). Synaptic and behavioral profile of multiple glutamatergic inputs to the nucleus accumbens. *Neuron* **76**(4): 790-803.

Brog JS, Salyapongse A, Deutch AY, Zahm DS (1993). The patterns of afferent innervation of the core and shell in the "accumbens" part of the rat ventral striatum: immunohistochemical detection of retrogradely transported fluoro-gold. *J Comp Neurol* **338**(2): 255-278.

Brons JF, Woody CD (1980). Long-term changes in excitability of cortical neurons after Pavlovian conditioning and extinction. *J Neurophysiol* **44**(3): 605-615.

Brown EE, Robertson GS, Fibiger HC (1992). Evidence for conditional neuronal activation following exposure to a cocaine-paired environment: role of forebrain limbic structures. *The Journal of neuroscience : the official journal of the Society for Neuroscience* **12**(10): 4112-4121.

Brown LL, Smith DM, Goldbloom LM (1998). Organizing principles of cortical integration in the rat neostriatum: corticostriate map of the body surface is an ordered lattice of curved laminae and radial points. *J Comp Neurol* **392**(4): 468-488.

Brown MT, Bellone C, Mameli M, Labouebe G, Bocklisch C, Balland B*, et al* (2010). Drug-driven AMPA receptor redistribution mimicked by selective dopamine neuron stimulation. *PLoS One* **5**(12): e15870.

Brown PL, Jenkins HM (1968). Auto-shaping of the pigeon's key-peck. *J Exp Anal Behav* **11**(1): 1-8.

Bush RR, Mosteller F (1951). A mathematical model for simple learning. *Psychol Rev* **58**(5): 313-323.

Calipari ES, Huggins KN, Mathews TA, Jones SR (2012). Conserved dorsal-ventral gradient of dopamine release and uptake rate in mice, rats

and rhesus macaques. *Neurochem Int* **61**(7): 986-991.

Campeau S, Hayward MD, Hope BT, Rosen JB, Nestler EJ, Davis M (1991). Induction of the c-fos proto-oncogene in rat amygdala during unconditioned and conditioned fear. *Brain Res* **565**(2): 349-352.

Caprioli D, Venniro M, Zhang M, Bossert JM, Warren BL, Hope BT*, et al* (2017). Role of Dorsomedial Striatum Neuronal Ensembles in Incubation of Methamphetamine Craving after Voluntary Abstinence. *J Neurosci* **37**(4): 1014-1027.

Cardinal RN, Parkinson JA, Hall J, Everitt BJ (2003). The contribution of the amygdala, nucleus accumbens, and prefrontal cortex to emotion and motivated behaviour. *International Congress Series* **1250**: 23.

Carelli RM, Deadwyler SA (1994). A comparison of nucleus accumbens neuronal firing patterns during cocaine self-administration and water reinforcement in rats. *J Neurosci* **14**(12): 7735-7746.

Carelli RM, Wightman RM (2004). Functional microcircuitry in the accumbens underlying drug addiction: insights from real-time signaling during behavior. *Curr Opin Neurobiol* **14**(6): 763-768.

Carew TJ, Pinsker HM, Kandel ER (1972). Long-term habituation of a defensive withdrawal reflex in aplysia. *Science* **175**(4020): 451-454.

Carr DB, Sesack SR (2000). Projections from the rat prefrontal cortex to the ventral tegmental area: target specificity in the synaptic associations with mesoaccumbens and mesocortical neurons. *J Neurosci* **20**(10): 3864-3873.

Carr GD, White NM (1983). Conditioned place preference from intra-accumbens but not intra-caudate amphetamine injections. *Life Sci* **33**(25): 2551-2557.

Carter AG, Soler-Llavina GJ, Sabatini BL (2007). Timing and location of synaptic inputs determine modes of subthreshold integration in striatal medium spiny neurons. *J Neurosci* **27**(33): 8967-8977.

Cascio M (2004). Structure and function of the glycine receptor and related nicotinicoid receptors. *J Biol Chem* **279**(19): 19383-19386.

Chatterjee D, Tran S, Shams S, Gerlai R (2015). A Simple Method for Immunohistochemical Staining of Zebrafish Brain Sections for c-fos Protein Expression. *Zebrafish* **12**(6): 414-420.

Chaudhuri A (1997). Neural activity mapping with inducible transcription factors. *Neuroreport* **8**(13): iii-vii.

Chauvet C, Lardeux V, Jaber M, Solinas M (2011). Brain regions associated with the reversal of cocaine conditioned place preference by environmental enrichment. *Neuroscience* **184**: 88-96.

Chen RQ, Wang SH, Yao W, Wang JJ, Ji F, Yan JZ*, et al* (2011). Role of glycine receptors in glycine-induced LTD in hippocampal CA1 pyramidal neurons. *Neuropsychopharmacology* **36**(9): 1948-1958.

Chergui K, Bouron A, Normand E, Mulle C (2000). Functional GluR6 kainate receptors in the striatum: indirect downregulation of synaptic transmission. *J Neurosci* **20**(6): 2175-2182.

Chudasama Y, Robbins TW (2003). Dissociable contributions of the orbitofrontal and infralimbic cortex to pavlovian autoshaping and discrimination reversal learning: further evidence for the functional heterogeneity of the rodent frontal cortex. *J Neurosci* **23**(25): 8771-8780.

Chuhma N, Tanaka KF, Hen R, Rayport S (2011). Functional connectome of the striatal medium spiny neuron. *J Neurosci* **31**(4): 1183-1192.

Cifani C, Koya E, Navarre BM, Calu DJ, Baumann MH, Marchant NJ*, et al* (2012). Medial prefrontal cortex neuronal activation and synaptic alterations after stress-induced reinstatement of palatable food seeking: a study using c-fos-GFP transgenic female rats. *J Neurosci* **32**(25): 8480-8490.

Colle L, Wise RA (1988). Concurrent facilitory and inhibitory effects of amphetamine on stimulation-induced eating. *Brain Res* **459**(2): 356-360.

Conde F, Maire-Lepoivre E, Audinat E, Crepel F (1995). Afferent connections of the medial frontal cortex of the rat. II. Cortical and subcortical afferents. *J Comp Neurol* **352**(4): 567-593.

Contractor A, Mulle C, Swanson GT (2011). Kainate receptors coming of age: milestones of

two decades of research. *Trends Neurosci* **34**(3): 154-163.

Crombag HS, Sutton JM, Takamiya K, Holland PC, Gallagher M, Huganir RL (2008a). A role for alpha-amino-3-hydroxy-5-methylisoxazole-4-propionic acid GluR1 phosphorylation in the modulatory effects of appetitive reward cues on goal-directed behavior. *Eur J Neurosci* **27**(12): 3284-3291.

Crombag HS, Sutton JM, Takamiya K, Lee HK, Holland PC, Gallagher M*, et al* (2008b). A necessary role for GluR1 serine 831 phosphorylation in appetitive incentive learning. *Behav Brain Res* **191**(2): 178-183.

Cruz FC, Koya E, Guez-Barber DH, Bossert JM, Lupica CR, Shaham Y*, et al* (2013). New technologies for examining the role of neuronal ensembles in drug addiction and fear. *Nat Rev Neurosci* **14**(11): 743-754.

Czubayko U, Plenz D (2002). Fast synaptic transmission between striatal spiny projection neurons. *Proc Natl Acad Sci U S A* **99**(24): 15764-15769.

Dalley JW, Cardinal RN, Robbins TW (2004). Prefrontal executive and cognitive functions in rodents: neural and neurochemical substrates. *Neurosci Biobehav Rev* **28**(7): 771-784.

Dalley JW, Laane K, Theobald DE, Armstrong HC, Corlett PR, Chudasama Y*, et al* (2005). Time-limited modulation of appetitive Pavlovian memory by D1 and NMDA receptors in the nucleus accumbens. *Proc Natl Acad Sci U S A* **102**(17): 6189-6194.

Day JJ, Carelli RM (2007). The nucleus accumbens and Pavlovian reward learning. *Neuroscientist* **13**(2): 148-159.

Day JJ, Wheeler RA, Roitman MF, Carelli RM (2006). Nucleus accumbens neurons encode Pavlovian approach behaviors: evidence from an autoshaping paradigm. *Eur J Neurosci* **23**(5): 1341-1351.

Descartes R (1975). *The philosophical works of Descartes (*Cambridge University Press: London. Vol 1.

Delfs JM, Zhu Y, Druhan JP, Aston-Jones, GS (1998). Origin of noradrenergic afferents to the shell subregion of the nucleus accumbens: anterograde and retrograde tract-tracing studies in the rat.*Brain Res* **806**(2): 127-40.

Di Chiara G (1999). Drug addiction as dopamine-dependent associative learning disorder. *Eur J Pharmacol* **375**(1-3): 13-30.

Di Chiara G, Imperato A (1988). Drugs abused by humans preferentially increase synaptic dopamine concentrations in the mesolimbic system of freely moving rats. *Proc Natl Acad Sci U S A* **85**(14): 5274-5278.

Dickinson A (1985). Actions and Habits: The Development of Behavioural Autonomy. *Philos Trans R Soc Lond B Biol Sci* **308**: 11.

Dickinson A (2010). Instrumental Conditioning. In: Stolerman I (ed). *Encyclopedia of Psycho-pharmacology*. Springer-Verlag: Berlin.

Dong Y, Green T, Saal D, Marie H, Neve R, Nestler EJ*, et al* (2006). CREB modulates excitability of nucleus accumbens neurons. *Nat Neurosci* **9**(4): 475-477.

Dube L, Smith AD, Bolam JP (1988). Identification of synaptic terminals of thalamic or cortical origin in contact with distinct medium-size spiny neurons in the rat neostriatum. *J Comp Neurol* **267**(4): 455-471.

Durieux PF, Schiffmann SN, de Kerchove d'Exaerde A (2011). Targeting neuronal populations of the striatum. *Front Neuroanat* **5**: 40.

Esteban JA, Shi SH, Wilson C, Nuriya M, Huganir RL, Malinow R (2003). PKA phosphorylation of AMPA receptor subunits controls synaptic trafficking underlying plasticity. *Nat Neurosci* **6**(2): 136-143.

Everitt BJ, Cardinal RN, Hall J, Parkinson JA, Robbins TW (2000). Differential involvement of amygdala subsystems in appetitive conditioning and drug addiction In: Aggleton JP (ed). *The amygdala: a functional analysis*. Oxford University Press: Oxford.

Everitt BJ, Morris KA, O'Brien A, Robbins TW (1991). The basolateral amygdala-ventral striatal system and conditioned place preference: further evidence of limbic-striatal interactions underlying reward-related processes. *Neuroscience* **42**(1): 1-18.

Everitt BJ, Robbins TW (2013). From the ventral to the dorsal striatum: devolving views of their roles in drug addiction. *Neurosci Biobehav Rev* **37**(9 Pt A): 1946-1954.

Everitt BJ, Robbins TW, Evenden JL, Marston HM, Jones GH, Sirkia TE (1987). The effects of excitotoxic lesions of the substantia innominata, ventral and dorsal globus pallidus on the acquisition and retention of a conditional visual discrimination: implications for cholinergic hypotheses of learning and memory. *Neuroscience* **22**(2): 441-469.

Fanselow MS, Dong HW (2010). Are the dorsal and ventral hippocampus functionally distinct structures? *Neuron* **65**(1): 7-19.

Ferrario CR, Loweth JA, Milovanovic M, Wang X, Wolf ME (2011). Distribution of AMPA receptor subunits and TARPs in synaptic and extrasynaptic membranes of the adult rat nucleus accumbens. *Neurosci Lett* **490**(3): 180-184.

Flagel SB, Cameron CM, Pickup KN, Watson SJ, Akil H, Robinson TE (2011). A food predictive cue must be attributed with incentive salience for it to induce c-fos mRNA expression in cortico-striatal-thalamic brain regions. *Neuroscience* **196**: 80-96.

Francis TC, Chandra R, Friend DM, Finkel E, Dayrit G, Miranda J*, et al* (2015). Nucleus accumbens medium spiny neuron subtypes mediate depression-related outcomes to social defeat stress. *Biol Psychiatry* **77**(3): 212-222.

Franklin TR, Druhan JP (2000). Expression of Fos-related antigens in the nucleus accumbens and associated regions following exposure to a cocaine-paired environment. *The European journal of neuroscience* **12**(6): 2097-2106.

Freund TF, Buzsaki G (1996). Interneurons of the hippocampus. *Hippocampus* **6**(4): 347-470.

Fujiyama F, Kuramoto E, Okamoto K, Hioki H, Furuta T, Zhou L*, et al* (2004). Presynaptic localization of an AMPA-type glutamate receptor in corticostriatal and thalamostriatal axon terminals. *Eur J Neurosci* **20**(12): 3322-3330.

Gabbott PL, Warner TA, Jays PR, Salway P, Busby SJ (2005). Prefrontal cortex in the rat: projections to subcortical autonomic, motor, and limbic centers. *J Comp Neurol* **492**(2): 145-177.

Gao YJ, Ji RR (2009). c-Fos and pERK, which is a better marker for neuronal activation and central sensitization after noxious stimulation and tissue injury? *Open Pain J* **2**: 11-17.

Garcia-Munoz M, Lopez-Huerta VG, Carrillo-Reid L, Arbuthnott GW (2015). Extrasynaptic glutamate NMDA receptors: key players in striatal function. *Neuropharmacology* **89**: 54-63.

Geinisman Y, Berry RW, Disterhoft JF, Power JM, Van der Zee EA (2001). Associative learning elicits the formation of multiple-synapse boutons. *J Neurosci* **21**(15): 5568-5573.

Georgopoulos AP, Schwartz AB, Kettner RE (1986). Neuronal population coding of movement direction. *Science* **233**(4771): 1416-1419.

Gertler TS, Chan CS, Surmeier DJ (2008). Dichotomous anatomical properties of adult striatal medium spiny neurons. *J Neurosci* **28**(43): 10814-10824.

Ghitza UE, Fabbricatore AT, Prokopenko VF, West MO (2004). Differences between accumbens core and shell neurons exhibiting phasic firing patterns related to drug-seeking behavior during a discriminative-stimulus task. *J Neurophysiol* **92**(3): 1608-1614.

Giese KP, Mizuno K (2013). The roles of protein kinases in learning and memory. *Learn Mem* **20**(10): 540-552.

Glimcher PW (2011). Understanding dopamine and reinforcement learning: the dopamine reward prediction error hypothesis. *Proc Natl Acad Sci U S A* **108 Suppl 3**: 15647-15654.

Gotz T, Kraushaar U, Geiger J, Lubke J, Berger T, Jonas P (1997). Functional properties of AMPA and NMDA receptors expressed in identified types of basal ganglia neurons. *J Neurosci* **17**(1): 204-215.

Gravante G, Sorbera F, Sabatino M, La Grutta V (1985). [Feeding behavior of the cat in response to stimulation of the caudate nucleus]. *Boll Soc Ital Biol Sper* **61**(2): 249-254.

Grimm JW, Fyall AM, Osincup DP (2005). Incubation of sucrose craving: effects of reduced training and sucrose pre-loading. *Physiol Behav* **84**(1): 73-79.

Grimm JW, Hope BT, Wise RA, Shaham Y (2001). Neuroadaptation. Incubation of cocaine craving after withdrawal. *Nature* **412**(6843): 141-142.

Groenewegen HJ (2003). The basal ganglia and motor control. *Neural Plast* **10**(1-2): 107-120.

Groenewegen HJ, Berendse HW, Haber SN (1993). Organization of the output of the ventral striatopallidal system in the rat: ventral pallidal efferents. *Neuroscience* **57**(1): 113-142.

Guire ES, Oh MC, Soderling TR, Derkach VA (2008). Recruitment of calcium-permeable AMPA receptors during synaptic potentiation is regulated by CaM-kinase I. *J Neurosci* **28**(23): 6000-6009.

Gulley JM, Kosobud AE, Rebec GV (2002). Behavior-related modulation of substantia nigra pars reticulata neurons in rats performing a conditioned reinforcement task. *Neuroscience* **111**(2): 337-349.

Haber SN (2011). Neuroanatomy of Reward: A View from the Ventral Striatum. In: Gottfried JA (ed). *Neurobiology of Sensation and Reward*: Boca Raton (FL).

Haber SN, Fudge JL, McFarland NR (2000). Striatonigrostriatal pathways in primates form an ascending spiral from the shell to the dorsolateral striatum. *J Neurosci* **20**(6): 2369-2382.

Hagan CE, Bolin B, Dirk Keene CD (2011). Nervous System. In: Piper Treuting SD (ed). *Comparative Anatomy and Histology*. Academic Press: London, UK.

Hajnal A, Norgren R, Kovacs P (2009). Parabrachial coding of sapid sucrose: relevance to reward and obesity. *Ann N Y Acad Sci* **1170**: 347-364.

Hammond C (2014). Firing patterns of neurons. In: Hammond C (ed). *Cellular and molecular neurophysiology*. Academic Press: Cambridge, MI. Vol 4th.

Hansing RA, Schwartzbaum JS, Thompson JB (1968). Operant behavior following unilateral and bilateral caudate lesion in the rat. *J Comp Physiol Psychol* **66**(2): 378-388.

Hawkins RD, Abrams TW, Carew TJ, Kandel ER (1983). A cellular mechanism of classical conditioning in Aplysia: activity-dependent amplification of presynaptic facilitation. *Science* **219**(4583): 400-405.

Hawkins RD, Byrne JH (2015). Associative learning in invertebrates. *Cold Spring Harb Perspect Biol* **7**(5).

Hayton SJ, Olmstead MC, Dumont EC (2011). Shift in the intrinsic excitability of medial prefrontal cortex neurons following training in impulse control and cued-responding tasks. *PLoS One* **6**(8): e23885.

Hebb DO (1949). *The Organization of Behavior: A Neuropsychological Theory* John Wiley & Sons: New York.

Heidbreder CA, Groenewegen HJ (2003). The medial prefrontal cortex in the rat: evidence for a dorso-ventral distinction based upon functional and anatomical characteristics. *Neurosci Biobehav Rev* **27**(6): 555-579.

Heimer L, Alheid G, Zaborszky L (1985). Basal Ganglia. In: Paxinos G (ed). *The Rat Nervous System*. Academic Press: Australia.

Heimer L, Zahm DS, Churchill L, Kalivas PW, Wohltmann C (1991). Specificity in the Projection Patterns of Accumbal Core and Shell in the Rat. *Neuroscience* **41**(1): 89-125.

Hernandez PJ, Andrzejewski ME, Sadeghian K, Panksepp JB, Kelley AE (2005). AMPA/kainate, NMDA, and dopamine D1 receptor function in the nucleus accumbens core: a context-limited role in the encoding and consolidation of instrumental memory. *Learn Mem* **12**(3): 285-295.

Hernandez PJ, Sadeghian K, Kelley AE (2002). Early consolidation of instrumental learning requires protein synthesis in the nucleus accumbens. *Nat Neurosci* **5**(12): 1327-1331.

Hibino H, Inanobe A, Furutani K, Murakami S, Findlay I, Kurachi Y (2010). Inwardly rectifying potassium channels: their structure, function, and physiological roles. *Physiol Rev* **90**(1): 291-366.

Higley MJ (2014). Localized GABAergic inhibition of dendritic Ca(2+) signalling. *Nat Rev Neurosci* **15**(9): 567-572.

Holland PC (1992). Occasion setting in Pavlovian conditioning. In: Medin DL (ed). *The psychology of learning and motivation*. Academic Press: San Diego, CA.

Holland PC, Rescorla RA (1975). The effect of two ways of devaluing the unconditioned stimulus after first- and second-order appetitive conditioning. *J Exp Psychol Anim Behav Process* **1**(4): 355-363.

Honey RC, Good M (1993). Selective hippocampal lesions abolish the contextual specificity of latent inhibition and conditioning. *Behav Neurosci* **107**(1): 23-33.

Hong S, Hikosaka O (2008). The globus pallidus sends reward-related signals to the lateral habenula. *Neuron* **60**(4): 720-729.

Hotsenpiller G, Horak BT, Wolf ME (2002). Dissociation of conditioned locomotion and Fos induction in response to stimuli formerly paired with cocaine. *Behav Neurosci* **116**(4): 634-645.

Huang CH, Yu YJ, Chang CH, Gean PW (2016). Involvement of metabotropic glutamate receptor 5 in the inhibition of methamphetamine-associated contextual memory after prolonged extinction training. *J Neurochem* **137**(2): 216-225.

Huang YH, Mogenson GJ (1972). Neural pathways mediating drinking and feeding in rats. *Exp Neurol* **37**(2): 269-286.

Hubel DH, Wiesel TN (1959). Receptive fields of single neurones in the cat's striate cortex. *J Physiol* **148**: 574-591.

Hughes P, Lawlor P, Dragunow M (1992). Basal expression of Fos, Fos-related, Jun, and Krox 24 proteins in rat hippocampus. *Brain Res Mol Brain Res* **13**(4): 355-357.

Hull CL (1940). *Mathematico-Deductive Theory of Rote Learning* Yale University Press: New Haven, Yale.

Hunt SP, Pini A, Evan G (1987). Induction of c-fos-like protein in spinal cord neurons following sensory stimulation. *Nature*, **328**(6131): 632-634.

Igelstrom KM, Herbison AE, Hyland BI (2010). Enhanced c-Fos expression in superior colliculus, paraventricular thalamus and septum during learning of cue-reward association. *Neuroscience* **168**(3): 706-714.

Ikemoto S (2007). Dopamine reward circuitry: two projection systems from the ventral midbrain to the nucleus accumbens-olfactory tubercle complex. *Brain Res Rev* **56**(1): 27-78.

Impey S, Obrietan K, Wong ST, Poser S, Yano S, Wayman G*, et al* (1998). Cross talk between ERK and PKA is required for Ca2+ stimulation of CREB-dependent transcription and ERK nuclear translocation. *Neuron* **21**(4): 869-883.

Ito R, Hayen A (2011). Opposing roles of nucleus accumbens core and shell dopamine in the modulation of limbic information processing. *J Neurosci* **31**(16): 6001-6007.

Ito R, Robbins TW, Everitt BJ (2004). Differential control over cocaine-seeking behavior by nucleus accumbens core and shell. *Nat Neurosci* **7**(4): 389-397.

Ito R, Robbins TW, McNaughton BL, Everitt BJ (2006). Selective excitotoxic lesions of the hippocampus and basolateral amygdala have dissociable effects on appetitive cue and place conditioning based on path integration in a novel Y-maze procedure. *Eur J Neurosci* **23**(11): 3071-3080.

Ito R, Robbins TW, Pennartz CM, Everitt BJ (2008). Functional interaction between the hippocampus and nucleus accumbens shell is necessary for the acquisition of appetitive spatial context conditioning. *J Neurosci* **28**(27): 6950-6959.

Jaeger D, Kita H, Wilson CJ (1994). Surround inhibition among projection neurons is weak or nonexistent in the rat neostriatum. *J Neurophysiol* **72**(5): 2555-2558.

Janak PH, Chang JY, Woodward DJ (1999). Neuronal spike activity in the nucleus accumbens of behaving rats during ethanol self-administration. *Brain Res* **817**(1-2): 172-184.

Janak PH, Tye KM (2015). From circuits to behaviour in the amygdala. *Nature* **517**(7534): 284-292.

John J, Manchanda R (2011). Modulation of synaptic potentials and cell excitability by dendritic KIR and KAs channels in nucleus accumbens medium spiny neurons: a computational study. *J Biosci* **36**(2): 309-328.

Johnson CM, Peckler H, Tai LH, Wilbrecht L (2016). Rule learning enhances structural plasticity of long-range axons in frontal cortex. *Nat Commun* **7**: 10785.

Kandel ER (2012). The molecular biology of memory: cAMP, PKA, CRE, CREB-1, CREB-2, and CPEB. *Mol Brain* **5**: 14.

Kawaguchi Y (1993). Physiological, morphological, and histochemical characterization of three classes of interneurons

in rat neostriatum. *J Neurosci* **13**(11): 4908-4923.

Kawaguchi Y, Kubota Y (1997). GABAergic cell subtypes and their synaptic connections in rat frontal cortex. *Cereb Cortex* **7**(6): 476-486.

Kawashima T, Okuno H, Bito H (2014). A new era for functional labeling of neurons: activity-dependent promoters have come of age. *Front Neural Circuits* **8**: 37.

Kelley AE (2004). Ventral striatal control of appetitive motivation: role in ingestive behavior and reward-related learning. *Neurosci Biobehav Rev* **27**(8): 765-776.

Kelley AE, Schiltz CA, Landry CF (2005). Neural systems recruited by drug- and food-related cues: studies of gene activation in corticolimbic regions. *Physiol Behav* **86**(1-2): 11-14.

Kemenes I, Straub VA, Nikitin ES, Staras K, O'Shea M, Kemenes G*, et al* (2006). Role of delayed nonsynaptic neuronal plasticity in long-term associative memory. *Curr Biol* **16**(13): 1269-1279.

Kemp JM, Powell TP (1971a). The site of termination of afferent fibres in the caudate nucleus. *Philos Trans R Soc Lond B Biol Sci* **262**(845): 413-427.

Kemp JM, Powell TP (1971b). The structure of the caudate nucleus of the cat: light and electron microscopy. *Philos Trans R Soc Lond B Biol Sci* **262**(845): 383-401.

Kessels HW, Malinow R (2009). Synaptic AMPA receptor plasticity and behavior. *Neuron* **61**(3): 340-350.

Kirouac GJ (2015). Placing the paraventricular nucleus of the thalamus within the brain circuits that control behavior. *Neurosci Biobehav Rev* **56**: 315-329.

Kleppe IC, Robinson HP (1999). Determining the activation time course of synaptic AMPA receptors from openings of colocalized NMDA receptors. *Biophys J* **77**(3): 1418-1427.

Kobilka BK (2007). G protein coupled receptor structure and activation. *Biochim Biophys Acta* **1768**(4): 794-807.

Kolb B (1984). Functions of the frontal cortex of the rat: a comparative review. *Brain Res* **320**(1): 65-98.

Kolb B, Gibb R, Robinson TE (2003). Brain Plasticity and Behavior. *Current Directions in Psychological Science* **12**(1): 5.

Konorski J (1948). *Conditioned reflexes and neuron organization* Cambridge University PRess: Cambridge.

Konorski J (1967). *Integrative activity of the brain: An interdisciplinary* Chicago Press: Chicago, US.

Konorski J, Scwejkowska G (1956). Reciprocal transformation of heterogeneous conditioned reflexes *Acta Biologiae Experimentalis* **17**(1): 19.

Konradi C, Leveque JC, Hyman SE (1996). Amphetamine and dopamine-induced immediate early gene expression in striatal neurons depends on postsynaptic NMDA receptors and calcium. *J Neurosci* **16**(13): 4231-4239.

Koob GF, Volkow ND (2010). Neurocircuitry of addiction. *Neuropsychopharmacology* **35**(1): 217-238.

Koos T, Tepper JM (1999). Inhibitory control of neostriatal projection neurons by GABAergic interneurons. *Nat Neurosci* **2**(5): 467-472.

Koos T, Tepper JM (2002). Dual cholinergic control of fast-spiking interneurons in the neostriatum. *J Neurosci* **22**(2): 529-535.

Korb E, Finkbeiner S (2011). Arc in synaptic plasticity: from gene to behavior. *Trends Neurosci* **34**(11): 591-598.

Kourrich S, Calu DJ, Bonci A (2015). Intrinsic plasticity: an emerging player in addiction. *Nat Rev Neurosci* **16**(3): 173-184.

Kourrich S, Thomas MJ (2009). Similar neurons, opposite adaptations: psychostimulant experience differentially alters firing properties in accumbens core versus shell. *J Neurosci* **29**(39): 12275-12283.

Kourrich S, Rothwell, PE, Klug JR, Thomas MJ. (2007). Cocaine experience controls bidirectional synaptic plasticity in the nucleus accumbens. *J Neurosci*, **27**(30): 7921–7928.

Koya E, Cruz FC, Ator R, Golden SA, Hoffman AF, Lupica CR*, et al* (2012). Silent synapses in selectively activated nucleus accumbens neurons following cocaine sensitization. *Nat Neurosci* **15**(11): 1556-1562.

Koya E, Golden SA, Harvey BK, Guez-Barber DH, Berkow A, Simmons DE*, et al* (2009). Targeted disruption of cocaine-activated nucleus accumbens neurons prevents context-specific sensitization. *Nat Neurosci* **12**(8): 1069-1073.

Krasne FB, Glanzman DL (1995). What we can learn from invertebrate learning. *Annual Reveiws of Psychology* **46**: 39.

Kumaresan V, Yuan M, Yee J, Famous KR, Anderson SM, Schmidt HD*, et al* (2009). Metabotropic glutamate receptor 5 (mGluR5) antagonists attenuate cocaine priming- and cue-induced reinstatement of cocaine seeking. *Behav Brain Res* **202**(2): 238-244.

Kupchik YM, Brown RM, Heinsbroek JA, Lobo MK, Schwartz DJ, Kalivas PW (2015). Coding the direct/indirect pathways by D1 and D2 receptors is not valid for accumbens projections. *Nat Neurosci* **18**(9): 1230-1232.

Lanciego JL, Luquin N, Obeso JA (2012). Functional neuroanatomy of the basal ganglia. *Cold Spring Harb Perspect Med* **2**(12): a009621.

Lashley KS (1930). Basic neural mechanisms in behavior. *Psychological Review* **37**(1): 23.

Lavenex P, Amaral DG (2000). Hippocampal-neocortical interaction: a hierarchy of associativity. *Hippocampus* **10**(4): 420-430.

Lavoie AM, Mizumori SJ (1994). Spatial, movement- and reward-sensitive discharge by medial ventral striatum neurons of rats. *Brain Res* **638**(1-2): 157-168.

Lazarus M, Huang ZL, Lu J, Urade Y, Chen JF (2012). How do the basal ganglia regulate sleep-wake behavior? *Trends Neurosci* **35**(12): 723-732.

Le Merrer J, Stephens DN (2006). Food-induced behavioral sensitization, its cross-sensitization to cocaine and morphine, pharmacological blockade, and effect on food intake. *J Neurosci* **26**(27): 7163-7171.

Lee AT, Vogt D, Rubenstein JL, Sohal VS (2014). A class of GABAergic neurons in the prefrontal cortex sends long-range projections to the nucleus accumbens and elicits acute avoidance behavior. *J Neurosci* **34**(35): 11519-11525.

Lee HJ, Gallagher M, Holland PC (2010). The central amygdala projection to the substantia nigra reflects prediction error information in appetitive conditioning. *Learn Mem* **17**(10): 531-538.

Lenoir M, Serre F, Cantin L, Ahmed SH (2007). Intense sweetness surpasses cocaine reward. *PLoS One* **2**(8): e698.

Leri F, Flores J, Rajabi H, Stewart J (2003). Effects of cocaine in rats exposed to heroin. *Neuropsychopharmacology* **28**(12): 2102-2116.

Levey AI, Kitt CA, Simonds WF, Price DL, Brann MR (1991). Identification and localization of muscarinic acetylcholine receptor proteins in brain with subtype-specific antibodies. *J Neurosci* **11**(10): 3218-3226.

Levitan L (1975). Tests of the Rescorla-Wagner model of Pavlovian conditioning. *Bulletin of the Psychonomic Society* **6**(3): 3.

Li Y, Acerbo MJ, Robinson TE (2004). The induction of behavioural sensitization is associated with cocaine-induced structural plasticity in the core (but not shell) of the nucleus accumbens. *Eur J Neurosci* **20**(6): 1647-1654.

Liang J, Suryanarayanan A, Chandra D, Homanics GE, Olsen RW, Spigelman I (2008). Functional consequences of GABAA receptor alpha 4 subunit deletion on synaptic and extrasynaptic currents in mouse dentate granule cells. *Alcohol Clin Exp Res* **32**(1): 19-26.

Liu S, Globa AK, Mills F, Naef L, Qiao M, Bamji SX*, et al* (2016). Consumption of palatable food primes food approach behavior by rapidly increasing synaptic density in the VTA. *Proc Natl Acad Sci U S A* **113**(9): 2520-2525.

Lobo MK (2009). Molecular profiling of striatonigral and striatopallidal medium spiny neurons past, present, and future. *Int Rev Neurobiol* **89**: 1-35.

Lopatin AN, Makhina EN, Nichols CG (1995). The mechanism of inward rectification of potassium channels: "long-pore plugging" by cytoplasmic polyamines. *J Gen Physiol* **106**(5): 923-955.

Loussouarn G, Park KH, Bellocq C, Baro I, Charpentier F, Escande D (2003). Phosphatidylinositol-4,5-bisphosphate, PIP2, controls KCNQ1/KCNE1 voltage-gated potassium channels: a functional homology between voltage-gated and inward rectifier K+ channels. *EMBO J* **22**(20): 5412-5421.

Lubow RE (1973). Latent inhibition. *Psychol Bull* **79**(6): 398-407.

Luckman SM, Dyball RE, Leng G (1994). Induction of c-fos expression in hypothalamic magnocellular neurons requires synaptic activation and not simply increased spike activity. *J Neurosci* **14**(8): 4825-4830.

Luscher C, Malenka RC. (2011). Drug-evoked synaptic plasticity in addiction: from molecular changes to circuit remodelling. *Neuron* **69**(4): 650-663.

Luscher C, Slesinger PA (2010). Emerging roles for G protein-gated inwardly rectifying potassium (GIRK) channels in health and disease. *Nat Rev Neurosci* **11**(5): 301-315.

Ma YY, Guo CY, Yu P, Lee DY, Han JS, Cui CL (2006). The role of NR2B containing NMDA receptor in place preference conditioned with morphine and natural reinforcers in rats. *Exp Neurol* **200**(2): 343-355.

Mackintosh NJ (1974). *The psychology of animal learning* Academic Press: London.

MacLeod NK, James TA, Kilpatrick IC, Starr MS (1980). Evidence for a GABAergic nigrothalamic pathway in the rat. II. Electrophysiological studies. *Exp Brain Res* **40**(1): 55-61.

Magnus R (1924). *Körperstellung* Springer: Berlin.

Maki BA, Popescu GK (2014). Extracellular Ca(2+) ions reduce NMDA receptor conductance and gating. *J Gen Physiol* **144**(5): 379-392.

Malenka RC, Nicoll RA (1999). Long-term potentiation--a decade of progress? *Science* **285**(5435): 1870-1874.

Man HY (2011). GluA2-lacking, calcium-permeable AMPA receptors – inducers of plasticity? *Curr Opin Neurobiol,* **21**(2): 291-298.

Mangiavacchi S, Wolf ME (2004). D1 dopamine receptor stimulation increases the rate of AMPA receptor insertion onto the surface of cultured nucleus accumbens neurons through a pathway dependent on protein kinase A. *J Neurochem* **88**(5): 1261-1271.

Martin-Iverson MT, Szostak C, Fibiger HC (1986). 6-Hydroxydopamine lesions of the medial prefrontal cortex fail to influence intravenous self-administration of cocaine. *Psychopharmacology (Berl)* **88**(3): 310-314.

Mattson BJ, Bossert JM, Simmons DE, Nozaki N, Nagarkar D, Kreuter JD*, et al* (2005). Cocaine-induced CREB phosphorylation in nucleus accumbens of cocaine-sensitized rats is enabled by enhanced activation of extracellular signal-related kinase, but not protein kinase A. *J Neurochem* **95**(5): 1481-1494.

Maurin Y, Banrezes B, Menetrey A, Mailly P, Deniau JM (1999). Three-dimensional distribution of nigrostriatal neurons in the rat: relation to the topography of striatonigral projections. *Neuroscience* **91**(3): 891-909.

Mazur JE (2012). *Learning and behaviour* Routledge: London.

McCutcheon JE, Ebner SR, Loriaux AL, Roitman MF (2012). Encoding of aversion by dopamine and the nucleus accumbens. *Front Neurosci* **6**: 137.

McKay BM, Matthews EA, Oliveira FA, Disterhoft JF (2009). Intrinsic neuronal excitability is reversibly altered by a single experience in fear conditioning. *J Neurophysiol* **102**(5): 2763-2770.

McKay BM, Oh MM, Disterhoft JF (2013). Learning increases intrinsic excitability of hippocampal interneurons. *J Neurosci* **33**(13): 5499-5506.

Meil WM, See RE (1997). Lesions of the basolateral amygdala abolish the ability of drug associated cues to reinstate responding during withdrawal from self-administered cocaine. *Behav Brain Res* **87**(2): 139-148.

Mermelstein PG, Song WJ, Tkatch T, Yan Z, Surmeier DJ (1998). Inwardly rectifying potassium (IRK) currents are correlated with IRK subunit expression in rat nucleus accumbens medium spiny neurons. *J Neurosci* **18**(17): 6650-6661.

Mikkelsen JD, Larsen MH (2006). Effects of stress and adrenalectomy on activity-regulated cytoskeleton protein (Arc) gene expression. *Neurosci Lett* **403**(3): 239-243.

Mogenson GJ, Jones DL, Yim CY (1980). From motivation to action: functional interface between the limbic system and the motor system. *Prog Neurobiol* **14**(2-3): 69-97.

Moyer JR, Jr., Thompson LT, Disterhoft JF (1996). Trace eyeblink conditioning increases CA1 excitability in a transient and learning-specific manner. *J Neurosci* **16**(17): 5536-5546.

Mtchedlishvili Z, Kapur J (2006). High-affinity, slowly desensitizing GABAA receptors mediate tonic inhibition in hippocampal dentate granule cells. *Mol Pharmacol* **69**(2): 564-575.

Mu P, Moyer JT, Ishikawa M, Zhang Y, Panksepp J, Sorg BA*, et al* (2010). Exposure to cocaine dynamically regulates the intrinsic membrane excitability of nucleus accumbens neurons. *J Neurosci* **30**(10): 3689-3699.

Mucha RF, Iversen SD (1986). Increased food intake after opioid microinjections into nucleus accumbens and ventral tegmental area of rat. *Brain Res* **397**(2): 214-224.

Murray JE, Belin D, Everitt BJ (2012). Double dissociation of the dorsomedial and dorsolateral striatal control over the acquisition and performance of cocaine seeking. *Neuropsychopharmacology* **37**(11): 2456-2466.

Nagy JI, Carter DA, Fibiger HC (1978). Anterior striatal projections to the globus pallidus, entopeduncular nucleus and substantia nigra in the rat: the GABA connection. *Brain Res* **158**(1): 15-29.

Nakanishi S (1992). Molecular diversity of glutamate receptors and implications for brain function. *Science* **258**(5082): 597-603.

Nestler EJ (2001). Molecular basis of long-term plasticity underlying addiction. *Nat Rev Neurosci* **2**(2): 119-128.

Nguyen TV, Kosofsky BE, Birnbaum R, Cohen BM, Hyman SE (1992). Differential expression of c-fos and zif268 in rat striatum after haloperidol, clozapine, and amphetamine. *Proc Natl Acad Sci U S A* **89**(10): 4270-4274.

Nisenbaum ES, Wilson CJ (1995). Potassium currents responsible for inward and outward rectification in rat neostriatal spiny projection neurons. *J Neurosci* **15**(6): 4449-4463.

Nordquist RE, Pennartz CM, Uylings HB, Joosten RN, Jonker AJ, Groenewegen HJ*, et al* (2003). C-fos activation patterns in rat prefrontal cortex during acquisition of a cued classical conditioning task. *Behav Brain Res* **146**(1-2): 65-75.

Oginsky MF, Maust JD, Corthell JT, Ferrario CR (2016). Enhanced cocaine-induced locomotor sensitization and intrinsic excitability of NAc medium spiny neurons in adult but not in adolescent rats susceptible to diet-induced obesity. *Psychopharmacology (Berl)* **233**(5): 773-784.

Oh MM, Disterhoft JF (2015). Increased Excitability of Both Principal Neurons and Interneurons during Associative Learning. *Neuroscientist* **21**(4): 372-384.

Oliva I, Wanat MJ (2016). Ventral Tegmental Area Afferents and Drug-Dependent Behaviors. *Front Psychiatry* **7**: 30.

Ongur D, Price JL (2000). The organization of networks within the orbital and medial prefrontal cortex of rats, monkeys and humans. *Cereb Cortex* **10**(3): 206-219.

Ottersen OP (1982). Connections of the amygdala of the rat. IV: Corticoamygdaloid and intraamygdaloid connections as studied with axonal transport of horseradish peroxidase. *J Comp Neurol* **205**(1): 30-48.

Paoletti P, Neyton J (2007). NMDA receptor subunits: function and pharmacology. *Curr Opin Pharmacol* **7**(1): 39-47.

Parent A, Hazrati LN (1995). Functional anatomy of the basal ganglia. I. The cortico-basal ganglia-thalamo-cortical loop. *Brain Res Brain Res Rev* **20**(1): 91-127.

Parker JG, Beutler LR, Palmiter RD (2011). The contribution of NMDA receptor signaling in the corticobasal ganglia reward network to appetitive Pavlovian learning. *J Neurosci* **31**(31): 11362-11369.

Parkinson JA, Cardinal RN, Everitt BJ (2000a). Limbic cortical-ventral striatal systems underlying appetitive conditioning. *Prog Brain Res* **126**: 263-285.

Parkinson JA, Dalley JW, Cardinal RN, Bamford A, Fehnert B, Lachenal G*, et al* (2002). Nucleus accumbens dopamine depletion impairs both acquisition and performance of appetitive Pavlovian approach behaviour: implications for

mesoaccumbens dopamine function. *Behav Brain Res* **137**(1-2): 149-163.

Parkinson JA, Willoughby PJ, Robbins TW, Everitt BJ (2000b). Disconnection of the anterior cingulate cortex and nucleus accumbens core impairs Pavlovian approach behavior: further evidence for limbic cortical-ventral striatopallidal systems. *Behav Neurosci* **114**(1): 42-63.

Pavlov IP (1927). *Conditioned reflexes: an investigation of the physiological activity of the cerebral cortex.* Oxford University Press: Oxford, UK.

Pennartz CM, Groenewegen HJ, Lopes da Silva FH (1994). The nucleus accumbens as a complex of functionally distinct neuronal ensembles: an integration of behavioural, electrophysiological and anatomical data. *Prog Neurobiol* **42**(6): 719-761.

Perrin-Terrin AS, Jeton F, Pichon A, Frugiere A, Richalet JP, Bodineau L*, et al* (2016). The c-FOS Protein Immunohistological Detection: A Useful Tool As a Marker of Central Pathways Involved in Specific Physiological Responses In Vivo and Ex Vivo. *J Vis Exp*(110).

Perry CJ, McNally GP (2013). A role for the ventral pallidum in context-induced and primed reinstatement of alcohol seeking. *Eur J Neurosci* **38**(5): 2762-2773.

Phillips AG, Fibiger HC (1978). The role of dopamine in maintaining intracranial self-stimulation in the ventral tegmentum, nucleus accumbens, and medial prefrontal cortex. *Can J Psychol* **32**(2): 58-66.

Pickens CL, Airavaara M, Theberge F, Fanous S, Hope BT, Shaham Y (2011). Neurobiology of the incubation of drug craving. *Trends Neurosci* **34**(8): 411-420.

Pickens CL, Saddoris MP, Gallagher M, Holland PC (2005). Orbitofrontal lesions impair use of cue-outcome associations in a devaluation task. *Behav Neurosci* **119**(1): 317-322.

Pin JP, Duvoisin R (1995). The metabotropic glutamate receptors: structure and functions. *Neuropharmacology* **34**(1): 1-26.

Pirker S, Schwarzer C, Wieselthaler A, Sieghart W, Sperk G (2000). GABA(A) receptors: immunocytochemical distribution of 13 subunits in the adult rat brain. *Neuroscience* **101**(4): 815-850.

Prescott SA, De Koninck Y (2003). Gain control of firing rate by shunting inhibition: roles of synaptic noise and dendritic saturation. *Proc Natl Acad Sci U S A* **100**(4): 2076-2081.

Ralevic V, Burnstock G (1998). Receptors for purines and pyrimidines. *Pharmacol Rev* **50**(3): 413-492.

Raybuck JD, Lattal KM (2014). Differential effects of dorsal hippocampal inactivation on expression of recent and remote drug and fear memory. *Neurosci Lett* **569**: 1-5.

Reiner A, Medina L, Veenman CL (1998). Structural and functional evolution of the basal ganglia in vertebrates. *Brain Res Brain Res Rev* **28**(3): 235-285.

Rescorla RA, Wagner AR (1972). A theory of Pavlovian conditioning: Variations in the effectiveness of reinforcement and nonreinforcement. In: Black AH, Prokasy WF (eds). *Classical conditioning II: current research and theory*. Appleton-Century-Crofts: New York.

Rhodes JS, Ryabinin AE, Crabbe JC (2005). Patterns of brain activation associated with contextual conditioning to methamphetamine in mice. *Behavioral neuroscience* **119**(3): 759-771.

Roberts DC, Koob GF (1982). Disruption of cocaine self-administration following 6-hydroxydopamine lesions of the ventral tegmental area in rats. *Pharmacol Biochem Behav* **17**(5): 901-904.

Roberts DC, Koob GF, Klonoff P, Fibiger HC (1980). Extinction and recovery of cocaine self-administration following 6-hydroxydopamine lesions of the nucleus accumbens. *Pharmacol Biochem Behav* **12**(5): 781-787.

Robinson TE, Flagel SB (2009). Dissociating the predictive and incentive motivational properties of reward-related cues through the study of individual differences. *Biol Psychiatry* **65**(10): 869-873.

Rosenkilde CE, Bauer RH, Fuster JM (1981). Single cell activity in ventral prefrontal cortex of behaving monkeys. *Brain Res* **209**(2): 375-394.

Ryabinin AE, Criado JR, Henriksen SJ, Bloom FE, Wilson MC (1997). Differential sensitivity of c-Fos expression in hippocampus and other brain regions to moderate and low doses of alcohol. *Molecular psychiatry* **2**(1): 32-43.

Salgado S, Kaplitt MG (2015). The Nucleus Accumbens: A Comprehensive Review. *Stereotact Funct Neurosurg* **93**(2): 75-93.

Sassone-Corsi P (2012). The cyclic AMP pathway. *Cold Spring Harb Perspect Biol* **4**(12).

Schoenbaum G, Setlow B, Nugent SL, Saddoris MP, Gallagher M (2003). Lesions of orbitofrontal cortex and basolateral amygdala complex disrupt acquisition of odor-guided discriminations and reversals. *Learn Mem* **10**(2): 129-140.

Schotanus SM, Chergui K (2008a). Dopamine D1 receptors and group I metabotropic glutamate receptors contribute to the induction of long-term potentiation in the nucleus accumbens. *Neuropharmacology* **54**(5): 837-844.

Schotanus SM, Chergui K (2008b). Long-term potentiation in the nucleus accumbens requires both NR2A- and NR2B-containing N-methyl-D-aspartate receptors. *Eur J Neurosci* **27**(8): 1957-1964.

Schroeder BE, Binzak JM, Kelley AE (2001). A common profile of prefrontal cortical activation following exposure to nicotine- or chocolate-associated contextual cues. *Neuroscience* **105**(3): 535-545.

Schultz W, Dayan P, Montague PR (1997). A neural substrate of prediction and reward. *Science* **275**(5306): 1593-1599.

Schwarz LA, Luo L (2015). Organization of the Locus Coeruleus-Norepinephrine system. *Curr Biol,* **25**(21): 1051-1056.

Sergeeva OA, Chepkova AN, Haas HL (2002). Guanidinoethyl sulphonate is a glycine receptor antagonist in striatum. *Br J Pharmacol* **137**(6): 855-860.

Sesack SR, Deutch AY, Roth RH, Bunney BS (1989). Topographical organization of the efferent projections of the medial prefrontal cortex in the rat: an anterograde tract-tracing study with Phaseolus vulgaris leucoagglutinin. *J Comp Neurol* **290**(2): 213-242.

Sesack SR, Pickel VM (1990). In the rat medial nucleus accumbens, hippocampal and catecholaminergic terminals converge on spiny neurons and are in apposition to each other. *Brain Res* **527**(2): 266-279.

Shen W, Hernandez-Lopez S, Tkatch T, Held JE, Surmeier DJ (2004). Kv1.2-containing K+ channels regulate subthreshold excitability of striatal medium spiny neurons. *J Neurophysiol* **91**(3): 1337-1349.

Shen W, Tian X, Day M, Ulrich S, Tkatch T, Nathanson NM*, et al* (2007). Cholinergic modulation of Kir2 channels selectively elevates dendritic excitability in striatopallidal neurons. *Nat Neurosci* **10**(11): 1458-1466.

Sherrington CS (1906). *The Integrative Action of the Nervous System* Oxford University Press: Oxford.

Shiflett MW, Balleine BW (2010). At the limbic-motor interface: disconnection of basolateral amygdala from nucleus accumbens core and shell reveals dissociable components of incentive motivation. *Eur J Neurosci* **32**(10): 1735-1743.

Shiflett MW, Balleine BW (2011). Contributions of ERK signaling in the striatum to instrumental learning and performance. *Behav Brain Res* **218**(1): 240-247.

Shirayama Y, Chaki S (2006). Neurochemistry of the nucleus accumbens and its relevance to depression and antidepressant action in rodents. *Curr Neuropharmacol* **4**(4): 277-291.

Sigel E, Steinmann ME (2012). Structure, function, and modulation of GABA(A) receptors. *J Biol Chem* **287**(48): 40224-40231.

Simonyi A, Schachtman TR, Christoffersen GR (2005). The role of metabotropic glutamate receptor 5 in learning and memory processes. *Drug News Perspect* **18**(6): 353-361.

Skinner BF (1938). *The Behavior of organisms: An experimental analysis.* Appleton-Century: New York.

Skinner BF (1969). *Contingencies of reinforcement: A theoretical analysis* Meredith: New York.

Smeyne RJ, Schilling K, Robertson L, Luk D, Oberdick J, Curran T*, et al* (1992). fos-lacZ transgenic mice: mapping sites of gene induction in the central nervous system. *Neuron* **8**(1): 13-23.

Smith KS, Tindell AJ, Aldridge JW, Berridge KC (2009). Ventral pallidum roles in reward and motivation. *Behav Brain Res* **196**(2): 155-167.

Smith RJ, Lobo MK, Spencer S, Kalivas PW (2013). Cocaine-induced adaptations in D1 and D2 accumbens projection neurons (a dichotomy not necessarily synonymous with direct and indirect pathways). *Curr Opin Neurobiol* **23**(4): 546-552.

Smith Y, Bevan MD, Shink E, Bolam JP (1998). Microcircuitry of the direct and indirect pathways of the basal ganglia. *Neuroscience* **86**(2): 353-387.

Solomon PR, Groccia-Ellison ME (1996). Classic conditioning in aged rabbits: delay, trace, and long-delay conditioning. *Behav Neurosci* **110**(3): 427-435.

Somogyi P, Bolam JP, Smith AD (1981). Monosynaptic cortical input and local axon collaterals of identified striatonigral neurons. A light and electron microscopic study using the Golgi-peroxidase transport-degeneration procedure. *J Comp Neurol* **195**(4): 567-584.

Song C, Ehlers VL, Moyer JR, Jr. (2015). Trace Fear Conditioning Differentially Modulates Intrinsic Excitability of Medial Prefrontal Cortex-Basolateral Complex of Amygdala Projection Neurons in Infralimbic and Prelimbic Cortices. *J Neurosci* **35**(39): 13511-13524.

Sripanidkulchai K, Sripanidkulchai B, Wyss JM (1984). The cortical projection of the basolateral amygdaloid nucleus in the rat: a retrograde fluorescent dye study. *J Comp Neurol* **229**(3): 419-431.

Staley K, Smith R (2001). A new form of feedback at the GABAA receptor. *Nature Neuroscience* **4**: 3.

Stalnaker TA, Cooch NK, Schoenbaum G (2015). What the orbitofrontal cortex does not do. *Nat Neurosci* **18**(5): 620-627.

Stefanik MT, Kalivas PW (2013). Optogenetic dissection of basolateral amygdala projections during cue-induced reinstatement of cocaine seeking. *Front Behav Neurosci* **7**: 213.

Steinberg EE, Boivin JR, Saunders BT, Witten IB, Deisseroth K, Janak PH (2014). Positive reinforcement mediated by midbrain dopamine neurons requires D1 and D2 receptor activation in the nucleus accumbens. *PLoS One* **9**(4): e94771.

Stewart J, Vezina P (1989). Microinjections of Sch-23390 into the ventral tegmental area and substantia nigra pars reticulata attenuate the development of sensitization to the locomotor activating effects of systemic amphetamine. *Brain Res* **495**(2): 401-406.

Struthers WM, DuPriest A, Runyan J (2005). Habituation reduces novelty-induced FOS expression in the striatum and cingulate cortex. *Exp Brain Res* **167**(1): 136-140.

Stuber GD, Hnasko TS, Britt JP, Edwards RH, Bonci A (2010). Dopaminergic terminals in the nucleus accumbens but not the dorsal striatum corelease glutamate. *J Neurosci* **30**(24): 8229-8233.

Stuber GD, Klanker M, de Ridder B, Bowers MS, Joosten RN, Feenstra MG*, et al* (2008). Reward-predictive cues enhance excitatory synaptic strength onto midbrain dopamine neurons. *Science* **321**(5896): 1690-1692.

Stuber GD, Sparta DR, Stamatakis AM, van Leeuwen WA, Hardjoprajitno JE, Cho S*, et al* (2011). Excitatory transmission from the amygdala to nucleus accumbens facilitates reward seeking. *Nature* **475**(7356): 377-380.

Suto N, Laque A, De Ness GL, Wagner GE, Watry D, Kerr T*, et al* (2016). Distinct memory engrams in the infralimbic cortex of rats control opposing environmental actions on a learned behavior. *Elife* **5**.

Sutton MA, McGibney K, Beninger RJ (2000). Conditioned locomotion in rats following amphetamine infusion into the nucleus accumbens: blockade by coincident inhibition of protein kinase A. *Behav Pharmacol* **11**(5): 365-376.

Taylor JR, Robbins TW (1984). Enhanced behavioural control by conditioned reinforcers following microinjections of d-amphetamine into the nucleus accumbens. *Psychopharmacology (Berl)* **84**(3): 405-412.

Taylor JR, Robbins TW (1986). 6-Hydroxydopamine lesions of the nucleus accumbens, but not of the caudate nucleus, attenuate enhanced responding with reward-related stimuli produced by intra-accumbens d-amphetamine. *Psychopharmacology (Berl)* **90**(3): 390-397.

Tepper JM, Plenz D (2006). Microcircuits in the striatum: Striatal cell types and their interaction. In: Grillner S, Graybiel AM (eds). *The Interface*

*between Neurons and Global Brain Function*. The MIT Press: Cambridge, MA:.

Tepper JM, Tecuapetla F, Koos T, Ibanez-Sandoval O (2010). Heterogeneity and diversity of striatal GABAergic interneurons. *Front Neuroanat* **4**: 150.

Thomas MJ, Beurrier C, Bonci A, Malenka RC (2001). Long-term depression in the nucleus accumbens: a neural correlate of behavioral sensitization to cocaine. *Nat Neurosci* **4**(12): 1217-1223.

Thorndike EL (1905). *The elements of psychology* A. G. Seiler.

: New York.

Tilson HA, Rech RH (1973). Conditioned Drug Effects and Absence of Tolerance to d-Amphetamine Induced Motor Activity *Pharmacology Biochemistry and Behavior* **1**(2): 4.

Tritsch NX, Ding JB, Sabatini BL (2012). Dopaminergic neurons inhibit striatal output through non-canonical release of GABA. *Nature* **490**(7419): 262-266.

Tropea TF, Kosofsky BE, Rajadhyaksha AM (2008). Enhanced CREB and DARPP-32 phosphorylation in the nucleus accumbens and CREB, ERK, and GluR1 phosphorylation in the dorsal hippocampus is associated with cocaine-conditioned place preference behavior. *J Neurochem* **106**(4): 1780-1790.

Tsai HC, Zhang F, Adamantidis A, Stuber GD, Bonci A, de Lecea L*, et al* (2009). Phasic firing in dopaminergic neurons is sufficient for behavioral conditioning. *Science* **324**(5930): 1080-1084.

Tunstall BJ, Kearns DN (2016). Cocaine can generate a stronger conditioned reinforcer than food despite being a weaker primary reinforcer. *Addict Biol* **21**(2): 282-293.

Ulrich D, Bettler B (2007). GABA(B) receptors: synaptic functions and mechanisms of diversity. *Curr Opin Neurobiol* **17**(3): 298-303.

Ungless MA, Magill PJ, Bolam JP (2004). Uniform inhibition of dopamine neurons in the ventral tegmental area by aversive stimuli. *Science* **303**(5666): 2040-2042.

Ungless MA, Whistler JL, Malenka RC, Bonci A (2001). Single cocaine exposure in vivo induces long-term potentiation in dopamine neurons. *Nature* **411**(6837): 583-587.

Uslaner JM, Norton CS, Watson SJ, Akil H, Robinson TE (2003). Amphetamine-induced c-fos mRNA expression in the caudate-putamen and subthalamic nucleus: interactions between dose, environment, and neuronal phenotype. *Journal of neurochemistry* **85**(1): 105-114.

Usuda I, Tanaka K, Chiba T (1998). Efferent projections of the nucleus accumbens in the rat with special reference to subdivision of the nucleus: biotinylated dextran amine study. *Brain Res* **797**(1): 73-93.

Uylings HB, Groenewegen HJ, Kolb B (2003). Do rats have a prefrontal cortex? *Behav Brain Res* **146**(1-2): 3-17.

van Aerde KI, Feldmeyer D (2015). Morphological and physiological characterization of pyramidal neuron subtypes in rat medial prefrontal cortex. *Cereb Cortex* **25**(3): 788-805.

Van Bockstaele EJ, Pickel VM (1995). GABA-containing neurons in the ventral tegmental area project to the nucleus accumbens in rat brain. *Brain Res* **682**(1-2): 215-221.

van der Kooy D, Kuypers HG (1979). Fluorescent retrograde double labeling: axonal branching in the ascending raphe and nigral projections. *Science* **204**(4395): 873-875.

Van der Werf YD, Witter MP, Groenewegen HJ (2002). The intralaminar and midline nuclei of the thalamus. Anatomical and functional evidence for participation in processes of arousal and awareness. *Brain Res Brain Res Rev* **39**(2-3): 107-140.

Voglis G, Tavernarakis N (2006). The role of synaptic ion channels in synaptic plasticity. *EMBO Rep* **7**(11): 1104-1110.

Voorn P, Vanderschuren LJ, Groenewegen HJ, Robbins TW, Pennartz CM (2004). Putting a spin on the dorsal-ventral divide of the striatum. *Trends Neurosci* **27**(8): 468-474.

Watabe-Uchida M, Zhu L, Ogawa SK, Vamanrao A, Uchida, N (2012). Whole-brain mapping of direect inputs to midbrain dopamine neurons. *Neuron,* **74**(5): 858-873.

Waltereit R, Dammermann B, Wulff P, Scafidi J, Staubli U, Kauselmann G*, et al* (2001). Arg3.1/Arc mRNA induction by Ca2+ and cAMP requires protein kinase A and mitogen-activated

protein kinase/extracellular regulated kinase activation. *J Neurosci* **21**(15): 5484-5493.

Wang Y, Prywes R (2000). Activation of the c-fos enhancer by the erk MAP kinase pathway through two sequence elements: the c-fos AP-1 and p62TCF sites. *Oncogene* **19**(11): 1379-1385.

Ward RP, Dorsa DM (1996). Colocalization of serotonin receptor subtypes 5-HT2A, 5-HT2C, and 5-HT6 with neuropeptides in rat striatum. *J Comp Neurol* **370**(3): 405-414.

Warren EB, Sillivan SE, Konradi C (2010). Receptors and Second Messengers in the Basal Ganglia. In: Steiner H, Tseng K, Y; (eds). *Handbook of Basal Ganglia Structure and Function*. Academic Press: London, UK.

West EA, Carelli RM (2016). Nucleus Accumbens Core and Shell Differentially Encode Reward-Associated Cues after Reinforcer Devaluation. *J Neurosci* **36**(4): 1128-1139.

Whitaker LR, Carneiro de Oliveira PE, McPherson KB, Fallon RV, Planeta CS, Bonci A*, et al* (2016). Associative Learning Drives the Formation of Silent Synapses in Neuronal Ensembles of the Nucleus Accumbens. *Biol Psychiatry* **80**(3): 246-256.

Whitelaw RB, Markou A, Robbins TW, Everitt BJ (1996). Excitotoxic lesions of the basolateral amygdala impair the acquisition of cocaine-seeking behaviour under a second-order schedule of reinforcement. *Psychopharmacology (Berl)* **127**(3): 213-224.

Wickens JR, Alexander ME, Miller R (1991). Two dynamic modes of striatal function under dopaminergic-cholinergic control: simulation and analysis of a model. *Synapse* **8**(1): 1-12.

Williams DR, Williams H (1969). Auto-maintenance in the pigeon: sustained pecking despite contingent non-reinforcement. *J Exp Anal Behav* **12**(4): 511-520.

Wilson CJ, Kawaguchi Y (1996). The origins of two-state spontaneous membrane potential fluctuations of neostriatal spiny neurons. *J Neurosci* **16**(7): 2397-2410.

Windholz G (1986). A comparative analysis of the conditional reflex discoveries of Pavlov and Twitmyer, and the birth of a paradigm. *Pavlov J Biol Sci* **21**(4): 141-147.

Wong R, Hadjiyanni I, Wei HC, Polevoy G, McBride R, Sem KP*, et al* (2005). PIP2 hydrolysis and calcium release are required for cytokinesis in Drosophila spermatocytes. *Curr Biol* **15**(15): 1401-1406.

Xenias HS, Ibanez-Sandoval O, Koos T, Tepper JM (2015). Are striatal tyrosine hydroxylase interneurons dopaminergic? *J Neurosci* **35**(16): 6584-6599.

Xia Y, Driscoll JR, Wilbrecht L, Margolis EB, Fields HL, Hjelmstad GO (2011). Nucleus accumbens medium spiny neurons target non-dopaminergic neurons in the ventral tegmental area. *J Neurosci* **31**(21): 7811-7816.

Xu TX, Ma Q, Spealman RD, Yao WD (2010). Amphetamine modulation of long-term potentiation in the prefrontal cortex: dose dependency, monoaminergic contributions, and paradoxical rescue in hyperdopaminergic mutant. *J Neurochem* **115**(6): 1643-1654.

Yin HH, Knowlton BJ, Balleine BW (2004). Lesions of dorsolateral striatum preserve outcome expectancy but disrupt habit formation in instrumental learning. *Eur J Neurosci* **19**(1): 181-189.

Zaborszky L, Cullinan WE (1992). Projections from the nucleus accumbens to cholinergic neurons of the ventral pallidum: a correlated light and electron microscopic double-immunolabeling study in rat. *Brain Res* **570**(1-2): 92-101.

Zangenehpour S, Chaudhuri A (2002). Differential induction and decay curves of c-fos and zif268 revealed through dual activity maps. *Brain Res Mol Brain Res* **109**(1-2): 221-225.

Zhang W, Linden DJ (2003). The other side of the engram: experience-driven changes in neuronal intrinsic excitability. *Nat Rev Neurosci* **4**(11): 885-900.

Zhang W, Tingare A, Ng DC, Johnson HW, Schell MJ, Lord RL*, et al* (2012). IP3-dependent intracellular Ca2+ release is required for cAMP-induced c-fos expression in hippocampal neurons. *Biochem Biophys Res Commun* **425**(2): 450-455.

Zhang XF, Hu XT, White FJ (1998). Whole-cell plasticity in cocaine withdrawal: reduced sodium currents in nucleus accumbens neurons. *J Neurosci* **18**(1): 488-498.

Zhou FM, Lee CR (2011). Intrinsic and integrative properties of substantia nigra pars reticulata neurons. *Neuroscience* **198**: 69-94.

Zhu Y, Auerbach A (2001). Na(+) occupancy and Mg(2+) block of the n-methyl-d-aspartate receptor channel. *J Gen Physiol* **117**(3): 275-286.

Zombeck JA, Chen GT, Johnson ZV, Rosenberg DM, Craig AB, Rhodes JS (2008). Neuroanatomical specificity of conditioned responses to cocaine versus food in mice. *Physiol Behav* **93**(3): 637-650.

# Chapter 2.

# Materials and Methods

## 2.1. Animals

Male *Fos-GFP* mice (https://www.jax.org/strain/014135) previously bred onto a C57BL/6 background were bred with wild-type C57BL/6 females obtained from Charles River Laboratories at the University of Sussex (Figure 1A). Heterozygous *Fos-GFP* male mice continued to be bred at the University of Sussex ancillary unit with wild-type C57BL/6 females obtained from Charles River Laboratories UK. *Fos-GFP* male mice were used for electrophysiology and immunofluorescence experiments and C57BL/6 wild-type males were used for *in situ* hybridisation and immunofluorescence/immunohistochemical studies.

All mice were housed under a 12 h light/dark cycle (lights on at 7:00 A.M.) at the maintained temperature of 21±1°C and 50±5% relative humidity. Animals were aged 10-12 weeks at the beginning of behavioural testing. In Pavlovian approach studies (Chapter 3 and 4) mice were food restricted to 90% *ad libitum* body weight 1 week before behavioural testing until the completion of the behavioural experiments. All experiments were conducted in accordance with the UK 1986 Animal Scientific Procedures Act and received approval from the University of Sussex Ethics Committee.

## 2.2. Behavioural Experiments

### 2.2.1. Pavlovian Approach Experiments (Chapter 3 and 4)

*Apparatus*

All behavioural experiments were performed in standard mouse operant chambers (15.9 x 14 x 12.7 cm; Med Associates; Figure 1B), each housed within a sound-attenuating and light-resistant cubicle. The conditioning chamber front and rear access panels and ceiling were constructed from clear Plexiglas and the side walls were made from removable aluminium panels atop a stainless steel grid floor. Each chamber was

fitted with a recessed magazine situated in the centre of one side wall that dispensed a 10% sucrose solution serving as the unconditioned stimulus (US). An infrared beam detected head entries into the food magazine. The house light was situated in the side panel and was on for the duration of the behavioural experiments. A mechanical click generator provided a broad-frequency (0-15 kHz) sound, which served as a conditioned stimulus (CS) (Med Associates). Initiation and running of behavioural protocols, including the recording of head entries into the food magazine, was performed using Med-PC IV (Med Associates).

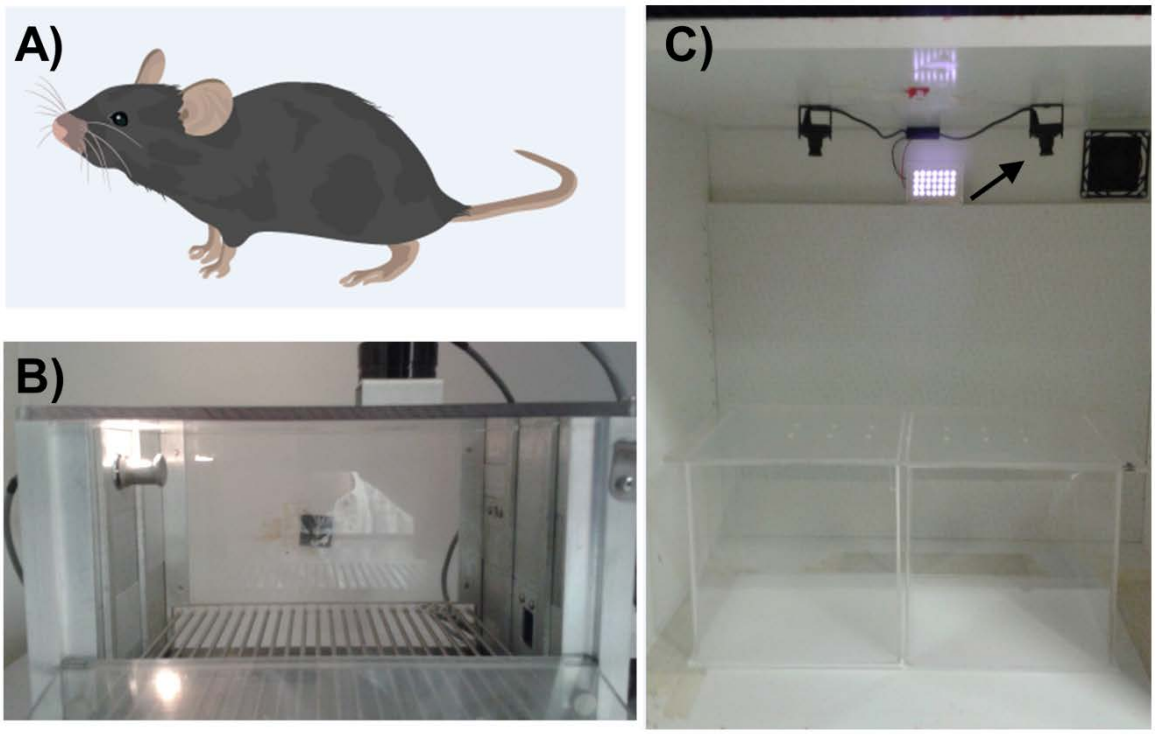


**Figure 1.** Behavioural experimentation with *Mus musculus* (C57BL/6). **A)** The C57BL/6 strain of mouse (cartoon). **B)** Skinner box used for Pavlovian approach experiments. House light (left), sucrose-delivery magazine (bottom right) and mechanical click generator (top) are shown. **C)** Experimental chambers for cocaine conditioned locomotion experiments. Video recordings of experimental chambers (clear acrylic) were captured from cameras (top, arrow). Animals were run in the dark, with light for recording provided by an infrared light source.

*Procedures*

Magazine training and Pavlovian conditioning: Mice were randomly assigned to the Paired or Unpaired groups that underwent identical procedures except that Unpaired mice only received sucrose in the home cage 1-4 h at random times before or after each conditioning session (Chapter 5 includes Paired mice only). One day after magazine training (in which Paired mice were pre-trained to the sucrose-delivery magazine with a 10% sucrose solution under a random interval-30 (RI-30) schedule) mice underwent 12 acquisition sessions over a 7 d period in the morning (8:00 A.M. to 12:00 P.M.) and/or afternoon (12:00 P.M. to 5:00 P.M.) for 1-2 sessions per day. Each acquisition session lasted approximately 24 min and consisted of six 120 s CS presentations separated by 120 s RI intertrial interval (ITI) periods. During each 120 s CS period, 13.3 µl of 10% sucrose solution was delivered into the magazine on an RI-30 s schedule (Paired mice) or was unrewarded (Unpaired mice). Twelve acquisition sessions produced selective responding to the CS.

Behavioural testing for Pavlovian approach conditioning: At 7-9 d (histology experiments) or 7-13 d (electrophysiology experiments) after the last acquisition session, both Paired and Unpaired mice were tested for Pavlovian approach. The testing schedule was identical to that used in conditioning, however under extinction conditions.

Behavioural testing for extinction learning: After magazine training and acquisition, mice in the extinction (EXT) experiments (Paired EXT and Unpaired EXT) underwent either 8 (histology) or 7-13 (electrophysiology) once-daily extinction sessions until test day (the final extinction session). During each extinction session, only the CS was presented in the absence of sucrose delivery. In the histology experiments, a third

group (Paired No EXT) was included and the experiment was conducted identically to the Paired mice in the previous Pavlovian approach experiments

Spontaneous recovery (SR) of Pavlovian approach: An additional group of Paired wild-type mice underwent conditioning and extinction sessions similar to the Paired EXT mice described above. After the last extinction session (EXT final), they remained in the colony room for an additional 6-7 d and were subsequently tested for SR of Pavlovian approach responding.

### 2.2.2. Cocaine Conditioned Locomotion Experiments (Chapter 5)

*Apparatus*

The behavioural experiments were performed in square clear acrylic locomotor chambers (20 x 20 x 20 cm) (Figure 1C). A CCTV camera with Ethovision$^{Tm}$ software (Noldus) was used for automated behavioural tracking. Light for image recording was provided by an infrared light source (Kemo, UK).

*Procedures*

Cocaine Locomotor Conditioning: Mice were randomly assigned to conditioned locomotion (CL) groups “Paired CL” or “Unpaired CL” in which cocaine injections (20 mg/kg, i.p.; MacFarlan Smith, UK) were paired with a novel context (locomotor chamber) or with the home cage, respectively. Mice received 2 injection sessions per day; on one session, the Paired and Unpaired CL mice received a cocaine and saline injection, respectively, before being placed in the locomotor chambers for 30 min. In an alternate session, Paired and Unpaired CL mice received saline and cocaine injections, respectively, in the home cage. Conditioning proceeded for five sessions with cocaine

injections counterbalanced between morning (8 A.M. – 12 P.M.) and afternoon (3 P.M. – 6 P.M.) sessions.

Conditioned Locomotion Test: Locomotor tests were conducted 7-13 (electrophysiology) or 7-11 (immunohistochemistry) days following the final conditioning session. Mice received a single saline injection and were placed in the locomotor chamber for 90 min after which their brains were extracted for electrophysiological and immunohistochemical analyses.

Extinction (EXT) learning and behavioural testing: Paired and Unpaired EXT mice received cocaine locomotor conditioning as described above (similar to Paired and Unpaired CL, respectively). However, one day following the final conditioning session, both groups of mice underwent 1-2 x daily extinction sessions, consisting of a saline injection preceding a 30 min locomotor chamber exposure. Saline injections were administered before Paired and Unpaired EXT mice were placed in the locomotor chamber to ensure stress due to injection was comparable across groups**.** Following 7-13 (10-16 sessions; electrophysiology) or 7-11 (10-14 sessions; immunohistochemistry) days of extinction, a 90 min extinction test session was conducted.

## 2.3. Histological Experiments

### 2.3.1. GFP immunofluorescence histochemistry (Chapter 3)

Ninety minutes after initiating the final test session, *Fos-GFP* mice were anesthetised with 200 mg/kg sodium pentobarbital and transcardially perfused with 4% paraformaldehyde. GFP immunofluorescence was performed as described (Koya *et al*, 2009) and, unless specified otherwise, all steps were performed at room temperature. To assess GFP expression, free-floating sections were washed in Tris-buffered saline (TBS; 0.025 M Tris-HCl, 0.5 M NaCl, pH 7.5) and blocked in 10% normal goat serum

(catalog #S-1000, Vector Laboratories) in TBST (TBS, 0.2% Triton X-100). Slices were then incubated at 4°C overnight in anti-GFP primary antibody (catalog #ab13970, Abcam) diluted 1/16000 in 3% normal goat serum TBST. The following day, slices were incubated for 2 h in anti-chicken 568 (catalog #SAB4600039, Sigma-Aldrich) at 1/200 in TBST. Slices were mounted on Superfrost Plus slides (catalog #UY-48512-00; Cole Parmer) air-dried, and coverslipped with PermaFluor (catalog #TA-030-FM, Thermo Scientific). Fluorescence images of GFP staining from left and right hemispheres of the NAc shell and OFC of 1-2 coronal sections per animal, corresponding to approximately bregma 1.18 and 2.46 (Paxinos and Franklin, 2001) respectively, were captured using a QI click camera (Qimaging) attached to an Olympus Bx53 microscope. GFP nuclei were quantified using iVision software (version 4.0.15, Biovision Technologies). The shell portion of the NAc was selected for this study because pilot experiments revealed sucrose-cue-induced GFP in this area.

### 2.3.2. In situ hybridisation (Chapter 3)

Forty-five minutes after the final test session, mice were killed and their brains were removed and rapidly frozen in isopentane at -50°C. Then, 10 µm sections containing the NAc shell (bregma 1.18) and OFC (bregma 2.46) were prepared using a Leica CM1900 cryostat. RNA-scope *in situ* hybridisation was performed as described previously (Rubio *et al*, 2015). All target probes were designed by Advanced Cell Diagnostics and targeted the mRNA of *Fos* (GenBank accession number NM_010234.2: target region, 443-1447), *Slc17a7* (glutamate transporter; GenBank accession number NM_ 182993.2: target region, 464-1415), *Slc32a1* (GABA transporter; GenBank accession number NM_009508.2: target region, 894-2037), Drd1a (dopamine receptor1; GenBank accession number NM_010076.3: target region, 444-1358), and Drd2 (dopamine receptor 2; GenBank accession number NM_010077.2: target region, 69-1175). Probes were incubated with sections for 2 h at

40°C. Fos, *Drd1a*, and *Drd2* mRNA were used as a marker for activated D1R- or D2R-expressing cells in the NAc shell, which form the direct and indirect pathways, respectively, that target overlapping but also distinct basal ganglia structures (Smith *et al*, 2013). OFC-containing sections were hybridised with probes against Fos, *Slc17a7a* (vesicular glutamate transporter; *VGLUT1*) and *Slc32a1* (vesicular GABA transporter; *VGAT*) to visualise *Fos*+ pyramidal neurons or GABAergic interneurons, respectively. Sections were then incubated with three-step preamplifier and amplifier probes before being incubated with fluorescently labelled probes (Alexa Fluor 488, Atto 568, and Atto 647). Finally, a DAPI solution was briefly applied (for visualisation of nuclei) and the slides were coverslipped with Vectashield Hard Set Anti-fade mounting medium (catalog #H-1400, Vector Laboratories). Images of the NAc shell and OFC were taken using a Leica TCS SP8 confocal system attached to a DMI 6000 AFC Inverted Motorised Research Microscope at 20x magnification (HC PL APO 20 /0.70 CS), zoom factor 0.75. The images were collected using Leica Application Suite X Confocal Software and analysed in Fiji (Schindelin *et al*, 2012).

### 2.3.3. Fos immunohistochemistry (Chapter 5)

Ninety min following conditioned locomotion or extinction test sessions, mice were deeply anaesthetised with 200 mg/kg sodium pentobarbital and transcardially perfused with ice cold phosphate-buffered saline (PBS; in mM NaCl 137, KCl 2.7, $Na_2HPO_4$ 10, $KH_2PO_4$ 1.8, pH 7.5) for 5 min, then 4% paraformaldehyde (PFA) in PBS for 20 min. Brains were removed and post-fixated in 4% PFA for 20 h, cryoprotected in 30% sucrose-PBS solution and frozen in crushed dry ice. 30 µm thick sections of the striatum were prepared on a Leica CM1900 cryostat. Free-floating striatal sections were incubated in 0.3% hydrogen peroxide in PBS, blocked in 3% normal goat serum in 0.2% Triton X-100 PBS (PBS-Tx) and stained overnight at 4$^{o}$C in rabbit anti-Fos primary antibody (1/7000 in PBS-Tx; SC-52, Santa Cruz). Secondary labelling with

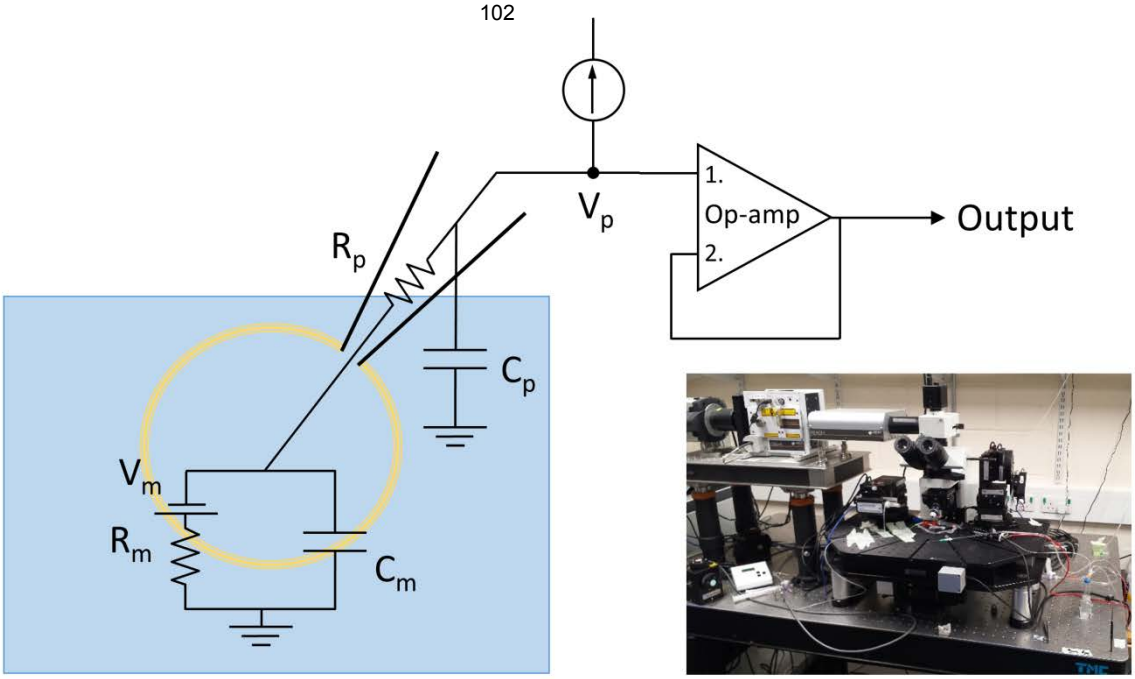


**Figure 2**. Patch-clamp electrophysiology recording in current clamp (CC) mode. Figure adapted from Barbour (2014). The cell is modelled as the membrane capacitance ($C_m$), membrane resistance ($R_m$) and the membrane voltage ($V_m$). The ground is provided by an electrode placed in the bath solution (blue) and connected to the amplifier ground. The recording pipette, patched onto the neuron in whole-cell mode, has a resistance at its pore ($R_p$) and capacitance across its glass ($C_p$). The voltage at the pipette ($V_p$) will follow $V_m$ but with an additional error caused by the voltage drop over $R_p$. **CC Operation:** The operational amplifier (op-amp) adjusts its output to balance the voltage at its inputs (1. and 2., through which close to zero current flows). The output of the op amp ("Output") will match the $V_p$ (which is the potential at input 1.), as the output is driving input 2. to match input 1. through the feedback connection. In this configuration the setup is a *voltage follower* and the output will reflex $V_m$. Current may be injected into the cell through the current source. **Series Resistance:** It is important to note the series resistance of $R_p$ and $R_m$. When current is injected to the cell from the current source, it creates a voltage-drop across $R_p$, causing an error in the measured voltage. As such, to measure precise voltages from the cell the series resistance can be compensated, through a "bridge balance" circuit. This cosmetic modification may be applied to reduce the error and bring $V_p$ closer to the physiological $V_m$. **Note**: While this schematic is used to illustrate the fundamental theory underlying current-clamp, the Axopatch 200B amplifier used in the present experiments utilises a current-follower (rather than a voltage-follower) recording device, with an additional feedback circuit used to simulate current clamp (Axon Instruments Inc., 1999; Magistretti *et al*, 1996). **Right:** The electrophysiological setup on which the present experiments were conducted.

1/600 goat anti-rabbit antibody in PBS-Tx (BA-1000, Vector Labs) was amplified with a commercial avidin-biotin kit (PK-4000, Vectorlabs) and developed in DAB nickel for ~15 min. Sections were mounted onto Superfrost slides (WZ-48512-00, Cole-Parmer), dried overnight, hydrated in de-ionised $H_20$ then dehydrated in graded ethanol baths (2 min in 30%, 60%, 90%, 95%, 100%, 100%) and cleared in Histoclear III (HS-204, National Diagnostics) then coverslipped in Histomount mounting medium (HS-103, National Diagnostics).

## 2.4. Electrophysiological Experiments

### 2.4.1. Slice preparation and recording solutions

*Chapter 3*

Ninety minutes after the final behavioural test, mice were anesthetised with a ketamine (100 mg/kg) xylazine (16 mg/kg) mix and brains were removed and placed in ice-cold cutting aCSF containing the following (in mM): 75 sucrose, 87 NaCl, 2.5 KCl, 0.5 CaCl2, 7.0 MgCl2, 1.25 NaH2PO4, 25 NaHCO3, and 10 D-glucose (bubbled with 95% O2/5% CO2, pH 7.4) for 2 min. Then, 250-mm-thick coronal slices that corresponded to approximately bregma 1.18-1.10 for the NAc shell and 3.08-2.68 for the OFC were sectioned on a Leica VT1200S vibratome. After slicing, sections were briefly held in cutting aCSF for 5 min at 32°C before resting in recovery aCSF containing the following (in mM): 125 NaCl, 3 KCl, 0.5 CaCl2, 3.5 MgCl2, 1.25 NaH2PO4, 25 NaHCO3, and 10 D-glucose (bubbled with 95% O2/5% CO2, pH 7.4) at room temperature. Sections were recorded in aCSF containing the following (in mM): 125 NaCl, 3 KCl, 2 CaCl2, 2 MgCl2, 1.25 NaH2PO4, 25 NaHCO3, and 10 D-glucose (bubbled with 95% O2/5% CO2, pH 7.4) at room temperature. The liquid junction potential was -11.1 mV and was not corrected.

*Chapter 4 and 5*

Ninety minutes following Pavlovian approach test, mice were deeply anaesthetised with 200 mg/kg sodium pentobarbital (Chapter 4) or 150 mg/kg ketamine and 20 mg/kg xylazine (Chapter 5) and transcardially perfused with ice cold NMDG-HEPES recovery aCSF (in mM, 93 NMDG, 2.5 KCl, 1.2 $NaH_2PO_4$, 30 $NaHCO_3$, 20 HEPES, 25 glucose, 2 thiourea, 5 Na-ascorbate, 3 Na-pyruvate, 0.5 $CaCl_2 \cdot 4H_2O$ and 10 $MgSO_4 \cdot 7H_2O$, bubbled with 95% $O_2$/ 5% $CO_2$, pH 7.4) (Ting *et al*, 2014). The brain was quickly removed and sliced in NMDG-HEPES aCSF on a Leica VT1200S vibratome. Striatal

sections were incubated in 34$^{o}$C NMDG-HEPES aCSF for 5 min and transferred to recording aCSF (in mM, 126 NaCl, 4.5 KCl, 1 $MgCl_2$, 2.5 $CaCl_2$, 1.2 $NaH_2PO_4$ 11 D-(+)-Glucose, 26 $NaHCO_3$ bubbled with 95% $O_2$/5% $CO_2$, pH 7.4) at room temperature for the remainder of the recording day. The liquid junction potential was -13.7 mV and was not corrected.

### 2.4.2. Slice imaging (All Chapters)

Slices were transferred to a recording chamber perfused with 30-32$^{o}$C recording aCSF. Whole-cell recordings on NAc medium spiny neurons (MSNs) or OFC pyramidal neurons were performed using borosilicate capillary glass-pipettes (1.5 mm outer diameter, 0.86 mm inner diameter) filled with a potassium gluconate solution (current clamp recording) (in mM): 135 K-gluconate, 3 MgCl2, 4 NaCl, 5 HEPES, 5 EGTA, 2 Mg-ATP, 0.3 Na3-GTP (pH 7.25) and 100 µM Alexa 568 dye (A10437, ThermoFisher Scientific) or cesium based intracellular solution (voltage clamp recording) (in mM): 0.1 Spermine tetrahydrochloride, 120 CsCH3SO3, 5 NaCl, 10 TEA-Cl, 10 HEPES, 4 Mg-ATP, 0.3 Na-GTP, 0.001 QX314 (Lidocaine; L7757 Sigma-Aldrich) and 100 µM Alexa 568 dye (A10437, ThermoFisher Scientific). Pipette resistances ranged from 4-7 mΩ. Neurons were visualised using an Olympus BX51WI microscope attached to a Revolution XD spinning disk confocal system (Andor 252 Technology Ltd) to permit fluorescence microscopy. GFP+ neurons were identified with a 488 nm excitation wavelength; neurons which did not express visible GFP were considered to be GFP negative (GFP–). Pyramidal neurons were identified based on their morphology under DIC microscopy (e.g., a prominent apical dendrite) and by their distinct firing patterns in response to current injections in current-clamp mode (e.g., action potential (AP) frequency accommodation (Cifani et al, 2012). MSNs were identified based on their morphology, and additionally resting membrane potential, AP waveform and response

to a 100 pA hyperpolarising during current clamp experiments (Kourrich and Thomas, 2009).

### 2.4.3. Current clamp recordings (Chapter 3 and 5)

Theory of current clamp electrophysiology is described in Figure 2. MSNs were held at -75 mV and pyramidal neurons were held at -70 mV for the duration of recordings. Data were collected with a Multiclamp 200B amplifier (Molecular Devices) combined with Digidata BNC-20190 A (Molecular Devices) and WinWCP Software (courtesy of Dr. John Dempster, University of Strathclyde, Glasgow, UK; http://spider.science.strath.ac.uk/sipbs/software_ses.htm. Signals were digitised at 10 kHz and filtered at 5 kHz (PCI6024E; National Instruments) and 50 kHz noise was filtered out using a HumBug (Quest Scientific) module. Spike kinetics were calculated using Mini Analysis Software (version 6.0; Synaptosoft) or manually (fast afterhyperpolarisation (fAHP) and medium afterhyperpolarisation (mAHP)). The current-clamp protocol consisted of 1 s positive current injections beginning at 30 pA and incrementing in 2 pA and 5 pA steps for MSNs and pyramidal neurons, respectively in Chapter 3. In Chapter 5, the current clamp protocol consisted of one-second positive current injections beginning at -30 pA and incrementing in 10 pA steps.

### 2.4.4. Voltage Clamp Recordings (Chapter 4)

*Experiment 1 - AMPA receptor (AMPAR) and GABA receptor (GABAR) –mediated currents following Pavlovian approach responding*

Theory of voltage clamp electrophysiology is described in Figure 3. Whole-cell recordings of AMPAR currents (excitatory postsynaptic currents; EPSC) were undertaken in the presence of the $GABA_A$ channel blocker picrotoxin (100 μM; P1675,

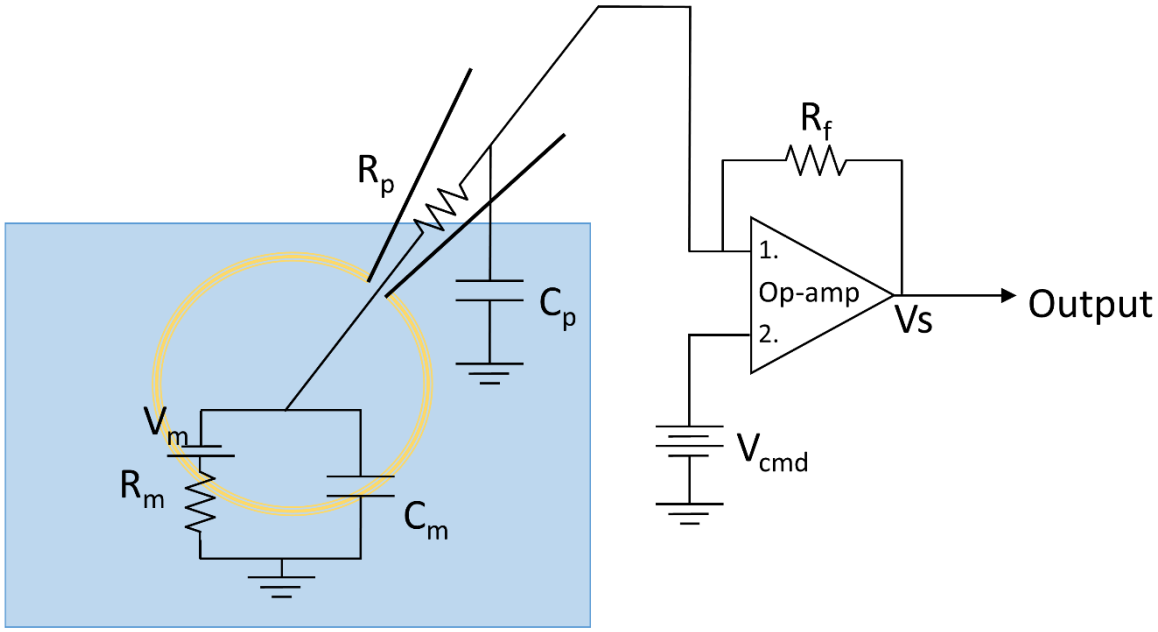


**Figure 3.** Patch-clamp electrophysiology recording in voltage-clamp (VC) mode. Figure adapted from Harrison *et al* (2015) and Barbour (2014). The cell membrane is modelled as the membrane capacitance ($C_m$), membrane resistance ($R_m$) and the membrane voltage ($V_m$) The ground is provided by an electrode placed in the bath solution (in blue) and connected to amplifier ground. **VC Operation.** The recording pipette, patched onto the neuron in whole-cell mode, has a resistance at it's pore ($R_p$) and capacitance across its glass ($C_p$). An operational amplifier (op-amp) is used to measure cell responses and clamp the membrane voltage to a command voltage ($V_{cmd}$). An op-amp will adjust its output to balance the voltage at its inputs (1. and 2.). In voltage clamp mode, the pipette potential can be set by $V_{cmd}$. This permits the measurement of membrane currents ($I_{cell}$, not pictured), as these cause a voltage drop across the reference resistor ($R_f$) proportional to $I_{cell}$. The op-amp will adjust its output to oppose this voltage change and as such the change its output ("Output") is equal, but opposite, to $I_{cell}$. **Series Resistance.** It is important to note the series resistors $R_p$ and $R_m$. When current flows through the series resistor, the voltage of the cell begins to deviate from $V_{cmd}$ in proportion to the magnitude of the current, as $R_m$ and $R_p$ act a voltage divider (Sontheimer and Olsen, 2007). To ensure the effective clamping of $V_m$, it is important that the access resistance during recording is >10x smaller than the membrane resistance. Furthermore, $C_m$ in conjunction with this voltage divider acts as a low-past filter, limiting the measurement of high-frequency currents such as fast ionic membrane currents. Thus if $R_p$ increases during recording, due to cellular debris blocking the pipette tip, measured synaptic currents are reduced. As such, when drugs are applied during recording, it is imperative to measure series resistance and exclude cells in which the series resistance ($R_s$) changes following drug application.

Sigma) at -70 mV. GABAR currents were detected at the reversal potential for excitatory synapses (0 mV) in the presence of NMDA receptor blocker APV (50 μM; A5282, Sigma). Paired-pulse and spontaneous transmission recordings were taken

from excitatory and GABAR synapses (spontaneous EPSCs and spontaneous inhibitory postsynaptic currents (IPSCs) respectively); paired-pulse ratios were calculated by dividing the first and second evoked peaks, across inter-spike intervals of 20, 40, 60, 80, 100, 150, 200 and 250 milliseconds. Evoked responses were elicited by stimulating directly in the NAc shell with single pulses (0.1 ms) at 0.033 Hz, from a bipolar Tungsten microelectrode (Matrix, FHC). Stimulation amplitude was adjusted to elicit approximately half the maximum evoked current.

*Experiment 2 - Cyclothiazide (CTZ) effects on AMPAR transmission following Pavlovian approach responding*

We measured AMPAR currents during application of the positive AMPAR allosteric modulator cyclothiazide (100 μM) (Sigma, C9847). Evoked EPSC (eEPSC) and sEPSC recordings were completed in standard recording aCSF (control) or in CTZ-aCSF. Following eEPSC and sEPSC recordings, CTZ-aCSF was perfused through the slice chamber for 20 min before eEPSC and sPESC recordings were repeated. CTZ action was confirmed by visual observation of markedly increased AMPAR current decay times.

Series resistance was monitored using –10 mV voltage steps (200 ms); cells exhibiting >15% change in access resistance during recording were discarded. Spontaneous EPSCs were acquired using WinEDR (courtesy of J. Dempster, University of Strathclyde) and analysed using Mini Analysis (Synaptosoft).

## 2.5 Data Analysis

### 2.5.1. Data presentation and outlier exclusion

All data were analysed using GraphPad Prism (Graphpad Software) and SPSS (IBM). Group data are presented as mean±SEM. Where possible, graphs displaying individual data points of representative behavioural, histological and electrophysiological findings are displayed in Appendix A. Post-hoc tests were conducted using Fisher's LSD. For all experiments, histological/physiological experiments contain lower animal numbers than in behavioural experiments; this is due to the loss of samples during perfusion/slice preparation, poor staining or failure to obtain electrophysiological recordings due to cell death. In addition, for these experiments, cell counts that exhibited frequencies that were 2 SDs from the mean were excluded from analysis; outliers were additionally confirmed using a 1% GRUBBS test. The details on number of animals run and cases of differences between 2SD and GRUBBS test outlier detection can be found in Appendix B.

### 2.5.2. Normality testing

The Kolmogorov-Smirnoff (KS) test was used to assess the distribution of independent samples alongside visual inspection of histograms to identify deviation in skew and kurtosis. For repeat measure samples, the standardised residuals were subject to KS testing. If the KS test indicated non-Gaussian distribution for independent samples or the majority of standardised residuals were non-normally distributed, results were confirmed using a non-parametric test and listed in the corresponding results section. However, in figures data was presented using parametric test analyses, due to the inherent issues with normality testing and non-parametric analyses in small samples (Ghasemi and Zahediasl, 2012; Potvin and Roff, 1993) as well as to correspond with published versions of the data.

### 2.5.3. Power testing

Power analyses were conducted on behavioural pilot experiments for both Pavlovian approach and conditioned locomotion experiments. These indicated that a sample size of n=10 (alpha=0.05, beta=0.95, power=0.8, effect size=1.17) and n=6 (alpha=0.05, beta=0.95, power=0.8, effect size=1.75), respectively, was required to resolve the behavioural differences. Due to the novel nature of the immunohistochemical and electrophysiological studies, power analyses were not conducted for these experiments.

### 2.5.4. Data Analysis

*Chapter 3*

Behaviour: Total head entries into the sucrose-delivery magazine during CS and ITI presentation during acquisition and extinction were analysed using a three-way mixed ANOVA including the factors of Condition (Paired, Unpaired), CS Presentation (CS, ITI) and a repeated-measures factor of session (1-12 for acquisition, 1-7 for extinction). Pavlovian approach test data were analysed using a two-way ANOVA using CS Presentation (CS, ITI) and Training Condition (Paired, Unpaired). Spontaneous recovery test data were analysed using a two-way ANOVA using CS Presentation (CS, ITI) and Test (EXT Final, SR Test) as factors. Pavlovian approach test data following extinction learning were analysed using a two-way ANOVA using CS Presentation (CS, ITI), and Group (Paired No EXT, Unpaired EXT, Paired EXT) as factors.

GFP and Fos mRNA expression: In Experiments 1 and 2, t-tests on the number GFP/*Fos* neurons per square millimetre were conducted independently in the NAc shell and OFC using Condition (Paired, Unpaired) as a factor. In Experiment 3, a one-way

ANOVA between Groups (Paired No EXT, Paired EXT, Unpaired EXT) was conducted on the number of *Fos* neurons per square millimetre.

Electrophysiology: Resting membrane potential, input resistance, rheobase, and spike kinetics data were analysed using two-way ANOVAs for Experiments 1 and 2 using Condition (Paired, Unpaired) and GFP (GFP+, GFP–) as factors. Spike counts for Experiments 1 and 2 were analysed using a three-way mixed ANOVA including the factors of Condition (Paired, Unpaired), GFP (GFP+, GFP–), and a repeated measures factor of Current Injections.

*Chapter 4*

Behaviour: Head entries into the magazine during the CS and inter-trial interval (ITI) across acquisition sessions were analysed using a two-way mixed ANOVA with factors CS (CS, ITI) and Session (Acquisition sessions 1-12). Test data was analysed using a paired *t* test comparing CS and ITI head entries in Paired mice.

Electrophysiology - Spontaneous and Evoked Currents: In experiment 1, sEPSC and spontaneous inhibitory postsynaptic current (sIPSC) parameters (frequency, amplitude, decay, rise time, half-width) were analysed using *t* tests. As the number of tests undertaken was small and some parameters were not independent (e.g. decay time/rise-times and half-width), no correction for multiple comparisons was used. Cumulative probability plots were analysed using the Mann-Whitney test directly on cumulative probability frequencies. In experiment 2, sEPSC and eEPSC parameters were analysed using a two-way ANOVA with GFP (GFP+, GFP–) and Cyclothiazide (CTZ-free aCSF, CTZ-aCSF) as factors.

Electrophysiology - Paired-pulse Ratio: Paired-pulse ratios across stimulation intervals were analysed using a two-way mixed ANOVA with factors GFP (GFP+, GFP–) and Inter-Spike Interval (20, 40, 60, 80, 100, 150, 200, 250 seconds

*Chapter 5*

Behaviour and Immunohistochemistry: Distance travelled in the locomotor chamber and Fos+ neurons per $mm^2$ (analysed independently for the NAc shell, NAc core and DS) were analysed using a two-way ANOVA including the factors Group (Paired vs. Unpaired) and Extinction (EXT vs. no EXT). Three mice were excluded from the immunohistochemical analysis due to poor perfusion and/or section quality.

Electrophysiology: Spike counts were analysed using a three-way mixed ANOVA including the factors of Group (Paired, Unpaired), GFP (GFP+, GFP–) and a repeated measures factor of Current (30 pA increments). Active and passive membrane properties (Tables 1-3) were analysed using a two-way ANOVA with Group (Paired, Unpaired) and GFP (GFP+, GFP–) as factors. Electrophysiological parameters were analysed separately for conditioned locomotion and extinction experiments.

## References


Axon Instruments Inc (1999). *Axopatch 200B patch clamp theory and operation*. [online]. Available at: https://www.autom8.com/wp-content/uploads/2016/07/Axopatch-200B.pdf Accessed on: 03/12/2017.

Barbour B (2014). Electronics for electrophysiologists. [online]. Available at: http://www.biologie.ens.fr/~barbour/electronics_for_electrophysiologists.pdf [Accessed 29/11/2017).

Cifani C, Koya E, Navarre BM, Calu DJ, Baumann MH, Marchant NJ*, et al* (2012). Medial prefrontal cortex neuronal activation and synaptic alterations after stress-induced reinstatement of palatable food seeking: a study using c-fos-GFP transgenic female rats. *J Neurosci* **32**(25): 8480-8490.

Ghasemi A, Zahediasl S (2012). Normality tests for statistical analysis: a guide for non-statisticians. *Int J Endocrinol Metab* **10**(2): 486-489.

Harrison RR, Kolb I, Kodandaramaiah SB, Chubykin AA, Yang A, Bear MF*, et al* (2015). Microchip amplifier for in vitro, in vivo, and automated whole cell patch-clamp recording. *J Neurophysiol* **113**(4): 1275-1282.

Kourrich S, Thomas MJ (2009). Similar neurons, opposite adaptations: psychostimulant experience differentially alters firing properties in accumbens core versus shell. *J Neurosci* **29**(39): 12275-12283.

Koya E, Golden SA, Harvey BK, Guez-Barber DH, Berkow A, Simmons DE*, et al* (2009). Targeted disruption of cocaine-activated nucleus accumbens neurons prevents context-specific sensitization. *Nat Neurosci* **12**(8): 1069-1073.

Magistretti J, Mantegazza M, Guatteo E, Wanke E (1996). Action potentials recorded with patch-clamp amplifiers: are they genuine? *Trends Neurosci* **19**(12): 530-534.

Paxinos G, Franklin K (2001). *The Mouse Brain in Stereotaxic Coordinates* Academic Press: San Diego, CA.

Potvin C, Roff DA (1993). Distribution-free and robust statistical methods: viable alternatives to parametric statistics. *Ecology* **74**(6): 1617-1628.

Rubio FJ, Liu QR, Li X, Cruz FC, Leao RM, Warren BL*, et al* (2015). Context-induced reinstatement of methamphetamine seeking is associated with unique molecular alterations in Fos-expressing dorsolateral striatum neurons. *J Neurosci* **35**(14): 5625-5639.

Schindelin J, Arganda-Carreras I, Frise E, Kaynig V, Longair M, Pietzsch T*, et al* (2012). Fiji: an open-source platform for biological-image analysis. *Nat Methods* **9**(7): 676-682.

Smith RJ, Lobo MK, Spencer S, Kalivas PW (2013). Cocaine-induced adaptations in D1 and D2 accumbens projection neurons (a dichotomy not necessarily synonymous with direct and indirect pathways). *Curr Opin Neurobiol* **23**(4): 546-552.

Sontheimer H, Olsen ML (2007). Whole-cell patch-clamp recordings. In: Walz W (ed). *Patch-Clamp Analysis: Advanced Techniques*, 2nd. edn. Humana: Totowa, N.J., pp 35-68.

Ting JT, Daigle TL, Chen Q, Feng G (2014). Acute brain slice methods for adult and aging animals: application of targeted patch clamp analysis and optogenetics. *Methods Mol Biol* **1183**: 221-242.

# Chapter 3.

# Changes in Appetitive Associative Strength Modulates Nucleus Accumbens, But Not Orbitofrontal Cortex Neuronal Ensemble Excitability

*Ziminski JJ, Hessler S, Margetts-Smith G, Sieburg MC, Crombag HS, Koya E (2017). Changes in Appetitive Associative Strength Modulates Nucleus Accumbens, But Not Orbitofrontal Cortex Neuronal Ensemble Excitability. J Neurosci 37(12): 3160-3170.*

**Abstract**

Cues that predict the availability of food rewards influence motivational states and elicit food-seeking behaviours. If a cue no longer predicts food availability, then animals may adapt accordingly by inhibiting food-seeking responses. Sparsely activated sets of neurons, coined “neuronal ensembles,” have been shown to encode the strength of reward-cue associations. Although alterations in intrinsic excitability have been shown to underlie many learning and memory processes, little is known about these properties specifically on cue-activated neuronal ensembles. We examined the activation patterns of cue-activated orbitofrontal cortex (OFC) and nucleus accumbens (NAc) shell ensembles using wild-type and *Fos-GFP* mice, which express green fluorescent protein (GFP) in activated neurons, after appetitive conditioning with sucrose and extinction learning. We also investigated the neuronal excitability of recently activated, GFP+ neurons in these brain areas using whole-cell electrophysiology in brain slices. Exposure to a sucrose cue elicited activation of neurons in both the NAc shell and OFC. In the NAc shell, but not the OFC, these activated GFP+ neurons were more excitable than surrounding GFP– neurons. After extinction, the number of neurons activated in both areas was reduced and activated ensembles in neither area exhibited altered excitability. These data suggest that learning-induced alterations in the intrinsic excitability of neuronal ensembles is regulated dynamically across different brain areas. Furthermore, we show that changes in associative strength modulate the excitability profile of activated ensembles in the NAc shell.

## Introduction

Animals use cues that predict the availability of food rewards to guide their behaviour and maximize food-seeking strategies (Petrovich, 2011). In humans and nonhuman animals, stimuli that are associated with palatable foods powerfully shape behaviour and increase motivation to consume food (Anschutz *et al*, 2011; Petrovich and Gallagher, 2007; van Strien *et al*, 2012). Conversely, animals rapidly inhibit such learned appetitive responses when previously food-associated cues no longer predict food availability (Mackintosh, 1983; Pavlov, 1927). Identifying how these learned associations are encoded neuronally is crucial to illuminating the mechanisms underlying disorders characterized by excessive food intake, such as obesity.

Exposure to food-associated cues activates brain areas that subserve motivational processes, such as the nucleus accumbens (NAc) and prefrontal cortex, which also play a pivotal role in encoding food-predictive cues and changes in cue-reinforcer contingencies (Annett *et al*, 1989; Burger and Berner, 2014; Day *et al*, 2006; Flagel *et al*, 2011; Petrovich, 2011; Schoenbaum *et al*, 2007; Schoenbaum *et al*, 2003; Singh *et al*, 2010; Warren *et al*, 2016). Moreover, there is now evidence indicating that, within both of these regions, associative memories may be encoded in sparsely activated subsets of neurons called neuronal ensembles (Cruz *et al*, 2013; Fanous *et al*, 2012; Koya *et al*, 2009; Pennartz *et al*, 1994; Warren *et al*, 2016; Whitaker *et al*, 2016). These ensembles exhibit synaptic adaptations that are not observed in surrounding nonactivated neurons after learning (Gouty-Colomer *et al*, 2016; Koya *et al*, 2012; Whitaker *et al*, 2016). Therefore, appetitive associations may be encoded through adaptations occurring in multiple neuronal ensembles existing across multiple brain areas.

During experience-dependent plasticity, neurons may fine-tune information transfer by modifying their connectivity to surrounding neurons at the synapse, but also by adapting their intrinsic excitability (Dong *et al*, 2006; Kourrich *et al*, 2015). Alterations in neuronal excitability modulate neuronal firing properties and thus the ability of neurons

to influence the activity of local and distal postsynaptic neurons (Daoudal and Debanne, 2003; Nisenbaum and Wilson, 1995; Santini *et al*, 2008). These excitability changes have been widely observed after aversive conditioning in brain areas that encode emotionally salient stimuli, such as the amygdala and prefrontal cortex (Quirk and Mueller, 2008; Santini *et al*, 2008; Sehgal *et al*, 2014). However, in these studies, neuronal excitability was measured from a randomly sampled neuronal population within a given brain area without taking neuronal activation history into account. Therefore, little is known about changes in the intrinsic excitability of neurons that occur in behaviourally relevant ensembles activated by appetitive cues.

The aim of this study was to characterize intrinsic excitability changes of cue-activated neuronal ensembles in the shell portion of the NAc and orbitofrontal cortex (OFC) after appetitive conditioning with sucrose reward and extinction learning using *Fos-GFP* mice, which express green fluorescent protein (GFP) in strongly activated neurons (Barth *et al*, 2004; Koya *et al*, 2012; Whitaker *et al*, 2016). Both the NAc shell and OFC are activated by food-associated cues and are implicated in appetitive behaviours that are guided by learned associations and updating changes in learned contingencies (e.g., extinction) (Day *et al*, 2006; Fanous *et al*, 2012; Moorman and Aston-Jones, 2014; Schoenbaum *et al*, 2007; Schoenbaum *et al*, 2003; Singh *et al*, 2010). We hypothesized that changes in associative strength may modulate the excitability properties of the cue-activated neuronal ensembles in these areas.

## Results

### Pavlovian approach and neuronal activation in the NAc and OFC

In order for mice to acquire the relationship between the sucrose reward and a cue that predicts its availability, we utilized an appetitive Pavlovian conditioning procedure (Figure 1A). To this end, we trained two groups of *Fos-GFP* mice, in which mice in the Paired group received auditory cue (CS) presentations paired with 10% sucrose

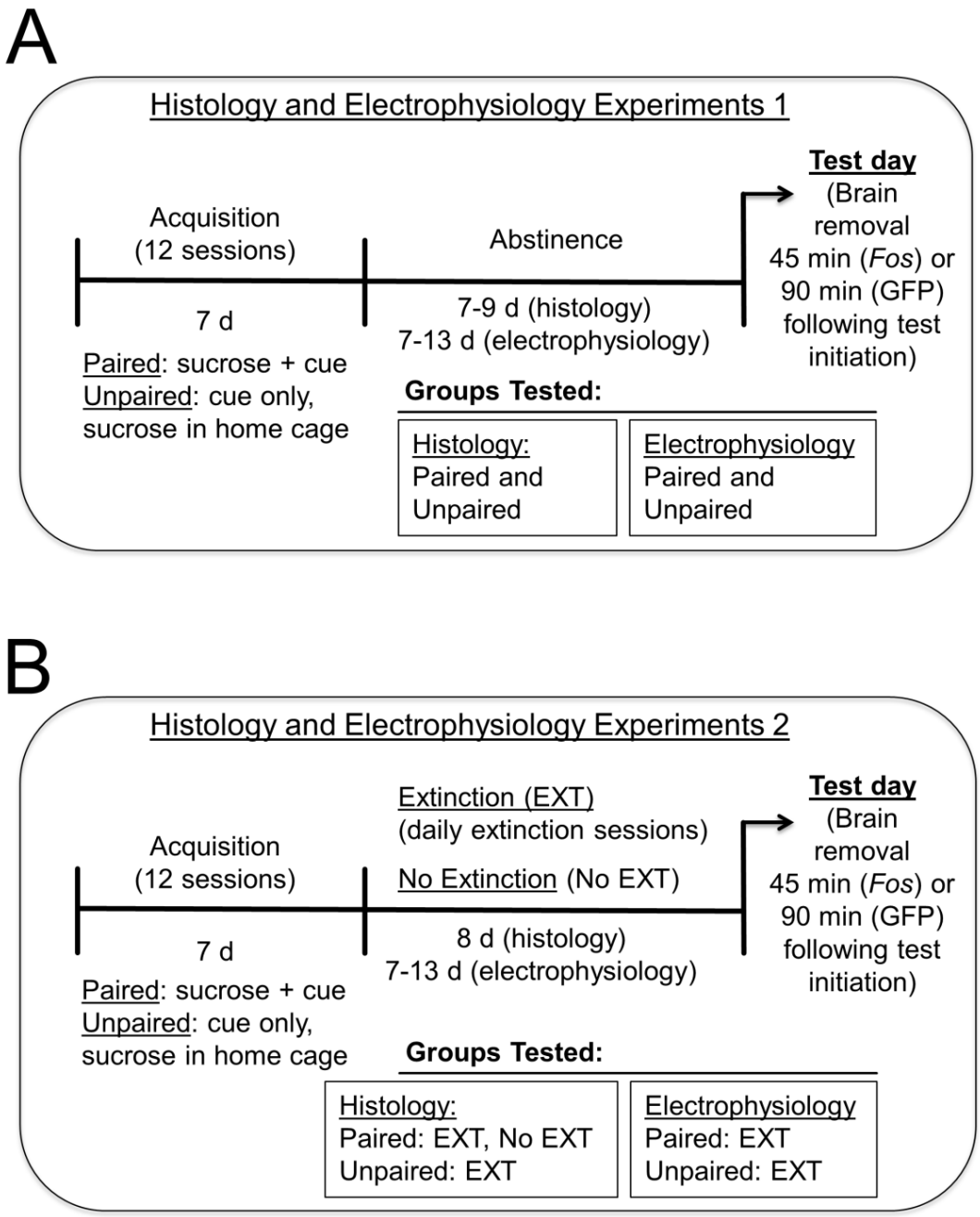


**Figure 1.** Timeline for Pavlovian approach and extinction experiments. **(A)** In Pavlovian approach experiments, two groups of mice underwent 12 acquisition (Pavlovian conditioning) sessions. In each session, Paired mice received sucrose during CS presentations in the conditioning chamber, whereas Unpaired mice received only CS presentations and instead were given sucrose in their home cage at random times before or after each session. At 7-9 d (histology experiments) or 7-13 d (electrophysiology experiments) after the last acquisition session, on test day, all mice were tested under extinction conditions and their brains were removed at 45 (Fos analysis) or 90 min (GFP immunohistochemistry and electrophysiology) after initiating testing. **(B)** In Extinction experiments, Paired and Unpaired mice underwent similar acquisition sessions as during Pavlovian approach experiments. One day after the last acquisition session a group of Paired and a group of Unpaired mice (EXT) underwent an extinction phase in which only the cue was presented. Another group of Paired mice did not undergo extinction learning (No EXT). One extinction session was conducted per day and this phase lasted 8 d (histology experiments) or 7–13 d (electrophysiology experiments). Mice were killed on the final extinction session and their brains were removed at 45 min (Fos analysis) or 90 min (electrophysiology) after initiating testing.

solution (US) during each acquisition session for a total of 12 sessions. In contrast, the Unpaired group received only cue presentations during each session, and received similar amounts of sucrose in their home cages at random times before or after each session. Thus, the CS in these mice remained neutral. As the training progressed, mice in the Paired group made significantly more CS-entries compared to ITI-entries (Figure 2A). In contrast, CS- and ITI-entries remained low throughout the 12 acquisition sessions in mice in the Unpaired group. A three-way ANOVA revealed a significant effect of Condition X CS Presentation X Session interaction ($F_{11,836}$=3.34, p<0.001) indicating that mice in the Paired group had reliably acquired the CS-US association. When Paired and Unpaired mice were tested one week following acquisition, Paired mice demonstrated a significant increase in number of head entries during presentation of the CS, a two-way ANOVA revealed a significant interaction of Condition X CS presentation ($F_{1,76}$=10.65, p<0.01; Figure 2B). Post-hoc analysis revealed significantly higher CS (cue presentation) compared to ITI (no cues) responses in the Paired group (p<0.001), but not in the Unpaired group (p=0.73).

| | NAc shell | | | | OFC | | | |
|---|---|---|---|---|---|---|---|---|
| | Unpaired | | Paired | | Unpaired | | Paired | |
| | GFP– | GFP+ | GFP– | GFP+ | GFP– | GFP+ | GFP– | GFP+ |
| Resting Vm (mV) | -80.43 ±0.47 | -79.00 ±1.05 | -79.94 ±0.64 | -76.77 ±1.14 | -77.08 ±1.49 | -77.92 ±1.28 | -77.33 ±1.20 | -76.05 ±1.16 |
| Rheobase (pA) | 52.43 ±4.39 | 52.00 ±4.76 | 51.79 ±3.41 | 39.38 ±3.24 | 108.54 ±16.81 | 120.71 ±13.75 | 107.08 ±23.72 | 106.46 ±13.75 |
| Ri (mΩ) | 387.60 ±24.17 | 385.52 ±46.69 | 351.23 ±14.77 | 498.15*# ±39.64 | 158.36 ±15.63 | 162.74 ±15.29 | 227.28# ±26.90 | 186.79# ±18.19 |
| AP Amplitude (mV) | 60.8 ±2.36 | 61.62 ±4.37 | 71.05 ±2.00 | 67.40 ±3.24 | 82.19 ±2.01 | 77.34 ±2.43 | 78.53 ±2.28 | 79.50 ±1.73 |
| Half-Width (ms) | 1.78 ±0.04 | 1.79 ±0.12 | 1.62 ±0.09 | 1.67 ±0.10 | 1.22 ±0.03 | 1.33 ±0.5 | 1.25 ±0.03 | 1.18 ±0.04 |
| fAHP (mV) | -9.66 ±0.60 | -10.15 ±0.76 | -10.95 ±0.54 | -9.86 ±0.79 | -7.21 ±1.37 | -9.10 ±0.67 | -10.47† ±0.95 | -10.27† ±0.62 |
| mAHP (mV) | -8.77 ±0.47 | -8.99 ±0.50 | -8.31 ±0.45 | -7.95 ±0.77 | -6.86 ±1.18 | -6.42 ±0.83 | -7.83 ±0.87 | -7.84 ±1.38 |

**Table 1.** Basic membrane properties from the NAc shell (MSNs) and OFC (pyramidal neurons) after Pavlovian approach test. Data are expressed as mean±SEM (*p<0.05, †p<0.05, #p 0.05). #Significant interaction of Condition GFP; *significant differences between Paired GFP+ compared with Paired GFP–; †main effect of Condition. Liquid junction potential was -11.1 mV and was not adjusted for. Spike characteristics were determined from the first action potential (AP) of spike runs consisting of 6-8 spikes. Input resistance was calculated from slope of the I/V curve measured in response to 2 pA (NAc shell) or 5 pA (OFC) current steps. The AP threshold was calculated by the third-order derivative method (Cotel *et al*, 2013) using Mini Analysis software. (In this method, the maximum value of the third derivative of the AP trace (d3Vm/dt3) was utilized to determine onset time of the AP and then the critical membrane voltage that was required to elicit an AP (AP threshold) was determined). The AP peak was calculated as the difference between the AP peak and the AP threshold. Half-width was measured as the AP width at half-maximal spike. Postspike fAHPs and mAHPs were measured 3 and 30 ms after the AP threshold, respectively, similar to Ishikawa *et al* (2009).

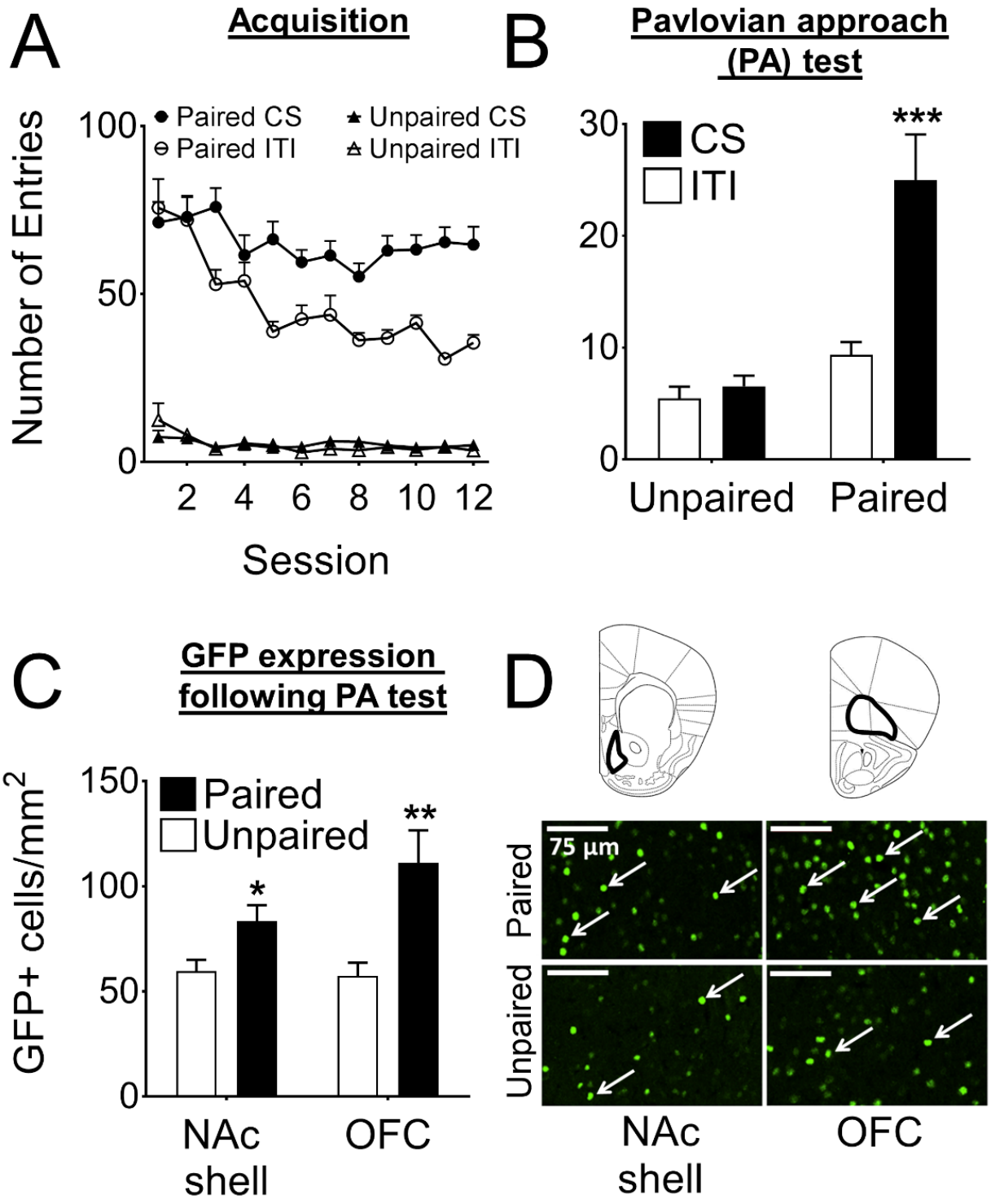


**Figure 2.** Sucrose cues evoke Pavlovian approach responses and enhance GFP expression in the NAc shell and OFC. **(A)** Head entries into the magazine in Unpaired and Paired mice during the CS and ITI periods (n=20/group) during acquisition. **(B)** Head entries at test; CS head entries are significantly higher than ITI entries in the Paired, but not Unpaired group (***p<0.001). Asterisk indicates Paired CS compared with Paired ITI. **(C)** GFP expression in the NAc shell and OFC; GFP expression is significantly higher in the Paired group compared with the Unpaired group for both brain areas (**p<0.01, *p<0.05; NAc shell n=16-17/group, OFC n=16/group). **(D)** Representative images of GFP–immunohistochemistry in the NAc shell and OFC in Unpaired and Paired mice; white arrows indicate GFP+ neurons. Data are expressed as mean±SEM.

Next, we examined neuronal activation in the NAc and the OFC in the same mice by counting GFP expressing (GFP+) neurons in these brain areas. The number of GFP+ neurons in the Paired mice was significantly higher compared to Unpaired mice in both the NAc (144% increase) ($t_{31}$=2.75, p<0.05) and the OFC (193% increase) ($t_{30}$=3.23, p<0.01) (Figure 2C). Thus, mice in the Paired, but not Unpaired group exhibited Pavlovian approach responses, and significant activation of NAc and OFC neurons, suggesting that these areas are activated by sucrose memories.

*Phenotype of Fos-expressing neurons in the NAc and OFC*

We next examined the phenotype of activated neurons in the NAc and OFC using RNAscope-based *in situ* hybridization. In line with the immunohistochemical findings, we found that *Fos* mRNA expression levels were significantly increased in the NAc (156% increase) ($t_{14}$=2.57, p<0.05) and OFC (208% increase) ($t_{20}$=2.31, p<0.05) of Paired compared to Unpaired mice (Figure 3A).

In the NAc, we delineated *Fos*+ MSNs by their expression of either the Dopamine D1 receptor (*Drd1*), or Dopamine D2 receptor (*Drd2*) mRNAs (Figure 3D). In the OFC, Pyramidal neurons and interneurons were distinguished by their expression of their respective vesicular transporter mRNAs, VGLUT1 and VGAT (Figure 3D). In these brain areas, these neurons play important yet distinct roles in information processing (Dilgen *et al*, 2013; Smith *et al*, 2013).

The phenotype distribution of D1R- or D2R-expressing *Fos*+ neurons in NAc was similar between Paired and Unpaired mice (*Drd1* 48.7% vs 48.7%; *Drd2* 43.8% vs 34.5%; Paired vs Unpaired; Figure 3B). A small proportion of *Fos*+ neurons expressed both *Drd1* and *Drd2* (3.2% vs 11.5%) or could not be identified as *Drd1* or *Drd2*-expressing (3.8% vs 5.3%; Paired vs Unpaired; data not shown). This suggests a similar proportion of D1R- and D2R-expressing neurons were activated following the Pavlovian approach test.

The OFC *Fos*+ ensemble consisted largely of *VGLUT1*+ neurons (97.5% vs. 94.4%; Paired vs. Unpaired) and a small minority of *VGAT1*+ neurons in (2.3% and 4.9%; Paired vs. Unpaired) (Figure 3C). This suggests that primarily pyramidal neurons were activated in the OFC following Pavlovian approach test.

**Experiment 2: Electrophysiological properties of GFP+ and GFP– neurons in the NAc and OFC following Pavlovian approach**

*NAc*

We measured the firing capacity of MSNs following depolarizing current injections across a 0-100 pA range. A three-way ANOVA revealed a significant interaction of Condition X GFP X Current Injection ($F_{9,486}$=2.76, p<0.01) and GFP X Current Injection ($F_{9,486}$=4.23, p<0.001) and main effect for GFP ($F_{1,54}$=4.92, p<0.05) with no other effects (Figure 4A). Thus, following sucrose memory retrieval, GFP+ neurons were more excitable compared to the surrounding GFP– neurons.

We assessed the possible source of this enhanced firing capacity by examining other active and passive membrane properties. No significant interactions for Condition X GFP were observed for the resting membrane potential, rheobase or spike kinetics of GFP+ and GFP– neurons in either group (Table 1). However, a two-way ANOVA revealed a significant interaction of Condition X GFP ($F_{1,54}$=5.63, p<0.05; Table 1) for the input resistance. Post-hoc analysis indicated a significant increase in the input resistance of GFP+ neurons compared to GFP– neurons in Paired (p<0.001) but not Unpaired mice (p=0.97). Furthermore, the increase in the input resistance in the Paired group was associated with a shift in the I/V curve at both positive and negative potentials; Condition X GFP X Current ($F_{25,1175}$=4.96, p<0.001; Figure 4A).

*OFC*

In the OFC, spike counts of pyramidal neurons were measured across a 20-300 pA range. A three-way ANOVA did not reveal a significant interaction of Condition X GFP

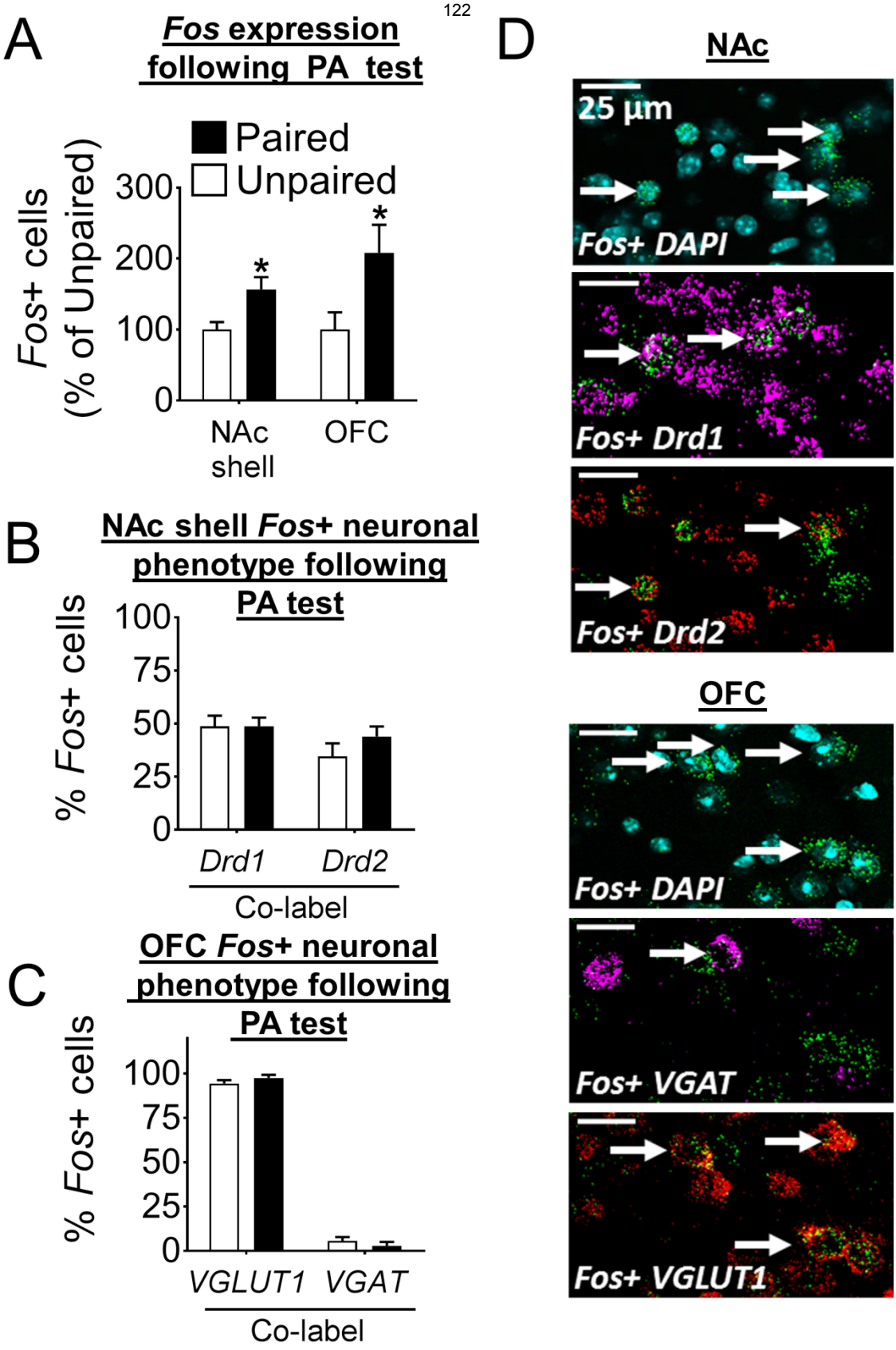


**Figure 3.** Characterization of activated neurons in the NAc shell and OFC after Pavlovian approach responding. **(A)** Fos expression in the NAc shell and OFC after Pavlovian approach test expressed as percentage of Unpaired group; Fos expression is significantly higher in the Paired compared with the Unpaired group for both areas (*p<0.05; n=7-11/group). **(B)** Proportion of Fos neurons coexpressing either *Drd1* (Fos *Drd1*) or *Drd2* (Fos *Drd2*) in the NAc shell. **(C)** Proportion of Fos neurons coexpressing either *VGLUT1* (*Fos VGLUT1*) or *VGAT* (Fos *VGAT* ). The vast majority of the Fos neurons are pyramidal neurons and only a small minority are interneurons. For A–D, data are expressed as mean±SEM. **(D)** Representative images of *Fos*, *Drd1*, and *Drd2* labelling from the NAc shell (top) and *Fos*, *VGLUT1*, and *VGAT* labelling from the *OFC* (bottom). DAPI (blue) was used to visualize cell nuclei. White arrows indicate colabeled *Fos* cells.

X Current Injection ($F_{14,700}$=0.53, p=0.92; Figure 4B), and thus Pavlovian conditioning did not modulate the excitability of GFP+ neurons. However, there was a significant interaction of Condition X Current ($F_{14,700}$=2.28, p<0.01). We then compared only the GFP– neurons in the Paired and Unpaired mice to investigate generalized changes to the majority of neurons, but we found no significant difference in spike counts of GFP– neurons between Paired and Unpaired mice in the OFC ($F_{14,294}$=1.26, p=0.23).

There was no significant interaction for Condition X GFP and there were no main effects for Condition or GFP for the resting membrane potential or spike kinetics of GFP+ and GFP– neurons in the OFC (Table 1). However, there was a main effect of Condition for the input resistance ($F_{1,51}$=5.69, p<0.05) and fAHP ($F_{1,51}$=6.09, p<0.05). Comparison of GFP– neurons from both groups revealed that the input resistance ($F_{1,22}$=4.89, p<0.05), but not the fAHP ($F_{1,22}$=3.84, p=0.06) was larger in Paired compared to Unpaired mice. Furthermore, there was a significant shift in the I/V curve between Paired and Unpaired GFP– neurons ($F_{12,264}$=4.77, p<0.001; Figure 4C). Thus, conditioning produced generalized changes to passive membrane properties that were reflective of ion channel opening at rest.

Pyramidal neurons can be categorised based on their firing patterns as ‘regular spiking’ or ‘intrinsic bursting’ cells (Hedrick and Waters, 2012). These differential firing patterns are thought to influence the information content that is sent to postsynaptic neurons (Reinagel *et al*, 1999). Next we characterised the composition of the OFC pyramidal neuronal ensemble. In GFP+ neurons in Paired mice, 78% were regular spiking (14/18 neurons) and 22% were weak bursting (4/18 neurons), and for GFP– neurons, 82% were regular spiking (9/11 neurons) and 18% (2/11 neurons) were weak bursting. In GFP+ neurons in Unpaired mice 88% (15/17 neurons) were regular spiking and 12% (2/17) were weak bursting, and for GFP– neurons 93% (14/15 neurons) were regular

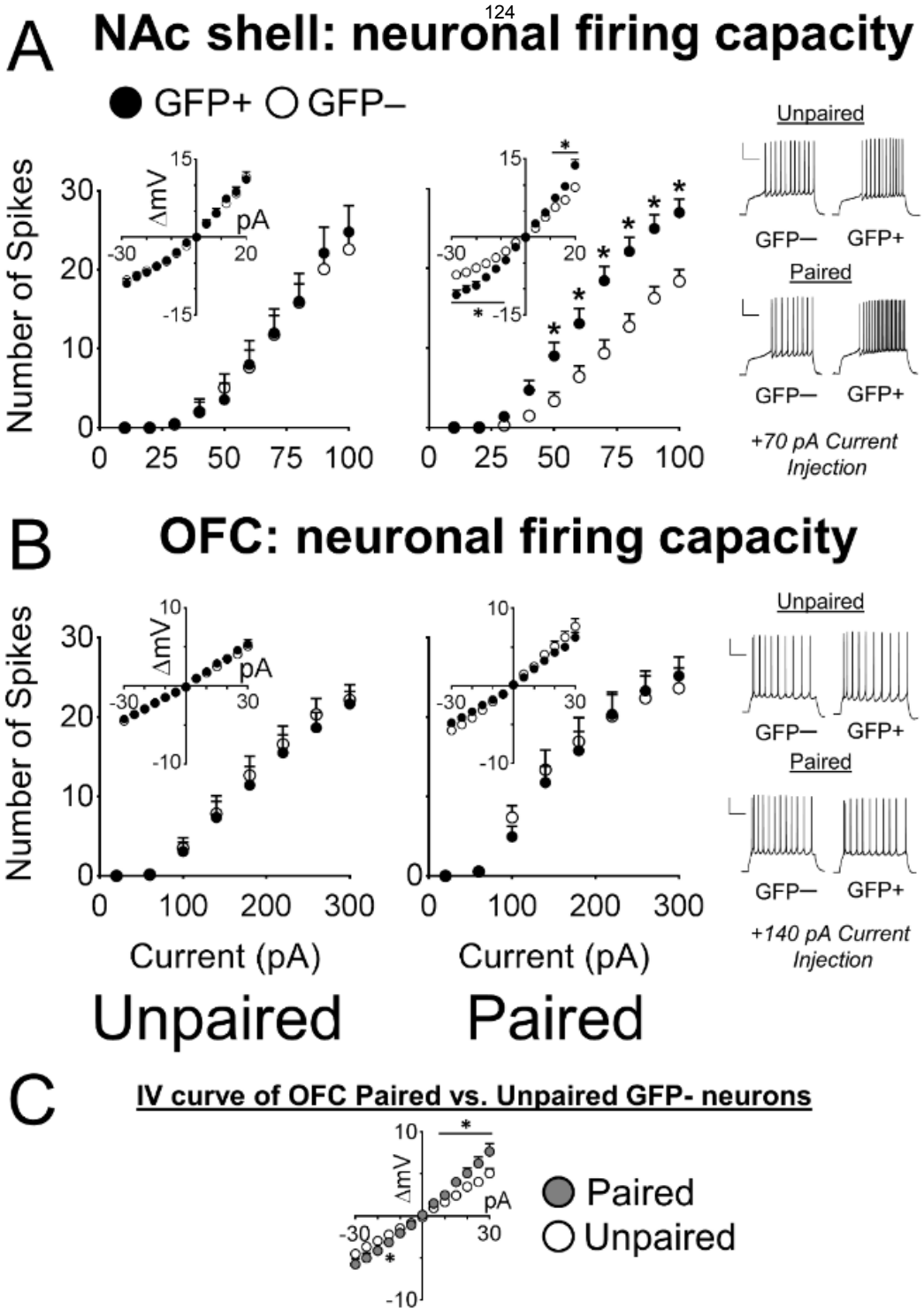


**Figure 4.** GFP+ neurons activated by sucrose cues are more excitable compared with their surrounding GFP– neurons in theNAc shell but not the OFC**. (A)** In the NAc shell, the spike counts of Paired group GFP+ neurons were significantly increased compared with the GFP– neurons after current injections (GFP–, n=19/9; GFP+, n=16/9). *p<0.01. In contrast, in the Unpaired groups, the spike counts of GFP+ and GFP– neurons were similar (GFP–, n=14/7; GFP+, n=9/5). The I/V curve (inset) indicated that there was a large increase in the input resistance of GFP+ neurons in Paired mice, but no difference in the Unpaired mice. *p<0.05. Example traces of GFP+ and GFP– neurons at 70 pA from the NAc shell of Paired and Unpaired mice. Scale bar, 25 mV, 250 ms. **(B)** In the OFC, no difference in spike counts was observed between GFP+ and GFP– neurons in the Unpaired mice (GFP–, n=12/5; GFP+, n=14/5) and in Paired mice (GFP–, n=11/5; GFP+, n=17/5). The I/V curves of GFP+ and GFP– neurons in Paired and Unpaired mice are shown in the inset. Example traces of GFP+ and GFP– neurons in the OFC of Paired and Unpaired mice at 140 pA are shown. Scale bar, 25 mV, 250 ms. **C,** I/V curves of GFP+ neurons from Paired and Unpaired mice from the OFC. *p<0.05. Data are expressed as mean±SEM; values to the right of GFP+ and GFP– denote number of cells recorded/number of mice used.

spiking and 7% (1/15 neurons) were weak bursting. These data, together with the increased levels of *Fos+VGLUT1* expressing cells in Paired mice suggests that sucrose memory retrieval in the OFC is encoded by an increased recruitment of pyramidal neurons which are composed primarily of regular spiking neurons.

## Experiment 3: Extinction of Pavlovian approach and NAc and OFC *Fos* expression

We examined the effect of extinction learning (EXT; Figure 1B) on the size and phenotype distribution of NAc and OFC ensembles in Paired no EXT, Paired EXT and Unpaired EXT mice. On test day, a two-way ANOVA revealed a significant interaction of Group X CS ($F_{2,29}$=11.38, p<0.001; Figure 5A). Post-hoc analysis revealed no differences between CS and ITI responses in the Paired EXT group (p=0.61) or in the Unpaired EXT group (p=0.06), but Paired no EXT mice made significantly more head entries into the magazine during the CS compared to ITI period (p<0.001).

Extinction is thought to be a process in which the original CS-US association is actively supressed or 'masked', rather than passively forgotten (Bouton, 2004; Quirk *et al*, 2008). We investigated whether the Pavlovian approach response could spontaneously recover following extinction, which would suggest that the original CS-US association was supressed rather than masked. A separate group of wild-type mice underwent acquisition and extinction similar to the Paired EXT mice described above, and were then tested for spontaneous recovery 6-7 days following the final extinction session (Figure 5B). A repeated two-way ANOVA revealed a significant interaction of CS Presentation X Test ($F_{1,44}$=5.30, p<0.05) and main effects for CS Presentation ($F_{1,44}$=6.48, p<0.05) and Test ($F_{1,44}$=28.83, p<0.001). Post-hoc analysis revealed a significant difference between CS and ITI entries at the spontaneous recovery test (p<0.001) but not following the final extinction session (p=0.73). As the distribution of independent samples was non-normal, results were confirmed using a

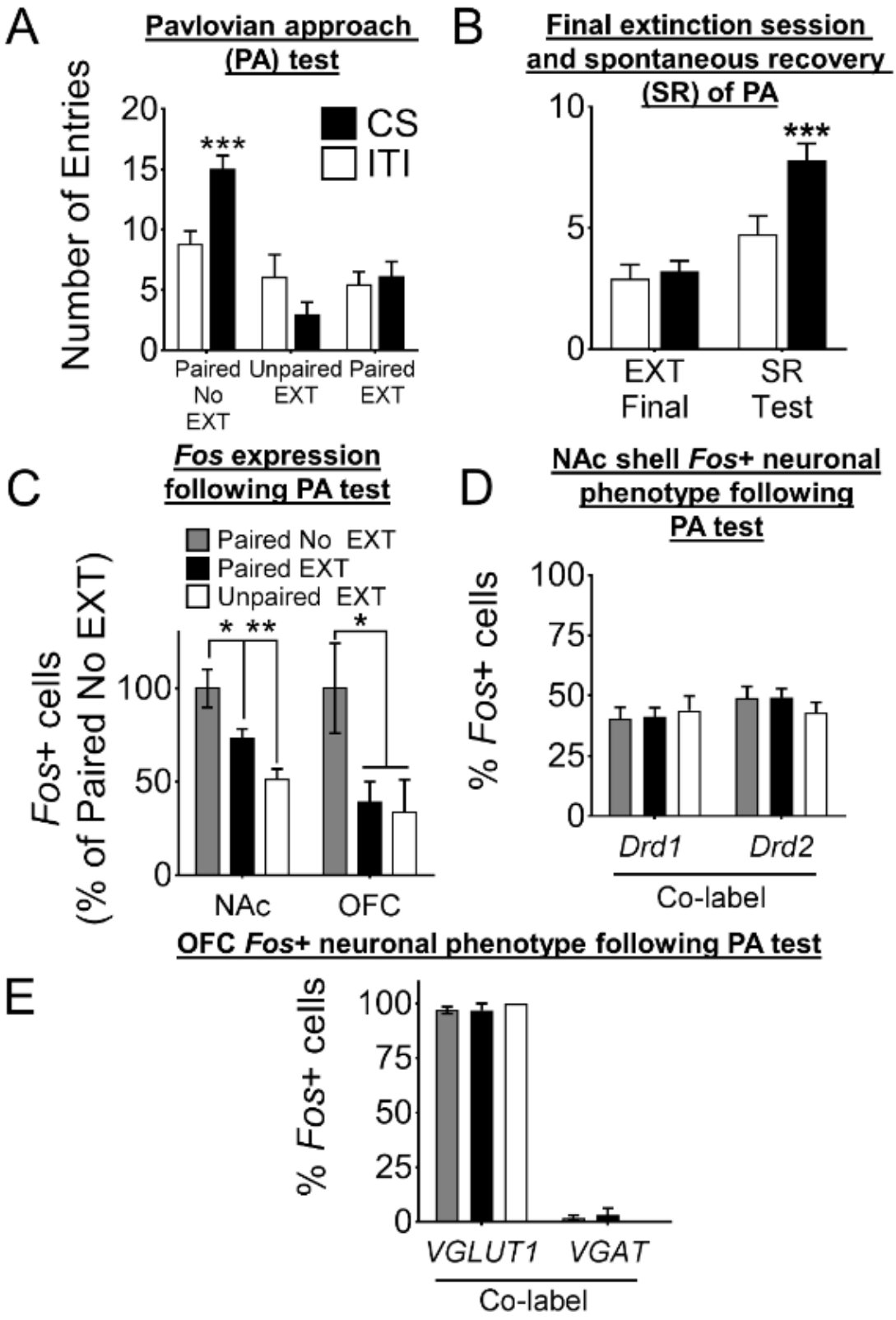


**Figure 5.** Characterization of activated neurons in the NAc shell and OFC after extinction of Pavlovian approach responding. **(A)** Head entries of mice used in in situ hybridization extinction experiments at test (n=8-12/group; ***p<0.001 comparing CS entries and ITI entries). After extinction, head entries made during the CS presentation are reduced in Paired mice. **(B)** Extinction of Pavlovian approach responding can recover spontaneously (SR test) after exposure to the CS 6-7 d after the final extinction session (EXT final; n=24; ***p<0.001 comparing CS entries and ITI entries). **(C)** *Fos* expression in the NAc shell and OFC of Paired No EXT, Paired EXT, and Unpaired EXT mice at testing expressed as a percentage of the Paired EXT group. Fos expression is significantly reduced after extinction in both areas (**p<0.01; *p<0.05; n=5-11/group). **(D)** Percentage of NAc shell *Fos*+ neurons that coexpress *Drd1* or *Drd2*; the proportion of *Fos*+ *Drd1* and *Fos*+ *Drd2* neurons was similar between groups. **(E)** Proportion of *Fos*+ neurons in the OFC coexpressing *VGLUT1* or *VGAT*. *Fos*+ neurons were primarily *VGLUT1* expressing in all groups. All data are expressed as mean±SEM.

Bonferroni -corrected Wilcoxon-signed ranks test (Spontaneous Recovery $Z$ = -3.81, p<0.005, Extinction $Z$ = -0.5, p = 0.62). This data suggests that the suppression of Pavlovian approach we observed here represents an active masking of the CS-US memory.

We next investigated the size of the NAc ensemble following extinction by quantifying *Fos*+ neurons in Paired no EXT, Paired EXT and Unpaired EXT mice. A one-way ANOVA revealed a significant effect of group on *Fos* expression in the NAc (Percent of Paired no EXT: Paired EXT = 73.2%; Unpaired EXT = 51.2%) ($F_{2,21}$=8.68, p<0.01) and OFC (Percent of Paired no EXT: Paired EXT = 39.1%; Unpaired EXT = 35.5%) ($F_{2,22}$=4.06, p<0.05) (Figure 5C). Post-Hoc analyses revealed that *Fos* levels were significantly lower in the Paired EXT group compared to the Paired no EXT group for both brain areas (NAc & OFC, p<0.05). Thus following extinction, the number of CS-activated neurons was reduced.

*Phenotype of NAc and OFC neurons following extinction*

In the NAc, the number of *Fos*+ neurons which co-expressed either *Drd1* or *Drd2* was similar across all groups (*Drd1* 38.2% vs 43.9% vs 42.9%; *Drd2* 48.9% vs 43.06% vs 49.28%; Paired No EXT vs Unpaired EXT vs Paired EXT) (Figure 5D). A small proportion of *Fos*+ neurons expressed both *Drd1* and *Drd2* (6.8% vs 5.3% vs 3.3%) or could not be identified as *Drd1* or *Drd2*-expressing (6.1% vs 7.7% vs 4.1%; Paired No EXT vs Unpaired EXT vs Paired EXT data not shown).

In the OFC, the *Fos*+ neuronal ensemble consisted of almost entirely *VGLUT1* neurons (97% vs. 100% vs. 96.9%) in all conditions and only an extremely small proportion were VGAT neurons (1.9% vs 0% vs 3.1%; Paired No EXT vs Unpaired EXT vs Paired EXT; Figure 5E).

**Experiment 4: Electrophysiological properties of GFP+ and GFP– neurons in the NAc and OFC following extinction of Pavlovian approach**

We examined the excitability properties of Paired EXT and Unpaired EXT mice in the NAc and OFC. Following extinction, we found no difference in the firing capacity of either NAc or OFC neurons. In the NAc, a three-way ANOVA did not reveal a significant interaction of Condition X GFP X Current Injection ($F_{9,414}$=0.87, p=0.55); Figure 6A) and no significant main effects (Current Injection nor Condition) or further interactions. In the OFC, no main interaction ($F_{14,1008}$=0.45, p=0.96; Figure 6B) or further effects were observed.

No significant interactions in any other measured electrophysiological parameters were observed (Table 2). However, there was a main effect of GFP for the fAHP ($F_{1,73}$=4.46, p<0.05) in the OFC. Post-hoc analysis demonstrated that there was no GFP effect between the Paired or Unpaired groups but between Paired GFP– and Unpaired GFP+ (p<0.05). Overall, following extinction of Pavlovian responding, no increases in the excitability of GFP+ neurons were observed in either the NAc or the OFC of Paired EXT mice.

As previously, we also characterised the composition of the OFC pyramidal neuronal ensemble. In GFP+ neurons in Paired mice 87.0% were regular spiking (20/23 neurons) and 13.0% were weak bursting (3/23 neurons), and for GFP– neurons, 81.0% were regular spiking (17/21 neurons) and 19.0% (4/17 neurons) were weak bursting. In GFP+ neurons in Unpaired mice 66.7% (12/18 neurons) were regular spiking and 33.3% (6/18) were weak bursting, and for GFP– neurons 88.0% (22/25 neurons) were regular spiking and 12.0% (3/25 neurons) were weak bursting. These data, together with the decreased levels of *Fos+VGLUT1* expressing cells in Paired EXT mice suggests that extinction memory retrieval in the OFC is encoded by a smaller pyramidal neuronal ensemble compared to sucrose memory retrieval, but that this ensemble is still composed primarily of regular spiking neurons.

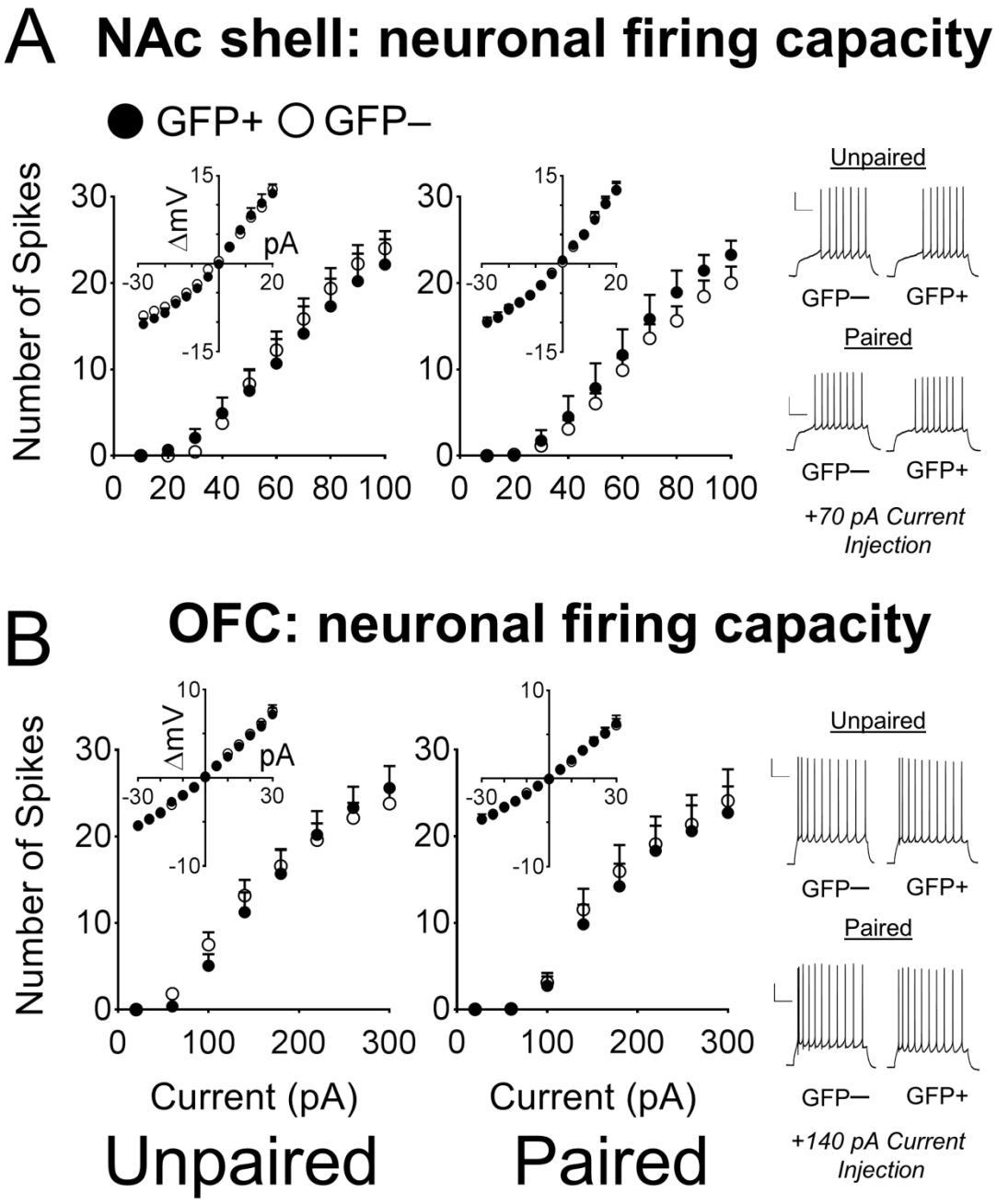


**Figure 6**. GFP+ neurons activated after extinction are of similar excitability to surrounding GFP– neurons in both the NAc shell and OFC. **A)** There was no significant difference between spike counts of GFP+ and GFP– neurons in the NAc shell of Paired EXT mice (GFP–, n=18/6; GFP+, n=12/6). In the Unpaired EXT group, spike counts of GFP+ and GFP– neurons were also similar (GFP–, n=13/7; GFP+, n=12/6). Example traces of GFP+ and GFP– neurons at 70 pA from NAc shell Paired EXT mice are shown. Scale bar, 25 mV, 250 ms. **(B)** In the OFC, there was no difference between spike counts of GFP+ and GFP– neurons in the Paired EXT group (GFP–, n=19/7; GFP+, n=18/6) or the Unpaired EXT group (GFP–, n=24/7; GFP+, n=16/8). Example traces of GFP+ and GFP– neurons at 140 pA from OFC Paired EXT mice. Scale bar, 25 mV, 250 ms. Data are expressed as mean±SEM; values to the right of GFP+ and GFP– denote number of cells recorded/number of mice used.

## Discussion

We examined the size, phenotype, and excitability of NAc shell and OFC ensembles after changes in reward-cue association strength; that is, after sucrose conditioning and after extinction learning. We found that exposure to a sucrose-predictive cue activated neurons in both the NAc shell and OFC, whereas cue-induced activation was reduced after extinction learning. In the NAc shell, similar levels of D1R- and D2R-expressing neurons were activated across conditions, whereas in the OFC, the majority of activated neurons were pyramidal cells.

We observed dynamic adaptations in the excitability of neuronal ensembles involved in encoding associative memories, which did not generalize across brain areas. In the NAc shell, but not the OFC, neurons activated after sucrose cue exposure were more excitable than surrounding neurons. Furthermore, after extinction learning, the behaviourally activated ensemble in the NAc shell was no longer more excitable. Our findings provide novel insight into how NAc shell ensembles encode changes in associative strength by recruiting neurons with a different excitability phenotype compared with their surrounding neurons.

### *Investigating neuronal excitability in the Fos-GFP mouse: methodological considerations*

We have characterized recently behaviourally activated neurons that express GFP (which is highly correlated with Fos expression) from *Fos-GFP* mice (Koya *et al*, 2012). It has been shown previously that Fos labels ensembles that are causally involved in the expression of conditioned behaviours (Cruz *et al*, 2013; Fanous *et al*, 2012; Koya *et al*, 2009; Warren *et al*, 2016). In addition, Fos expression requires sustained calcium signalling and ERK/MAPK

| | NAc shell | | | | OFC | | | |
|---|---|---|---|---|---|---|---|---|
| | Unpaired | | Paired | | Unpaired | | Paired | |
| | GFP– | GFP+ | GFP– | GFP+ | GFP– | GFP+ | GFP– | GFP+ |
| Resting Vm (mV) | -79.09 ±1.00 | -76.18 ±0.86 | -77.60 +0.66 | -76.83 ±1.05 | -77.71 ±0.63 | -77.13 ±1.19 | -76.16 ±0.94 | -77.11 ±0.82 |
| Rheobase (pA) | 41.15 ±4.96 | 38.18 ±5.50 | 45.56 ±4.72 | 45.00 ±4.99 | 88.13 ±10.00 | 107.72 ±11.99 | 121.05 ±18.30 | 119.38 ±14.56 |
| Ri (mΩ) | 418.36 ±24.83 | 475.79 ±52.81 | 438.83 ±37.22 | 454.78 ±48.13 | 207.12 ±14.67 | 196.56 ±14.38 | 182.57 ±18.97 | 169.24 ±21.71 |
| AP Amplitude (mV) | 62.99 ±3.81 | 66.18 ±3.12 | 67.82 ±2.85 | 61.55 ±3.26 | 107.11 ±1.72 | 102.51 ±3.40 | 106.52 ±1.71 | 98.61 ±2.81 |
| Half-Width (ms) | 1.71 ±0.07 | 1.78 ±0.09 | 1.62 ±0.04 | 1.79 ±0.08 | 1.01 ±0.03 | 1.04 ±0.04 | 0.96 ±0.03 | 1.00 ±0.04 |
| fAHP (mV) | -10.68 ±0.61 | -12.00 ±1.03 | -10.72 ±0.72 | -9.28 ±0.88 | -19.17 ±2.26 | -25.57* ±2.54 | -17.37 ±2.40 | -21.38* ±2.79 |
| mAHP (mV) | -8.77 ±0.47 | -8.99 ±0.50 | -8.31 ±0.45 | -7.95 ±0.77 | -6.86 ±1.18 | -6.42 ±0.83 | -7.83 ±0.87 | -7.84 ±1.38 |

**Table 2.** Basic membrane properties from the NAc shell (MSNs) and OFC (pyramidal neurons) following extinction of Pavlovian approach. Data are expressed as mean±SEM (*p<0.05). Asterisk indicates main effect of GFP. Liquid junction potential was -11.1 mV and was not adjusted for. Spike kinetics were calculated as detailed in Table 1. Vm, Resting membrane potential; Ri, input resistance; fAHP, fast AHP; mAHP, medium AHP.

phosphorylation (Cruz *et al*, 2013) but it is not necessarily a direct correlate of spike activity (Luckman *et al*, 1994). Therefore, similar to other *Fos-GFP* mice studies (Koya *et al*, 2012; Whitaker *et al*, 2016), we suggest that we are mainly recording from neurons with robust, prolonged activation after cue exposure. It should also be noted that certain NAc neurons decrease their firing rate in response to appetitive Pavlovian cues and this decrease is thought to play an important role in appetitive behaviours (Day *et al*, 2006; Pennartz *et al*, 1994; Wan and Peoples, 2006). Therefore, intrinsic excitability changes on inhibitory neuronal ensembles may also underlie sucrose and extinction memory recall. However, methods to characterize inhibited neurons electrophysiologically are currently unavailable.

*Potential implications and mechanisms for increased excitability of NAc shell ensemble after sucrose memory retrieval*

GFP neurons in the NAc shell were more excitable than surrounding GFP neurons after sucrose cue exposure. This excitability change was associated with an increase in the input resistance, which was underpinned by a shift in the I/V curve at both depolarized and hyperpolarized potentials. MSNs express a pronounced inwardly rectifying potassium current, $I K_{IR}$, as well as voltage-gated currents such as A-type currents, which regulate the voltage response at hyperpolarized and depolarized potentials, respectively (Hibino *et al*, 2010; Nisenbaum *et al*, 1995; Perez *et al*, 2006).

At depolarized potentials, shifts in the I/V curve may also be influenced by voltage-gated $Ca^{2+}$ and $Na^{+}$ currents (Nisenbaum *et al*, 1995). Therefore, it is possible that the change in input resistance was primarily due to a modulation of intrinsic $K^{+}$ or $Na^{+}/Ca^{+2}$ currents at the dendritic/somatic level. Interestingly, similar adaptations have been observed in the NAc of obesity-prone rats that consume more food (Oginsky *et al*, 2016). It is tempting to speculate that the increase in the relative excitability of GFP neurons represents a potential mechanism to promote “normal” adaptive and “out-of-control” appetitive and consummatory behaviours by increasing the sensitivity to reward-associated cues. Further electrophysiological investigation is necessary to identify the precise intrinsic factors underlying these excitability changes in GFP neurons after Pavlovian conditioning.

It is possible that the changes that we observed are short-term homeostatic mechanisms that are elicited after acute activation. Homeostatic adaptations in response to high-frequency stimulation or prolonged excitation are, however, typically hyperpolarizing (Barth *et al*, 2004; Turrigiano, 1999), whereas increased excitability usually occurs after decreased excitatory input (Ishikawa *et al*, 2009). Furthermore, we did not observe such changes in strongly activated neurons in the OFC and NAc shell after exposure to a cocaine-associated context (Ziminski *et al*, 2017). Therefore, we favour the argument that the enhanced excitability that we observed occurred before testing is related to associative memory encoding.

Similar levels of Fos and *Drd1*- and *Drd2*-expressing neurons were observed in the NAc shell after Pavlovian approach. This finding indicates recruitment of ensembles from both direct (*Drd1*) and indirect (*Drd2*) pathways that target overlapping, but also distinct structures (Smith et al., 2013), and is consistent with studies that have examined Fos expression during motivated behaviours (Caprioli *et al*, 2017; Li *et al*, 2015; Rubio *et al*, 2015; Soares-Cunha *et al*, 2016). However, the functional roles of accumbens D1R- and D2R-expressing neurons are complex. Previous studies that used global manipulations of D1R- or D2R-expressing accumbens neurons indicated

opposing (Chandra *et al*, 2015; Lobo *et al*, 2010; Robinson and Berridge, 2001) and similar (Soares-Cunha *et al*, 2016) roles for motivated behaviours mediated by drug and natural rewards, respectively. Such discrepancies may arise from globally manipulating neurons regardless of their behavioural relevance, which may have different effects from neuronal ensemble specific manipulations. For example, neuronal ensemble, but not global, lesioning of the infralimbic cortex altered cue-elicited reward-seeking behaviour (Pfarr *et al*, 2015). To elucidate precisely the functions of D1- and D2R-expressing neurons in appetitive behaviours, future studies should use methods that manipulate Fos-expressing neurons from these populations selectively.

*Potential implications and mechanisms for the lack of excitability changes in NAc shell ensemble after extinction*

After extinction, it is possible that we recorded from a small portion of the original ensemble activated during the initial Pavlovian approach responding. This is consistent with the idea that extinction learning represents a suppression of the original memory (Bouton, 2004; Mackintosh, 1983; Pavlov, 1927; Quirk *et al*, 2008). Supporting this, we observed SR of responding after extinction. Therefore, it is possible that the excitability of the original NAc shell ensemble activated during appetitive memory recall is reduced after extinction. Extinction learning induces neural adaptations that have been shown to suppress reward seeking (Knackstedt *et al*, 2010; Sutton *et al*, 2003), whereas manipulating the excitability of the NAc shell is sufficient to modulate shell-dependent behaviours such as drug-induced locomotor activity (Dong *et al*, 2006). This suggests that decreasing the excitability in a CS-US coding ensemble in the NAc shell may be sufficient to modify conditioned approach behaviours.

However, recent studies have also suggested that extinction learning may result in the creation of a new neuronal ensemble that mediates the new CS-US contingency (Orsini *et al*, 2013; Warren *et al*, 2016). Warren *et al* (2016) performed pharmacogenetic lesioning of ventromedial prefrontal cortex Fos-expressing neurons in

an operant food self-administration procedure and demonstrated that ablation of Fos-expressing neurons after extinction and food self-administration disinhibited and attenuated nonreinforced food-seeking, respectively. This suggests that, in this area, extinction learning results in the recruitment of a new ensemble distinct from the ensemble activated during initial memory recall. Therefore, in our extinction experiments, GFP neurons after extinction may represent a new “extinction” ensemble rather than the same ensemble that encoded the original CS-US association.

*Potential reasons for lack of differences in OFC ensemble excitability after sucrose memory retrieval*

Unlike the NAc shell, OFC GFP neurons did not differ in their excitability compared with GFP neurons after sucrose memory retrieval despite associated increases in the number of GFP neurons. This lack of excitability may be due to the fact that these neurons may have undergone transient changes in neuronal excitability during conditioning to confer a permissive learning state (Mozzachiodi and Byrne, 2010; Saar *et al*, 1998). In support, previous studies have demonstrated that excitability changes in cortical areas may be transient and uncorrelated to the expression of learned behaviours (Moyer *et al*, 1996). Alternatively, OFC GFP neurons may encode a sudden unexpected change in cue-reward associations rather than the retrieval of sucrose memories. However, in vivo electrophysiology studies suggest that the activity of OFC neurons is most robust during presentation of a reward-associated stimulus and reward seeking (Moorman *et al*, 2014) . In addition, pharmacogenetic lesioning of Fos-expressing OFC neurons activated by drug-associated cues attenuate subsequent cue-induced drug seeking (Fanous *et al*, 2012). Therefore, we favour the explanation that the recruitment of GFP neurons in the OFC represents the retrieval of sucrose memory into an ensemble that does not differ in its excitability compared with surrounding neurons rather than recruitment of neurons into an “extinction” ensemble.

*Concluding remarks*

By recording selectively from behaviourally activated neurons, here, we illuminate a potentially novel ensemble coding mechanism that reflects changes in appetitive strength associations in the NAc shell. One issue that needs to be resolved here is whether these changes in ensemble excitability in the NAc play a causal role in encoding sucrose and extinction memories. Therefore, future studies may use transgenic tools to manipulate the excitability of these NAc neuronal ensembles directly, for example, by altering Kv channel expression (Dong *et al*, 2006) in Fos-expressing neurons using the *Fos-tTA* mouse (Kandel *et al*, 2014) and testing their effects on appetitive and extinction memory recall.

## References


Annett LE, McGregor A, Robbins TW (1989). The effects of ibotenic acid lesions of the nucleus accumbens on spatial learning and extinction in the rat. *Behav Brain Res* **31**(3): 231-242.

Anschutz DJ, Engels RC, van der Zwaluw CS, Van Strien T (2011). Sex differences in young adults' snack food intake after food commercial exposure. *Appetite* **56**(2): 255-260.

Barth AL, Gerkin RC, Dean KL (2004). Alteration of neuronal firing properties after in vivo experience in a FosGFP transgenic mouse. *J Neurosci* **24**(29): 6466-6475.

Bouton ME (2004). Context and behavioral processes in extinction. *Learn Mem* **11**(5): 485-494.

Burger KS, Berner LA (2014). A functional neuroimaging review of obesity, appetitive hormones and ingestive behavior. *Physiol Behav* **136**: 121-127.

Caprioli D, Venniro M, Zhang M, Bossert JM, Warren BL, Hope BT*, et al* (2017). Role of Dorsomedial Striatum Neuronal Ensembles in Incubation of Methamphetamine Craving after Voluntary Abstinence. *J Neurosci* **37**(4): 1014-1027.

Chandra R, Francis TC, Konkalmatt P, Amgalan A, Gancarz AM, Dietz DM*, et al* (2015). Opposing role for Egr3 in nucleus accumbens cell subtypes in cocaine action. *J Neurosci* **35**(20): 7927-7937.

Cifani C, Koya E, Navarre BM, Calu DJ, Baumann MH, Marchant NJ*, et al* (2012). Medial prefrontal cortex neuronal activation and synaptic alterations after stress-induced reinstatement of palatable food seeking: a study using c-fos-GFP transgenic female rats. *J Neurosci* **32**(25): 8480-8490.

Cotel F, Exley R, Cragg SJ, Perrier JF (2013). Serotonin spillover onto the axon initial segment of motoneurons induces central fatigue by inhibiting action potential initiation. *Proc Natl Acad Sci U S A* **110**(12): 4774-4779.

Cruz FC, Koya E, Guez-Barber DH, Bossert JM, Lupica CR, Shaham Y*, et al* (2013). New technologies for examining the role of neuronal ensembles in drug addiction and fear. *Nat Rev Neurosci* **14**(11): 743-754.

Daoudal G, Debanne D (2003). Long-term plasticity of intrinsic excitability: learning rules and mechanisms. *Learn Mem* **10**(6): 456-465.

Day JJ, Wheeler RA, Roitman MF, Carelli RM (2006). Nucleus accumbens neurons encode Pavlovian approach behaviors: evidence from an autoshaping paradigm. *Eur J Neurosci* **23**(5): 1341-1351.

Dilgen J, Tejeda HA, O'Donnell P (2013). Amygdala inputs drive feedforward inhibition in the medial prefrontal cortex. *J Neurophysiol* **110**(1): 221-229.

Dong Y, Green T, Saal D, Marie H, Neve R, Nestler EJ*, et al* (2006). CREB modulates excitability of nucleus accumbens neurons. *Nat Neurosci* **9**(4): 475-477.

Fanous S, Goldart EM, Theberge FR, Bossert JM, Shaham Y, Hope BT (2012). Role of orbitofrontal cortex neuronal ensembles in the expression of incubation of heroin craving. *J Neurosci* **32**(34): 11600-11609.

Flagel SB, Cameron CM, Pickup KN, Watson SJ, Akil H, Robinson TE (2011). A food predictive cue must be attributed with incentive salience for it to induce c-fos mRNA expression in cortico-striatal-thalamic brain regions. *Neuroscience* **196**: 80-96.

Gouty-Colomer LA, Hosseini B, Marcelo IM, Schreiber J, Slump DE, Yamaguchi S*, et al* (2016). Arc expression identifies the lateral amygdala fear memory trace. *Mol Psychiatry* **21**(3): 364-375.

Hedrick T, Waters J (2012). Effect of temperature on spiking patterns of neocortical layer 2/3 and layer 6 pyramidal neurons. *Front Neural Circuits* **6**: 28.

Hibino H, Inanobe A, Furutani K, Murakami S, Findlay I, Kurachi Y (2010). Inwardly rectifying potassium channels: their structure, function, and physiological roles. *Physiol Rev* **90**(1): 291-366.

Ishikawa M, Mu P, Moyer JT, Wolf JA, Quock RM, Davies NM*, et al* (2009). Homeostatic synapse-driven membrane plasticity in nucleus accumbens neurons. *J Neurosci* **29**(18): 5820-5831.

Kandel ER, Dudai Y, Mayford MR (2014). The molecular and systems biology of memory. *Cell* **157**(1): 163-186.

Knackstedt LA, Moussawi K, Lalumiere R, Schwendt M, Klugmann M, Kalivas PW (2010). Extinction training after cocaine self-administration induces glutamatergic plasticity to inhibit cocaine seeking. *J Neurosci* **30**(23): 7984-7992.

Kourrich S, Calu DJ, Bonci A (2015). Intrinsic plasticity: an emerging player in addiction. *Nat Rev Neurosci* **16**(3): 173-184.

Koya E, Cruz FC, Ator R, Golden SA, Hoffman AF, Lupica CR*, et al* (2012). Silent synapses in selectively activated nucleus accumbens neurons following cocaine sensitization. *Nat Neurosci* **15**(11): 1556-1562.

Koya E, Golden SA, Harvey BK, Guez-Barber DH, Berkow A, Simmons DE*, et al* (2009). Targeted disruption of cocaine-activated nucleus accumbens neurons prevents context-specific sensitization. *Nat Neurosci* **12**(8): 1069-1073.

Li X, Rubio FJ, Zeric T, Bossert JM, Kambhampati S, Cates HM*, et al* (2015). Incubation of methamphetamine craving is associated with selective increases in expression of Bdnf and trkb, glutamate receptors, and epigenetic enzymes in cue-activated fos-expressing dorsal striatal neurons. *J Neurosci* **35**(21): 8232-8244.

Lobo MK, Covington HE, 3rd, Chaudhury D, Friedman AK, Sun H, Damez-Werno D*, et al* (2010). Cell type-specific loss of BDNF signaling mimics optogenetic control of cocaine reward. *Science* **330**(6002): 385-390.

Luckman SM, Dyball RE, Leng G (1994). Induction of c-fos expression in hypothalamic magnocellular neurons requires synaptic activation and not simply increased spike activity. *J Neurosci* **14**(8): 4825-4830.

Mackintosh N (1983). *Conditioning and associative learning.* Clarendon: Oxford.

Moorman DE, Aston-Jones G (2014). Orbitofrontal cortical neurons encode expectation-driven initiation of reward-seeking. *J Neurosci* **34**(31): 10234-10246.

Moyer JR, Jr., Thompson LT, Disterhoft JF (1996). Trace eyeblink conditioning increases CA1 excitability in a transient and learning-specific manner. *J Neurosci* **16**(17): 5536-5546.

Mozzachiodi R, Byrne JH (2010). More than synaptic plasticity: role of nonsynaptic plasticity in learning and memory. *Trends Neurosci* **33**(1): 17-26.

Nisenbaum ES, Wilson CJ (1995). Potassium currents responsible for inward and outward rectification in rat neostriatal spiny projection neurons. *J Neurosci* **15**(6): 4449-4463.

Oginsky MF, Goforth PB, Nobile CW, Lopez-Santiago LF, Ferrario CR (2016). Eating 'Junk-Food' Produces Rapid and Long-Lasting Increases in NAc CP-AMPA Receptors: Implications for Enhanced Cue-Induced Motivation and Food Addiction. *Neuropsychopharmacology* **41**(13): 2977-2986.

Orsini CA, Yan C, Maren S (2013). Ensemble coding of context-dependent fear memory in the amygdala. *Front Behav Neurosci* **7**: 199.

Pavlov IP (1927). *Conditioned reflexes: an investigation of the physiological activity of the cerebral cortex.* Oxford University Press: Oxford, UK.

Paxinos G, Franklin K (2001). *The Mouse Brain in Stereotaxic Coordinates* Academic Press: San Diego, CA.

Pennartz CM, Groenewegen HJ, Lopes da Silva FH (1994). The nucleus accumbens as a complex of functionally distinct neuronal ensembles: an integration of behavioural, electrophysiological and anatomical data. *Prog Neurobiol* **42**(6): 719-761.

Perez MF, White FJ, Hu XT (2006). Dopamine D(2) receptor modulation of K(+) channel activity regulates excitability of nucleus accumbens neurons at different membrane potentials. *J Neurophysiol* **96**(5): 2217-2228.

Petrovich GD (2011). Learning and the motivation to eat: forebrain circuitry. *Physiol Behav* **104**(4): 582-589.

Petrovich GD, Gallagher M (2007). Control of food consumption by learned cues: a forebrain-hypothalamic network. *Physiol Behav* **91**(4): 397-403.

Pfarr S, Meinhardt MW, Klee ML, Hansson AC, Vengeliene V, Schonig K*, et al* (2015). Losing Control: Excessive Alcohol Seeking after Selective Inactivation of Cue-Responsive Neurons in the Infralimbic Cortex. *J Neurosci* **35**(30): 10750-10761.

Quirk GJ, Mueller D (2008). Neural mechanisms of extinction learning and retrieval. *Neuropsychopharmacology* **33**(1): 56-72.

Reinagel P, Godwin D, Sherman SM, Koch C (1999). Encoding of visual information by LGN bursts. *J Neurophysiol* **81**(5): 2558-2569.

Robinson TE, Berridge KC (2001). Incentive-sensitization and addiction. *Addiction* **96**(1): 103-114.

Rubio FJ, Liu QR, Li X, Cruz FC, Leao RM, Warren BL*, et al* (2015). Context-induced reinstatement of methamphetamine seeking is associated with unique molecular alterations in Fos-expressing dorsolateral striatum neurons. *J Neurosci* **35**(14): 5625-5639.

Saar D, Grossman Y, Barkai E (1998). Reduced after-hyperpolarization in rat piriform cortex pyramidal neurons is associated with increased learning capability during operant conditioning. *Eur J Neurosci* **10**(4): 1518-1523.

Santini E, Quirk GJ, Porter JT (2008). Fear conditioning and extinction differentially modify

the intrinsic excitability of infralimbic neurons. *J Neurosci* **28**(15): 4028-4036.

Schindelin J, Arganda-Carreras I, Frise E, Kaynig V, Longair M, Pietzsch T*, et al* (2012). Fiji: an open-source platform for biological-image analysis. *Nat Methods* **9**(7): 676-682.

Schoenbaum G, Saddoris MP, Stalnaker TA (2007). Reconciling the roles of orbitofrontal cortex in reversal learning and the encoding of outcome expectancies. *Ann N Y Acad Sci* **1121**: 320-335.

Schoenbaum G, Setlow B, Saddoris MP, Gallagher M (2003). Encoding predicted outcome and acquired value in orbitofrontal cortex during cue sampling depends upon input from basolateral amygdala. *Neuron* **39**(5): 855-867.

Sehgal M, Ehlers VL, Moyer JR, Jr. (2014). Learning enhances intrinsic excitability in a subset of lateral amygdala neurons. *Learn Mem* **21**(3): 161-170.

Singh T, McDannald MA, Haney RZ, Cerri DH, Schoenbaum G (2010). Nucleus Accumbens Core and Shell are Necessary for Reinforcer Devaluation Effects on Pavlovian Conditioned Responding. *Front Integr Neurosci* **4**: 126.

Smith RJ, Lobo MK, Spencer S, Kalivas PW (2013). Cocaine-induced adaptations in D1 and D2 accumbens projection neurons (a dichotomy not necessarily synonymous with direct and indirect pathways). *Curr Opin Neurobiol* **23**(4): 546-552.

Soares-Cunha C, Coimbra B, David-Pereira A, Borges S, Pinto L, Costa P*, et al* (2016). Activation of D2 dopamine receptor-expressing neurons in the nucleus accumbens increases motivation. *Nat Commun* **7**: 11829.

Sutton MA, Schmidt EF, Choi KH, Schad CA, Whisler K, Simmons D*, et al* (2003). Extinction-induced upregulation in AMPA receptors reduces cocaine-seeking behaviour. *Nature* **421**(6918): 70-75.

Turrigiano GG (1999). Homeostatic plasticity in neuronal networks: the more things change, the more they stay the same. *Trends Neurosci* **22**(5): 221-227.

van Strien T, Peter Herman C, Anschutz D (2012). The predictive validity of the DEBQ-external eating scale for eating in response to food commercials while watching television. *Int J Eat Disord* **45**(2): 257-262.

Wan X, Peoples LL (2006). Firing patterns of accumbal neurons during a pavlovian-conditioned approach task. *J Neurophysiol* **96**(2): 652-660.

Warren BL, Mendoza MP, Cruz FC, Leao RM, Caprioli D, Rubio FJ*, et al* (2016). Distinct Fos-Expressing Neuronal Ensembles in the Ventromedial Prefrontal Cortex Mediate Food Reward and Extinction Memories. *J Neurosci* **36**(25): 6691-6703.

Whitaker LR, Carneiro de Oliveira PE, McPherson KB, Fallon RV, Planeta CS, Bonci A*, et al* (2016). Associative Learning Drives the Formation of Silent Synapses in Neuronal Ensembles of the Nucleus Accumbens. *Biol Psychiatry* **80**(3): 246-256.

Ziminski J, Sieburg MC, Margetts-Smith G, Crombag HS, Koya E (2017). Regional Differences In Striatal Neuronal Ensemble Excitability Following Cocaine And Extinction Memory Retrieval In Fos-GFP Mice. *Neuropsychopharmacology*. [online] Available at: https://www.nature.com/articles/npp2017101

# Chapter 4.

# Excitatory and Inhibitory synaptic properties of neuronal ensembles activated following Pavlovian approach.

**Abstract**

Associative memories are thought to be encoded by neuroadaptations on selectively activated neuronal ensembles. These neuroadaptations may increase the intrinsic excitability of individual neurons, or alternatively strengthen the connectivity between neurons through alterations at the synapse. We have previously demonstrated modulation of intrinsic excitability on ensembles activated following exposure to sucrose-associated stimuli. However, possible adaptations occurring at the synapse remain unknown. As such, we assayed the strength of glutamatergic and GABAergic synapses on ensembles activated following the expression of Pavlovian approach behaviors in the *Fos-GFP* mouse. We observed that the frequency of spontaneous excitatory postsynaptic currents (sEPSC) was increased onto GFP+, but not surrounding non-activated GFP– neurons. This increase in synaptic strength occurred in the absence of changes to presynaptic release probability ($p_r$) or sEPSC amplitude, suggesting an increased number of functional synapses. We also observed no selective effect of the AMPAR-allosteric modulator cyclothiazide, which preferentially binds the AMPAR “flip” splice variant, suggesting AMPAR splice variants are not selectively regulated in GFP+ neurons. Finally, spontaneous transmission at inhibitory synapses was similar across activated and non-activated neurons. These data suggest that excitatory synaptic transmission is potentiated in neurons selectively activated following the expression of Pavlovian approach behaviours.

## Introduction

Stimuli associated with the presentation of high-calorie foods exert a powerful influence over motivated behaviors, increasing food consumption in humans (Harris *et al*, 2009) and inducing approach behaviors in rodents (Holland, 1980; Mackintosh, 1983). The ability for food-associated cues to elicit psychological and behavioral responses is dependent on complex biophysical adaptations in the motivational system of the brain (Day and Carelli, 2007; Shiflett *et al*, 2008). Understanding these neuroadaptations is crucial in the design of therapeutic interventions against disorders characterized by hypersensitive responses to food-associated cues, such as obesity (Boswell and Kober, 2016).We have previously shown that exposure to a sucrose-associated cue elicits activation of a more excitable neuronal ensemble in the nucleus accumbens (NAc) shell (Ziminski *et al*, 2017). Previous studies have shown that such ensembles are necessary for the expression of conditioned responses (Cruz *et al*, 2014) and are the site of selective learning-induced neuroadaptations (Cifani *et al*, 2012; Gouty-Colomer *et al*, 2016; Koya *et al*, 2012; Whitaker *et al*, 2016). Thus adaptations which occur selectively on neuronal ensembles may be particularly important to the encoding of appetitive associations.

Learning-induced neuroadaptations may occur at the synapse, or involve functional alterations in ion channels which modulate the intrinsic excitability of the neuron (Hayton *et al*, 2011; Hyman *et al*, 2006; Kourrich *et al*, 2015; Wolf, 2010). While synaptic and intrinsic changes have been demonstrated following associative learning with appetitive reinforcers (Hutter and Chapman, 2013; Stuber *et al*, 2008; Ziminski *et al*, 2017), they are not usually measured in the same experiment. As such, little is known about how these distinct set of neuroadaptations interact at the neuronal level following the encoding of food-associated cues.

The aim of this study was to further characterize the neuroadaptations on NAc shell ensembles activated by sucrose-associated stimuli by examining the properties of their

glutamatergic and GABAergic synapses. The NAc shell is a subcortical brain area important for the expression of motivated behavior and is involved in encoding Pavlovian responding to food-associated cues (Blaiss and Janak, 2009). As previously, we utilized the *Fos-GFP* mouse to visualize neurons activated following sucrose-cue elicited Pavlovian approach behaviors. We hypothesize that neurons activated by exposure to a sucrose-associated cue may undergo both synaptic alternations alongside changes in intrinsic excitability.

## Results

### Pavlovian approach behavior

To examine approach behaviors following exposure to a sucrose-associated cue, we trained Paired mice in the Pavlovian approach procedure (Figure 1A). During the conditioning phase, presentation of the CS predicted delivery of a 10% sucrose solution; Paired mice readily acquired selective approach behaviors, making more head entries to the food-delivery magazine during presentation of the CS than the ITI (CS X Session $F_{11,198}$=2.14, p<0.05; Session $F_{11,198}$=9.69, p<0.001; CS $F_{18,198}$=49.44, p<0.001) (Figure 1B). At test, mice made significantly more head entries during presentation of the CS than the inter-trial interval ($t_8$=3.71, p<0.01) (Figure 1C). Thus mice robustly demonstrated Pavlovian approach responding at test, suggesting successful recall of the sucrose-cue association.

### Experiment 1: Inhibitory and excitatory synaptic transmission following Pavlovian approach responding

We next examined excitatory (AMPAR) and inhibitory (GABAR) transmission at GFP+ and GFP– synapses in the NAc shell following Pavlovian approach responding. Small

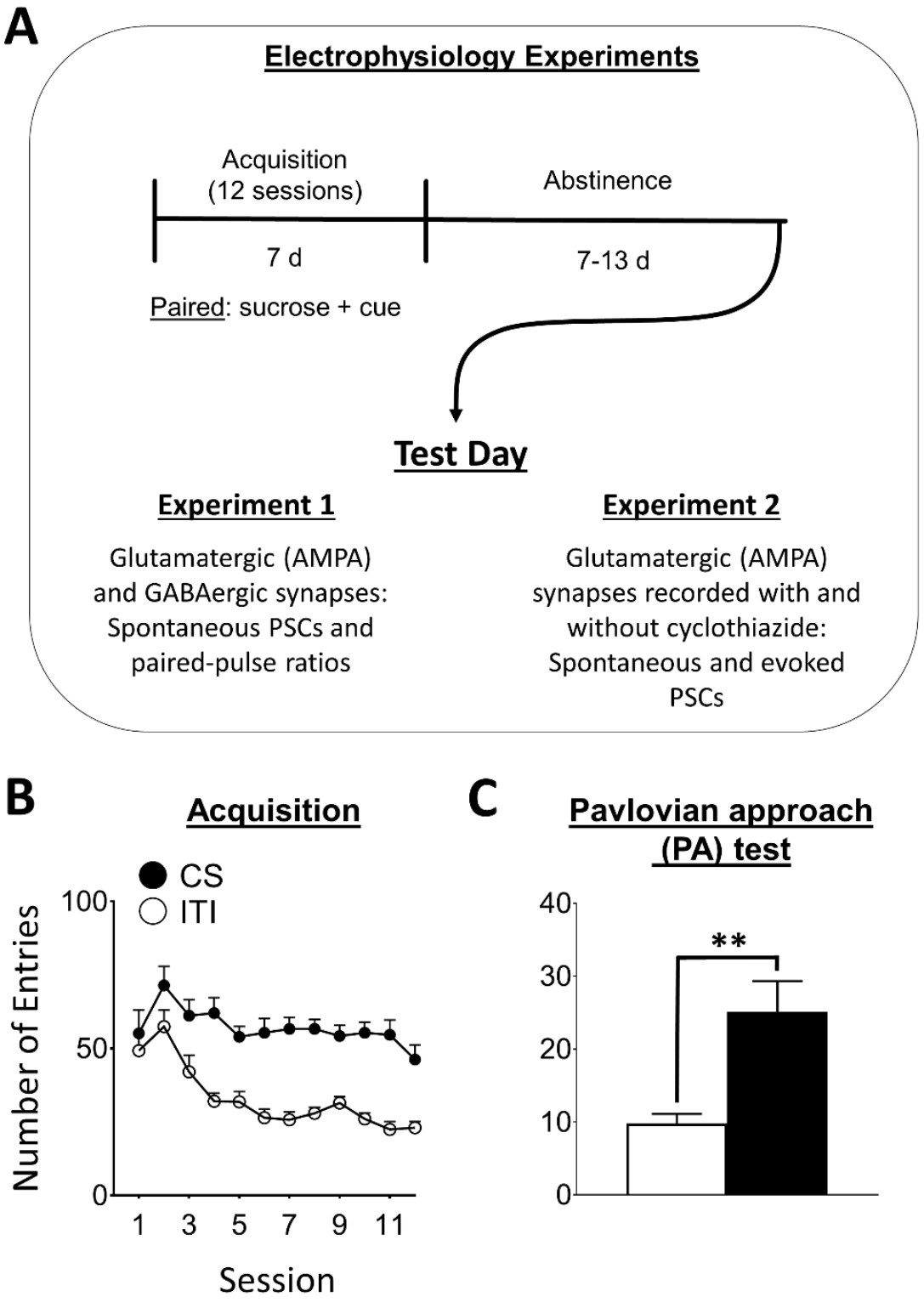


**Figure 1.** Experimental schedule and Pavlovian approach responding. **(A)** Paired mice underwent Pavlovian conditioning during which presentation of the CS was accompanied by delivery of a 10% sucrose solution. Following 12 acquisition sessions, no experimental procedures were undertaken for 7 d before mice were tested for Pavlovian approach responding under extinction conditions. 90 min following the start of the behavioural test, mice were killed for further experiments. Electrophysiological recordings of AMPA currents were undertaken at -70 mV in the presence of the $GABA_A$ channel-blocker picrotoxin. GABAergic currents were recorded at 0 mV (the EPSC reversal potential). During cyclothiazide (CTZ) recordings, evoked and spontaneous EPSCs were recorded in CTZ-free aCSF before CTZ-aCSF was perfused for 20-minutes and further recordings taken. **(B)** Head entries into the magazine during acquisition of Paired mice (n=12). Mice rapidly acquire CS-induced magazine approach behaviours **(C)** At test mice show robust Pavlovian approach responding, making significantly more head entries into the magazine during CS presentation than the ITI (n=12). **p<0.01. Data are expressed as mean±SEM.

postsynaptic currents elicited by spontaneous presynaptic vesicle release can be detected using patch-clamp electrophysiology. Differences in the amplitudes and time courses of these spontaneous postsynaptic currents (sPSC) may indicate functional changes in the efficacy of both pre- and postsynaptic transmission; as such, we measured the frequency, amplitude, decay, rise times, and half-widths of these spontaneous responses. Additionally, we examined the probability of presynaptic release ($p_r$) at glutamatergic and GABAergic synapses using the paired-pulse ratio method.

*AMPAR transmission: spontaneous excitatory postsynaptic currents (sEPSC)*

Following Pavlovian approach responding in *Fos-GFP* mice, sEPSC frequencies were significantly increased in GFP+ neurons $t_{12}$=2.36, p<0.05 (Figure 2A). Cumulative frequency distributions demonstrate that sEPSC frequencies were uniformly shifted across the range of inter-spike intervals (Mann-Whitney; $U$=2327, p<0.001). No significant change in sEPSC amplitudes were observed between GFP+ and GFP– neurons ($t_{11}$=0.70, p=0.49, $U$=811, p=0.06) (Figure 2B) nor were differences found in any other measured sEPSC parameter (Table 1). Thus sEPSC frequencies, but not other sEPSC waveform kinetics, were significantly increased on GFP+ neurons following Pavlovian approach.

*Paired-pulse ratios (AMPA)*

There were no significant differences between paired-pulse ratios from GFP+ and GFP– neurons following Pavlovian approach responding (GFP X ISI $F_{6,54}$=1.04, p=0.41, GFP $F_{1,9}$=0.97, p=.20, ISI $F_{6,54}$=2.81, p<0.05) (Figure 2D). This suggests that the increased sEPSC frequencies we observed were not due to an increase in vesicular $p_r$ at excitatory synapses.

| | Experiment 1. | | | | Experiment 2. | | | |
|---|---|---|---|---|---|---|---|---|
| | sEPSC | | sIPSC | | No CTZ | | CTZ | |
| | GFP– | GFP+ | GFP– | GFP+ | GFP– | GFP+ | GFP– | GFP+ |
| Frequency (Hz) | 0.68 ±0.14 | 1.55* ±0.29 | 1.33 ±0.26 | 1.31 ±0.51 | 0.95 ±0.18 | 2.45 ±0.67 | 1.51 ±0.78 | 2.63 ±0.51 |
| Amplitude (pA) | 12.74 ±0.74 | 14.15 ±1.25 | 18.85 ±1.11 | 20.14 ±0.78 | 15.37 ±0.49 | 18.69 ±1.71 | 16.87 ±1.80 | 17.96 ±1.71 |
| Decay (ms) | 3.11 ±0.16 | 2.92 ±0.14 | 9.52 ±0.38 | 9.82 ±1.77 | 2.55 ±0.45 | 2.91 ±0.13 | 4.75## ±0.42 | 4.05## ±0.75 |
| Rise time(ms) | 1.86 ±0.02 | 1.74 ±0.19 | 3.59 ±0.13 | 3.51 ±0.31 | 1.85 ±0.15 | 1.91 ±0.9 | 1.96 ±0.17 | 2.31 ±0.08 |
| Half-width (ms) | 2.70 ±0.08 | 2.46 ±0.31 | 6.85 ±0.34 | 6.72 ±0.87 | 2.27 ±0.38 | 2.71 ±0.18 | 4.01## ±0.39 | 3.58## ±0.33 |

**Table 1.** Spontaneous postsynaptic currents (sPSC) from GFP+ and GFP– neurons following Pavlovian approach.* indicates t-test between GFP+ and GFP- neurons, # indicates main effect of cyclothiazide (CTZ) application. *p<0.05, ##p<0.01. sPSCs were detected using Mini Analysis software. Frequency was calculated as number of detected spontaneous currents divided by duration of recording (s). All sPSC waveform kinetics were calculated using Mini Analysis software. Peak was calculated as difference between sPSC threshold (as calculated using the 2$^{nd}$ differential) and sPSC peak. Half-width was measured as the sPSC width at half of the maximal amplitude. Rise time indicates the time between sPSC threshold and peak. Decay was calculated as the time between sPSC peak and sPSC decay. Data are expressed as mean±SEM.

*$GABA_AR$ transmission: spontaneous inhibitory postsynaptic currents (sIPSC)*

We observed no changes in sIPSC parameters between GFP+ and GFP– neurons following Pavlovian approach responding. We observed no changes in sIPSC frequencies ($F_{10}$=0.03, p=0.97, $U$=4018, p=0.86) (Figure 3A), amplitudes ($F_{10}$=0.03, p=0.97, $U$=3114, p=0.57) (Figure 3B), nor any other sIPSC parameter measured (Table 1). Thus, the expression of Pavlovian approach did not selectively alter synaptic GABAergic transmission between GFP+ and GFP– neurons.

*Paired-pulse ratios (GABA)*

There was no significant difference between paired-pulse ratios from GFP+ and GFP– neurons following Pavlovian approach responding (GFP X ISI $F_{6,36}$=1.01, p=0.44, GFP $F_{1,6}$=0.49, p=.51, ISI $F_{6,36}$=1.79, p=1.27) (Figure 3D). This suggest that vesicular $p_r$ at inhibitory synapses was not selectively altered following exposure to sucrose-cues.

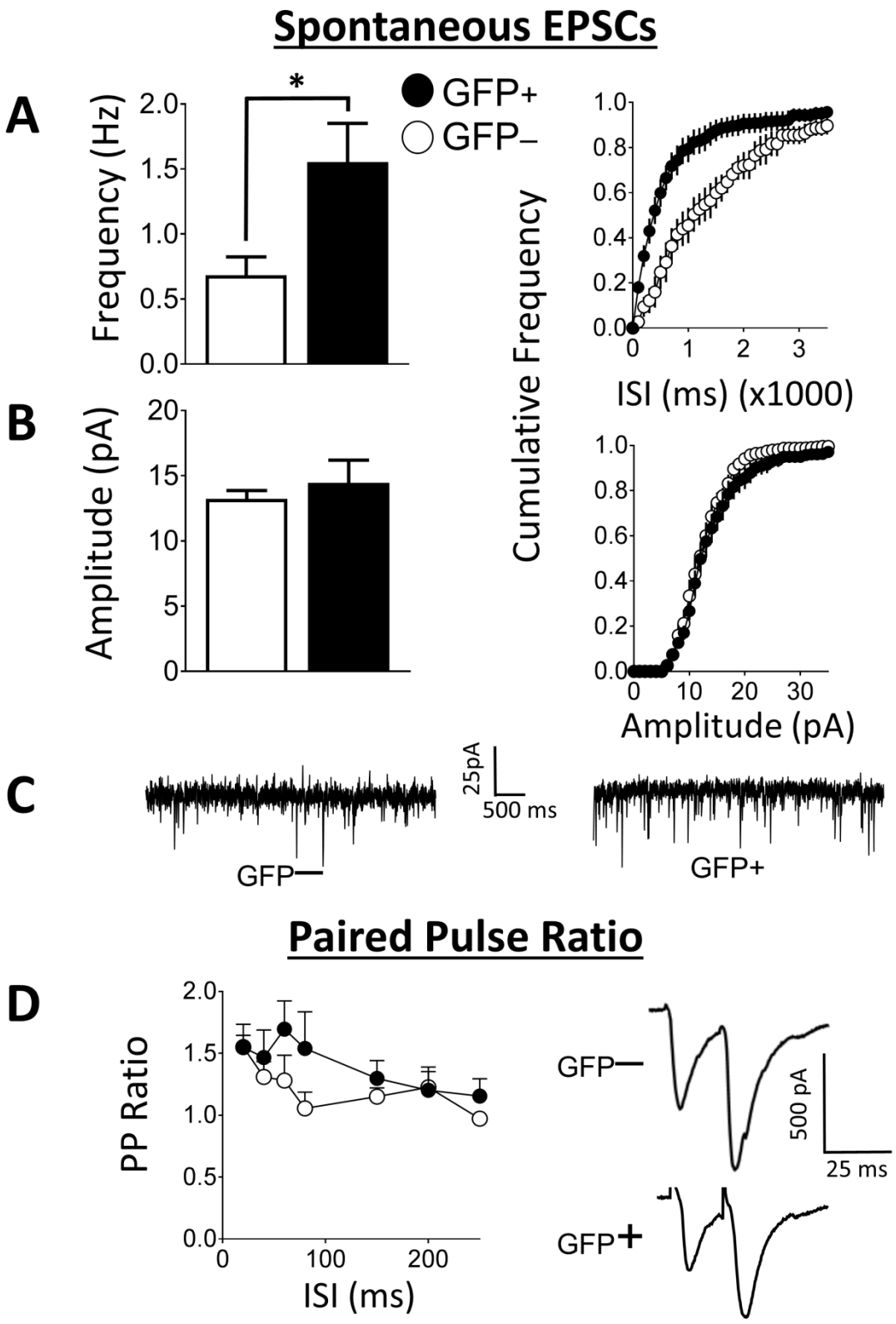


**Figure 2.** AMPA transmission is increased in GFP+ neurons following exposure to sucrose cues **(A)** sEPSC frequencies were increased in GFP+ neurons following Pavlovian approach responding (GFP+, n=8/4; GFP–, n=6/4). **(B)** There were no significant differences in sEPSC amplitudes between GFP+ and GFP– neurons of Paired mice (GFP+, n=9/4; GFP–, n=8/4). **(C)** Representative 5 s traces from GFP+ and GFP– neurons of Paired mice. Scale bar 25 pA, 500 ms **(D)** There were no significant differences in the paired-pulse (PP) ratios of GFP+ and GFP–neurons of Paired mice, suggesting sEPSC changes were not due to pre-synaptic adaptations (GFP+, n=5/3; GFP–, n=6/3). *Right*: Representative images of paired-pulse recordings from GFP+ and GFP– neurons of Paired mice. Scale bar 500 pA, 25 ms. Images were edited to remove stimulus artefacts. Data are expressed as mean±SEM. *p<0.05. Values to the right of GFP+ and GFP– denote number of cells recorded/number of mice used.

**Experiment 2: The effects of cyclothiazide application at glutamatergic synapses following Pavlovian approach responding**

Alternative splicing of AMPAR subunits (GluR1-4) generates heterogeneous “flip” and “flop” variants characterized by an extracellular region change of 9-11 amino acids. In some subunits (GluR2-3) these changes alter the deactivation kinetics of the “flop” isoform, whereas in GluR1 the change is silent (Pei *et al*, 2009). We used cyclothiazide, an allosteric modulator of the AMPA receptor with a pronounced preference for the flip variant (Kessler *et al*, 2000), to probe potential differences in AMPAR subunit isoform expression between GFP+ and GFP- neurons. This permits detection of subtle changes in splice variant expression; furthermore, this may provide putative pharmacological targets for therapeutic drug interventions against diseases characterized by hypersensitive responses to food-cues, such as obesity.

*Modulation of evoked EPSCs by cyclothiazide*

Following cyclothiazide application, there was a significant increase in the decay of evoked EPSCs following cyclothiazide application, however the magnitude of this increase was similar between GFP+ and GFP– neurons (GFP X Cyclothiazide $F_{1,8}$=0.59, p=0.46; Cyclothiazide $F_{1,8}$=52.42, p<0.0001; GFP $F_{1,8}$=1.53, p=0.25) (Figure 4A). We observed no general nor GFP selective change in the amplitude of evoked EPSCs (GFP X Cyclothiazide $F_{1,8}$=0.17, p=0.69; Cyclothiazide $F_{1,8}$=1.49, p=0.26; GFP $F_{1,8}$=0.30, p=0.59) (Figure 4A). Thus cyclothiazide non-selectively increased the decay times of evoked EPSCs in NAc shell neurons.

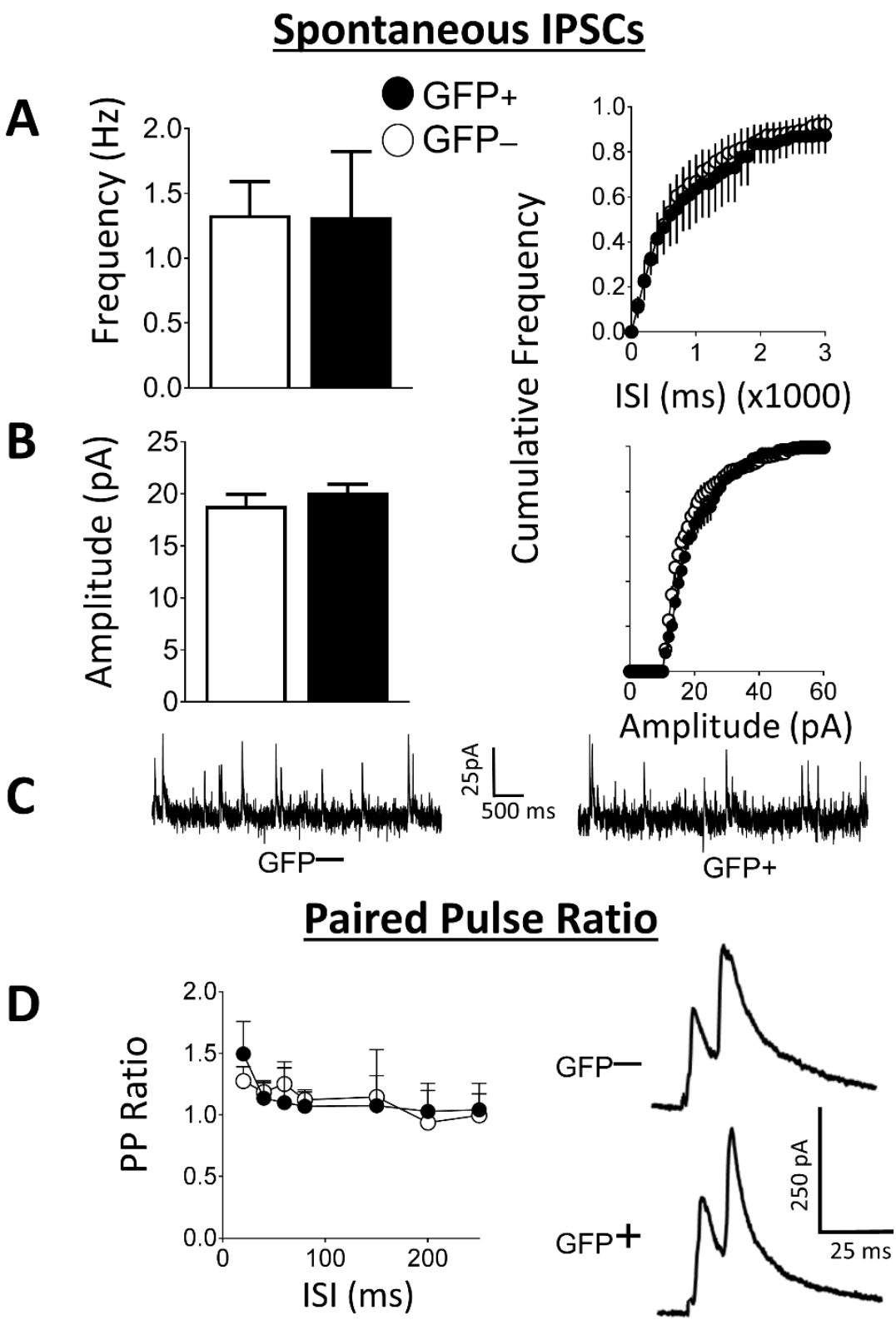


**Figure 3.** GABAergic transmission in GFP+ neurons is not altered following exposure to sucrose cues. **(A)** sIPSC frequencies were similar between GFP+ and GFP– neurons following Pavlovian approach responding (GFP+, n=4/2; GFP–, n=8/3). **(B)** sIPSC amplitudes were similar between GFP+ and GFP– neurons following Pavlovian approach responding (GFP+, n=4/2; GFP–, n=8/3). **(C)** Representative 5 s traces from GFP+ and GFP– neurons. Scale bar 25 pA, 500 ms **(D)** There were no significant differences in the paired-pulse ratios of GABAergic currents between GFP+ and GFP– neurons of Paired mice (GFP+, n=3/3; GFP–, n=5/2). *Right*: Representative images of GABAergic paired-pulse recordings from GFP+ and GFP– neurons of Paired mice. Images were edited to remove stimulus artefacts. Scale bar 500 pA, 25 ms. Data are expressed as mean±SEM. Values to the right of GFP+ and GFP– denote number of cells recorded/number of mice used.

*Modulation of spontaneous EPSCs by cyclothiazide*

We next examined the effects of cyclothiazide application on sEPSCs in GFP+ and GFP– neurons. Due to a low number of recorded cells in this experiment, a qualitative analysis of spontaneous properties was conducted (Figure 4). Cyclothiazide application increased the decay times (Figure 4B) and half-width of sEPSCs (Table 1), however this effect did not appear to be selective between GFP+ and GFP– neurons. Furthermore, there appeared to be no effect of cyclothiazide on MSN amplitudes (Figure 4C) or frequencies (Figure 4D). Thus cyclothiazide non-selectively increased the decay times of spontaneous sEPSCs in NAc shell neurons.

## Discussion

We examined excitatory and inhibitory transmission in GFP+ and GFP– neurons of the NAc shell following Pavlovian approach responding. Spontaneous EPSC frequencies on GFP+ neurons were significantly increased following exposure to a sucrose-associated cue, in the absence of adaptations in other sEPSC kinetic adaptations or changes in presynaptic release probability ($p_r$). We observed no changes in spontaneous currents or presynaptic $p_r$ at GABAergic synapses, nor selective responses to the AMPAR allosteric modulator cyclothiazide in GFP+ neurons. These data suggest that adaptations at glutamatergic synapses occur selectively in neurons activated by sucrose cues and function to potentiate excitatory transmission.

*Methodological considerations of the Fos-GFP mouse*

We utilized the *Fos-GFP* mouse to visualize neurons activated following Pavlovian approach responding. As discussed in several previous studies using the *Fos-GFP* mouse, we suggest we were recording from only the most strongly activated neurons

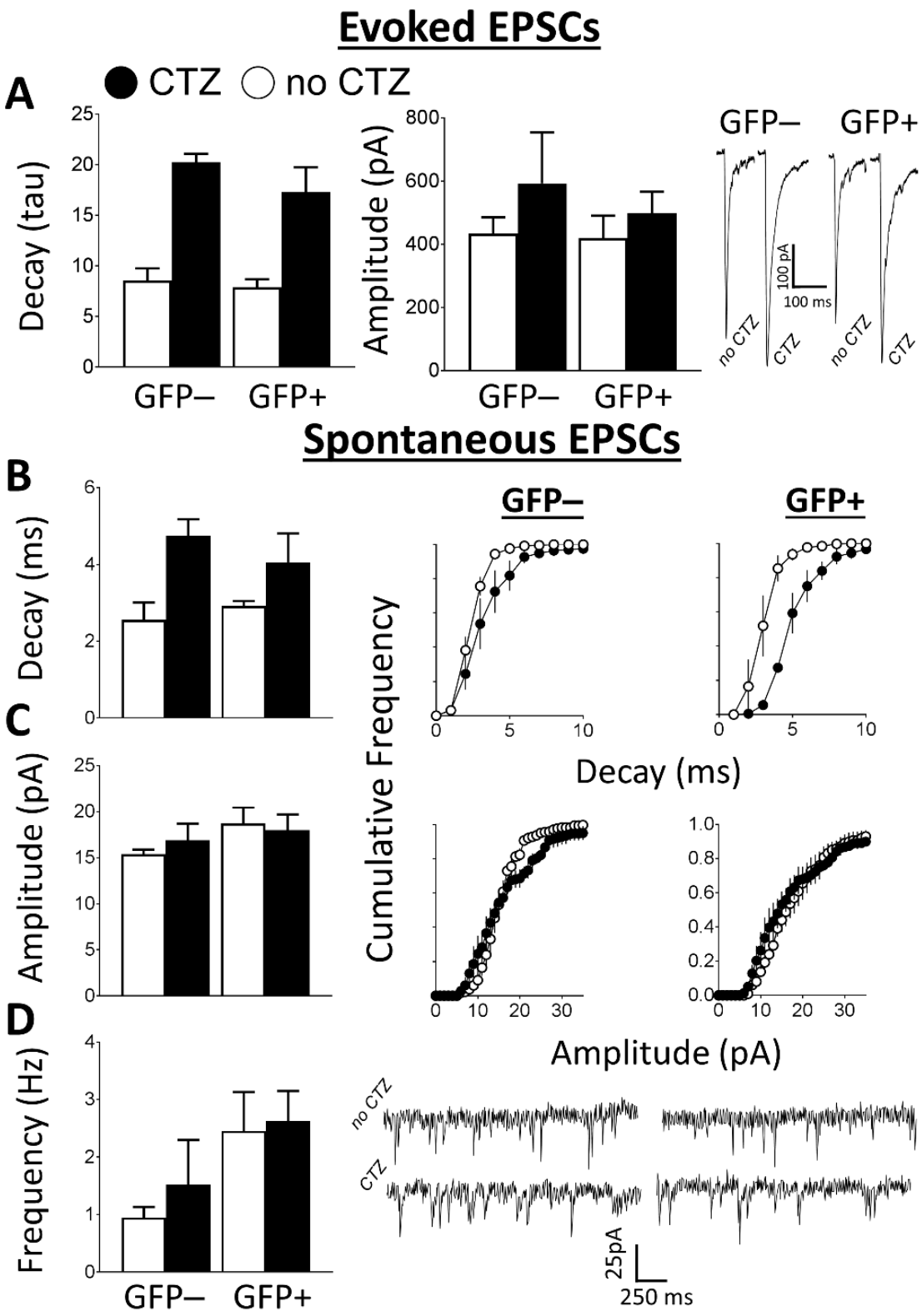


**Figure 4.** Cyclothiazide does not selectively alter AMPA transmission in GFP+ neurons following exposure to sucrose cues. **(A)** Cyclothiazide modulation of evoked EPSCs following exposure to sucrose cues. CTZ generally increased the decay times of evoked EPSCs but this was not selective between GFP+ and GFP– neurons (GFP+, n=3/2; GFP–, n=3/3). *Right:* Representative traces of evoked EPSCs under CTZ and CTZ-free conditions **(B)** There was a general increase in the decay time of following cyclothiazide application but this was not selective between GFP+ and GFP– neurons. **(C)** There was no general nor selective changes in sEPSC amplitudes following cyclothiazide application **(D)** Cyclothiazide did not generally nor selectively modulate sEPSC frequencies in NAc shell neurons following Pavlovian approach responding. *Right:* Representative 2 s traces of GFP+ and GFP– neurons during CTZ-free or CTZ application. Scale bar 25 pA, 250 ms. Group sizes were equal for all sEPSC (GFP+: CTZ-free n=2/2, CTZ n=3/3; GFP–: CTZ-free n=2/2, CTZ n=3,3). Scale bar 100 pA, 100 ms. Data are expressed as mean±SEM. Values to the right of GFP+ and GFP– denote number of cells recorded/number of mice used.

(Koya *et al*, 2012; Whitaker *et al*, 2016; Ziminski *et al*, 2017); it should be noted that this technology does not permit identification of neurons which may decrease their firing following exposure to food-associated cues. See Ziminski *et al* (2017) for further discussion.

**Adaptations at excitatory synapses following appetitive learning**

We observed a significant increase in the sEPSC frequencies on GFP+ neurons in the NAc shell following Pavlovian approach responding. Synaptic adaptations on neuronal ensembles following associative learning have previously been demonstrated (Cifani *et al*, 2012; Gouty-Colomer *et al*, 2016; Whitaker *et al*, 2016); thus associative learning may selectively induce synaptic adaptations in behaviorally relevant neurons.

We observed increased sEPSC frequencies on GFP+ neurons without concurrent changes in presynaptic vesicle probability ($p_r$), indicative of a selective increase in functional neurotransmitter release sites (Turrigiano and Nelson, 2004). This increase in synaptic release sites may represent the growth of new functional presynaptic boutons, or alternatively, the activation of postsynaptic silent synapses. Previous studies observing increased sEPSC frequencies following food exposure have demonstrated a presynaptic mechanism. Similar to our findings, Liu *et al* (2016) detected increased sEPSC frequencies, but not amplitudes nor changes to the vesicle $p_r$, in the ventral tegmental area (VTA) following palatable-food priming of food-approach behaviors. Increased sEPSC frequencies appeared necessary for the expression of food-primed approach behaviors, and occurred during 24 h of free access to the palatable food. Using immunoelectron microscopy, they observed growth of new presynaptic release sites onto dopaminergic VTA neurons simultaneously with the increases in sEPSC frequencies. Thus suggests that new presynaptic release sites may form onto neurons following exposure to high-calorie foods and are important for

the expression of approach behaviors; use of synapse-visualization techniques could be used to further explore the increases in sEPSC frequencies we observed.

Distinct adaptations in GFP+ sEPSC frequencies may occur as a function of conditioning procedure or, alternatively, following an acute learning experience. For example, repeated cocaine injections in a non-home cage environment, which induce in behavioral sensitization, result in decreased sEPSC frequencies on GFP+ neurons, while acute cocaine administration in cocaine-naïve mice lead to *increased* sEPSC frequencies on GFP+ neurons (Koya *et al*, 2012; Whitaker *et al*, 2016). Thus the type of learning experience may differentially modulate glutamatergic release onto GFP+ neurons. Growth of new functional presynaptic release sites as well as rapid activation of postsynaptic silent synapses can occur within the time-scale of our behavioral test (Liao *et al*, 2001; Lucido *et al*, 2009; Ma *et al*, 1999; Nesler *et al*, 2016). As such, the increases in sEPSC frequencies on GFP+ neurons we observed may be an acute adaptation following the behavioral test, or may have occurred during the conditioning procedure as a function of CS-US conditioning or by sucrose exposure alone (Liu *et al*, 2016). Further experimentation utilizing the *Fos-tTA x TRE-H2B-GFP* mouse (Tayler *et al*, 2013), in which GFP is expressed for weeks rather than hours, will aid in distinguishing the nature of these synaptic adaptations.

*Further investigation of glutamatergic synapses following Pavlovian approach responding*

While sEPSC and paired-pulse ratios are valuable measures of synaptic efficacy, additional experimental techniques can further aid characterization of glutamatergic synapses. The ratio of functional AMPA/NMDA receptors expressed in the neuronal membrane is a widely used measure of synaptic strength (Hyman *et al*, 2006). Changes in AMPAR/NMDAR current ratios have previously been observed following

high-calorie food conditioning (Counotte *et al*, 2014) as well as selectively on GFP+ neurons following stress-primed reinstatement of food-seeking (Cifani *et al*, 2012). Indeed, measurement of AMPAR/NMDAR ratios responding may elucidate the mechanism underlying the increase in sEPSC frequencies we observed. Activation of silent synapses increases AMPAR/NMDAR ratios (Beique *et al*, 2006; Lu *et al*, 2001) whereas generation of new presynaptic boutons will not necessarily modulate AMPAR/NMDAR ratios (see Yang & Calakos, 2013 for full discussion). Thus, increased sEPSC frequencies in the absence of changes to the AMPAR/NMDAR ratio would strongly suggest a presynaptic mechanism. Hence, more detailed characterization of synaptic transmission should be included in future studies of sucrose-cue activated ensembles

**Relationship between synaptic and intrinsic excitability adaptations in sucrose-cue activated neurons**

We have previously observed increased membrane excitability in GFP+ neurons following Pavlovian approach responding (Ziminski *et al*, 2017). These combined data suggest that sucrose-cue activated neurons demonstrate both increased intrinsic excitability and glutamatergic synaptic strength compared to their surrounding, non - activated neurons.

*Effects of increased synaptic transmission on measures of intrinsic excitability*

It is plausible that increased glutamatergic tone onto GFP+ neurons may have led directly to the potentiated firing rate and input resistance we previously measured. While neuronal gain (the current input- spike output relationship) is modulated *in vivo* by synaptic input (Cardin *et al*, 2008), the effect of spontaneous neurotransmitter release on measures of membrane excitability *in vitro* are less clear. Previous

observations suggest changes in sEPSC frequencies are not usually accompanied by alterations in intrinsic measures of excitability. Application of the AMPAR blocker CNQX-eliminates spontaneous EPSC frequencies but has no effect on the input resistance of both mammalian and invertebrate neurons (Hanganu *et al*, 2001; Li and Burrell, 2008b), while in the hypothalamus of hypertensive rats, increased sEPSC frequencies lead to potentiated neuronal firing rates in the absence of changes in the input resistance (Li *et al*, 2008a)**.** Furthermore, we observed decreased inward rectification in response to hyperpolarizing stimuli, an effect primarily mediated by inwardly rectifying potassium current $K_{ir}$ (Nisenbaum and Wilson, 1995) and not consistent with the excitatory effect of increasing sEPSC frequency. Additionally, neuronal gain is not thought to be affected by shunting inhibition provided by extrasynaptic $GABA_A$ α4 receptors (Pavlov *et al*, 2009), excluding this possible influence on the input resistance. This suggests that the membrane adaptations we observed in GFP+ neurons following exposure to sucrose cues are independent from the detected increases in basal glutamatergic tone.

*The function of concurrent increases in synaptic and intrinsic excitability in neurons activated by sucrose-cues*

We observed concurrent increases in the synaptic and intrinsic excitability of neurons strongly activated by sucrose cues (Ziminski *et al*, 2017). This is in contrast to previous descriptions of homeostatic adaptations to synaptic and intrinsic excitability, whereby intrinsic excitability is increased in response to *decreased* synaptic drive, and vice-versa (Ishikawa *et al*, 2009; Schulz, 2006), a regulatory process thought to be crucial in maintaining network stability (Turrigiano, 2011). The number of strongly activated neurons observed after expression of conditioned and sensitized behaviors is commonly in the range of 3-5% (Koya *et al*, 2009; Warren *et al*, 2016). As such, it is possible homeostatic processes may govern in the majority of weakly activated

neurons following learning-induced network perturbations (Turrigiano, 2011), while behaviorally relevant cue-activated ensembles are selectively potentiated.

Concurrent increases in intrinsic excitability and synaptic transmission have previously been observed *in vitro* following use of the long-term potentiation (LTP) induction procedure (Zhang and Linden, 2003). Theta burst stimulation (stimulation in the frequency range of the endogenous hippocampal theta rhythm (Larson and Munkacsy, 2015)) in cerebellar mossy fiber-granule cell synapses resulted in increased excitability of the postsynaptic neuron concurrent with potentiated synaptic transmission (Armano *et al*, 2000). While such observations following associative conditioning are rare, Antonov *et al* (2001) observed, at the sensory-motor neuron synapse of *Aplysia* following conditioning of the siphon withdrawal reflex, increases in presynaptic input resistance and firing frequency alongside both pre- and postsynaptic facilitation of glutamatergic transmission (Roberts and Glanzman, 2003). Thus high-frequency stimulation can simultaneously potentiate synaptic and intrinsic excitability at the level of a single neuron. It is thus tempting to speculate that during associative learning in *Fos-GFP* mice, strongly activated GFP+ neurons undergo LTP-like processes caused by high-frequency stimulation. NMDAR-mediated transmission may be of particular importance as NMDAR activation is necessary for both LTP-induced simultaneous increases in synaptic and intrinsic excitability (Armano *et al*, 2000), as well as GFP induction in the *Fos-GFP mice (Cruz et al, 2013).*

The function of the neuroadaptations we observed in GFP+ neurons following Pavlovian responding is presently unclear. While strengthening of excitatory synaptic transmission permits selective increases in connectivity between specific neurons (Bliss and Collingridge, 1993), potentiation of intrinsic excitability is thought to maximize downstream information transfer and/or facilitate synapse-driven plasticity (Daoudal and Debanne, 2003; Kourrich *et al*, 2015; Stemmler and Koch, 1999). Electrophysiological studies following associative conditioning have demonstrated

transient, learning induced increases in excitability that are dissociable from expression of conditioned behavior (Moyer *et al*, 1996); alternatively, persisting (1 month) increases in conditioning-induced intrinsic excitability have also been detected (Schreurs *et al*, 1998). Thus we may have recorded during a short-term transitionary phase in which brief changes in intrinsic excitability, which functioned to transiently facilitate synaptic-plasticity, overlap with the long-term potentiation of glutamatergic synapses. Alternatively, persistent increases in both synaptic and intrinsic excitability may function to potentiate the output of interconnected, behaviorally relevant ensembles. Further work examining the time scale of ensemble adaptations would aid in determining the nature of the adaptations we have observed.

*Confirming concurrent synaptic and intrinsic changes in GFP+ neurons*

Sucrose-cue activated neurons did not uniformly show increased synaptic or intrinsic excitability above the baseline (averaged response) of surrounding, non-activated GFP– neurons (Appendix B). Thus it is possible that individual GFP+ neurons regulated their synaptic and intrinsic excitability in a mutually exclusive manner i.e. no single GFP+ neuron displayed *both* the synaptic and intrinsic adaptations we observed. However, while there is a significant overlap in the intracellular signaling cascades regulating synaptic and intrinsic adaptations (Kotaleski and Blackwell, 2010), suggesting this possibility is unlikely, further experiments recording both current and voltage responses in the same neuron (Zuo *et al*, 2016) would be necessary to confirm our observations.

**Exposure to a sucrose-associated cue did not result in selective regulation of inhibitory synapses or AMPAR splice-variant expression**

*Inhibitory synapses*

We observed no alterations in spontaneous inhibitory postsynaptic currents (sIPSC) or in presynaptic release probabilities at GABAergic synapses, suggesting that the net effect of increased sEPSC frequencies onto GFP+ neurons was excitatory (Froemke, 2015).

Transient reductions in GABAergic transmission (coined “transient disinhibition) is an important mechanism of synaptic potentiation observed sensory networks which facilitates synaptic plasticity (Froemke, 2015). This is an energy efficient way of increasing excitatory transmission, as decreasing inhibition requires less metabolic activity than increasing excitation (Waldvogel *et al*, 2000). Thus it is interesting that we did not see any adaptations in GABAergic synaptic strength in the NAc shell following Pavlovian approach responding. Limbic system projections to the NAc are primarily glutamatergic, with GABA afferents sparse and GABAergic tone provided by local interneurons; furthermore, glutamate-dopamine interactions are crucial for the expression of many motivated behaviors (Lee *et al*, 2014; Russo and Nestler, 2013; Salgado and Kaplitt, 2015; Sesack and Pickel, 1990; Totterdell and Smith, 1989; Wu *et al*, 1993). Thus in NAc circuitry, modulation of the glutamatergic system may provide a higher degree of neuronal specificity than the GABAergic system.

Additional measures of inhibitory transmission will permit further characterization of GABAergic synapses on GFP+ neurons. For example, coincident pre- and postsynaptic activity can cause adaptations in the chloride transporter, altering the Cl- reversal potential and thus GABA current magnitude (Woodin *et al*, 2003). Furthermore, probability of neurotransmitter release following evoked IPSCs can be assayed using the coefficient of variation of IPSC amplitudes (Hefft *et al*, 2002; Kerchner and Nicoll, 2008; Kullmann and Lamsa, 2007). It is possible that interneurons

may differentially regulate the probability of GABA release onto GFP+ and GFP- neurons; dual-recording experiments between GABAergic interneurons and GFP+ MSNs can be used to explore this possibility.

*Cyclothiazide application*

We observed no selective adaptations in the responses of sucrose-cue activated neurons to the AMPA receptor allosteric modulator cyclothiazide. We report pronounced generalized increased in AMPAR-mediated EPSC decay times and modest increase in EPSC amplitudes following cyclothiazide application, in accordance with other studies of cyclothiazide action (Liu and Cull-Candy, 2002; Rammes *et al*, 1994).

AMPA receptor subunits exist in flip/flop splice isoforms which heterogeneously combine into functional receptors; as such flip and flop variants may exist in the same receptor (Liu *et al*, 2002). Cyclothiazide has a pronounced binding preference for the flip splice variant of AMPA receptor subunits (Kessler *et al*, 2000). Our data suggest that there are no selective changes in flip vs. flop AMPAR subunit expression in neurons activated by sucrose-associated cues. Thus, cyclothiazide or related drugs with flip/flop binding preferences may be of limited utility in the design of pharmacological interventions aiming to reduce the behavioral influence of food-associated cues (Boswell *et al*, 2016). It should be noted that cyclothiazide affinity for flip-containing AMPAR receptors may non-linearly scale dependent on the proportion of flip vs. flop subunits present in the receptor (Liu *et al*, 2002); thus large increases in the proportion of flip-subunits expressed in the AMPAR population may be masked by subtle changes in homogenous flip-subunit containing AMPA receptors. Molecular identification of AMPAR subunit composition in GFP+ vs. GFP- neurons could be

further elucidated using single-cell RNA quantification following electrophysiological experiments (Lu *et al*, 2009).

**Concluding Remarks**

We report that exposure to sucrose-associated cues elicits activation of a NAc shell ensemble with increased synaptic and intrinsic excitability compared to surrounding, non-activated neurons. These concurrent adaptations may function to increase both the activity and connectivity of the sucrose-cue activated ensemble. It is necessary to further identify the time-scale of the neuroadaptations we observed, as to whether these changes are transient adaptations or, alternatively, persistent network alterations which occur following Pavlovian approach conditioning. At the present time, the behavioral relevance of the neurons recently activated following the Pavlovian approach test is unclear. Further investigations utilizing the Daun02 ensemble-inactivation method (Koya *et al*, 2012) would elucidate the contribution of the sucrose-cue activated ensembles we are presently measuring to conditioned behavior.

## References


Antonov I, Antonova I, Kandel ER, Hawkins RD (2001). The contribution of activity-dependent synaptic plasticity to classical conditioning in Aplysia. *J Neurosci* **21**(16): 6413-6422.

Armano S, Rossi P, Taglietti V, D'Angelo E (2000). Long-term potentiation of intrinsic excitability at the mossy fiber-granule cell synapse of rat cerebellum. *J Neurosci* **20**(14): 5208-5216.

Beique JC, Lin DT, Kang MG, Aizawa H, Takamiya K, Huganir RL (2006). Synapse-specific regulation of AMPA receptor function by PSD-95. *Proc Natl Acad Sci U S A* **103**(51): 19535-19540.

Blaiss CA, Janak PH (2009). The nucleus accumbens core and shell are critical for the expression, but not the consolidation, of Pavlovian conditioned approach. *Behav Brain Res* **200**(1): 22-32.

Bliss TV, Collingridge GL (1993). A synaptic model of memory: long-term potentiation in the hippocampus. *Nature* **361**(6407): 31-39.

Boswell RG, Kober H (2016). Food cue reactivity and craving predict eating and weight gain: a meta-analytic review. *Obes Rev* **17**(2): 159-177.

Cardin JA, Palmer LA, Contreras D (2008). Cellular mechanisms underlying stimulus-dependent gain modulation in primary visual cortex neurons in vivo. *Neuron* **59**(1): 150-160.

Cifani C, Koya E, Navarre BM, Calu DJ, Baumann MH, Marchant NJ*, et al* (2012). Medial prefrontal cortex neuronal activation and synaptic alterations after stress-induced reinstatement of palatable food seeking: a study using c-fos-GFP transgenic female rats. *J Neurosci* **32**(25): 8480-8490.

Counotte DS, Schiefer C, Shaham Y, O'Donnell P (2014). Time-dependent decreases in nucleus accumbens AMPA/NMDA ratio and incubation of sucrose craving in adolescent and adult rats. *Psychopharmacology (Berl)* **231**(8): 1675-1684.

Cruz FC, Babin KR, Leao RM, Goldart EM, Bossert JM, Shaham Y*, et al* (2014). Role of nucleus accumbens shell neuronal ensembles in context-induced reinstatement of cocaine-seeking. *J Neurosci* **34**(22): 7437-7446.

Cruz FC, Koya E, Guez-Barber DH, Bossert JM, Lupica CR, Shaham Y*, et al* (2013). New technologies for examining the role of neuronal ensembles in drug addiction and fear. *Nat Rev Neurosci* **14**(11): 743-754.

Daoudal G, Debanne D (2003). Long-term plasticity of intrinsic excitability: learning rules and mechanisms. *Learn Mem* **10**(6): 456-465.

Day JJ, Carelli RM (2007). The nucleus accumbens and Pavlovian reward learning. *Neuroscientist* **13**(2): 148-159.

Froemke RC (2015). Plasticity of cortical excitatory-inhibitory balance. *Annu Rev Neurosci* **38**: 195-219.

Gouty-Colomer LA, Hosseini B, Marcelo IM, Schreiber J, Slump DE, Yamaguchi S*, et al* (2016). Arc expression identifies the lateral amygdala fear memory trace. *Mol Psychiatry* **21**(3): 364-375.

Hanganu IL, Kilb W, Luhmann HJ (2001). Spontaneous synaptic activity of subplate neurons in neonatal rat somatosensory cortex. *Cereb Cortex* **11**(5): 400-410.

Harris JL, Bargh JA, Brownell KD (2009). Priming effects of television food advertising on eating behavior. *Health Psychol* **28**(4): 404-413.

Hayton SJ, Olmstead MC, Dumont EC (2011). Shift in the intrinsic excitability of medial prefrontal cortex neurons following training in impulse control and cued-responding tasks. *PLoS One* **6**(8): e23885.

Hefft S, Kraushaar U, Geiger JR, Jonas P (2002). Presynaptic short-term depression is maintained during regulation of transmitter release at a GABAergic synapse in rat hippocampus. *J Physiol* **539**(Pt 1): 201-208.

Holland PC (1980). Influence of visual conditioned stimulus characteristics on the form of Pavlovian appetitive conditioned responding in rats. *J Exp Psychol Anim Behav Process* **6**(1): 81-97.

Hutter JA, Chapman CA (2013). Exposure to cues associated with palatable food reward results in a dopamine D(2) receptor-dependent suppression of evoked synaptic responses in the entorhinal cortex. *Behav Brain Funct* **9**: 37.

Hyman SE, Malenka RC, Nestler EJ (2006). Neural mechanisms of addiction: the role of reward-related learning and memory. *Annu Rev Neurosci* **29**: 565-598.

Ishikawa M, Mu P, Moyer JT, Wolf JA, Quock RM, Davies NM*, et al* (2009). Homeostatic synapse-driven membrane plasticity in nucleus accumbens neurons. *J Neurosci* **29**(18): 5820-5831.

Kerchner GA, Nicoll RA (2008). Silent synapses and the emergence of a postsynaptic mechanism for LTP. *Nat Rev Neurosci* **9**(11): 813-825.

Kessler M, Rogers G, Arai A (2000). The norbornenyl moiety of cyclothiazide determines the preference for flip-flop variants of AMPA receptor subunits. *Neurosci Lett* **287**(2): 161-165.

Kotaleski JH, Blackwell KT (2010). Modelling the molecular mechanisms of synaptic plasticity using systems biology approaches. *Nat Rev Neurosci* **11**(4): 239-251.

Kourrich S, Calu DJ, Bonci A (2015). Intrinsic plasticity: an emerging player in addiction. *Nat Rev Neurosci* **16**(3): 173-184.

Kourrich S, Thomas MJ (2009). Similar neurons, opposite adaptations: psychostimulant experience differentially alters firing properties in accumbens core versus shell. *J Neurosci* **29**(39): 12275-12283.

Koya E, Cruz FC, Ator R, Golden SA, Hoffman AF, Lupica CR*, et al* (2012). Silent synapses in selectively activated nucleus accumbens neurons following cocaine sensitization. *Nat Neurosci* **15**(11): 1556-1562.

Koya E, Golden SA, Harvey BK, Guez-Barber DH, Berkow A, Simmons DE*, et al* (2009). Targeted disruption of cocaine-activated nucleus accumbens neurons prevents context-specific sensitization. *Nat Neurosci* **12**(8): 1069-1073.

Kullmann DM, Lamsa KP (2007). Long-term synaptic plasticity in hippocampal interneurons. *Nat Rev Neurosci* **8**(9): 687-699.

Larson J, Munkacsy E (2015). Theta-burst LTP. *Brain Res* **1621**: 38-50.

Lee AT, Vogt D, Rubenstein JL, Sohal VS (2014). A class of GABAergic neurons in the prefrontal cortex sends long-range projections to the nucleus accumbens and elicits acute avoidance behavior. *J Neurosci* **34**(35): 11519-11525.

Li DP, Yang Q, Pan HM, Pan HL (2008a). Pre- and postsynaptic plasticity underlying augmented glutamatergic inputs to hypothalamic presympathetic neurons in spontaneously hypertensive rats. *J Physiol* **586**(6): 1637-1647.

Li Q, Burrell BD (2008b). CNQX and AMPA inhibit electrical synaptic transmission: a potential interaction between electrical and glutamatergic synapses. *Brain Res* **1228**: 43-57.

Liao D, Scannevin RH, Huganir R (2001). Activation of silent synapses by rapid activity-dependent synaptic recruitment of AMPA receptors. *J Neurosci* **21**(16): 6008-6017.

Liu S, Globa AK, Mills F, Naef L, Qiao M, Bamji SX*, et al* (2016). Consumption of palatable food primes food approach behavior by rapidly increasing synaptic density in the VTA. *Proc Natl Acad Sci U S A* **113**(9): 2520-2525.

Liu SJ, Cull-Candy SG (2002). Activity-dependent change in AMPA receptor properties in cerebellar stellate cells. *J Neurosci* **22**(10): 3881-3889.

Lu W, Man H, Ju W, Trimble WS, MacDonald JF, Wang YT (2001). Activation of synaptic NMDA receptors induces membrane insertion of new AMPA receptors and LTP in cultured hippocampal neurons. *Neuron* **29**(1): 243-254.

Lu W, Shi Y, Jackson AC, Bjorgan K, During MJ, Sprengel R*, et al* (2009). Subunit composition of synaptic AMPA receptors revealed by a single-cell genetic approach. *Neuron* **62**(2): 254-268.

Lucido AL, Suarez Sanchez F, Thostrup P, Kwiatkowski AV, Leal-Ortiz S, Gopalakrishnan G*, et al* (2009). Rapid assembly of functional presynaptic boutons triggered by adhesive contacts. *J Neurosci* **29**(40): 12449-12466.

Ma L, Zablow L, Kandel ER, Siegelbaum SA (1999). Cyclic AMP induces functional presynaptic boutons in hippocampal CA3-CA1 neuronal cultures. *Nat Neurosci* **2**(1): 24-30.

Mackintosh N (1983). *Conditioning and associative learning.* Clarendon: Oxford.

Moyer JR, Jr., Thompson LT, Disterhoft JF (1996). Trace eyeblink conditioning increases

CA1 excitability in a transient and learning-specific manner. *J Neurosci* **16**(17): 5536-5546.

Nesler KR, Starke EL, Boin NG, Ritz M, Barbee SA (2016). Presynaptic CamKII regulates activity-dependent axon terminal growth. *Mol Cell Neurosci* **76**: 33-41.

Nisenbaum ES, Wilson CJ (1995). Potassium currents responsible for inward and outward rectification in rat neostriatal spiny projection neurons. *J Neurosci* **15**(6): 4449-4463.

Pavlov I, Savtchenko LP, Kullmann DM, Semyanov A, Walker MC (2009). Outwardly rectifying tonically active GABAA receptors in pyramidal cells modulate neuronal offset, not gain. *J Neurosci* **29**(48): 15341-15350.

Pei W, Huang Z, Wang C, Han Y, Park JS, Niu L (2009). Flip and flop: a molecular determinant for AMPA receptor channel opening. *Biochemistry* **48**(17): 3767-3777.

Rammes G, Parsons C, Muller W, Swandulla D (1994). Modulation of Fast Excitatory Synaptic Transmission by Cyclothiazide and Gyki-52466 in the Rat Hippocampus. *Neuroscience Letters* **175**(1-2): 21-24.

Roberts AC, Glanzman DL (2003). Learning in Aplysia: looking at synaptic plasticity from both sides. *Trends Neurosci* **26**(12): 662-670.

Russo SJ, Nestler EJ (2013). The brain reward circuitry in mood disorders. *Nat Rev Neurosci* **14**(9): 609-625.

Salgado S, Kaplitt MG (2015). The Nucleus Accumbens: A Comprehensive Review. *Stereotact Funct Neurosurg* **93**(2): 75-93.

Schreurs BG, Gusev PA, Tomsic D, Alkon DL, Shi T (1998). Intracellular correlates of acquisition and long-term memory of classical conditioning in Purkinje cell dendrites in slices of rabbit cerebellar lobule HVI. *J Neurosci* **18**(14): 5498-5507.

Schulz DJ (2006). Plasticity and stability in neuronal output via changes in intrinsic excitability: it's what's inside that counts. *J Exp Biol* **209**(Pt 24): 4821-4827.

Sesack SR, Pickel VM (1990). In the rat medial nucleus accumbens, hippocampal and catecholaminergic terminals converge on spiny neurons and are in apposition to each other. *Brain Res* **527**(2): 266-279.

Shiflett MW, Martini RP, Mauna JC, Foster RL, Peet E, Thiels E (2008). Cue-elicited reward-seeking requires extracellular signal-regulated kinase activation in the nucleus accumbens. *J Neurosci* **28**(6): 1434-1443.

Stemmler M, Koch C (1999). How voltage-dependent conductances can adapt to maximize the information encoded by neuronal firing rate. *Nat Neurosci* **2**(6): 521-527.

Stuber GD, Klanker M, de Ridder B, Bowers MS, Joosten RN, Feenstra MG*, et al* (2008). Reward-predictive cues enhance excitatory synaptic strength onto midbrain dopamine neurons. *Science* **321**(5896): 1690-1692.

Tayler KK, Tanaka KZ, Reijmers LG, Wiltgen BJ (2013). Reactivation of neural ensembles during the retrieval of recent and remote memory. *Curr Biol* **23**(2): 99-106.

Ting JT, Daigle TL, Chen Q, Feng G (2014). Acute brain slice methods for adult and aging animals: application of targeted patch clamp analysis and optogenetics. *Methods Mol Biol* **1183**: 221-242.

Totterdell S, Smith AD (1989). Convergence of hippocampal and dopaminergic input onto identified neurons in the nucleus accumbens of the rat. *J Chem Neuroanat* **2**(5): 285-298.

Turrigiano G (2011). Too many cooks? Intrinsic and synaptic homeostatic mechanisms in cortical circuit refinement. *Annu Rev Neurosci* **34**: 89-103.

Turrigiano GG, Nelson SB (2004). Homeostatic plasticity in the developing nervous system. *Nat Rev Neurosci* **5**(2): 97-107.

Waldvogel D, van Gelderen P, Muellbacher W, Ziemann U, Immisch I, Hallett M (2000). The relative metabolic demand of inhibition and excitation. *Nature* **406**(6799): 995-998.

Warren BL, Mendoza MP, Cruz FC, Leao RM, Caprioli D, Rubio FJ*, et al* (2016). Distinct Fos-Expressing Neuronal Ensembles in the Ventromedial Prefrontal Cortex Mediate Food Reward and Extinction Memories. *J Neurosci* **36**(25): 6691-6703.

Whitaker LR, Carneiro de Oliveira PE, McPherson KB, Fallon RV, Planeta CS, Bonci A*, et al* (2016). Associative Learning Drives the Formation of Silent Synapses in Neuronal

Ensembles of the Nucleus Accumbens. *Biol Psychiatry* **80**(3): 246-256.

Wolf ME (2010). The Bermuda Triangle of cocaine-induced neuroadaptations. *Trends Neurosci* **33**(9): 391-398.

Woodin MA, Ganguly K, Poo MM (2003). Coincident pre- and postsynaptic activity modifies GABAergic synapses by postsynaptic changes in Cl- transporter activity. *Neuron* **39**(5): 807-820.

Wu M, Brudzynski SM, Mogenson GJ (1993). Functional interaction of dopamine and glutamate in the nucleus accumbens in the regulation of locomotion. *Can J Physiol Pharmacol* **71**(5-6): 407-413.

Yang Y, Calakos N (2013). Presynaptic long-term plasticity. *Front Synaptic Neurosci* **5**: 8.

Zhang W, Linden DJ (2003). The other side of the engram: experience-driven changes in neuronal intrinsic excitability. *Nat Rev Neurosci* **4**(11): 885-900.

Ziminski JJ, Hessler S, Margetts-Smith G, Sieburg MC, Crombag HS, Koya E (2017). Changes in Appetitive Associative Strength Modulates Nucleus Accumbens, But Not Orbitofrontal Cortex Neuronal Ensemble Excitability. *J Neurosci* **37**(12): 3160-3170.

Zuo W, Xiao C, Gao M, Hopf FW, Krnjevic K, McIntosh JM*, et al* (2016). Nicotine regulates activity of lateral habenula neurons via presynaptic and postsynaptic mechanisms. *Sci Rep* **6**: 32937.

# Chapter 5.

# Regional differences in striatal neuronal ensemble excitability following cocaine and extinction memory retrieval in *Fos-GFP* mice.

*Ziminski J, Sieburg MC, Margetts-Smith G, Crombag HS, Koya E (2017). Regional Differences In Striatal Neuronal Ensemble Excitability Following Cocaine And Extinction Memory Retrieval In Fos-GFP Mice. Neuropsychopharmacology. [online] Available at: https://www.nature.com/articles/npp201710*

**Abstract**

Learned associations between drugs of abuse and the drug administration environment play an important role in addiction. In rodents, exposure to a drug-associated environment elicits conditioned psychomotor activation, which may be weakened following extinction learning. While widespread drug-induced changes in neuronal excitability have been observed, little is known about specific changes within neuronal ensembles activated during the recall of drug-environment associations. Using a cocaine conditioned locomotion procedure, the present study assessed the excitability of neuronal ensembles in the nucleus accumbens (NAc) core and shell, and dorsal striatum (DS) following cocaine conditioning and extinction in *Fos-GFP* mice that express green fluorescent protein (GFP) in activated, GFP+, neurons. During conditioning, mice received repeated cocaine injections (20 mg/kg) paired with a locomotor activity chamber (Paired) or home cage (Unpaired). 7-13 days later both groups were re-exposed to the activity chamber under drug-free conditions, and Paired, but not Unpaired, mice exhibited conditioned locomotion. In a separate group of mice, conditioned locomotion was extinguished by repeatedly exposing mice to the activity chamber under drug-free conditions. Following the expression and extinction of conditioned locomotion, GFP+ neurons in the NAc core (but not NAc shell and DS) displayed greater firing capacity compared to surrounding GFP– neurons. This difference in excitability was due to a generalised decrease in GFP– excitability following conditioned locomotion, and a selective increase in GFP+ excitability following its extinction. These results suggest a role for both widespread and ensemble-specific changes in neuronal excitability following recall of drug-environment associations.

## Introduction

Exposure to drug-associated environmental cues or contexts elicits anticipatory responses including conditioned locomotor hyperactivity in rodents (Post *et al*, 1981) and conditioned emotional, behavioural, and physiological responses in humans (O'Brien *et al*, 1998). These learned associations between drug effects and the drug administration environment play an important role in addiction and may be weakened through extinction learning (Michel *et al*, 2003), and methods such as cue-exposure therapy utilise such inhibitory learning to reduce the impact of drug-associated stimuli (Conklin and Tiffany, 2002). Thus, understanding the neurobiological mechanisms of how the strength of these associations are modulated is crucial to better understanding drug addiction.

We and others have reported that drug-environment associations are encoded in sparsely activated populations of neurons, called neuronal ensembles (Carelli, 2002; Koya *et al*, 2009). Recent studies utilising *Fos-GFP* mice that express the green fluorescent protein (GFP) in behaviourally activated neurons, suggest that the ensembles which encode these associations exhibit unique adaptations at glutamatergic synapses compared to their surrounding neurons (Koya *et al*, 2012; Whitaker *et al*, 2016). These data indicate that ensemble-specific modifications may be implicated in the storage of drug-associative memories.

Neurons may alter their signal processing through synaptic adjustments or intrinsic excitability modulation (Wolf, 2010), such as changes in the firing capacity of neurons and/or in ion channel function. Widespread intrinsic excitability changes in the striatum, a brain area which subserves various cocaine-induced behaviours (Everitt and Robbins, 2013), have been observed following repeated cocaine exposure (Kourrich and Thomas, 2009; Ma *et al*, 2013; Mu *et al*, 2010; Zhang *et al*, 1998). These studies have enhanced our understanding of the long-term effects of repeated cocaine on

intrinsic excitability. However, to further understand how cocaine-environment associations are encoded in the brain, in addition to the widespread drug-induced changes, the neuronal excitability properties from neurons that are specifically activated by cocaine-associated memory recall must be characterised.

The aim of this study was to investigate neuronal excitability changes in striatal ensembles following cocaine and extinction memory retrieval utilising a cocaine conditioned locomotion procedure in *Fos-GFP* mice. We focused our investigation on the nucleus accumbens shell (NAc shell), core (NAc core) and dorsal striatum (DS), as these three striatal areas have been shown to have related yet distinct involvement in encoding drug-environment associations (Caprioli *et al*, 2017; Chaudhri *et al*, 2010; Everitt *et al*, 2013). We hypothesised that changes in the strength of a drug-environment association may be accompanied by alterations in neuronal excitability on striatal neuronal ensembles.

## Results

### Locomotor activity and striatal Fos expression following cocaine and extinction memory retrieval

We trained four groups of mice to assess the expression (CL: Paired CL, Unpaired CL) (Figure 1A) and extinction (EXT: Paired EXT, Unpaired EXT) (Figure 1B) of conditioned locomotor activity. A two-way ANOVA on the locomotor activity (indicated by distance travelled) during the test session revealed a significant interaction of Group X Extinction ($F_{1,40}$=4.17, p<0.05) and a significant main effect of Group ($F_{1,40}$=5.41, p<0.05) (A)**.** Post-hoc tests indicated that Paired CL mice displayed significantly higher locomotor activity compared to Unpaired CL mice (p<0.01). Also, Paired EXT mice displayed significantly lower locomotor activity compared to Paired CL mice (p<0.05), at levels similar to Unpaired EXT mice. These data indicate that Paired CL and Paired

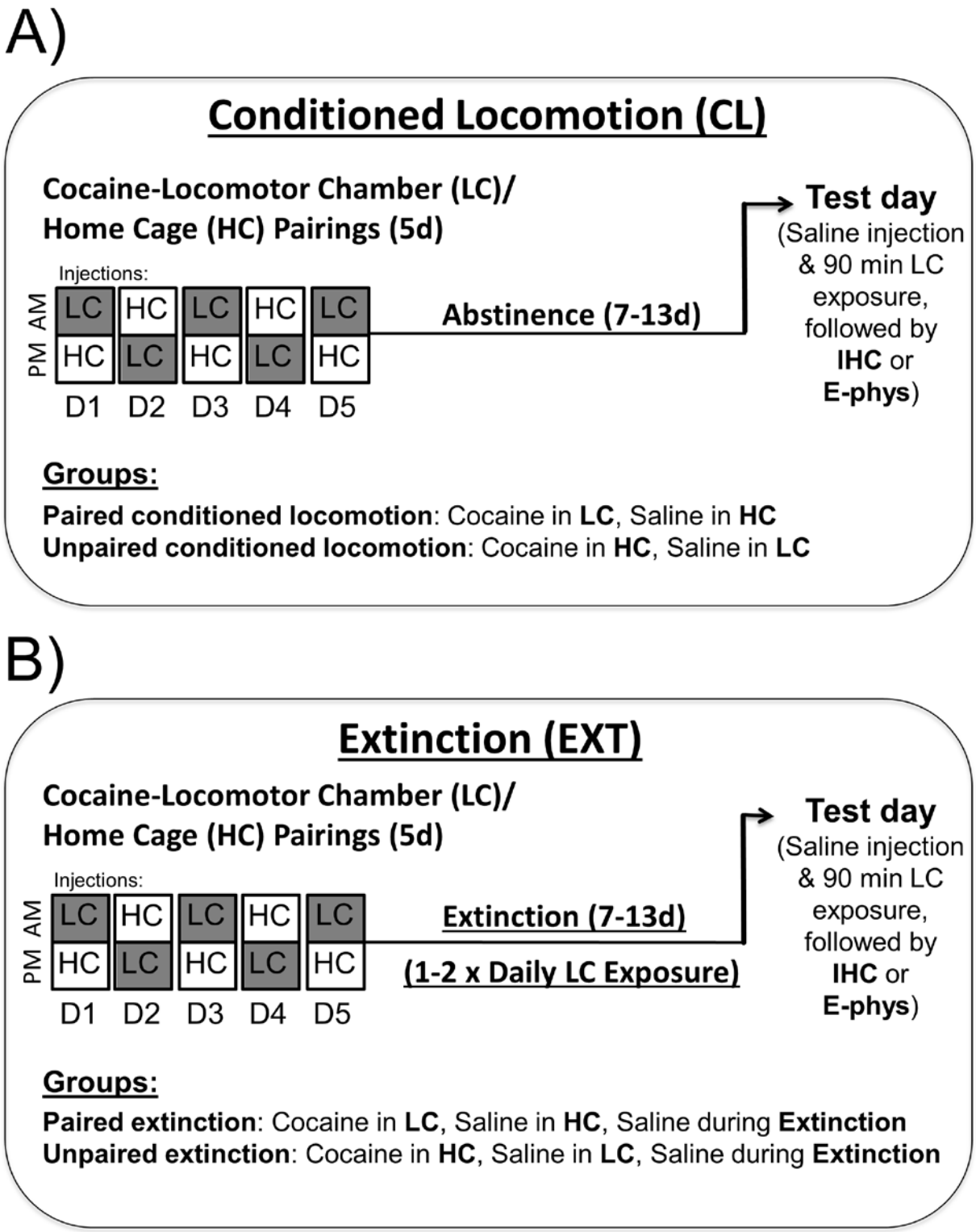


**Figure 1.** Timeline for conditioned locomotion and extinction experiments. **(A)** In conditioned locomotion (cocaine memory retrieval) experiments, two groups of mice were exposed to the locomotor chamber for once daily 30 minute sessions over a 5-day period; Paired CL mice received 20 mg/kg i.p. cocaine injections prior to these sessions while Unpaired CL mice received saline. Across the 5 acquisition days, Unpaired CL and Paired CL mice were given cocaine and saline injections in the home-cage, respectively. Home cage and locomotor chamber injections were counterbalanced across morning (8 A.M. - 12 A.M.) and afternoon (3 P.M. – 6 P.M.) sessions. This regime ensured that the psychostimulant effects of cocaine were paired with the locomotor chamber in the Paired CL group only. Following an abstinence period of 7-11 days (IHC; immunohistochemistry) or 7-13 days (E-phys; electrophysiology), free of experimental intervention, both Paired CL and Unpaired CL mice were given a single saline injection and placed in the locomotor chambers for 90 minutes, before being killed for further immunohistochemistry or electrophysiology experiments. **(B)** In extinction experiments (extinction memory retrieval), Paired EXT and Unpaired EXT mice underwent an identical cocaine injection procedure as during the conditioned locomotion experiments. One day following the final cocaine injection, Paired EXT and Unpaired EXT mice began an extinction phase consisting of 30 min, 1-2 x daily exposures to the locomotor chamber, each started immediately following a saline injection. Following 7-13 days (10-16 sessions; electrophysiology) or 7-11 days (10-14 sessions, immunohistochemistry) of extinction, mice were given a final 90 min extinction session before being killed for further experiments.

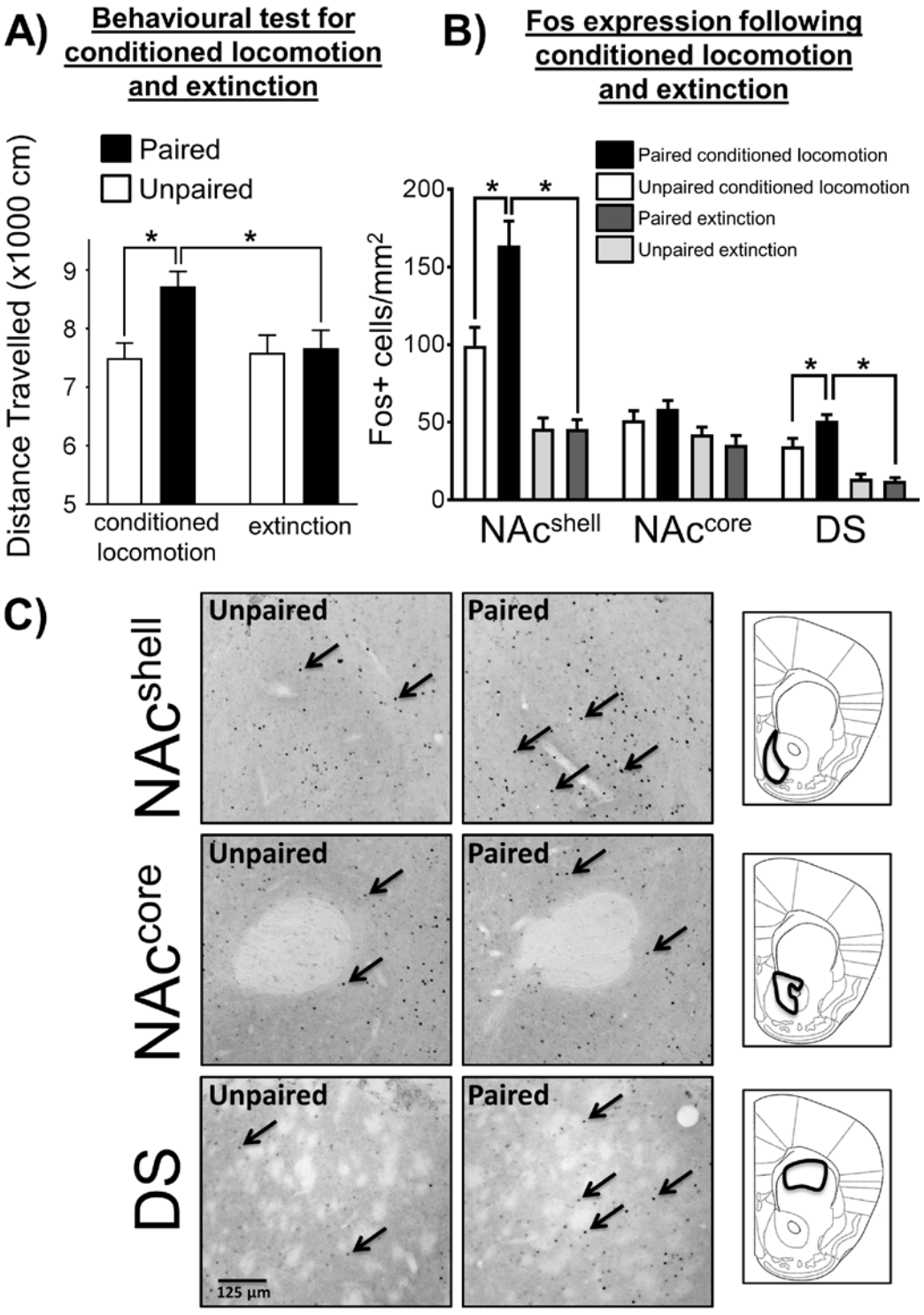


**Figure 2.** Behavioral response and neuronal activation following conditioned locomotion and extinction. **(A)** Distance travelled by Paired and Unpaired mice during the first 30 minutes of the conditioned locomotion and extinction test sessions in the immunohistochemistry study (n=10-12/group). Paired CL group mice show increased locomotion compared to Unpaired CL mice following cocaine memory retrieval. Following extinction memory retrieval, no increase in locomotion was observed (Paired EXT group). **(B)** Quantification of Fos+ neurons/mm$^2$ in the NAc shell, NAc core and DS following cocaine and extinction memory retrieval (n=10-12/group). **(C)** Representative images of Fos immunostaining in the NAc shell, NAc core and DS. Arrows indicate Fos+ neurons. Scale bar 125 µm. *Right:* Identification of sampling area for the NAc shell, NAc core and DS in both immunohistochemistry and electrophysiology experiments; coronal slice represents bregma 1.34 mm. All data are expressed as Mean±SEM. *p<0.05.

mice retrieved a cocaine and extinction memory, respectively.

We next examined neuronal ensemble activation in the NAc shell, NAc core and DS by quantifying the number of Fos+ neurons/mm$^2$.

*NAc shell*

In the NAc shell, a two-way ANOVA revealed a significant Group X Extinction interaction ($F_{1,41}$=8.31, p<0.01) and significant main effects of Group ($F_{1,41}$=8.20, p<0.01) and Extinction ($F_{1,41}$=58.24, p<0.001) (Figure 2B & 2C). Post-hoc tests indicated that Fos expression in Paired CL mice was significantly higher compared to Unpaired CL mice (p<0.001). Paired EXT mice displayed significantly lower Fos compared to Paired CL mice (p<0.001), at levels similar to Unpaired EXT mice.

*NAc core*

In the NAc core, a two-way ANOVA revealed no significant interaction between Group X Extinction ($F_{1,40}$=1.54, p=0.22), but a significant main effect of Extinction ($F_{1,40}$=8.03, p<0.01) (Figure 2B & 2C). Post-hoc tests indicated no differences in Fos expression between Paired CL and Unpaired CL mice (p=0.37).

*DS*

In the DS, there was a significant Group X Extinction interaction ($F_{1,39}$=6.09, p<0.05) and main effect of Group ($F_{1,39}$=4.43, p<0.05) and Extinction ($F_{1,39}$=69.66, p<0.001) (Figure 2B & 2C). Post-hoc tests revealed a significant difference between Paired CL and Unpaired CL mice (p<0.01). Paired EXT mice displayed significantly lower Fos compared to Paired CL mice (p<0.001), at levels similar to Unpaired EXT mice.

**Striatal medium spiny neuron (MSN) excitability following cocaine memory retrieval**

We next examined the excitability of 'activated', GFP-expressing (GFP+) and 'non-activated', non-expressing (GFP–) MSNs in the *Fos-GFP* mouse following cocaine memory retrieval. To that end, we examined the number of action potentials (firing capacity) across a range of positive current injection steps (30-210 pA), as a broad measure of excitability. We then examined active and passive membrane properties to investigate underlying adaptations to MSNs which may modulate firing capacity changes (indicated in Figure 5 and Tables 1-3).

*NAc shell*

We observed no selective firing capacity alterations between GFP+ and GFP– neurons, nor any generalised changes between Paired CL and Unpaired CL mice (Group X GFP X Current $F_{6,144}$=2.38, p<0.05, Group X Current $F_{6,144}$=0.27, p=0.95, GFP X Current $F_{6,144}$=0.68, p=0.67). While there was a main interaction effect, a Two-Way Mixed ANOVA in Paired and Unpaired mice separately revealed no GFP X Current interaction in either groups (Paired: $F_{6,66}$=2.03, p=0.07, Unpaired: $F_{6,78}$=0.83, p=0.57) (Figure 3A). Furthermore, we found no significant interaction effects in any of the passive or active membrane properties measured.

*NAc core*

In Paired CL mice, the firing capacity of GFP+ neurons was significantly increased compared to GFP– neurons (Group X GFP X Current $F_{6,174}$=5.76, p<0.001; Group X Current $F_{6,174}$=3.30, p<0.01, GFP X Current $F_{6,174}$=4.33, p<0.001) (Figure 3B). Comparison of the firing capacity of GFP+ and GFP– neurons across groups

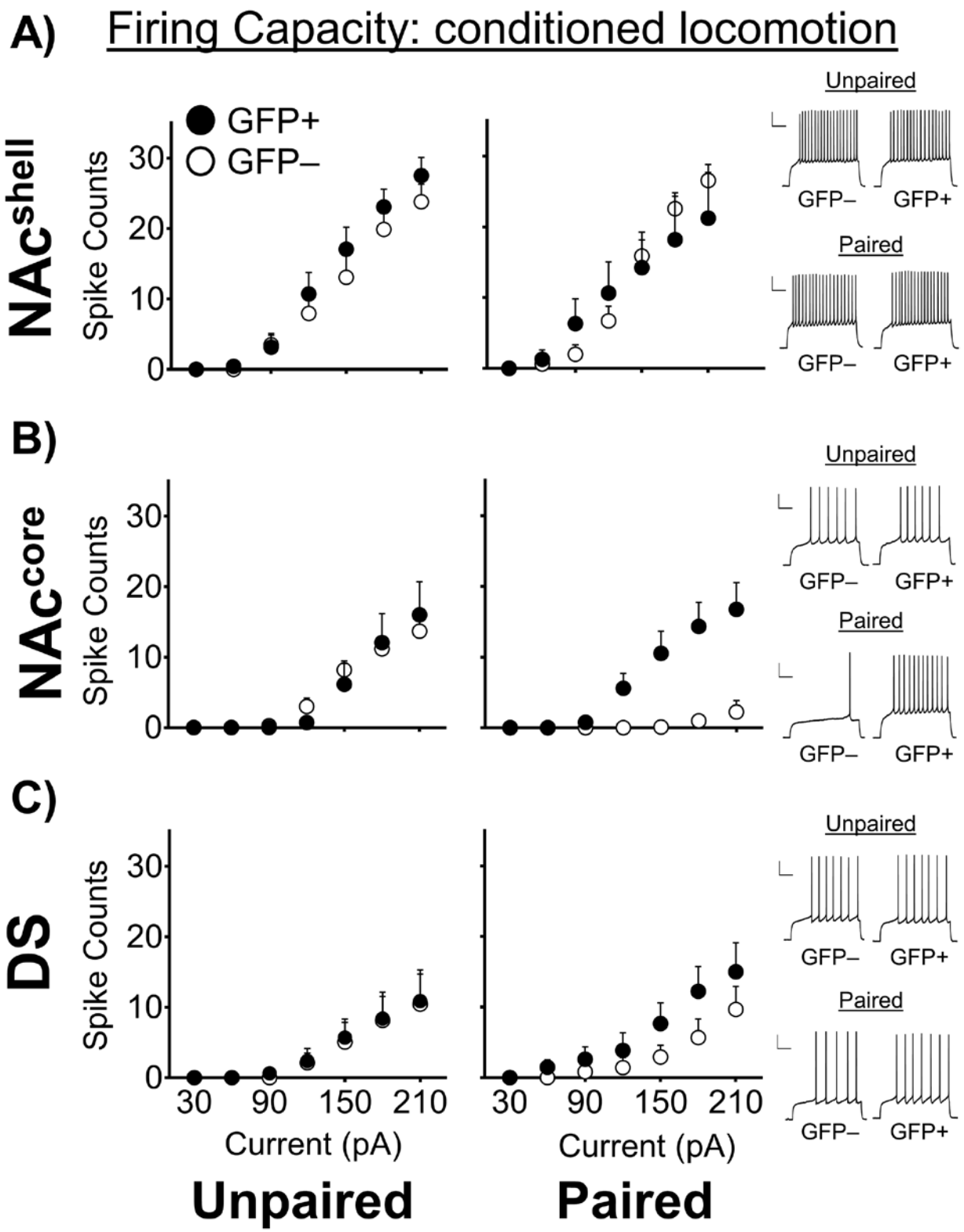


**Figure 3.** Excitability of GFP+ and GFP– neurons of the striatum following cocaine memory retrieval. **(A)** In the NAc shell, the spike counts of Paired CL mice were not significantly different between GFP+ neurons (n=5) and GFP– neurons (n=8); this was similar to the Unpaired CL group (GFP+ n=7; GFP– n=8). *Right:* Example traces of Paired CL and Unpaired CL GFP+ and GFP– neurons at 150 pA stimulation from the NAc shell following cocaine memory retrieval. **(B)** In the NAc core, GFP+ neurons were significantly more excitable than GFP– neurons in Paired CL mice (GFP+ n=9; GFP– n=9) but not Unpaired CL mice (GFP+ n=7; GFP– n=7) *Right:* Example traces of Paired CL and Unpaired CL GFP+ and GFP– neurons at 150 pA stimulation from the NAc core following cocaine memory retrieval. **(C)** Excitability of GFP+ and GFP– MSNs in the DS (GFP+; Paired CL n=7, Unpaired CL n=8), (GFP–; Paired CL n=6, Unpaired CL n=8). *Right:* Example traces of Paired CL and Unpaired CL GFP+ and GFP– neurons at 180 pA stimulation from the DS following cocaine memory retrieval. All data are expressed as Mean±SEM; n= number of animals (cells averaged for each animal). Scale bars 20 mV, 200 ms.

suggested that while Paired CL group GFP+ neurons were not significantly more excitable than Unpaired CL GFP+ neurons (Group (GFP+ neurons only) X Current $F_{6,84}$=0.53, p=0.78), the excitability of Paired CL GFP– neurons was significantly decreased compared to Unpaired CL GFP– neurons (Group (GFP– neurons only) X Current $F_{6,90}$=18.50, p<0.001). This suggests that in Paired CL mice following cocaine memory retrieval, GFP+ neurons of the NAc core were relatively more excitable than surrounding GFP– neurons due to a generalised decrease in the excitability of GFP– neurons.

We next examined changes in active and passive membrane properties which may indicate the potential mechanism by which the excitability of GFP– neurons was decreased. A two-way ANOVA indicated a significant interaction of Group X GFP for the rheobase (the minimum current required to elicit an action potential (AP)) ($F_{1,29}$=13.02, p<0.01), input resistance (indicator of the density of open ion channels) ($F_{1,29}$=10.65 p<0.01) (Figure 5A) and the fast and medium afterhyperpolarisation (fAHP and mAHP; components of the afterhyperpolarisation potential that dampens firing) (fAHP: $F_{1,29}$=8.54, p<0.01; mAHP: $F_{1,27}$=26.83, p<0.001) (Figure 5B). Post-hoc tests demonstrated that the input resistance of Paired CL GFP+ neurons was significantly increased compared to Paired CL GFP– neurons (p<0.01) while the rheobase, fAHP and mAHP were all significantly decreased (p<0.001, p<0.05, p<0.001 respectively). Furthermore, the input resistance of Paired CL GFP– compared to Unpaired CL GFP– was significantly decreased (p<0.05) while the rheobase, fAHP and mAHP were significantly increased (p<0.01, p<0.01, p<0.001 respectively). We also observed a significant increase in the mAHP of Unpaired CL GFP+ neurons compared to Unpaired CL GFP– neurons (p<0.05).

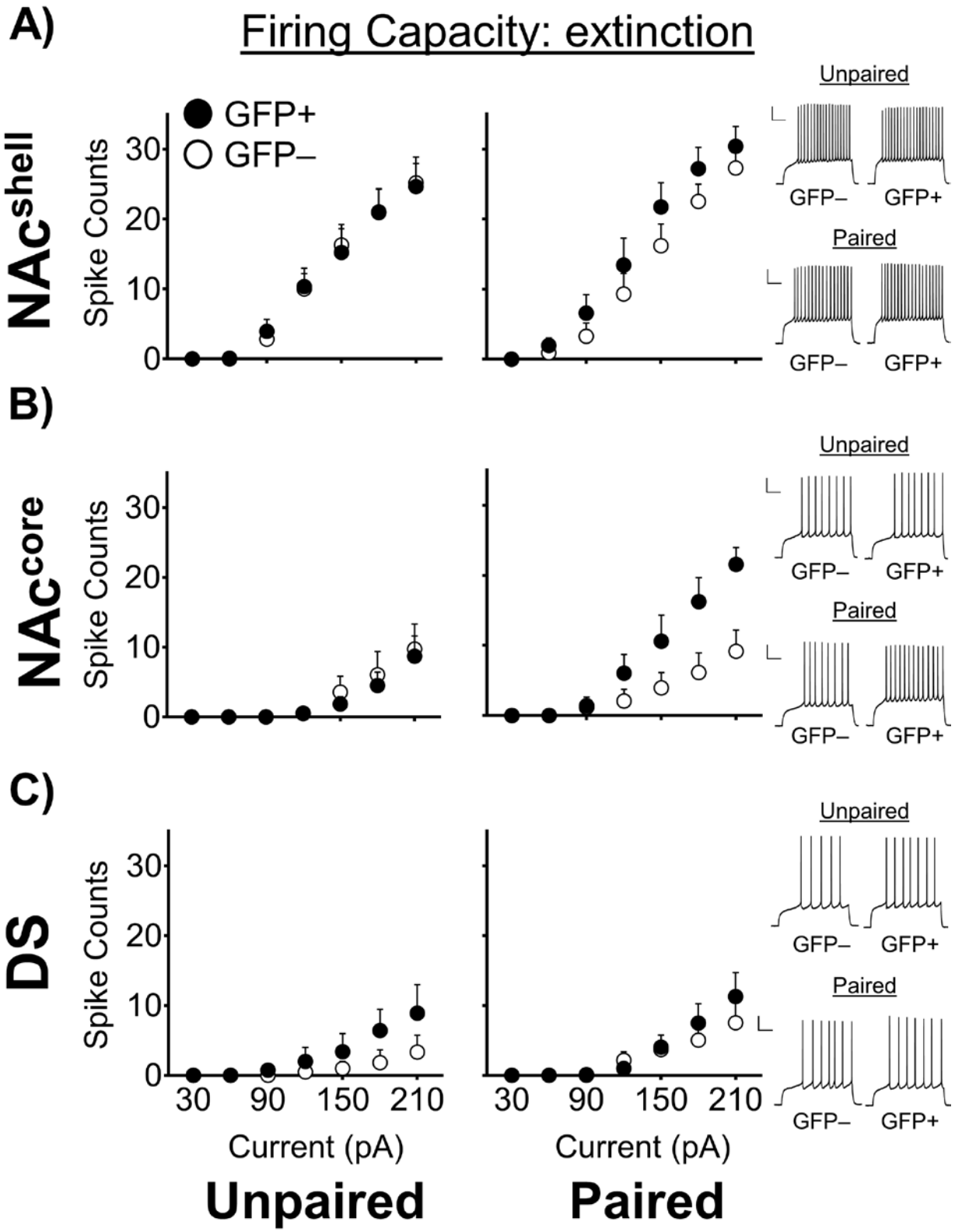


**Figure 4.** Excitability of GFP+ and GFP– neurons of the striatum following extinction memory retrieval. **(A)** The spike counts of NAc shell MSNs were not significantly different between Paired EXT GFP+ neurons (n=8) and Paired EXT GFP– neurons (n=10); this is similar to the Unpaired EXT group (GFP+ n=10, GFP– n=10). *Right:* Example traces of Paired EXT and Unpaired EXT GFP+ and GFP– neurons at 150 pA stimulation from the NAc shell following extinction memory retrieval. **(B)** In the NAc core, Paired EXT GFP+ neurons (n=10) were more excitable than Paired EXT GFP– neurons (n=10). In contrast, Unpaired EXT GFP+ neurons (n=10) were not more excitable than Unpaired EXT GFP– neurons (n=9). *Right:* Example traces of Paired EXT and Unpaired EXT GFP+ and GFP– neurons at 150 pA stimulation from the NAc core following extinction memory retrieval. **(C)** GFP+ and GFP– neurons in Paired EXT mice (GFP+ n=12, GFP– n=12) and Unpaired EXT mice (GFP+ n=6; GFP– n=9) following extinction memory retrieval. *Right:* Example traces of Paired EXT and Unpaired EXT GFP+ and GFP– neurons at 180 pA stimulation from the DS following extinction memory retrieval. All data are expressed as Mean±SEM; n= number of animals (cells averaged for each animal**).** Scale bars are 20 mV, 200 ms.

*DS*

We observed no selective firing capacity alterations between GFP+ and GFP– neurons (Group X GFP X Current $F_{6,150}$=0.36, p=0.91, Group X Current $F_{6,150}$=0.12, p=0.99, GFP X Current $F_{6,150}$=0.43, p=0.85) (Figure 3C). Also, there were no significant interaction effects for any of the aforementioned passive or active membrane properties.

**Striatal MSN excitability following extinction memory retrieval**

We next examined the excitability properties of striatal MSNs following the final extinction test (i.e. extinction memory retrieval) in Paired and Unpaired EXT mice.

*NAc shell*

We observed no selective firing capacity alterations between GFP+ and GFP– neurons (Group X GFP X Current $F_{6,204}$=0.36, p=0.84; Group X Current $F_{6,204}$=0.79, p=0.58; GFP X Current $F_{6,204}$=0.32, p=0.92) (Figure 4A). Furthermore, we found no significant interaction effects for any of the passive or active membrane properties that were measured.

*NAc core*

There was a significant increase in the firing capacity of Paired EXT GFP+ neurons compared to Paired EXT GFP– neurons (Group X GFP X Current $F_{6,168}$=4.22, p<0.001; Group X Current $F_{6,168}$=2.52, p<0.05, GFP X Current $F_{6,168}$=6.11, p<0.001) (Figure 4B). As the majority of standardised residuals were not normally distributed, a Mann-Whitney test applied to spike counts averaged across current injections also indicated

a significant increase in the excitability of GFP+ compared to GFP– neurons ($U$=22, p<0.05). The firing capacity of Paired EXT GFP+ neurons was significantly increased compared to the Unpaired EXT GFP+ baseline (Group (GFP+ neurons only) X Current $F_{6,108}$=6.99, p<0.001), but there were no significant differences in firing capacity between Paired EXT and Unpaired EXT GFP– neurons baseline (Group (GFP– neurons only) X Current $F_{6,102}$=0.250, p=0.12).

We next examined the membrane properties (Figure 5C & 5D), and a two-way ANOVA indicated a significant effect in the rheobase (Group X GFP $F_{1,35}$=9.12, p<0.01) and input resistance (Group X GFP $F_{1,35}$=11.29, p<0.01). Post-hoc tests comparing Paired EXT GFP+ and Paired EXT GFP– neurons indicated a decrease in the rheobase (p<0.01) and an increase in the input resistance (p<0.01) of Paired EXT GFP+ neurons (Figure 5C). This difference appeared to be due to changes in Paired EXT GFP+ neurons since no differences were observed in these properties from GFP– neurons of Paired EXT and Unpaired EXT mice

*DS*

We observed no selective firing capacity alterations between GFP+ and GFP– neurons (Group X GFP X Current $F_{6,210}$=0.13, p=0.99, Group X Current $F_{6,210}$=0.83, p=0.55, GFP X Current $F_{6,210}$=1.61, p=0.15) (Figure 4C). Also, there were no significant interaction effects for the passive or active membrane properties that were measured.

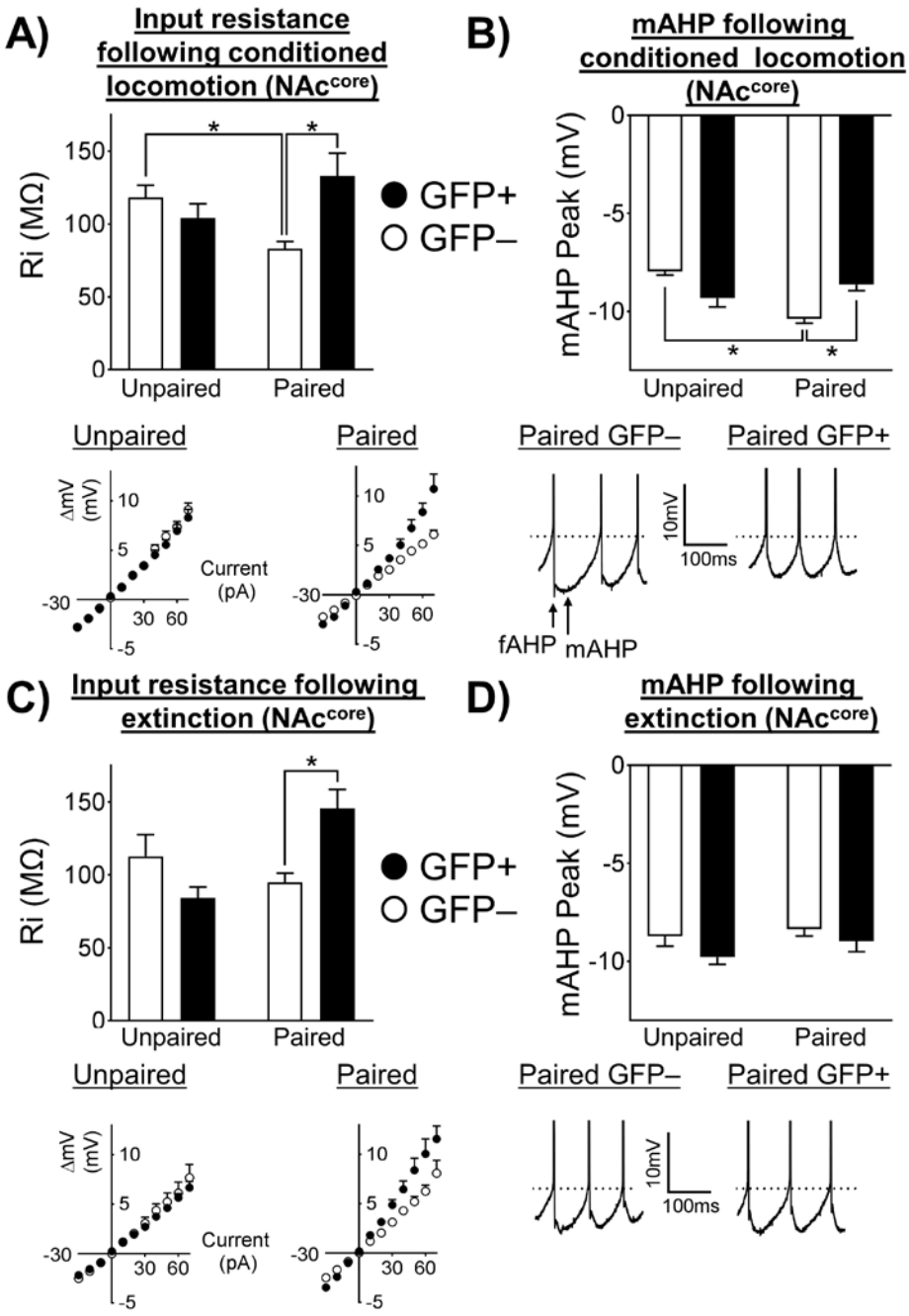


**Figure 5.** Modulation of input resistance and AHP underlies excitability changes following cocaine and extinction memory retrieval in the NAC core**. (A)** The input resistance of GFP+ neurons in Paired CL mice was increased compared to Paired CL GFP– neurons. In Unpaired CL mice, the input resistance of GFP+ and GFP– neurons was similar. *Below:* I/V curves of Paired CL and Unpaired CL GFP+ and GFP– neurons from which input resistance was calculated. In the Paired CL group, there was a significant shift in the I/V curve of GFP+ compared to GFP– neurons; in contrast, I/V curves of Unpaired CL GFP+ and GFP– neurons were similar. **(B)** Following cocaine memory retrieval, the mAHP of Paired CL GFP– neurons was significantly increased compared to Paired CL GFP+ and Unpaired CL GFP– neurons. *Below***:** Example traces of Paired CL GFP+ and GFP– neurons following cocaine memory retrieval, identifying the position of fAHP and mAHP peaks. Dashed line indicates the threshold of the first spike labelled with group means. The fAHP and mAHP of Paired CL GFP– neurons is increased following cocaine memory retrieval. Scale bar 10 mV, 100 ms **(C)** Following extinction memory retrieval, the input resistance of Paired EXT GFP+ neurons was increased compared to Paired EXT GFP– neurons. In the Unpaired EXT mice, the input resistance of GFP+ and GFP– neurons was similar. *Below:* I/V curves of Paired EXT and Unpaired EXT GFP+ and GFP– neurons from which input resistance was calculated. In the Paired EXT group, the I/V curve of GFP+ neurons was significantly shifted compared to GFP– neurons; in contrast, the I/V curves of Unpaired EXT GFP+ and GFP– neurons were similar. **(D)** The mAHP of GFP+ and GFP– neurons was not significantly different in either Paired EXT or Unpaired EXT mice. *Below:* Example traces of Paired EXT GFP+ and GFP– neurons. The fAHP, mAHP and of Paired EXT GFP+ and Paired EXT GFP– neurons were similar following extinction memory retrieval. Dashed line indicates the threshold of the first spike labeled with group means. Scale bar 10 mV, 100 ms. All data are expressed as Mean±SEM. *p<0.05.

## Discussion

We examined the size and excitability of NAc shell, NAc core and DS neuronal ensembles following cocaine and extinction memory retrieval using a cocaine conditioned locomotion procedure. In the NAc core we observed a relative increase in GFP+ neuron excitability following cocaine memory retrieval, which was attributable to a general decrease in the excitability of surrounding GFP– neurons. In contrast, following extinction memory retrieval, the excitability of GFP+ neurons was increased compared to GFP– neurons without a general decrease in GFP– neuron excitability. In the NAc shell and DS, we observed no changes in ensemble excitability following cocaine and extinction memory retrieval, despite the fact that conditioning and extinction processes regulated the size of the neuronal ensemble. These adaptations were likely related to drug-environment exposure, as other factors such as stress were controlled for in the Unpaired group that underwent similar levels of repeated handling, injections, and activity chamber and cocaine exposure. Collectively, these data provide novel insight into how distinct adaptations may serve to increase the sensitivity of neurons activated by exposure to a drug-associated environment and following extinction.

### Implications of changes in NAc core ensemble excitability following cocaine memory retrieval

We found adaptations in the rheobase, input resistance, I/V curve, fAHP and mAHP of NAc core GFP– MSNs in mice that underwent cocaine conditioning in a novel context outside of its home cage (i.e. Paired mice). Many of these factors have been previously shown to be regulated following repeated cocaine administration (Ma *et al*, 2013; Mu *et al*, 2010; Zhang *et al*, 1998).

| NAc Shell | Conditioned Locomotion | | | | Extinction | | | |
|---|---|---|---|---|---|---|---|---|
| | Unpaired | | Paired | | Unpaired | | Paired | |
| | GFP– | GFP+ | GFP– | GFP+ | GFP– | GFP+ | GFP– | GFP+ |
| Resting Vm (mV) | -70.63 ±0.80 | -71.00 ±0.93 | -70.19 ±0.46 | -68.80 ±0.41 | -71.06 ±0.49 | -70.56 ±0.52 | -70.39 ±0.39 | -70.87 ±0.85 |
| Rheobase (mV) | 115.63 ±11.78 | 110.71 ±12.84 | 116.88 ±6.74 | 134.33 ±30.50 | 115.00 ±12.38 | 107.22 ±12.34 | 108.75 ±9.99 | 92.14 ±13.35 |
| Ri (mΩ) | 207.34 ±22.89 | 228.63 ±28.97 | 200.22 ±15.06 | 223.86 ±53.98 | 185.38 ±16.30 | 223.48 ±25.07 | 205.65 ±19.12 | 260.76 ±33.26 |
| AP Amplitude (mV) | 68.21 ±3.88 | 70.46 ±2.30 | 69.53 ±2.01 | 66.99 ±2.31 | 71.99 ±2.99 | 68.14 ±4.32 | 70.39 ±0.96 | 72.11 ±3.07 |
| Half-Width (ms) | 1.40 ±0.06 | 1.55 ±0.14 | 1.41 ±0.08 | 1.42 ±0.09 | 1.32 ±0.03 | 1.38 ±0.04 | 1.34 ±0.04 | 1.45 ±0.05 |
| Threshold (mV) | -35.83 ±1.58 | -36.59 ±0.99 | -35.47 ±0.81 | -34.17 ±0.87 | -36.95 ±0.88 | -35.63 ±1.26 | -36.26 ±0.34 | -38.72 ±1.21 |
| fAHP (mV) | -6.72 ±0.57 | -6.81 ±0.89 | -8.30 ±0.49 | -6.86 ±0.24 | -7.75 ±0.73 | -7.60 ±0.56 | -6.92 ±0.39 | -7.16 ±0.88 |
| mAHP (mV) | -8.01 ±0.50 | -7.61 ±0.65 | -7.88 ±0.35 | -7.64 ±0.53 | -7.83 ±0.35 | -8.48 ±0.56 | -7.15 ±0.38 | -7.71 ±0.79 |

**Table 1.** Table of basic membrane properties from NAc$^{shell}$ MSNs of Paired and Unpaired mice following cocaine and extinction memory retrieval. Data are expressed as Mean±SEM. Liquid junction potential was -13.7 mV and was not adjusted for. Spike characteristics were determined from the first action potential (AP) of spike runs consisting of 6-8 spikes. Input resistance was calculated from the slope of the I/V curve measured in response to 10 pA current steps ranging from -30 pA to 70 pA. Spike threshold was measured using the third differential method (Cotel *et al*, 2013) with Mini Analysis software. The action potential peak was calculated as the difference between the AP peak and AP threshold. Half-width was measured as the AP width at half-maximal spike. Post-spike fAHPs and mAHPs were measured 3 and 30 ms following the AP threshold respectively, similar to (Ishikawa *et al*, 2009).

| NAc Core | Conditioned Locomotion | | | | Extinction | | | |
|---|---|---|---|---|---|---|---|---|
| | Unpaired | | Paired | | Unpaired | | Paired | |
| | GFP– | GFP+ | GFP– | GFP+ | GFP– | GFP+ | GFP– | GFP+ |
| Resting Vm (mV) | -70.16 ±0.48 | -71.33 ±0.67 | -71.93 ±0.57 | -70.38 ±0.75 | -71.37 ±0.60 | -72.06 ±0.24 | -71.81 ±0.47 | -71.25 ±0.69 |
| Rheobase (mV) | 169.06 ±11.81 | 180.71 ±19.34 | 248.24# ±14.59 | 143.88* ±16.75 | 189.44 ±14.91 | 211.50 ±11.21 | 197.30 ±16.27 | 135.30* ±12.68 |
| Ri (mΩ) | 123.66 ±8.21 | 104.24 ±9.75 | 83.12# ± 4.89 | 133.15* ±15.50 | 112.84 ±14.88 | 84.21 ±7.51 | 96.21 ±6.08 | 145.49* ±3.23 |
| AP Amplitude (mV) | 72.06 ±2.72 | 78.70 ±3.51 | 73.46 ±0.16 | 78.08 ±1.31 | 71.45 ±3.11 | 76.61 ±2.73 | 75.37 ±2.62 | 71.55 ±1.79 |
| Half-Width (ms) | 1.38 ±0.06 | 1.25 ±0.05 | 1.27 ±0.07 | 1.35 ±0.07 | 1.36 ±0.08 | 1.26 ±0.06 | 1.35 ±0.04 | 1.39 ±0.05 |
| Threshold (mV) | -34.50 ±1.04 | -34.53 ±1.32 | -32.08 ±0.87 | -35.61 ±0.98 | -32.91 ±0.96 | -34.78 ±0.79 | -34.54 ±1.35 | -33.24 ±1.06 |
| fAHP (mV) | -6.20 ±0.32 | -7.29 ±0.69 | -8.83# ±0.71 | -6.70* ±0.35 | -7.32 ±0.74 | -8.70 ±0.53 | -7.11 ±0.68 | -8.22 ±0.49 |
| mAHP (mV) | -7.95 ±0.20 | -9.31 ±0.45 | -10.37# ±0.22 | -8.63* ±0.30 | -8.88 ±0.53 | -9.78 ±0.36 | -8.39 ±0.36 | -8.96 ±0.55 |

**Table 2.** Table of basic membrane properties from NAc$^{core}$ MSNs of Paired and Unpaired mice following cocaine and extinction memory retrieval. Data are expressed as Mean±SEM. Asterisks indicates a significant interaction effect (*p<0.05, $^{\#}$ indicates differences between Paired GFP– vs. Unpaired GFP–). Spike kinetics were calculated as detailed in Table

| | Conditioned Locomotion | | | | Extinction | | | |
|---|---|---|---|---|---|---|---|---|
| | Unpaired | | Paired | | Unpaired | | Paired | |
| | GFP– | GFP+ | GFP– | GFP+ | GFP– | GFP+ | GFP– | GFP+ |
| Resting Vm (mV) | -71.00 ±0.66 | -71.57 ±0.53 | -72.41 ±0.64 | -72.46 ±0.72 | -71.87 ±0.74 | -72.58 ±1.04 | -71.10 ±0.37 | -72.00 ±0.33 |
| Rheobase (mV) | 237.86 ±41.13 | 205.00 ±24.84 | 233.33 ±40.55 | 171.90 ±30.22 | 236.25 ±17.62 | 176.95 ±22.25 | 248.33 ±20.73 | 210.00 ±23.53 |
| Ri (mΩ) | 101.95 ±13.06 | 116.69 ±18.90 | 102.62 ±13.06 | 132.73 ±23.39 | 73.44 ±5.18 | 100.01 ±17.97 | 89.77 ±10.02 | 94.24 ±9.11 |
| AP Amplitude (mV) | 76.86 ±4.82 | 85.04 ±2.82 | 84.50 ±6.41 | 91.91 ±1.63 | 86.74 ±5.01 | 83.99 ±4.00 | 80.03 ±3.21 | 85.89 ±2.79 |
| Half-Width (ms) | 1.24 ±0.07 | 1.18 ±0.11 | 1.24 ±0.08 | 1.24 ±0.10 | 1.16 ±0.05 | 1.26 ±0.09 | 1.22 ±0.05 | 1.17 ±0.05 |
| Threshold (mV) | -35.93 ±2.54 | -37.94 ±0.82 | -37.88 ±2.29 | -42.18 ±0.91 | -35.94 ±2.17 | -38.71 ±0.96 | -35.94 ±1.15 | -39.29 ±1.10 |
| fAHP (mV) | -8.39 ±1.09 | -9.00 ±1.09 | -7.85 ±1.14 | -9.47 ±0.92 | -10.21 ±1.38 | -9.20 ±1.71 | -8.59 ±1.07 | -9.27 ±1.00 |
| mAHP (mV) | -8.86 ±0.42 | -9.63 ±0.38 | -9.48 ±0.92 | -10.79 ±0.42 | -10.47 ±0.69 | -9.65 ±0.48 | -9.27 ±0.44 | -9.67 ±0.37 |

**Table 3.** Table of basic membrane properties from DS MSNs of Paired and Unpaired mice following cocaine and extinction memory retrieval. Data are expressed as Mean±SEM. Spike kinetics were calculated as detailed in Table 1.

The input resistance and I/V curve dynamics are primarily regulated by $K^+$ currents, including the inward-rectifying $K^+$ ($K_{ir}$) and A-type potassium currents (Nisenbaum and Wilson, 1995), though $Na^+$ and $Ca^{2+}$ currents also modulate near-threshold voltage responses (Bean, 2007; Nisenbaum *et al*, 1995). The regulation of the firing threshold, however, is dominated by voltage sensitive $Na^+$ currents (Cantrell and Catterall, 2001; Zhang *et al*, 1998), while the AHP (both fAHP and mAHP) is regulated by a class of voltage-dependent calcium-activated $K^+$ currents (Ishikawa *et al*, 2009; Vilchis *et al*, 2000). These membrane currents are carried by a complex and diverse host of ion channels (Bean, 2007), regulated by striatal monoamine neurotransmitters such as dopamine, and thus are a potential target for learning-induced plasticity (Cantrell *et al*, 2001; Nicola *et al*, 2000).

We observed a generalised decrease in the excitability of NAc core GFP– neurons, which resulted in a relative increase in the excitability of the activated GFP+ ensemble. The NAc core is necessary for the expression of conditioned locomotion following exposure to psychostimulant-associated environments (Sellings and Clarke, 2006) and for encoding cues that indicate the availability of cocaine (Suto *et al*, 2013). The alteration in global excitability we observed following the expression of conditioned locomotion may function to enhance the signal-to-noise ratio of glutamatergic input by depressing the activity of neurons encoding stimuli unrelated to the drug-associated environment. This increased signal-to-noise ratio may increase the information transfer from the activated ensemble to downstream targets, such as the ventral tegmental area, substantia nigra, and ventral pallidum (Heimer *et al*, 1991). This in turn, may facilitate attentional bias and increased salience of drug-associated stimuli (O'Donnell, 2003; Wanat *et al*, 2009), a phenomena often observed in drug addicts (Robinson and Berridge, 2008).

It remains to be determined here whether the excitability changes that we observed occurred prior to or immediately following the behavioural test. Psychostimulant

injections in a novel environment outside of the animal's home cage (Paired mice) produces more robust behavioural sensitisation, Fos expression and glutamatergic transmission than injections in the home cage (Unpaired mice) (Badiani *et al*, 1998; Hope *et al*, 2006; Hotsenpiller *et al*, 2001; Mattson *et al*, 2007). This suggests that our observed changes may have been due to baseline differences in excitability between Paired and Unpaired mice that occurred prior to test day. Alternatively, exposure to the cocaine-associated environment may have acutely altered the excitability of NAc core neurons through release of dopamine (Di Ciano *et al*, 1998); but see (Brown and Fibiger, 1992), which modulates MSN excitability (Nicola *et al*, 2000; O'Donnell, 2003).

An interesting point to raise here is that the GFP+ neurons exhibited relatively increased excitability, despite the lack of Fos expression increases in this area. However, this lack of increase does not necessarily imply the lack of neuronal ensemble recruitment following exposure to the cocaine-paired context, as distinct stimuli may recruit different neuronal ensembles without concomitant increases in the number of activated neurons. For example, Suto *et al* (2016) recently demonstrated that cues predictive of reward availability and omission both elicit activation of a similar number of Fos-expressing neurons in the infralimbic cortex, despite these two populations of cue-activated neurons mediating opposing behavioural responses.

**Implications for the increased excitability of GFP+ NAc core neurons following extinction memory retrieval**

Following extinction, we observed a relative increase in the excitability of Paired EXT GFP+ neurons in the NAc core, which was determined by an increase in GFP+ neuronal excitability, while GFP– neurons were comparable with baseline controls. Hence, the generalised adaptations observed following cocaine conditioning were no longer observed following extinction learning. Previous studies have demonstrated that

extinction of cocaine self-administration normalised drug-induced plasticity seen during withdrawal (Self *et al*, 2004), suggesting that extinction learning alone is enough to cause marked adaptations in the NAc following cocaine conditioning.

In this study, we did not examine whether the ensemble activated following conditioned locomotion includes the same neurons that were activated following extinction. Memories of cocaine-environment associations are robust and long-lasting (Hope *et al*, 2006; Robinson *et al*, 2008). Although extinction learning might suppress these drug-environment associations, exposure to certain stimuli (e.g. drugs) can re-activate this memory and thus reinstate drug conditioned behaviours that may contribute to relapse (Crombag *et al*, 2008; Mueller and Stewart, 2000). Interestingly, persistent increases in neuronal excitability have been observed following successful extinction learning (Brons and Woody, 1980). This increase may contribute to the 'memory savings effect', which facilitates re-acquisition of previously learned tasks (Ebbinghaus, 1913; Zhang and Linden, 2003). It is possible that the same NAc core neurons were activated both following cocaine and extinction memory retrieval, with relatively higher levels of excitability persisting after extinction. This persistently enhanced excitability may 'save' the cocaine associative memories. Such savings may explain the enduring, robust nature of drug memories and why addicts relapse even while undergoing cue exposure therapy that involves extinction learning (Conklin et al, 2002). However, one possible explanation for this persistent enhancement of excitability may be due to how we defined successful extinction learning by measuring the inhibition of conditioned general locomotor activity. Since cocaine produces changes on many behavioural dimensions (e.g. velocity of each movement bout, head movements) (Robinson et al, 2008), it is possible that we may not have observed a full extinction of conditioned responses if other parameters were measured. Thus we may be observing an enhanced excitability of the activated ensemble due to an incomplete, partial weakening of the CS-US association, and it remains to be seen whether a more robust

weakening would have resulted in the loss of the enhanced excitability. In future studies, we may examine multiple behavioural parameters when studying the extinction of conditioned locomotion, in order to better assess extinction learning effects.

Alternatively, it is possible that following extinction, we were recording from a distinct, neuronal ensemble that participates in suppression of the conditioned response. In support, recent studies have demonstrated that the suppressive effects of extinction training and omission cue exposure on food-seeking behaviours are relieved by pharmacogenetic lesioning of medial prefrontal cortex ensembles activated during extinction training and omission cue exposure, respectively (Suto *et al*, 2016; Warren *et al*, 2016). As such, it is possible that the relatively higher excitability we observed in GFP+ neurons may represent a functional adaptation in a newly recruited “extinction” ensemble whose recruitment is not associated with a net increase in the number of activated neurons following extinction. This newly recruited ensemble may, in turn**,** inhibit the retrieval of the cocaine-environment association (Quirk and Mueller, 2008).

**Lack of changes in the NAc shell and DS following cocaine and extinction memory retrieval**

We observed no selective changes in the excitability of NAc shell ensembles following cocaine and extinction memory retrieval, despite an increase and decrease in the size of the activated ensemble, respectively. A similar phenomenon has been observed previously (Jakkamsetti *et al*, 2013; Ziminski *et al*, 2017) in which exposure to novel or sucrose-conditioned stimuli increased the number of activated neurons in the hippocampus and orbitfrontal cortex respectively, in the absence of changes to the excitability of these activated neurons. Collectively, these findings add to a body of evidence indicating that intrinsic excitability alterations on neuronal ensembles and cue-evoked ensemble recruitment can be independently regulated.

However**,** in that same study we observed selective increases in NAc shell ensemble excitability following exposure to sucrose-associated cues (Ziminski *et al*, 2017), which were attenuated following extinction. These differences in ensemble excitability adaptations may be due to changes in conditioning parameters; drugs of abuse produce significantly more robust and longer lasting conditioned behaviours and neuroadaptations than food rewards (Lu *et al*, 2003; Zombeck *et al*, 2008), while conditioning to discrete cues and contextual stimuli is subserved by different anatomical substrates (Chaudhri *et al*, 2010). Thus, it is likely that striatal brain areas respond with a diverse set of adaptations following distinct types of learning.

We did not observe any changes in ensemble-selective excitability in the DS. This area consists of two related yet distinct subdivisions, the dorsomedial striatum (DMS) and the dorsolateral striatum (DLS), which have different roles in cocaine-related behaviours (Murray *et al*, 2012). Thus, by including both areas in our analysis, subtle ensemble excitability changes may not have been detected due to subregion-selective changes in ensemble or background neuronal excitability. In future studies these two subregions may be analyzed separately to better elucidate possible ensemble-specific adaptations following cocaine-conditioning. Also, striatal MSNs can be further distinguished based on their dopamine 1 and 2 receptor expression and these two neuronal subpopulations, which project to different brain areas, have distinct roles in cocaine-associated behaviours (Smith *et al*, 2013). In future studies, it would be crucial to identify whether GFP+ and GFP- cells are D1R- or D2R-expressing neurons using single-cell PCR, in order to determine whether associative learning induces pathway-specific neuronal ensemble changes in excitability**.**

**Concluding remarks**

These data provide novel insight into the regulation of striatal ensemble size and excitability in encoding cocaine-associative memories. Examining the complex

interaction of these factors which underlie memory encoding will be key to further understanding the contribution of drug-associated environments in addiction-related behaviours. Although the behavioural procedure used here is highly useful for studying cocaine-environment associations, it may not model certain features of drug addiction (e.g. drug-seeking). In future investigations, we may perform similar electrophysiological studies by using procedures that better model drug relapse, such as the contextual renewal of drug-seeking (Crombag et al 2008).

## References


Badiani A, Oates MM, Day HE, Watson SJ, Akil H, Robinson TE (1998). Amphetamine-induced behavior, dopamine release, and c-fos mRNA expression: modulation by environmental novelty. *J Neurosci* **18**(24): 10579-10593.

Bean BP (2007). The action potential in mammalian central neurons. *Nat Rev Neurosci* **8**(6): 451-465.

Brons JF, Woody CD (1980). Long-term changes in excitability of cortical neurons after Pavlovian conditioning and extinction. *J Neurophysiol* **44**(3): 605-615.

Brown EE, Fibiger HC (1992). Cocaine-induced conditioned locomotion: absence of associated increases in dopamine release. *Neuroscience* **48**(3): 621-629.

Cantrell AR, Catterall WA (2001). Neuromodulation of Na+ channels: an unexpected form of cellular plasticity. *Nat Rev Neurosci* **2**(6): 397-407.

Caprioli D, Venniro M, Zhang M, Bossert JM, Warren BL, Hope BT*, et al* (2017). Role of Dorsomedial Striatum Neuronal Ensembles in Incubation of Methamphetamine Craving after Voluntary Abstinence. *J Neurosci* **37**(4): 1014-1027.

Carelli RM (2002). The nucleus accumbens and reward: neurophysiological investigations in behaving animals. *Behav Cogn Neurosci Rev* **1**(4): 281-296.

Chaudhri N, Sahuque LL, Schairer WW, Janak PH (2010). Separable roles of the nucleus accumbens core and shell in context- and cue-induced alcohol-seeking. *Neuropsychopharmacology* **35**(3): 783-791.

Conklin CA, Tiffany ST (2002). Applying extinction research and theory to cue-exposure addiction treatments. *Addiction* **97**(2): 155-167.

Cotel F, Exley R, Cragg SJ, Perrier JF (2013). Serotonin spillover onto the axon initial segment of motoneurons induces central fatigue by inhibiting action potential initiation. *Proc Natl Acad Sci U S A* **110**(12): 4774-4779.

Crombag HS, Bossert JM, Koya E, Shaham Y (2008). Review. Context-induced relapse to drug seeking: a review. *Philos Trans R Soc Lond B Biol Sci* **363**(1507): 3233-3243.

Di Ciano P, Blaha CD, Phillips AG (1998). The relation between dopamine oxidation currents in the nucleus accumbens and conditioned increases in motor activity in rats following repeated administration of d-amphetamine or cocaine. *Eur J Neurosci* **10**(3): 1113-1120.

Ebbinghaus H (1913). *Memory. A Contribution to Experimental Psychology* Teachers College, Columbia University New York.

Everitt BJ, Robbins TW (2013). From the ventral to the dorsal striatum: devolving views of their roles in drug addiction. *Neurosci Biobehav Rev* **37**(9 Pt A): 1946-1954.

Heimer L, Zahm DS, Churchill L, Kalivas PW, Wohltmann C (1991). Specificity in the Projection Patterns of Accumbal Core and Shell in the Rat. *Neuroscience* **41**(1): 89-125.

Hope BT, Simmons DE, Mitchell TB, Kreuter JD, Mattson BJ (2006). Cocaine-induced locomotor activity and Fos expression in nucleus accumbens are sensitized for 6 months after repeated cocaine administration outside the home cage. *Eur J Neurosci* **24**(3): 867-875.

Hotsenpiller G, Giorgetti M, Wolf ME (2001). Alterations in behaviour and glutamate transmission following presentation of stimuli previously associated with cocaine exposure. *Eur J Neurosci* **14**(11): 1843-1855.

Ishikawa M, Mu P, Moyer JT, Wolf JA, Quock RM, Davies NM*, et al* (2009). Homeostatic synapse-driven membrane plasticity in nucleus accumbens neurons. *J Neurosci* **29**(18): 5820-5831.

Jakkamsetti V, Tsai NP, Gross C, Molinaro G, Collins KA, Nicoletti F*, et al* (2013). Experience-induced Arc/Arg3.1 primes CA1 pyramidal neurons for metabotropic glutamate receptor-dependent long-term synaptic depression. *Neuron* **80**(1): 72-79.

Kourrich S, Thomas MJ (2009). Similar neurons, opposite adaptations: psychostimulant experience differentially alters firing properties in

accumbens core versus shell. *J Neurosci* **29**(39): 12275-12283.

Koya E, Cruz FC, Ator R, Golden SA, Hoffman AF, Lupica CR*, et al* (2012). Silent synapses in selectively activated nucleus accumbens neurons following cocaine sensitization. *Nat Neurosci* **15**(11): 1556-1562.

Koya E, Golden SA, Harvey BK, Guez-Barber DH, Berkow A, Simmons DE*, et al* (2009). Targeted disruption of cocaine-activated nucleus accumbens neurons prevents context-specific sensitization. *Nat Neurosci* **12**(8): 1069-1073.

Lu L, Grimm JW, Shaham Y, Hope BT (2003). Molecular neuroadaptations in the accumbens and ventral tegmental area during the first 90 days of forced abstinence from cocaine self-administration in rats. *J Neurochem* **85**(6): 1604-1613.

Ma YY, Henley SM, Toll J, Jentsch JD, Evans CJ, Levine MS*, et al* (2013). Drug-primed reinstatement of cocaine seeking in mice: increased excitability of medium-sized spiny neurons in the nucleus accumbens. *ASN Neuro* **5**(4): 257-271.

Mattson BJ, Crombag HS, Mitchell T, Simmons DE, Kreuter JD, Morales M*, et al* (2007). Repeated amphetamine administration outside the home cage enhances drug-induced Fos expression in rat nucleus accumbens. *Behav Brain Res* **185**(2): 88-98.

Michel A, Tambour S, Tirelli E (2003). The magnitude and the extinction duration of the cocaine-induced conditioned locomotion-activated response are related to the number of cocaine injections paired with the testing context in C57BL/6J mice. *Behav Brain Res* **145**(1-2): 113-123.

Mu P, Moyer JT, Ishikawa M, Zhang Y, Panksepp J, Sorg BA*, et al* (2010). Exposure to cocaine dynamically regulates the intrinsic membrane excitability of nucleus accumbens neurons. *J Neurosci* **30**(10): 3689-3699.

Mueller D, Stewart J (2000). Cocaine-induced conditioned place preference: reinstatement by priming injections of cocaine after extinction. *Behav Brain Res* **115**(1): 39-47.

Murray JE, Belin D, Everitt BJ (2012). Double dissociation of the dorsomedial and dorsolateral striatal control over the acquisition and performance of cocaine seeking. *Neuropsychopharmacology* **37**(11): 2456-2466.

Nicola SM, Surmeier J, Malenka RC (2000). Dopaminergic modulation of neuronal excitability in the striatum and nucleus accumbens. *Annu Rev Neurosci* **23**: 185-215.

Nisenbaum ES, Wilson CJ (1995). Potassium currents responsible for inward and outward rectification in rat neostriatal spiny projection neurons. *J Neurosci* **15**(6): 4449-4463.

O'Brien CP, Childress AR, Ehrman R, Robbins SJ (1998). Conditioning factors in drug abuse: can they explain compulsion? *J Psychopharmacol* **12**(1): 15-22.

O'Donnell P (2003). Dopamine gating of forebrain neural ensembles. *Eur J Neurosci* **17**(3): 429-435.

Post RM, Lockfeld A, Squillace KM, Contel NR (1981). Drug-environment interaction: context dependency of cocaine-induced behavioral sensitization. *Life Sci* **28**(7): 755-760.

Quirk GJ, Mueller D (2008). Neural mechanisms of extinction learning and retrieval. *Neuropsychopharmacology* **33**(1): 56-72.

Robinson TE, Berridge KC (2008). Review. The incentive sensitization theory of addiction: some current issues. *Philos Trans R Soc Lond B Biol Sci* **363**(1507): 3137-3146.

Self DW, Choi KH, Simmons D, Walker JR, Smagula CS (2004). Extinction training regulates neuroadaptive responses to withdrawal from chronic cocaine self-administration. *Learn Mem* **11**(5): 648-657.

Sellings LH, Clarke PB (2006). 6-Hydroxydopamine lesions of nucleus accumbens core abolish amphetamine-induced conditioned activity. *Synapse* **59**(6): 374-377.

Smith RJ, Lobo MK, Spencer S, Kalivas PW (2013). Cocaine-induced adaptations in D1 and D2 accumbens projection neurons (a dichotomy not necessarily synonymous with direct and indirect pathways). *Curr Opin Neurobiol* **23**(4): 546-552.

Suto N, Elmer GI, Wang B, You ZB, Wise RA (2013). Bidirectional modulation of cocaine expectancy by phasic glutamate fluctuations in

the nucleus accumbens. *J Neurosci* **33**(21): 9050-9055.

Suto N, Laque A, De Ness GL, Wagner GE, Watry D, Kerr T*, et al* (2016). Distinct memory engrams in the infralimbic cortex of rats control opposing environmental actions on a learned behavior. *Elife* **5**.

Ting JT, Daigle TL, Chen Q, Feng G (2014). Acute brain slice methods for adult and aging animals: application of targeted patch clamp analysis and optogenetics. *Methods Mol Biol* **1183**: 221-242.

Vilchis C, Bargas J, Ayala GX, Galvan E, Galarraga E (2000). Ca2+ channels that activate Ca2+-dependent K+ currents in neostriatal neurons. *Neuroscience* **95**(3): 745-752.

Wanat MJ, Willuhn I, Clark JJ, Phillips PE (2009). Phasic dopamine release in appetitive behaviors and drug addiction. *Curr Drug Abuse Rev* **2**(2): 195-213.

Warren BL, Mendoza MP, Cruz FC, Leao RM, Caprioli D, Rubio FJ*, et al* (2016). Distinct Fos-Expressing Neuronal Ensembles in the Ventromedial Prefrontal Cortex Mediate Food Reward and Extinction Memories. *J Neurosci* **36**(25): 6691-6703.

Whitaker LR, Carneiro de Oliveira PE, McPherson KB, Fallon RV, Planeta CS, Bonci A*, et al* (2016). Associative Learning Drives the Formation of Silent Synapses in Neuronal Ensembles of the Nucleus Accumbens. *Biol Psychiatry* **80**(3): 246-256.

Wolf ME (2010). The Bermuda Triangle of cocaine-induced neuroadaptations. *Trends Neurosci* **33**(9): 391-398.

Zhang W, Linden DJ (2003). The other side of the engram: experience-driven changes in neuronal intrinsic excitability. *Nat Rev Neurosci* **4**(11): 885-900.

Zhang XF, Hu XT, White FJ (1998). Whole-cell plasticity in cocaine withdrawal: reduced sodium currents in nucleus accumbens neurons. *J Neurosci* **18**(1): 488-498.

Ziminski JJ, Hessler S, Margetts-Smith G, Sieburg MC, Crombag HS, Koya E (2017). Changes in Appetitive Associative Strength Modulates Nucleus Accumbens, But Not Orbitofrontal Cortex Neuronal Ensemble Excitability. *J Neurosci* **37**(12): 3160-3170.

Zombeck JA, Chen GT, Johnson ZV, Rosenberg DM, Craig AB, Rhodes JS (2008). Neuroanatomical specificity of conditioned responses to cocaine versus food in mice. *Physiol Behav* **93**(3): 637-650.

# Chapter 6.

# Discussion

## 6.1. Summary of Results

### 6.1.1. Differences in NAc shell ensemble neuroadaptations between Pavlovian Approach and conditioned locomotion experiments

We aimed to identify adaptations occurring selectively on neurons activated following exposure to food (sucrose) or drug (cocaine) associated stimuli, and their regulation following changes in associative strength. These studies demonstrate dynamic adaptations in the intrinsic and synaptic excitability of neurons activated following exposure to appetitive cues. These observations have important implications for our understanding of how the brain might encode highly detailed learned associations between rewards and environmental cues which predict their availability.

*Excitability differences in neurons activated following exposure to a sucrose-associated cue, and extinction*

In chapter 2, following exposure to a sucrose-associated CS, the number of Fos-expressing neurons in the NAc shell and OFC was increased. In the NAc shell, the number of activated D1R- or D2R-containing medium spiny neurons was similar, while in the OFC the majority of activated neurons were pyramidal cells. We observed that in the NAc shell of *Fos-GFP* mice, activated (GFP+) neurons were more excitable than surrounding, non-activated (GFP–) neurons, due to an increase in the input resistance of GFP+ cells. In chapter 3, we also observed that the synaptic strength of these GFP+ neurons was increased, as the frequency of spontaneous EPSCs was potentiated in the absence of facilitated presynaptic release probability, suggesting an increase in the number of functional synapses. In the OFC, we observed no selective increase in the intrinsic excitability of neurons activated following exposure to the food-associated CS.

Following extinction of the sucrose-cue association, exposure to the CS no longer increased the number of activated neurons NAc shell or OFC compared to control animals. Furthermore, in the NAc shell, the excitability of GFP+ neurons was no longer enhanced compared to surrounding GFP– neurons.

Hence, following exposure to a sucrose-associated CS the excitability of activated NAc shell was potentiated, while this potentiation was attenuated following weakening of the CS-US association through extinction learning.

### *Excitability differences in neurons activated following exposure to a cocaine-associated context, and extinction*

In chapter 4, We next investigated the nature of neuronal ensembles activated in the striatum (NAc shell, NAc core and dorsal striatum) following exposure to drug (cocaine) associated stimuli. Following exposure to a cocaine-associated environment, the number of activated neurons was increased in the NAc shell. However, the intrinsic excitability of GFP+ neurons in the NAc shell was not increased compared to the surrounding, GFP– neurons. Similar findings were observed in DS. Interestingly, while there was no increase in the number of activated neurons in the NAc core, the GFP+ neurons were significantly more excitable than GFP– neurons. This was due to a decrease in the excitability of the GFP– neurons determined by a decrease in the input resistance and increase in the afterhyperpolarisation.

Following extinction of the cocaine-environment association, the number of neurons activated in the NAc shell and DS was no longer increased compared to baseline controls. Similarly, there was no difference in the excitability of GFP+ and GFP– neurons in these brain areas. In the NAc core however, while there still no increase in the number of activated neurons in the NAc core the increase in the excitability of GFP+ neurons persisted. Interestingly, following extinction, this relative increase in the

excitability of GFP+ neurons was determined by an increase in the input resistance of GFP+ neurons.

### *Impact Summary*

Appetitive associations are thought to be encoded by neuronal ensembles activated across motivationally-relevant brain areas (Cruz *et al*, 2013; Josselyn *et al*, 2015; Warren *et al*, 2017). Through selective sampling of the neurons activated by reward-associated cues, we were able to reveal unique neuroadaptations on these ensembles. We demonstrate that following exposure to both food and drug-associated cues, the intrinsic and synaptic excitability of ensembles activated in the ventral striatum is increased. Interestingly, this increase was not universally observed across motivationally relevant brain areas, and was differentially regulated between food and drug rewards following extinction. These novel data suggest that neuroadaptations on neuronal ensembles are dynamically regulated following appetitive conditioning as a function of brain area and conditioning paradigm. Further investigations into the precise function of these selective neuroadaptations may elucidate their potential role in memory encoding.

## 5.2. Methodological considerations

### 5.2.1. Differences between Pavlovian approach and conditioned locomotion experiments

#### *NAc Shell GFP+ neuron excitability is differentially regulated following Pavlovian approach and conditioned locomotion*

We observed an increase in the excitability of NAc shell neurons activated following exposure to sucrose, but not cocaine-associated stimuli. This dissimilarity in NAc shell

ensemble excitability between experiments may be due to differences in the reinforcer and/or conditioning paradigm used. The NAc shell appears to play distinct functional roles in the expression of Pavlovian approach behaviours to a food reward and conditioned locomotion to a drug-associated context. Blaiss and Janak (2009) successfully disrupted Pavlovian approach behaviours using GABA agonist inactivation of the NAc shell. However, 6-OHDA lesions of the NAc shell do not attenuate expression of condition locomotion (Sellings and Clarke, 2006). As such, we may not have observed similar changes in the excitability of NAc shell GFP+ neurons due to differences in functional engagement of the NAc shell between conditioning paradigms.

Differences in the rate of learning between food or drug reinforcers may also determine the striatal areas recruited to processes associative cues. Pavlovian conditioned stimulus-response behaviours encoded by more dorsal striatal regions are more rapidly acquired using drug reinforcers than food (Belin and Everitt, 2008; Miles *et al*, 2003). Thus it is possible that the NAc core became more rapidly engaged in processing cocaine-associated stimuli while the influence of the NAc shell was reduced. It would be of interest to assay ensemble excitability at various time-points during cocaine-environment conditioning to determine whether a ventral-dorsal striatum transition in ensemble excitability may be observed.

Finally, conditioned sucrose availability to a discrete CS, but cocaine administration with a contextual cue. Encoding of contextual and discrete cues is subserved by different striatal brain areas (Chaudhri et al, 2010) and encoded through different NAc afferents such as the hippocampus and amygdala (Ito *et al*, 2006; Shiflett and Balleine, 2010). Thus, differences in the excitability of NAc shell GFP+ neurons may be directly due to the conditioning procedure used. Thus, where possible, similar conditioning paradigms must be used when comparing food and drug rewards; this is discussed in more detail below.

### *Increased excitability of NAc ensembles is attenuated following extinction of Pavlovian approach but not conditioned locomotion*

We observed a persistent increase in the excitability of NAc ensembles following extinction of the cocaine-context association. However, following extinction of a sucrose-CS association the excitability increase in GFP+ MSNs was completely attenuated. Upon cessation of use, cocaine causes significant withdrawal-induced neuroadaptations which are not observed following food consumption (Loweth *et al*, 2014; Self *et al*, 2004). For example, withdrawal from cocaine induces significantly depression of NAc MSN excitability while sucrose ingestion does not (Hopf *et al*, 2010). Furthermore, exposure to cocaine or cocaine-associated stimuli appear to reverse withdrawal induced adaptations following cessation of cocaine used (Hotsenpiller *et al*, 2001; Mu *et al*, 2010). Thus exposure to the locomotor chamber may dynamically interact with withdrawal-induced neuroadaptations in a unique manner following cocaine extinction (Schmidt *et al*, 2001; Self *et al*, 2004) which may profoundly alter the intrinsic excitability of NAc neurons.

### *Issues with assessing the affective state of animal models*

At test, the measurement of a behavioural response is typically used to infer that an association between the CS and US has been formed. However, it is impossible to directly measure any accompanying affective states or cognitive processes that CS exposure may elicit. In some animals the CS itself may be directly rewarding (i.e. sign trackers) while others may primarily direct their attention to the sucrose-delivery magazine (i.e. goal trackers) (Boakes, 1977). Alternatively, the CS may elicit recall of an explicit representation of the US (stimulus-stimulus relationship) or may elicit only the initiation of a habitual food-seeking response (stimulus-response relationship) (Mackintosh, 1974). Thus it is important to consider that the neurons we are recording

from following CS exposure may be underlying varied possible affective or cognitive processes which require extensive additional controls to investigate (Rescorla, 1967).

This issue is also relevant to the interpretation of the condition locomotion studies. It may be considered that exposure to a cocaine-associated context elicits a positive affective state associated with drug administration, and which in some settings may potentiate cocaine seeking (Fuchs *et al*, 2008). However, while humans report a "appetitive" affective state following exposure to drug cues (e.g. increased heart rate, craving) (O'Brien, 1998; Volkow, 2006) this may not be the case in the rodent model. For example, increased locomotion may also be observed following exposure to an appetitive CS due to frustration at the lack of expected reward (Amsel, 1958).

As such, it is important to consider that our measured behaviour can only inform us that an association has been formed between CS and US. The nature of this association however is less clear, as we cannot directly measure the animal's affective state during the expression of these behaviours. However, additional control experiments can be used to inform with more detail the precise nature of the CS-US association. For example, recently Sieburg (2017) working in our lab, has shown that our Pavlovian approach paradigm is sensitive to reinforcer devaluation, suggesting that CS exposure is eliciting a representation of the US.

### *Recommendations for future studies*

In future experiments, similar conditioning paradigms could be used to more effectively compare the neuroadaptations observed following learning with food and drug rewards. For example, sucrose and cocaine may be conditioned to contextual stimuli in a similar way, with conditioned locomotion also observed following exposure to a food-associated context (Ito *et al*, 2005). However, conditioning cocaine to a discrete cue in a comparable way to food is challenging.  Discrete cues may be paired with

intravenous infusion of cocaine, however due to the half-life of cocaine, it is necessary to use longer CS presentations (Hotsenpiller *et al*, 2002) or space conditioning trials between very long inter-trial intervals (Kearns and Weiss, 2004; Uslaner *et al*, 2006). Furthermore when conditioning with intravenous drug administration, the conditioned response cannot be goal-directed due to the passive infusion of cocaine (Kearns *et al*, 2004); conditioned responses measured following conditioning with cocaine to a discrete CS are usually increases in locomotor activity, or sign tracking behaviours (Hotsenpiller *et al*, 2002; Uslaner *et al*, 2006). These can in part be mediated by changes to procedure; for example, direct infusions of sucrose to the mouth of rodents, to reduce approach behaviours to a reward delivery site, can be made using intraoral cannula placement (Cone *et al*, 2016) while utilising a sucrose-cocaine liquid reward may permit approach behaviours when conditioning with cocaine (Miles *et al*, 2003).

While a perfect comparison between food and drug learning may be problematic, the present studies highlight the importance of comparing drug-induced neuroadaptations to those observed under natural reward learning. Psychoactive drugs of abuse elicit many unique and complex changes to the neurocircuitry of motivationally relevant brain areas in a manner not observed using natural rewards (Lu *et al*, 2003; Zombeck *et al*, 2008). Only by comparing the neuroadaptations observed following conditioning with drug reinforcers to natural rewards can we distinguish pathological drug-induced neuroadaptations from those which underlie normal learning processes.

### 6.2.2. Further subdivision of striatal and PFC neurocircuitry

We have utilised the activity marker ‘Fos’ to identify neuronal populations based upon their putative activation history following exposure to conditioning cues. However, neurons in the striatum and PFC may be further divided based on their molecular phenotype and connectivity. Failure to account for such differences may occlude

detection of subtype selective adaptations important in the encoding of associative memories.

### *The Striatum*

D1R- and D2R-expressing MSNs not only display different molecular and anatomical properties, but also demonstrate differences in baseline intrinsic excitability (Gertler *et al*, 2008; Planert *et al*, 2013). We did not assay the population of D1R/D2R GFP+ neurons following conditioned locomotion experiments. Selective activation of D1-containing MSNs is observed following psychostimulant administration (Bertran-Gonzalez *et al*, 2008; Graybiel *et al*, 1990), suggesting it is possible the differences we observed in GFP+ neuron excitability following conditioned locomotion may be due to shifts in the activated neuronal populations.

Furthermore, we did not distinguish between D1R- or D2R-containing MSNs during electrophysiological recording experiments. D1R activation typically leads to increases in intrinsic excitability, while D2R activation leads to decreased excitability (Planert *et al*, 2013). Thus it is possible that intrinsic excitability is differentially regulated in D1R and D2R MSNs following associative conditioning. In future studies it is crucial to identify the phenotype of GFP+ MSNs following electrophysiological recordings. *Post-hoc* identification of genetic phenotype can be accomplished by aspirating cell contents into the recording electrode then identifying gene expression using single-cell PCR (Planert *et al*, 2013). Thus in future studies, it would be beneficial to undertake single-cell PCR identification of striatal MSN phenotype following electrophysiological recording.

*The PFC*

Pyramidal neurons in the prefrontal cortex, including the OFC, are highly heterogeneous and may be subdivided into numerous classes based on their firing pattern and expression of certain membrane currents (Cao *et al*, 2009; Degenetais *et al*, 2002; Hedrick and Waters, 2012; Lee *et al*, 2014). Pyramidal subtypes broadly include regular spiking neurons (characterised by a constant inter-spike interval and lack of spike frequency adaptation) and bursting neurons (characterised by an initial burst of 2-3 action potentials followed by a spike train demonstrating firing adaptation) (Hedrick *et al*, 2012). However, varied classification systems are used across studies (Cao *et al*, 2009; Degenetais *et al*, 2002). When recording from the OFC we observed many pyramidal neurons exhibiting distinct firing patterns, however we did not record from a sufficient number of neurons to permit detailed subdivision of these pyramidal populations. It is possible that we observed no change in the excitability of GFP+ neurons in the OFC as by analysing all pyramidal subtypes together we may have occluded subtype-selective changes in excitability. Thus in future studies it will be necessary to record from a sufficient number of neurons to permit subtype-specific analysis.

### 6.2.3. We did not distinguish the cause of activation in GFP+ neurons visualised following Pavlovian approach and conditioned locomotion test

We have recorded from GFP+ MSNs activated during the recall of an appeitive association or extinction memory. *In vivo* electrophysiology experiments demonstrate that NAc neurons may encode many faucets of the conditioned experience, including training context exposure, CS presentation, and execution of goal directed instrumental behaviours (West and Carelli, 2016). As such, it is not clear whether the neuroadaptations we observed occur on neuron populations activated by the

conditioning environment, CS presentation, CR expression, or combinations of these. Due to the tempral congruency between CS presentation and the expression of a conditioned response, visualsing neuronal populations activated specifically by CS, CR, or both may be difficult (Day *et al*, 2006). Recently, new technologies permit the tagging of neurons regulated by light and high intracellualr calcium levels, allowing the visualisation of neuronal populations activated during specific behavioural epochs. These include the FLARE system, in which light exposure concurrent with high intraceullar calcium levels induces translocation and activation of a transcription factor, permitting the expression of specific transgenes in neurons activated during experimenter-determined periods (Wang *et al*, 2017). Similarly, in the CAMPARI system, light exposure alongside high intraceullar calcium levels permits the photoconversion a green flourscent protein to red (Fosque *et al*, 2015). These new techniologies will allow precise identification of neuronal subpopulations activated during specific epochs of the conditioned response.

## 6.3. Mechanisms and function of increased ensemble excitability

### 6.3.1. Increased input resistance in GFP+ neurons

We observed increases in the input resistance of GFP+ neurons following recall of a sucrose-cue association and cocaine extinction memory. Interestingly, increases in GFP+ input resistance have also been observed in the PFC following instrumental conditioning with sucrose (Whitaker et al, 2017; unpublished observations). This suggests that increases in GFP+ excitability observed following appetitive conditioning appears to preferentially accomplished by adaptations to the input resistance. Previously, changes in the input resistance has been observed in sensory neurons directly underlying the classical conditioning of the siphon withdrawal reflex in *Aplysia* (Antonov *et al*, 2001) and following LTP induction protocols in the hippocampus

(Campanac *et al*, 2008; Xu *et al*, 2005). The possible mechanisms of input resistance changes in the present studies and functional implications for memory encoding are discussed below.

### *I/V curve shifts at hyperpolarised potentials: inward rectifiers ($K_{IR}$) and leak (KCNK) channels*

The input resistance of MSNs is primarily regulated by potassium channel function (Nisenbaum and Wilson, 1995). Inwardly rectifying potassium channels ($K_{IR}$) and potassium leak channels (KCNK) regulate the voltage response of neurons at hyperpolarised ($K_{IR}$ and KCNK) and depolarised (KCNK only) potentials (Goldstein *et al*, 2001; Nisenbaum *et al*, 1995). We observed shifts in the I/V curve at hyperpolarised potentials, suggesting adaptations in both $K_{IR}$ and KCNK function. However, we did not observe concurrent changes in the resting membrane potential which is also regulated by these channels. How might $K_{IR}$ or KCNK adaptations result in adaptations to neuronal input resistance without simultaneous changes in the RMP? Campanac *et al* (2008) similarly observed increases in $R_{in}$ in the absence of RMP alterations (following hippocampal LTP), caused by a decrease in $I_h$ function, a potassium current which also regulates both membrane resistance and the RMP. They observed that the selective regulation of $I_h$ channels in the dendrites, but not the cell soma, led to alterations in the input resistance in the absence of RMP changes. In the striatum, $K_{IR}$ and KNCK are expressed in dendrites and regulate dendritic excitability (Cazorla *et al*, 2012; Pruss *et al*, 2003). Thus, we may have observed selective adaptations in dendritic ion channel function in GFP+ neurons following associative conditioning. Unfortunately, the anatomy of the striatum makes dendritic recordings extremely difficult. While the function of MSN dendrites can be elucidated using glutamate uncaging studies in which the neurotransmitter can be selectively released from caging molecules using photostimulation targeted to specific neuronal compartments (Plotkin *et al*, 2011), the

technology required to assay the input resistance of these dendrites is not currently available.

### *I/V curve shifts at depolarised potentials: Voltage-gated potassium channels*

Voltage-gated potassium currents also regulate voltage responses at depolarised potentials. These are primarily determined by A-type, delayed rectifier and KCNQ channels which are located on the cell soma, dendrites and axon (Fransen and Tigerholm, 2010; Manis, 2014). Voltage-gated potassium channels are highly diverse but typically activate at subthreshold voltages (A-type -10 mV observed in medium spiny neurons; Tkatch et al, 2000) (KCNQ -27 to -43 mV observed in the HEK cells; Kim et al, 2016). Thus while these channels may play a role in I/V curve shifts observed in GFP+ neurons at depolarised potentials, they cannot account for changes at more hyperpolarised potentials. As such, it is likely a combination of voltage-activated and other channels, such as KIR and KNCK, that regulate the input-output resistance of GFP+ neurons at both hyperpolarised and depolarised potentials.

### *Why might GFP+ neurons modify excitability through $R_{in}$?*

Modulation of intrinsic excitability following associative learning has been observed in randomly selected neurons to occur through many other mechanisms, including changes to the AHP (Moyer *et al*, 1996; Santini *et al*, 2008). Why might changes in GFP+ neuron excitability occurs primarily through changes in the input resistance? One unique consequence of altering input resistance is that it modulates transmission throughout the dendritic tree. Dendrites compute synaptic input in a non-linear fashion determined by input resistance and capacitance, regulated by ion channel expression and dendrite morphology (Stuart and Spruston, 2015). Voltage attenuation along dendrites is significant (Stuart and Spruston, 1998), thus synaptic transmission can be

robustly facilitated by improving the length-constant of dendrites through increasing the input resistance (Stuart *et al*, 2015). In GFP+ neurons following associative learning, changes to the input resistance may enhance transmission between nearby synapses along specific dendritic pathways and facilitate input-specific plasticity (Hyun *et al*, 2013). This may be especially important in striatal MSNs, which integrate a large number of glutamatergic afferents. Future studies may utilise identification of Fos-expressing neurons alongside high-resolution imaging of dendritic trees using 2-photon imaging and $Ca^{2+}$ dyes (MacAskill *et al*, 2014).

### 6.3.2. Generalised changes to the AHP and input resistance of GFP– neurons

*Decreases in intrinsic excitability and long-term depression (LTD)*

We also observed decreases in the excitability of surrounding, non-activated GFP– neurons following a cocaine extinction memory. This has similarly been observed this following acquisition of instrumental responding for sucrose (Whitaker et al, 2017; Unpublished observations). Thus it would appear in some instances, the excitability of surrounding, GFP– is decreased following associative learning, determined by changes in the AHP and input resistance (Ziminski et al 2017a; Ziminski et al 2017b; Whitaker, 2017; Unpublished observations). This is in accordance with previous studies observing regulation of AHP in randomly selected neurons following associative learning (Moyer *et al*, 1996; Santini *et al*, 2008).

Long-term depression of neuronal transmission is commonly associated with changes at the synapse, though long-term depression of intrinsic excitability has also been observed in Purkinje cells of the cerebellum (Shim *et al*, 2017). Shim *et al* (2017) utilised an LTD induction protocol in the cerebellum, in which concurrent stimulation of parallel fibre and climbing fibres (an error signal in the cerebellar motor circuit) results in LTD of the Parallel fibre to Purkinje cell synapses. They observed that the input

resistance of Purkinje neurons was significantly decreased following LTD induction, in a manner that was dependent on $Ca^{2+}$ and PKC. Thus stimulation protocols which induce synaptic LTD may also induce intrinsic LTD, suggesting that a decrease in the excitability of GFP– neurons may be determined by LTD-like processes.

### *In the striatum, LTD is triggered by mGluR1 and dopamine activation*

Many different forms of LTD have been observed in the brain. Hippocampal LTD at the Schaffer collateral pathway may be induced by low-frequency stimulation and is NMDAR dependent, whereas cerebellar LTD is dependent on mGluR1 receptors (Daniel *et al*, 1998; Luscher and Malenka, 2012). In the dorsal striatum, LTD can be induced by tetanic stimulation of cortical afferents (Calabresi *et al*, 1992) and requires concurrent mGluR1, D1 and D2 receptor activation, but is NMDAR-independent. mGluR1 receptors are necessary for decreases in intrinsic excitability following some forms of LTD in the hippocampus through modulation of the $I_h$ current (Brager and Johnston, 2007) and mGluR1 agonist application reduces excitability in the PFC through modification of sodium channels (Carlier *et al*, 2006). In both instances, PKC activation is critical (Daniel *et al*, 1998). Thus decreases in GFP– excitability following appetitive conditioning may be regulated in part by mGluR1 transmission.

Dopamine receptor activation appears to be crucial for striatal LTD (Calabresi *et al*, 1992), however the effect of dopamine on the excitability of MSNs is complex and multifaceted. D1-receptor antagonism has been observed to increase cell membrane excitability through depolarisation of the membrane voltage ($V_m$) through a cAMP-dependent mechanism *in vitro* (Podda *et al*, 2010). O'Donnell and Grace (1996) applied apomorphine, a nonspecific D1/D2 agonist as well as selective D1 and D2 agonists to NAc slices during whole cell recording of membrane voltages. They observed that apomorphine application led to a $V_m$ depolarisation in a majority of

neurons, however crucially, apomorphine application lead to a significant decrease in MSN firing due to an increase in the firing threshold. Application of D1 or D2 receptor agonists alone had no effect on membrane voltage nor overall excitability. This suggests that generalised activation of dopamine receptors in the NAc leads to hyperpolarisation of MSNs. Interestingly, dopamine has been observed to result in additional hyperpolarisation of down-state neurons while simultaneously stabilising the up-state of active neurons (O'Donnell, 2002). Supporting this, *in vitro* application of dopamine to NAc MSNs hyperpolarises these neurons unless the cell membrane potential is artificially raised (Perez *et al*, 2006). This suggests that following exposure to appetitive cues, neurons which are not significantly activated during dopamine release may be stabilised to the down-state and undergo LTD-like plasticity (O'Donnell, 2002).

## 6.4. Under what conditions might GFP+ neurons become more excitable?

Due to the kinetics of *Fos-GFP* expression, we assayed the excitability of neurons activated by exposure to appetitive cues shortly following activation. This means that we cannot determine at what time point the relative increased excitability of GFP+ neurons was increased. The enhanced excitability of GFP+ neurons may be an inherent property, have been potentiated during training, or transiently occur following the test session. Below, these possibilities are each explored.

### *GFP+ neurons may be recruited to ensembles due to enhanced baseline excitability*

Previous studies have suggested that neurons may be recruited to memory encoding ensembles based on pre-existing levels of intrinsic excitability. Han *et al* (2007) demonstrated that artificially increasing the excitability of a subset of lateral amygdala neurons through elevation of CREB increases the likelihood of these neurons been

recruited to a fear-memory encoding ensemble. Inhibition of these excitable CREB expressing neurons following fear conditioning is sufficient to disrupt fear memory recall (Han *et al*, 2009). Later studies which manipulated intrinsic excitability directly (through modulation of potassium channels) demonstrated that it was the excitability-modulating properties of CREB which were critical (Yiu *et al*, 2014). Furthermore, Gouty-Colomer *et al* (2016) observed that a population of Arc-expressing neurons in the lateral amygdala display increased baseline excitability and are preferentially recruited into a fear memory trace. This suggests that memory allocation based on relative levels of excitability may occur under physiological conditions. They also demonstrated, using an Unpaired group, that neurons with increased baseline excitability are more likely to be recruited into any activated ensemble, not necessarily a memory encoding ensemble (although it appeared they may be recruited to a memory encoding ensemble with higher likelihood). This suggests that the increase in GFP+ neuron excitability we observed following memory recall may be because these neurons are inherently excitable.

However, a number of lines of evidence suggest that in our studies, neurons included in *Fos-GFP* ensembles do not display baseline increases in excitability:

1) We have demonstrated many instances in which GFP+ populations activated following memory recall are not more excitable than surrounding neurons (for example, in the OFC or NAc shell following sucrose or cocaine memory retrieval, respectively). This is observed even in brain areas which demonstrated increased Fos expression following the test session.

2) NAc shell GFP+ neurons recording in behaviourally naïve mice are not more excitable than surrounding neurons (Ziminski et al 2016, unpublished observations), suggesting GFP+ neurons spontaneously activated under baseline conditions are not more excitable than surrounding neurons.

3) We have also observed in a recent study that, on day 1 of acquisition of a sucrose-CS association, the GFP+ neurons of Paired, but not Unpaired, mice in the anterior cingulate cortex are more excitable than surrounding neurons (Ziminski et al 2016, unpublished observations). This suggests that excitable neurons are not recruited into activated ensembles based on prior baseline excitability, but rather that associative conditioning induces an excitable phenotype in ACg neurons.

Together, these data suggest that in the striatum and PFC, GFP+ neurons may not be recruited to a memory encoding ensemble based on baseline differences in intrinsic excitability. It is clear from fear conditioning studies in the lateral amygdala that excitable neurons may be preferentially recruited into memory encoding ensembles due to baseline differences in excitability before training (Gouty-Colomer *et al*, 2016; Han *et al*, 2007; Han *et al*, 2009; Zhou *et al*, 2009). Nonetheless, while our data support the notion that increases in excitability may bias allocation of a neuron to a memory encoding ensemble, it does not appear that baseline levels of MSN excitability before training influences allocation to neuronal ensembles prior to appetitive conditioning.

### *GFP+ neuron excitability may be transiently increased following the test session*

Alternatively, it is possible that the excitability of neurons activated by appetitive cues in the striatum was transiently increased following activation in the test session. This could be due to reconsolidation processes following memory recall (Dudai, 2006) or related to the change in CS-US contingency as tests were conducted under extinction conditions (Schultz *et al*, 1997).

Why might certain sets of GFP+ neurons, but not others, demonstrate increased excitability following appetitive cue exposure? The striatum is a unique brain area which receives significant, convergent glutamatergic inputs from multiple cortical and

subcortical areas through a single-neuron layer (Tepper and Plenz, 2006). It appears that prolonged depolarisation of MSNs requires synchronous activity from afferents of different brain areas. Medium spiny neurons exhibit bistable membrane fluctuations between depolarised “up-states” and hyperpolarised “down-states”. Striatal up-states are dependent on synaptic drive, primarily from the hippocampus (O'Donnell and Grace, 1995) (though see Gruber and O'Donnell, 2009). Interestingly, PFC inputs are significantly influenced by MSN up-state/down-states and rarely induce firing during down-states, suggesting the influence of PFC input into NAc MSNs is gated by hippocampal drive. Furthermore, amygdala stimulation alone rarely induces firing in postsynaptic MSNs. These observations suggest that NAc MSNs may express Fos following synchronous activity from at least two glutamatergic projections areas, to permit sufficient membrane depolarisation inducing NMDAR-mediated transmission and extracellular-regulated kinase (ERK) pathway activation.

While synchronous glutamatergic stimulation and ERK activation in MSNs may be required for Fos expression in NAc MSNs, this alone appears insufficient to induce changes in the intrinsic excitability of these neurons. Evidence suggests that dopamine release concurrent with glutamatergic transmission may be important in the regulation of neuronal excitability. Both D1-receptor and NMDAR antagonists block LTP induction the NAc (Floresco *et al*, 2001; Kung *et al*, 2007). Furthermore, co-administration of low doses D1 and NMDA receptor agonists to cortical neurons results in synergistic increases in intrinsic excitability which are larger than when even large doses are used in isolation (Wang and O'Donnell, 2001). This suggests that combined glutamatergic and dopaminergic transmission may be required to induce excitability changes in NAc MSNs (O'Donnell, 2002). Interestingly Yuan *et al* (2002) demonstrate that ERK regulates A-type potassium channel function, increasing the input resistance of distal dendrites, in a manner dependent on PKA or PKC phosphorylation of ERK. Thus ERK may be a point of convergence between DA-receptor linked PKA/PKC transduction

pathways regulating neuronal excitability and NMDAR/CAMKII pathways crucial to the expression of Fos (Cruz *et al*, 2013; Yuan *et al*, 2002).

If synchronous glutamatergic and dopaminergic activity is required for excitability changes in Fos expressing neurons, this may explain why we did not observe universal changes in GFP+ neuron excitability. Subregion specific differences in Paired mice following conditioned locomotion may be due to differences in inherent afferent connectivity and dopamine release kinetics between areas (Brog *et al*, 1993; Haber, 2011; Ito *et al*, 2000; Salgado and Kaplitt, 2015; Voorn *et al*, 2004). For example, we observed an increase in intrinsic excitability of NAc core neurons, but not NAc shell neurons, following exposure to cocaine associated stimuli. Interestingly, exposure to cocaine-associated CS has been observed to selectively increase DA transmission in the NAc core but not NAc shell (Ito *et al*, 2000). Future experiments should observe the effects if dopamine antagonism on the excitability of GFP+ neurons following exposure to appetitive cues.

### *The enhanced excitability may result from repeated activation neurons during training*

Neurons activated during training are more likely to be activated during the test session than other less activated neurons; thus it is possible that we recorded from a population of neurons that had undergone long-term changes to intrinsic excitability during conditioning. Neurons repeatedly activated by cocaine administration in a locomotor chamber are more likely to be reactivated during a test session where either cocaine or saline is administered in the cocaine-paired environment (Mattson *et al*, 2008). Similarly, neurons activated during fear conditioning are more likely to be activated during the retrieval test session (Reijmers *et al*, 2007). Thus it is possible appetitive

conditioning induces persistence increase in excitability in a stable ensemble activated during training and test.

Future studies may utilise the *Fos-tTA* x TRE-H2BGFP mouse to record from neurons activated during training under baseline conditions. The *Fos-tTA* mouse utilises the tetracycline transactivator (tTA) system to permit control over the timing of transgene expression in recently activated neurons. tTA is an engineered fusion protein which is inactivate in the presence of the antibiotic doxycycline, but when active binds *TetO* operator sequences (usually combined with a promotor into tetracycline response elements (TRE)) permitting downstream gene expression in experimentally defined time windows. Researchers have combined the *Fos-tTA* mouse with the *TRE-H2BGFP* mouse (H2BGFP is retained in neurons for weeks following expression) permitting visualisation of Fos-expressing neurons *in vivo* or *ex vivo* weeks after neuronal activation (Tayler *et al*, 2013).

Future studies may utilise this mouse model to probe the excitability of GFP+ neurons activated after both conditioning and test sessions at rest. This would determine whether the excitability changes we observed are induced during training or at test and the time course of these adaptations.

## 6.5. Conclusions and Future studies

We have demonstrated that neuroadaptations to intrinsic and synaptic excitability occur selectively on neurons activated following exposure to reward-associated stimuli. Such changes which may serve to enhance neurotransmission between specific sets of neurons have long been hypothesised to underlie the encoding of memory (Daoudal and Debanne, 2003; Hebb, 1949; Malenka and Nicoll, 1999). To understand the role of the observed adaptations in memory encoding it is necessary to manipulate them selectively in activated neurons. Possible techniques which may be utilised to directly

interfere with the physiology and function of Fos-expressing neurons are explored below.

### *Manipulations of relevant cell populations*

Insertion of transgenes downstream of the *Fos* promoter region has been used to permit targeted ablation of Fos expressing ensembles. Insertion of the reporter gene *LacZ* (which encodes the reporter enzyme β-galactosidase) downstream to the Fos promotor leads to β-galactosidase expression in recently activated neurons. The Daun02 method (Koya *et al*, 2009) utilises the prodrug Daun02, which is converted to daunomycin in the presence of β-galactosidase. Daunomycin inhibits calcium-dependent action potentials and eventually kills neurons in which it is expressed (Farquhar *et al*, 2002; Santone *et al*, 1986), thus permitting selective destruction of Fos-expressing ensembles.

Many studies have demonstrated that the selective lesioning of neuronal ensembles is sufficient to disrupt the expression of conditioned behaviours. For example, context induced renewal of cocaine- and heroin-seeking behaviour (Bossert *et al*, 2011; Cruz *et al*, 2014) is reduced when ensembles activated following exposure to the conditioning context are selectively lesioned following extinction. Similarly, incubation of heroin craving following withdrawal (Fanous *et al*, 2012) is attenuated after ablation of neurons activated in response to drug-associated cues. Thus it is next important for us to selectively destroy the neuronal ensembles activated following the expression of Pavlovian approach and conditioned locomotion to determine the functional role of ensembles located in distinct striatal subregions.

Daun02 can be used to elucidate what is encoded by neurons activated during behavioural tests under extinction. Ensembles activated under these conditions could potentially encode recall of the associative memory, or rather consist of neurons

activated during extinction learning. Warren *et al* (2016) selectively lesioned neurons activated following either instrumental responding for a food reward, or during extinction of the conditioned response. They observed that selectively ablating neurons activated following reinforced instrumental responding reduced later food-seeking behaviour, while targeting neurons activated following extinction increased food seeking-behaviour. This was later supported by Suto *et al* (2016), who using a CS+/CS- omission paradigm observed that ablating CS+ activated neurons *decreased* food seeking behaviours, while destruction of CS- activated neurons *increased* food seeking. Thus the Daun02 method can be used to permit further insight into the precise functional role of NAc ensembles activated during the behavioural tests.

### *Targeted reversal of observed neuroadaptations*

Use of the *Fos-tTA* mouse permits virus-mediated expression of transgenes of interest directly to Fos-expressing ensembles. For example, Liu *et al* (2012) expressed channelrhodopsin-2 in neurons selectively activated following contextual fear conditioning, permitting optogenetic activation of this neuronal population. They observed freezing in mice when the neurons activated during fear conditioning were reactivated in the training context, however not in a different context distinct from that in which conditioning had taken place. Thus, optogenetic control of Fos-expressing neurons permits manipulation of ensembles with tight temporal control (allowing, for example, the inhibition of neurons only during CS presentation) (Tovote *et al*, 2015).

Intrinsic excitability may also be selectively manipulated in GFP+ neurons by virus-mediated expression of ion channels or regulatory proteins. For example, overexpression of potassium channels such as the $K_{IR}2.1$ can be used to manipulate the excitability of target neurons (Dong *et al*, 2006). Additionally, interference with the precise molecular processes which lead to adaptations in excitability and synaptic

strength might be undertaken following identification of the precise ion channels regulated in GFP+ neurons utilising single-cell quantitative PCR (Fuzik *et al*, 2016). For example, expression of dominant-negative ion channels or kinases involved in synapse activation and proliferation selectively in specifically in activated ensembles may be used to reverse the excitability and synaptic changes observed in the present studies (Halterman and Federoff, 1997; Hayashi *et al*, 2004; Schiemann *et al*, 2012).

### *Conclusion*

We have demonstrated adaptations to intrinsic and synaptic excitability selectively on neurons activated following appetitive memory recall. However, at present the functional relevance of these adaptations for memory encoding is unclear. To gain further insight into how NAc ensembles may encode associative memories, it would be advantageous to characterise a number of parameters surrounding Fos-ensemble formation and maintenance. Thus, it will be important to understand the time course of excitability changes in these activated ensembles, the precise chain of physiological and molecular events which lead to their formation, and their maintenance during memory recall. Due to the rapid growth in the sophistication of investigative experimental techniques, answering such questions is now possible.

## References


Amsel, A. (1958). The role of frustrative nonreward in noncontinous reward situations. Psychol Bull,**55**: 102-119.

Antonov I, Antonova I, Kandel ER, Hawkins RD (2001). The contribution of activity-dependent synaptic plasticity to classical conditioning in Aplysia. *J Neurosci* **21**(16): 6413-6422.

Belin D, Everitt BJ (2008). Cocaine seeking habits depend upon dopamine-dependent serial connectivity linking the ventral with the dorsal striatum. *Neuron* **57**(3): 432-441.

Bertran-Gonzalez J, Bosch C, Maroteaux M, Matamales M, Herve D, Valjent E*, et al* (2008). Opposing patterns of signaling activation in dopamine D1 and D2 receptor-expressing striatal neurons in response to cocaine and haloperidol. *J Neurosci* **28**(22): 5671-5685.

Blaiss CA, Janak PH (2009). The nucleus accumbens core and shell are critical for the expression, but not the consolidation, of Pavlovian conditioned approach. *Behav Brain Res* **200**(1): 22-32.

Bossert JM, Stern AL, Theberge FR, Cifani C, Koya E, Hope BT*, et al* (2011). Ventral medial prefrontal cortex neuronal ensembles mediate context-induced relapse to heroin. *Nat Neurosci* **14**(4): 420-422.

Brager DH, Johnston D (2007). Plasticity of intrinsic excitability during long-term depression is mediated through mGluR-dependent changes in I(h) in hippocampal CA1 pyramidal neurons. *J Neurosci* **27**(51): 13926-13937.

Brog JS, Salyapongse A, Deutch AY, Zahm DS (1993). The patterns of afferent innervation of the core and shell in the "accumbens" part of the rat ventral striatum: immunohistochemical detection of retrogradely transported fluoro-gold. *J Comp Neurol* **338**(2): 255-278.

Boakes RA (1977). Performance on learning to associate a stimulus with positive reinforcement. In: Hurwitz DH (ed). *Performance on learning to associate a stimulus with positive reinforcement*. Lawrence Erlbaum Associates: New Jersey.

Calabresi P, Maj R, Pisani A, Mercuri NB, Bernardi G (1992). Long-term synaptic

depression in the striatum: physiological and pharmacological characterization. *J Neurosci* **12**(11): 4224-4233.

Campanac E, Daoudal G, Ankri N, Debanne D (2008). Downregulation of dendritic I(h) in CA1 pyramidal neurons after LTP. *J Neurosci* **28**(34): 8635-8643.

Cao XY, Xu H, Wu LJ, Li XY, Chen T, Zhuo M (2009). Characterization of intrinsic properties of cingulate pyramidal neurons in adult mice after nerve injury. *Mol Pain* **5**: 73.

Carlier E, Sourdet V, Boudkkazi S, Deglise P, Ankri N, Fronzaroli-Molinieres L*, et al* (2006). Metabotropic glutamate receptor subtype 1 regulates sodium currents in rat neocortical pyramidal neurons. *J Physiol* **577**(Pt 1): 141-154.

Cazorla M, Shegda M, Ramesh B, Harrison NL, Kellendonk C (2012). Striatal D2 receptors regulate dendritic morphology of medium spiny neurons via Kir2 channels. *J Neurosci* **32**(7): 2398-2409.

Cone JJ, Fortin SM, McHenry JA, Stuber GD, McCutcheon JE, Roitman MF (2016). Physiological state gates acquisition and expression of mesolimbic reward prediction signals. *Proc Natl Acad Sci U S A* **113**(7): 1943-1948.

Cruz FC, Babin KR, Leao RM, Goldart EM, Bossert JM, Shaham Y*, et al* (2014). Role of nucleus accumbens shell neuronal ensembles in context-induced reinstatement of cocaine-seeking. *J Neurosci* **34**(22): 7437-7446.

Cruz FC, Koya E, Guez-Barber DH, Bossert JM, Lupica CR, Shaham Y*, et al* (2013). New technologies for examining the role of neuronal ensembles in drug addiction and fear. *Nat Rev Neurosci* **14**(11): 743-754.

Daniel H, Levenes C, Crepel F (1998). Cellular mechanisms of cerebellar LTD. *Trends Neurosci* **21**(9): 401-407.

Daoudal G, Debanne D (2003). Long-term plasticity of intrinsic excitability: learning rules and mechanisms. *Learn Mem* **10**(6): 456-465.

Day JJ, Wheeler RA, Roitman MF, Carelli RM (2006). Nucleus accumbens neurons encode Pavlovian approach behaviors: evidence from an autoshaping paradigm. *Eur J Neurosci* **23**(5): 1341-1351.

Degenetais E, Thierry AM, Glowinski J, Gioanni Y (2002). Electrophysiological properties of

pyramidal neurons in the rat prefrontal cortex: an in vivo intracellular recording study. *Cereb Cortex* **12**(1): 1-16.

Dong Y, Green T, Saal D, Marie H, Neve R, Nestler EJ*, et al* (2006). CREB modulates excitability of nucleus accumbens neurons. *Nat Neurosci* **9**(4): 475-477.

Dudai Y (2006). Reconsolidation: the advantage of being refocused. *Curr Opin Neurobiol* **16**(2): 174-178.

Fanous S, Goldart EM, Theberge FR, Bossert JM, Shaham Y, Hope BT (2012). Role of orbitofrontal cortex neuronal ensembles in the expression of incubation of heroin craving. *J Neurosci* **32**(34): 11600-11609.

Farquhar D, Pan BF, Sakurai M, Ghosh A, Mullen CA, Nelson JA (2002). Suicide gene therapy using E. coli beta-galactosidase. *Cancer Chemother Pharmacol* **50**(1): 65-70.

Floresco SB, Blaha CD, Yang CR, Phillips AG (2001). Dopamine D1 and NMDA receptors mediate potentiation of basolateral amygdala-evoked firing of nucleus accumbens neurons. *J Neurosci* **21**(16): 6370-6376.

Fosque BF, Sun Y, Dana H, Yang CT, Ohyama T, Tadross MR*, et al* (2015). Neural circuits. Labeling of active neural circuits in vivo with designed calcium integrators. *Science* **347**(6223): 755-760.

Fransen E, Tigerholm J (2010). Role of A-type potassium currents in excitability, network synchronicity, and epilepsy. *Hippocampus* **20**(7): 877-887.

Fuchs RA, Ramirez DR, Bell GH. (2008). Nucleus accumbens shell and core involvement in drug context-induced reinstatement of cocaine seeking in rats. *Psychopharmacology*, **200**(4): 545-556.

Fuzik J, Zeisel A, Mate Z, Calvigioni D, Yanagawa Y, Szabo G*, et al* (2016). Integration of electrophysiological recordings with single-cell RNA-seq data identifies neuronal subtypes. *Nat Biotechnol* **34**(2): 175-183.

Gertler TS, Chan CS, Surmeier DJ (2008). Dichotomous anatomical properties of adult striatal medium spiny neurons. *J Neurosci* **28**(43): 10814-10824.

Goldstein SA, Bockenhauer D, O'Kelly I, Zilberberg N (2001). Potassium leak channels and the KCNK family of two-P-domain subunits. *Nat Rev Neurosci* **2**(3): 175-184.

Gouty-Colomer LA, Hosseini B, Marcelo IM, Schreiber J, Slump DE, Yamaguchi S*, et al* (2016). Arc expression identifies the lateral amygdala fear memory trace. *Mol Psychiatry* **21**(3): 364-375.

Graybiel AM, Moratalla R, Robertson HA (1990). Amphetamine and cocaine induce drug-specific activation of the c-fos gene in striosome-matrix compartments and limbic subdivisions of the striatum. *Proc Natl Acad Sci U S A* **87**(17): 6912-6916.

Haber SN (2011). Neuroanatomy of Reward: A View from the Ventral Striatum. In: Gottfried JA (ed). *Neurobiology of Sensation and Reward*: Boca Raton (FL).

Halterman MW, Federoff HJ (1997). Molecular modification of neural networks: altering synaptic function through the use of viral mediated gene transfer. *Advances in Organ Biology* **2**: 22.

Han JH, Kushner SA, Yiu AP, Cole CJ, Matynia A, Brown RA*, et al* (2007). Neuronal competition and selection during memory formation. *Science* **316**(5823): 457-460.

Han JH, Kushner SA, Yiu AP, Hsiang HL, Buch T, Waisman A*, et al* (2009). Selective erasure of a fear memory. *Science* **323**(5920): 1492-1496.

Hayashi ML, Choi SY, Rao BS, Jung HY, Lee HK, Zhang D*, et al* (2004). Altered cortical synaptic morphology and impaired memory consolidation in forebrain- specific dominant-negative PAK transgenic mice. *Neuron* **42**(5): 773-787.

Hebb DO (1949). *The Organization of Behavior: A Neuropsychological Theory* John Wiley & Sons: New York.

Hedrick T, Waters J (2012). Effect of temperature on spiking patterns of neocortical layer 2/3 and layer 6 pyramidal neurons. *Front Neural Circuits* **6**: 28.

Hopf FW, Bowers MS, Chang SJ, Chen BT, Martin M, Seif T*, et al* (2010). Reduced nucleus accumbens SK channel activity enhances alcohol seeking during abstinence. *Neuron* **65**(5): 682-694.

Hotsenpiller G, Giorgetti M, Wolf ME (2001). Alterations in behaviour and glutamate

transmission following presentation of stimuli previously associated with cocaine exposure. *Eur J Neurosci* **14**(11): 1843-1855.

Hotsenpiller G, Horak BT, Wolf ME (2002). Dissociation of conditioned locomotion and Fos induction in response to stimuli formerly paired with cocaine. *Behav Neurosci* **116**(4): 634-645.

Hyun JH, Eom K, Lee KH, Ho WK, Lee SH (2013). Activity-dependent downregulation of D-type K+ channel subunit Kv1.2 in rat hippocampal CA3 pyramidal neurons. *J Physiol* **591**(22): 5525-5540.

Ito R, Dalley JW, Howes SR, Robbins TW, Everitt BJ (2000). Dissociation in conditioned dopamine release in the nucleus accumbens core and shell in response to cocaine cues and during cocaine-seeking behavior in rats. *J Neurosci* **20**(19): 7489-7495.

Ito R, Everitt BJ, Robbins TW (2005). The hippocampus and appetitive Pavlovian conditioning: effects of excitotoxic hippocampal lesions on conditioned locomotor activity and autoshaping. *Hippocampus* **15**(6): 713-721.

Ito R, Robbins TW, McNaughton BL, Everitt BJ (2006). Selective excitotoxic lesions of the hippocampus and basolateral amygdala have dissociable effects on appetitive cue and place conditioning based on path integration in a novel Y-maze procedure. *Eur J Neurosci* **23**(11): 3071-3080.

Josselyn SA, Kohler S, Frankland PW (2015). Finding the engram. *Nat Rev Neurosci* **16**(9): 521-534.

Kearns DN, Weiss SJ (2004). Sign-tracking (autoshaping) in rats: a comparison of cocaine and food as unconditioned stimuli. *Learn Behav* **32**(4): 463-476.

Koya E, Golden SA, Harvey BK, Guez-Barber DH, Berkow A, Simmons DE*, et al* (2009). Targeted disruption of cocaine-activated nucleus accumbens neurons prevents context-specific sensitization. *Nat Neurosci* **12**(8): 1069-1073.

Kung VW, Hassam R, Morton AJ, Jones S (2007). Dopamine-dependent long term potentiation in the dorsal striatum is reduced in the R6/2 mouse model of Huntington's disease. *Neuroscience* **146**(4): 1571-1580.

Lee AT, Gee SM, Vogt D, Patel T, Rubenstein JL, Sohal VS (2014). Pyramidal neurons in prefrontal cortex receive subtype-specific forms of excitation and inhibition. *Neuron* **81**(1): 61-68.

Liu X, Ramirez S, Pang PT, Puryear CB, Govindarajan A, Deisseroth K*, et al* (2012). Optogenetic stimulation of a hippocampal engram activates fear memory recall. *Nature* **484**(7394): 381-385.

Loweth JA, Tseng KY, Wolf ME (2014). Adaptations in AMPA receptor transmission in the nucleus accumbens contributing to incubation of cocaine craving. *Neuropharmacology* **76 Pt B**: 287-300.

Lu L, Grimm JW, Shaham Y, Hope BT (2003). Molecular neuroadaptations in the accumbens and ventral tegmental area during the first 90 days of forced abstinence from cocaine self-administration in rats. *J Neurochem* **85**(6): 1604-1613.

Luscher C, Malenka RC (2012). NMDA receptor-dependent long-term potentiation and long-term depression (LTP/LTD). *Cold Spring Harb Perspect Biol* **4**(6).

MacAskill AF, Cassel JM, Carter AG (2014). Cocaine exposure reorganizes cell type- and input-specific connectivity in the nucleus accumbens. *Nat Neurosci* **17**(9): 1198-1207.

Mackintosh NJ (1974). *The psychology of animal learning* Academic Press: London.

Malenka RC, Nicoll RA (1999). Long-term potentiation--a decade of progress? *Science* **285**(5435): 1870-1874.

Manis PB (2014). Delayed rectifier and A-type potassium channels. In: Jaeger D, Jung R (eds). *Encyclopedia of computational neuroscience*. Springer Science: New York.

Mattson BJ, Koya E, Simmons DE, Mitchell TB, Berkow A, Crombag HS*, et al* (2008). Context-specific sensitization of cocaine-induced locomotor activity and associated neuronal ensembles in rat nucleus accumbens. *Eur J Neurosci* **27**(1): 202-212.

Miles FJ, Everitt BJ, Dickinson A (2003). Oral cocaine seeking by rats: action or habit? *Behav Neurosci* **117**(5): 927-938.

Moyer JR, Jr., Thompson LT, Disterhoft JF (1996). Trace eyeblink conditioning increases CA1 excitability in a transient and learning-specific manner. *J Neurosci* **16**(17): 5536-5546.

Mu P, Moyer JT, Ishikawa M, Zhang Y, Panksepp J, Sorg BA*, et al* (2010). Exposure to cocaine dynamically regulates the intrinsic membrane excitability of nucleus accumbens neurons. *J Neurosci* **30**(10): 3689-3699.

Nisenbaum ES, Wilson CJ (1995). Potassium currents responsible for inward and outward rectification in rat neostriatal spiny projection neurons. *J Neurosci* **15**(6): 4449-4463.

O'Brien CP, Childress AR, Ehrman R, Robbins SJ. (1998). Conditioning factors in drug abuse: can the explain compulsion? J Psychopharmacology, **12(**1):15-22.

O'Donnell P (2002). Dopamine and ensemble coding in the striatum and nucleus accumbens. In: Graybiel AM, DeLong MR, Kitai ST (eds). *The Basal Ganglia VI*. Kluwer Academic: New York.

O'Donnell P, Grace AA (1995). Synaptic interactions among excitatory afferents to nucleus accumbens neurons: hippocampal gating of prefrontal cortical input. *J Neurosci* **15**(5 Pt 1): 3622-3639.

O'Donnell P, Grace AA (1996). Dopaminergic reduction of excitability in nucleus accumbens neurons recorded in vitro. *Neuropsychopharmacology* **15**(1): 87-97.

Perez MF, White FJ, Hu XT (2006). Dopamine D(2) receptor modulation of K(+) channel activity regulates excitability of nucleus accumbens neurons at different membrane potentials. *J Neurophysiol* **96**(5): 2217-2228.

Planert H, Berger TK, Silberberg G (2013). Membrane properties of striatal direct and indirect pathway neurons in mouse and rat slices and their modulation by dopamine. *PLoS One* **8**(3): e57054.

Plotkin JL, Day M, Surmeier DJ (2011). Synaptically driven state transitions in distal dendrites of striatal spiny neurons. *Nat Neurosci* **14**(7): 881-888.

Podda MV, Riccardi E, D'Ascenzo M, Azzena GB, Grassi C (2010). Dopamine D1-like receptor activation depolarizes medium spiny neurons of the mouse nucleus accumbens by inhibiting inwardly rectifying K+ currents through a cAMP-dependent protein kinase A-independent mechanism. *Neuroscience* **167**(3): 678-690.

Pruss H, Wenzel M, Eulitz D, Thomzig A, Karschin A, Veh RW (2003). Kir2 potassium channels in rat striatum are strategically localized to control basal ganglia function. *Brain Res Mol Brain Res* **110**(2): 203-219.

Reijmers LG, Perkins BL, Matsuo N, Mayford M (2007). Localization of a stable neural correlate of associative memory. *Science* **317**(5842): 1230-1233.

Rescrola RA (1967). Pavlovian conditioning and its proper control procedures. *Psych Rev,* **74**(1): 71-80.

Salgado S, Kaplitt MG (2015). The Nucleus Accumbens: A Comprehensive Review. *Stereotact Funct Neurosurg* **93**(2): 75-93.

Santini E, Quirk GJ, Porter JT (2008). Fear conditioning and extinction differentially modify the intrinsic excitability of infralimbic neurons. *J Neurosci* **28**(15): 4028-4036.

Santone KS, Oakes SG, Taylor SR, Powis G (1986). Anthracycline-induced inhibition of a calcium action potential in differentiated murine neuroblastoma cells. *Cancer Res* **46**(6): 2659-2664.

Schiemann J, Schlaudraff F, Klose V, Bingmer M, Seino S, Magill PJ*, et al* (2012). K-ATP channels in dopamine substantia nigra neurons control bursting and novelty-induced exploration. *Nat Neurosci* **15**(9): 1272-1280.

Schmidt EF, Sutton MA, Schad CA, Karanian DA, Brodkin ES, Self DW (2001). Extinction training regulates tyrosine hydroxylase during withdrawal from cocaine self-administration. *J Neurosci* **21**(7): RC137.

Schultz W, Dayan P, Montague PR (1997). A neural substrate of prediction and reward. *Science* **275**(5306): 1593-1599.

Self DW, Choi KH, Simmons D, Walker JR, Smagula CS (2004). Extinction training regulates neuroadaptive responses to withdrawal from chronic cocaine self-administration. *Learn Mem* **11**(5): 648-657.

Sellings LH, Clarke PB (2006). 6-Hydroxydopamine lesions of nucleus accumbens core abolish amphetamine-induced conditioned activity. *Synapse* **59**(6): 374-377.

Shiflett MW, Balleine BW (2010). At the limbic-motor interface: disconnection of basolateral amygdala from nucleus accumbens core and shell reveals dissociable components of

incentive motivation. *Eur J Neurosci* **32**(10): 1735-1743.

Shim HG, Jang DC, Lee J, Chung G, Lee S, Kim YG*, et al* (2017). Long-Term Depression of Intrinsic Excitability Accompanied by Synaptic Depression in Cerebellar Purkinje Cells. *J Neurosci* **37**(23): 5659-5669.

Sieburg, M. C., Margetts-Smith, G., Ziminski, J., Crombag, H. S., & Koya, E. The identification of sucrose cue-evoked corticostriatal neuronal ensemble activity patterns underlying hunger states. Program No. 837.07. 2017 Neuroscience Meeting Planner. Washington, DC: Society for Neuroscience, 2017. Online.

Stuart G, Spruston N (1998). Determinants of voltage attenuation in neocortical pyramidal neuron dendrites. *J Neurosci* **18**(10): 3501-3510.

Stuart GJ, Spruston N (2015). Dendritic integration: 60 years of progress. *Nat Neurosci* **18**(12): 1713-1721.

Suto N, Laque A, De Ness GL, Wagner GE, Watry D, Kerr T*, et al* (2016). Distinct memory engrams in the infralimbic cortex of rats control opposing environmental actions on a learned behavior. *Elife* **5**.

Tayler KK, Tanaka KZ, Reijmers LG, Wiltgen BJ (2013). Reactivation of neural ensembles during the retrieval of recent and remote memory. *Curr Biol* **23**(2): 99-106.

Tepper JM, Plenz D (2006). Microcircuits in the striatum: Striatal cell types and their interaction. In: Grillner S, Graybiel AM (eds). *The Interface between Neurons and Global Brain Function*. The MIT Press: Cambridge, MA:.

Tkatch T, Baranauskas G, Surmeier DJ (2000). Kv4.2 mRNA abundance and A-type K(+) current amplitude are linearly related in basal ganglia and basal forebrain neurons. *J Neurosci* **20**(2): 579-588.

Tovote P, Fadok JP, Luthi A (2015). Neuronal circuits for fear and anxiety. *Nat Rev Neurosci* **16**(6): 317-331.

Uslaner JM, Acerbo MJ, Jones SA, Robinson TE (2006). The attribution of incentive salience to a stimulus that signals an intravenous injection of cocaine. *Behav Brain Res* **169**(2): 320-324.

Volkow ND, Wang GJ, Telang F, Fowler JS, Logal J, Childress AR, Jayne M, Ma Y, Wong C. (2006). Cocaine cues and dopamine in dorsal striatum: mechanism of craving in cocaine addiction. J Neurosci, **26(**24): 6583-6588.

Voorn P, Vanderschuren LJ, Groenewegen HJ, Robbins TW, Pennartz CM (2004). Putting a spin on the dorsal-ventral divide of the striatum. *Trends Neurosci* **27**(8): 468-474.

Wang J, O'Donnell P (2001). D(1) dopamine receptors potentiate nmda-mediated excitability increase in layer V prefrontal cortical pyramidal neurons. *Cereb Cortex* **11**(5): 452-462.

Wang W, Wildes CP, Pattarabanjird T, Sanchez MI, Glober GF, Matthews GA*, et al* (2017). A light- and calcium-gated transcription factor for imaging and manipulating activated neurons. *Nat Biotechnol*.

Warren BL, Mendoza MP, Cruz FC, Leao RM, Caprioli D, Rubio FJ*, et al* (2016). Distinct Fos-Expressing Neuronal Ensembles in the Ventromedial Prefrontal Cortex Mediate Food Reward and Extinction Memories. *J Neurosci* **36**(25): 6691-6703.

Warren BL, Suto N, Hope BT (2017). Mechanistic Resolution Required to Mediate Operant Learned Behaviors: Insights from Neuronal Ensemble-Specific Inactivation. *Front Neural Circuits* **11**: 28.

West EA, Carelli RM (2016). Nucleus Accumbens Core and Shell Differentially Encode Reward-Associated Cues after Reinforcer Devaluation. *J Neurosci* **36**(4): 1128-1139.

Xu J, Kang N, Jiang L, Nedergaard M, Kang J (2005). Activity-dependent long-term potentiation of intrinsic excitability in hippocampal CA1 pyramidal neurons. *J Neurosci* **25**(7): 1750-1760.

Yiu AP, Mercaldo V, Yan C, Richards B, Rashid AJ, Hsiang HL*, et al* (2014). Neurons are recruited to a memory trace based on relative neuronal excitability immediately before training. *Neuron* **83**(3): 722-735.

Yuan LL, Adams JP, Swank M, Sweatt JD, Johnston D (2002). Protein kinase modulation of dendritic K+ channels in hippocampus involves a mitogen-activated protein kinase pathway. *J Neurosci* **22**(12): 4860-4868.

Zhou Y, Won J, Karlsson MG, Zhou M, Rogerson T, Balaji J*, et al* (2009). CREB regulates excitability and the allocation of memory to subsets of neurons in the amygdala. *Nat Neurosci* **12**(11): 1438-1443.

Ziminski JJ, Hessler S, Margetts-Smith G, Sieburg MC, Crombag HS, Koya E (2017a). Changes in Appetitive Associative Strength Modulates Nucleus Accumbens, But Not Orbitofrontal Cortex Neuronal Ensemble Excitability. *J Neurosci* **37**(12): 3160-3170.

Ziminski J, Sieburg MC, Margetts-Smith G, Crombag HS, Koya E (2017b). Regional Differences In Striatal Neuronal Ensemble Excitability Following Cocaine And Extinction Memory Retrieval In Fos-GFP Mice. *Neuropsychopharmacology*. [online] Available at: https://www.nature.com/articles/npp2017101

Zombeck JA, Chen GT, Johnson ZV, Rosenberg DM, Craig AB, Rhodes JS (2008). Neuroanatomical specificity of conditioned responses to cocaine versus food in mice. *Physiol Behav* **93**(3): 637-650.

# Appendix A; Individual data

## Chapter 3.

## Behaviour (Figure 4):

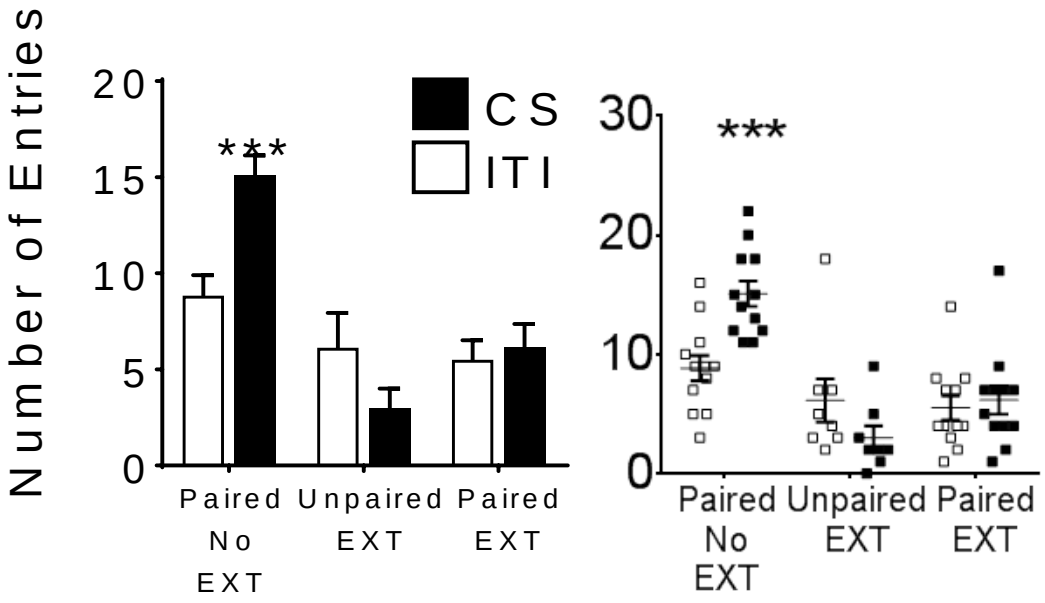


## Fos (Figure 4).

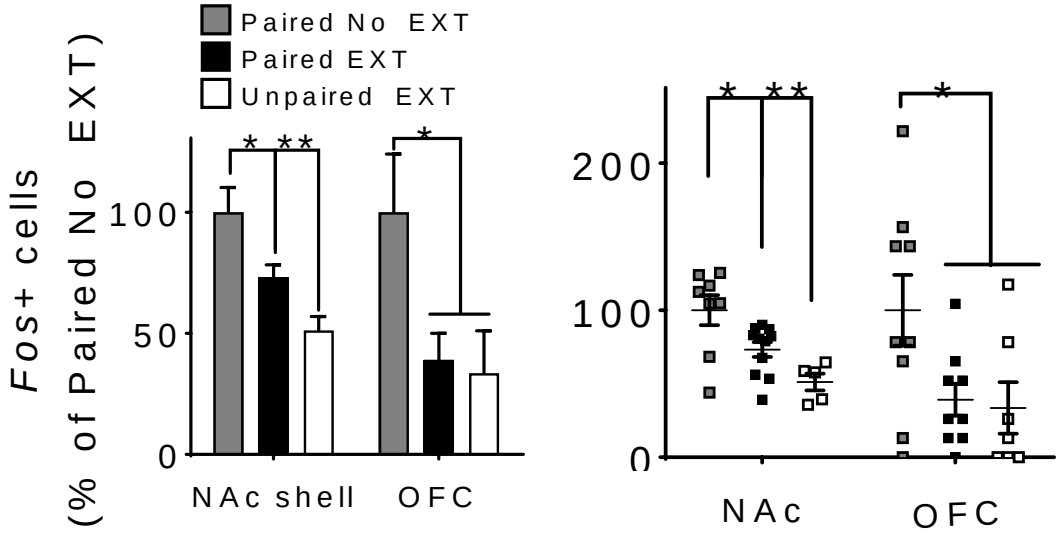

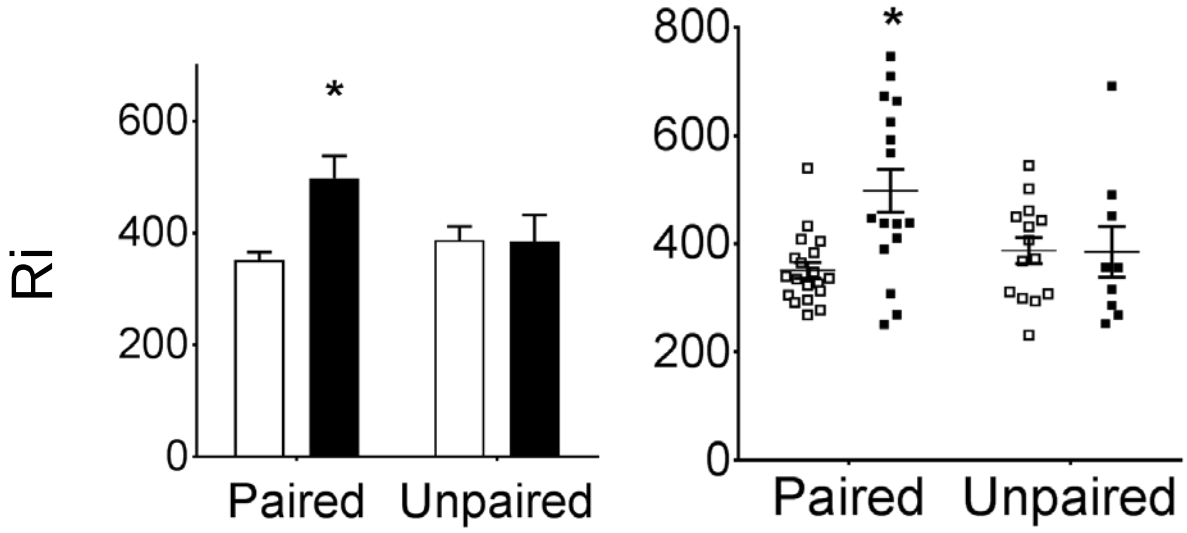
Ri
600
400
200
0
*
Paired
Unpaired
800
600
400
200
0
*
Paired
Unpaired

# Chapter 4.

## Electrophysiology

### AMPAR

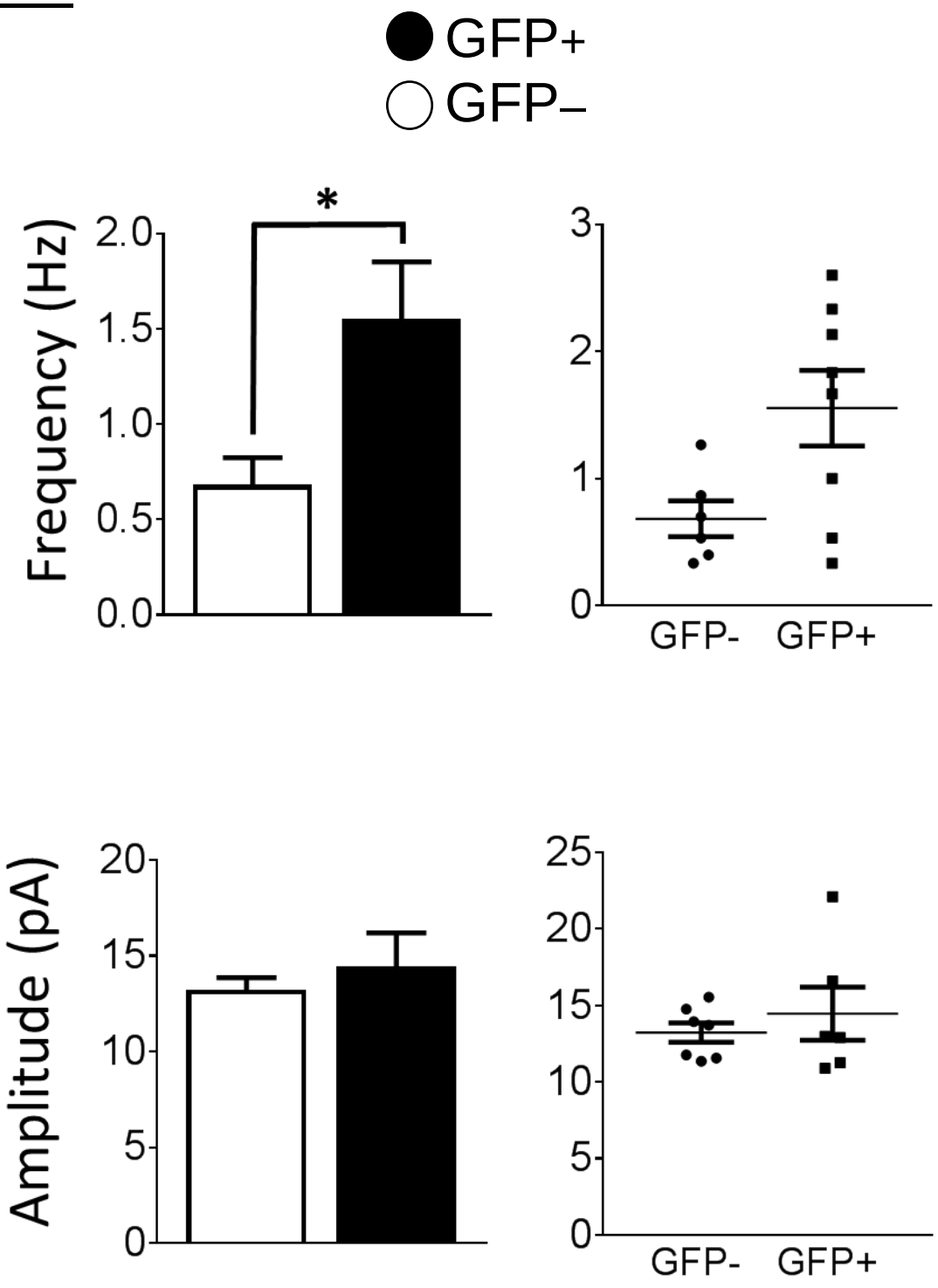

**GABAR**

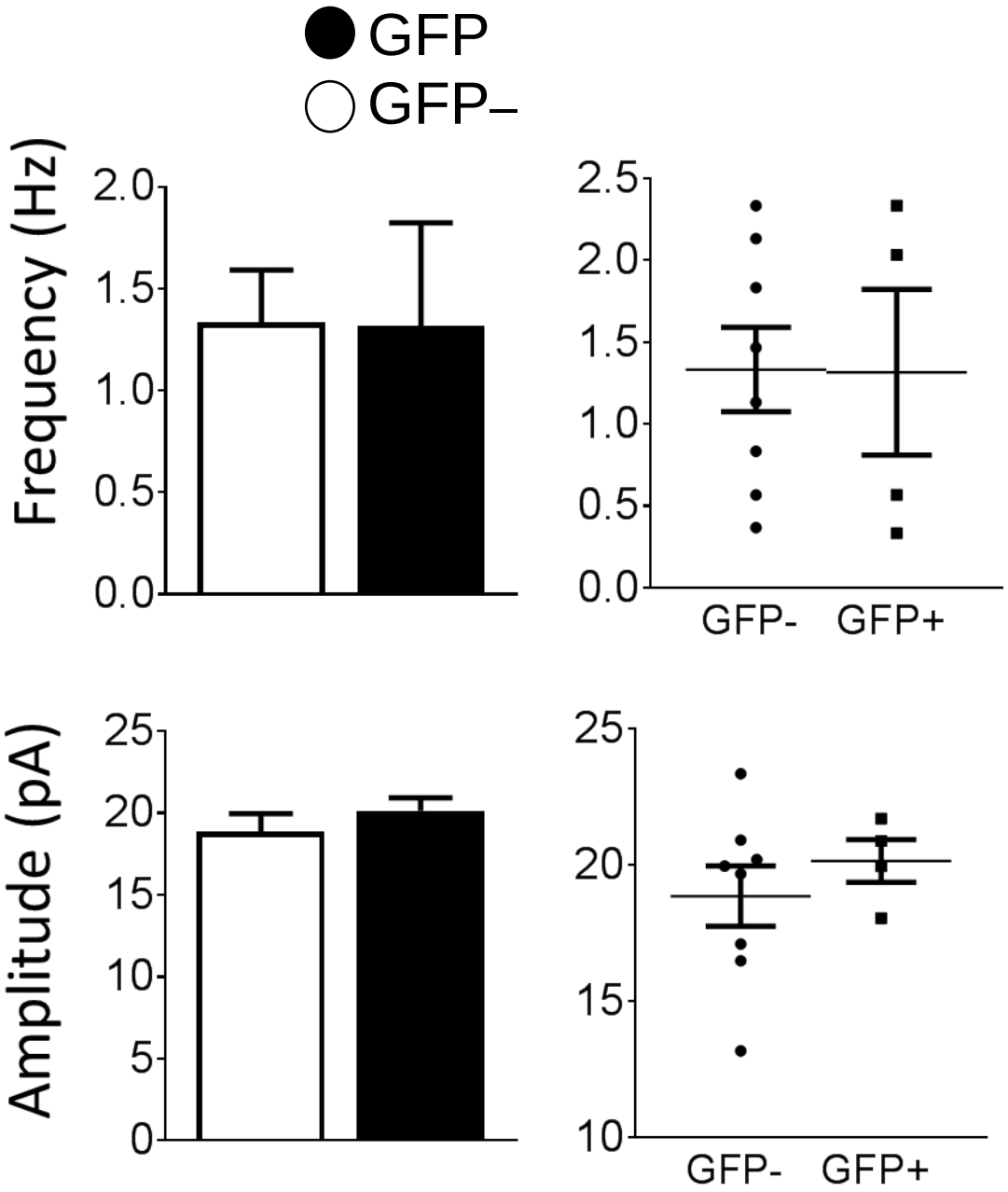
GFP
GFP–
Frequency (Hz)
2.0
1.5
1.0
0.5
0.0
2.5
2.0
1.5
1.0
0.5
0.0
GFP-
GFP+
Amplitude (pA)
25
20
15
10
5
0
25
20
15
10
GFP-
GFP+

## Cyclothiazide

## Evoked EPSCs

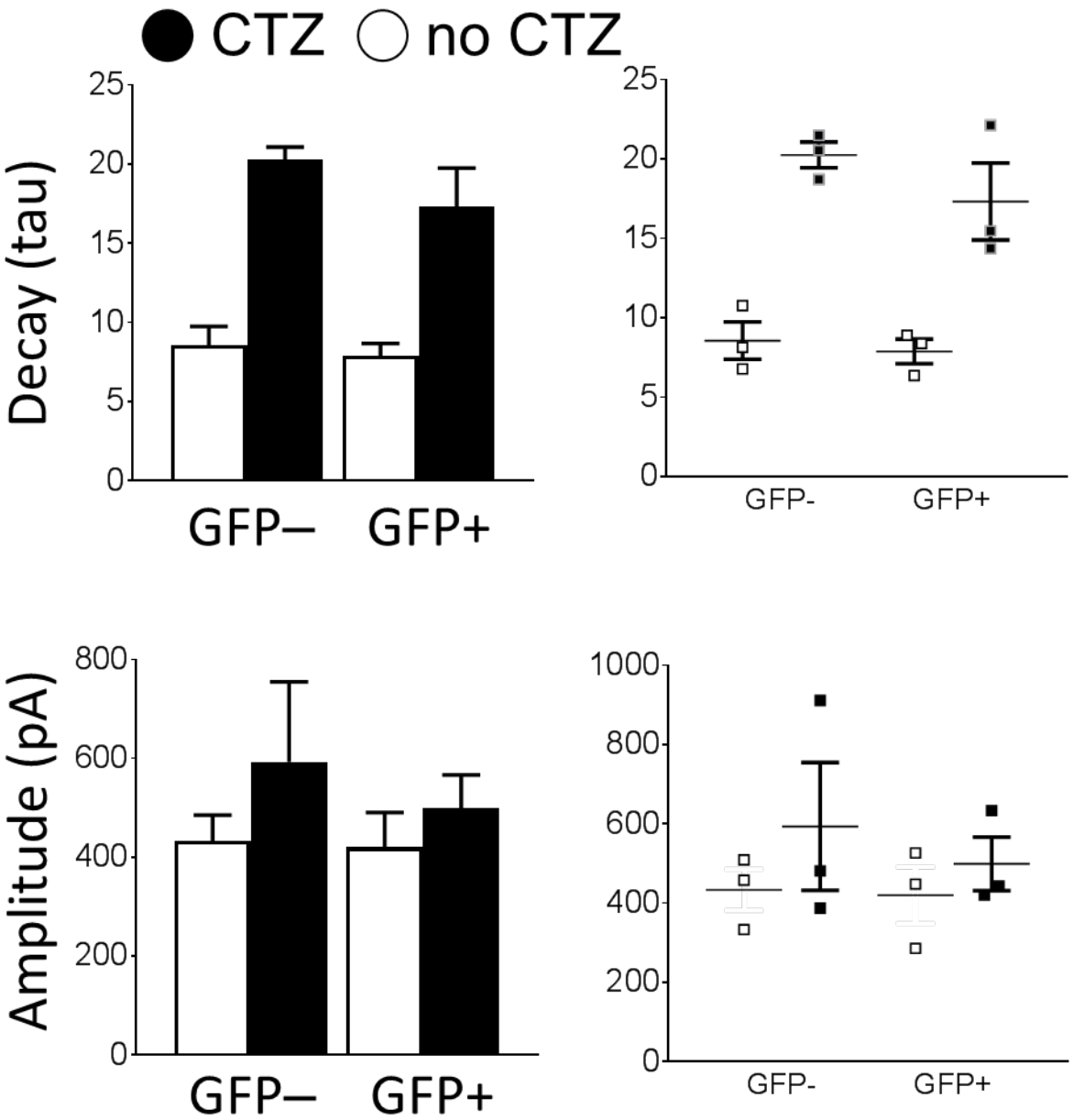

# Chapter 5.

## Behaviour

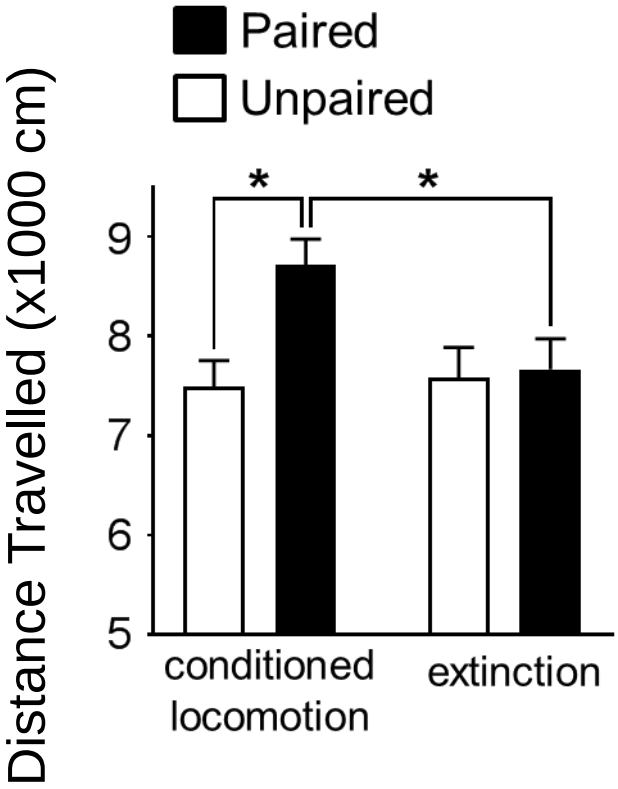


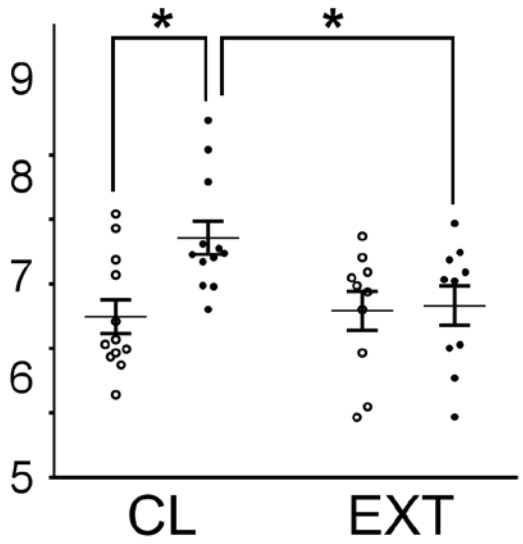


## Immunohistochemistry

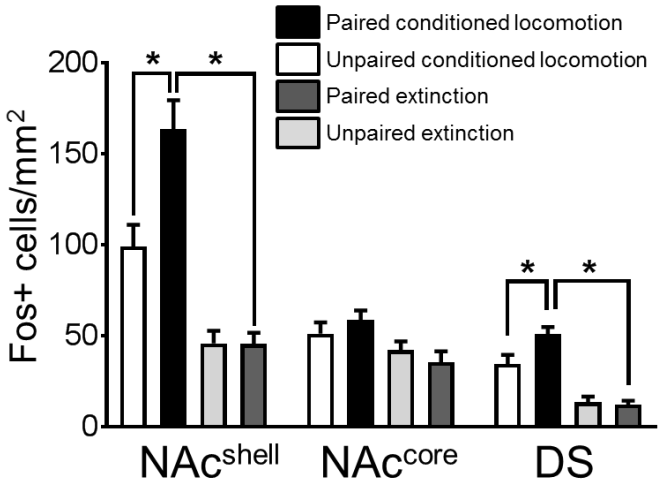


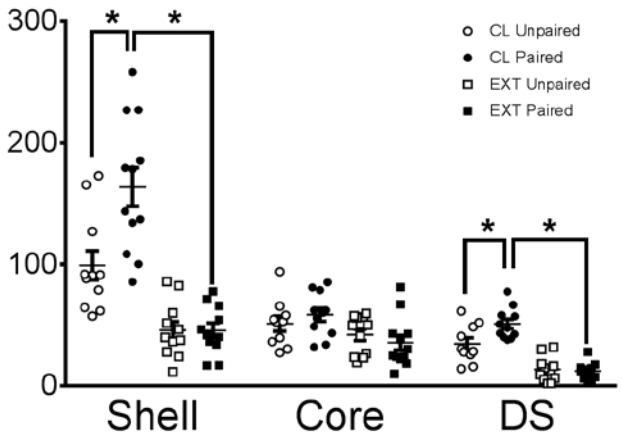

## Electrophysiology

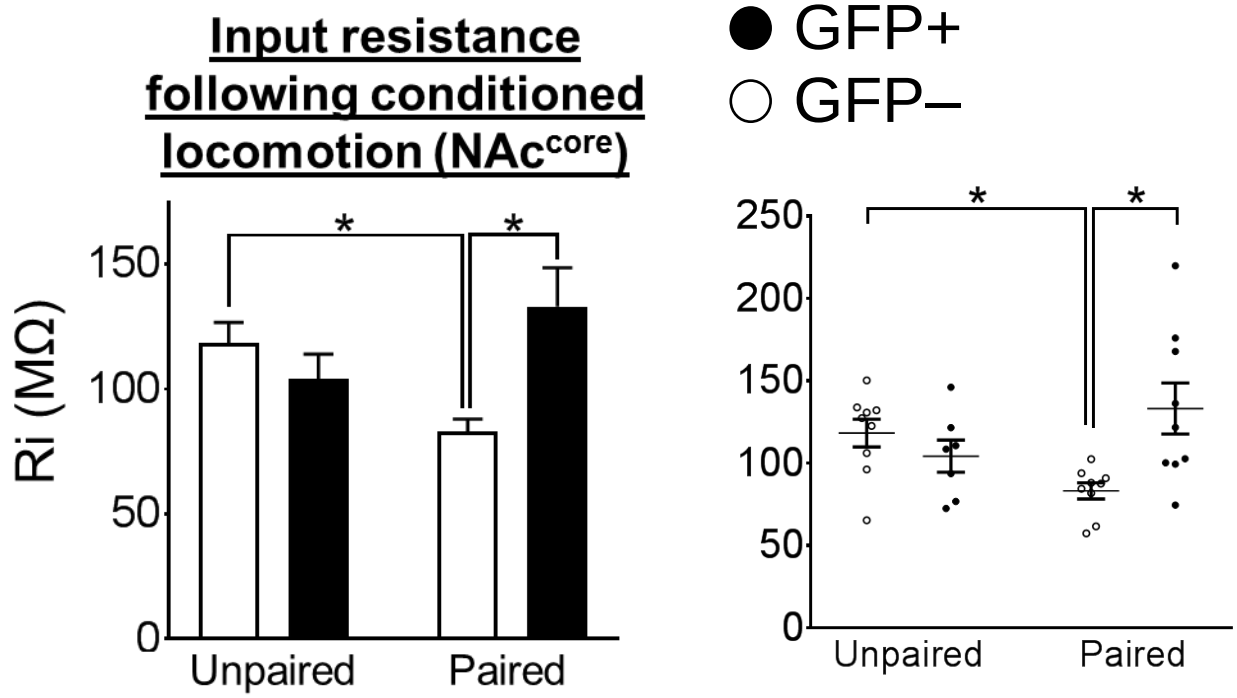


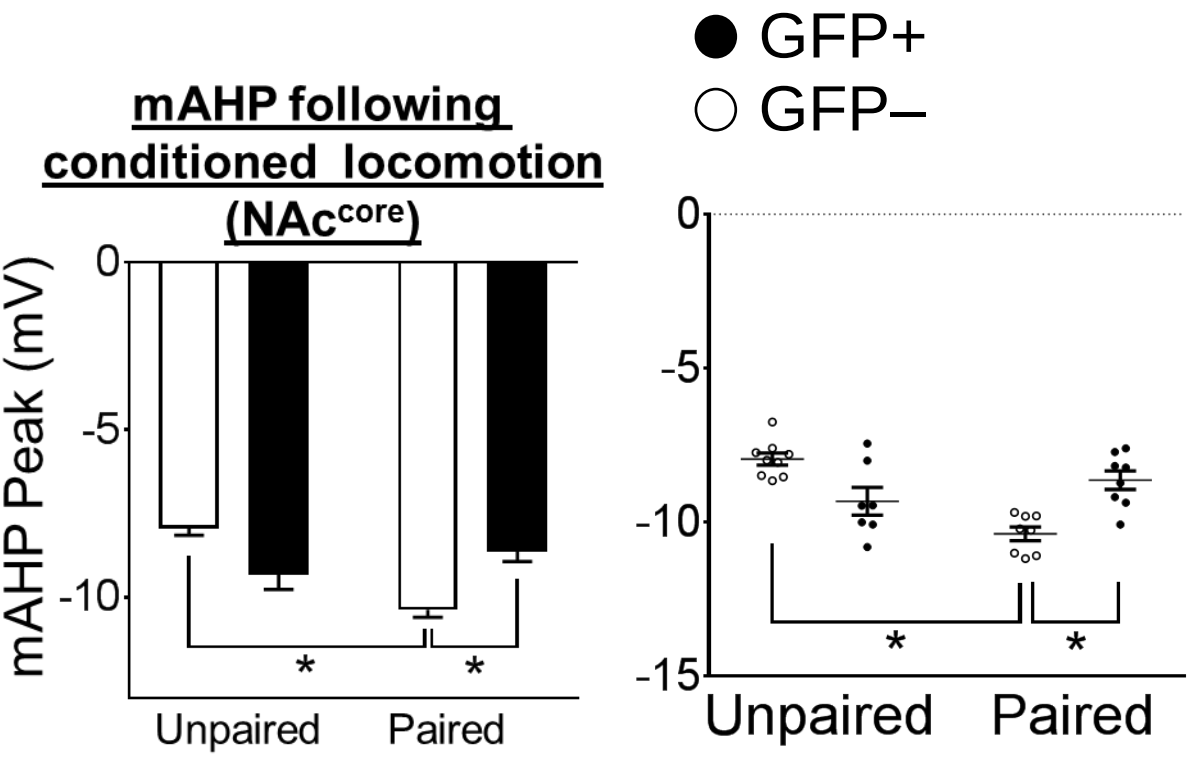

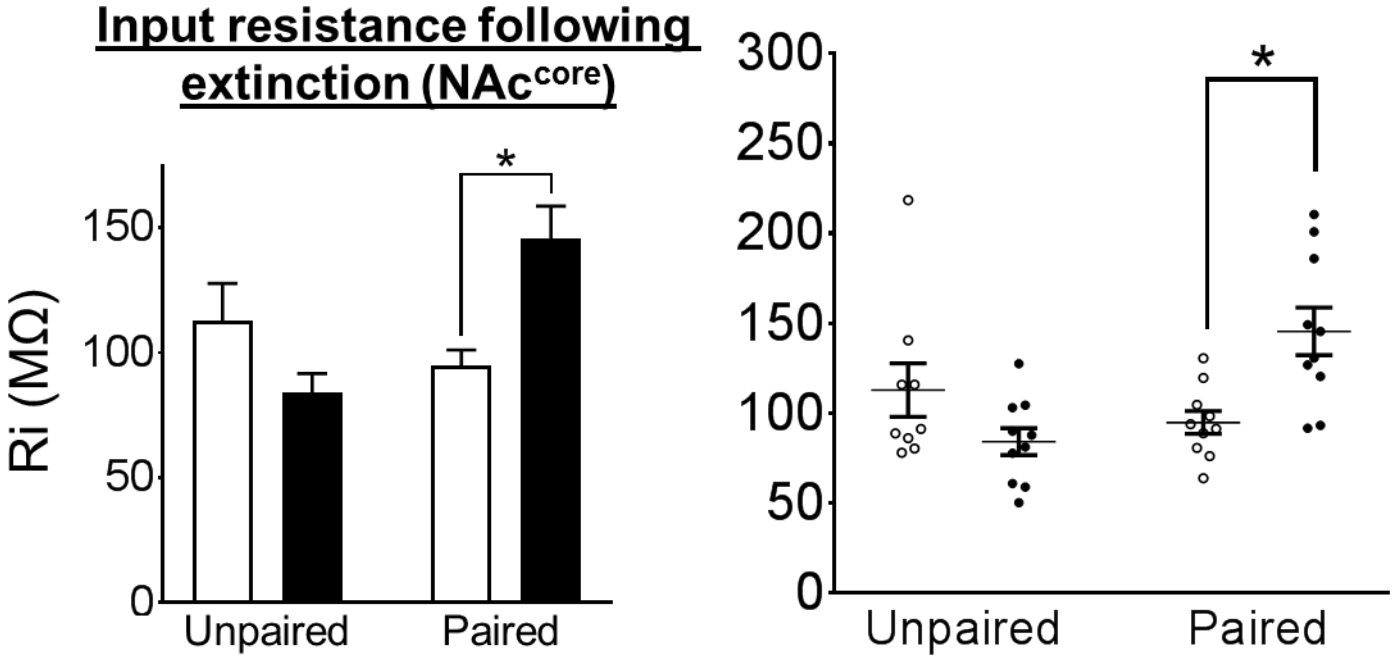
Input resistance following extinction (NAc^core)
Ri (MΩ)
150
100
50
0
*
Unpaired
Paired
300
250
200
150
100
50
0
*
Unpaired
Paired

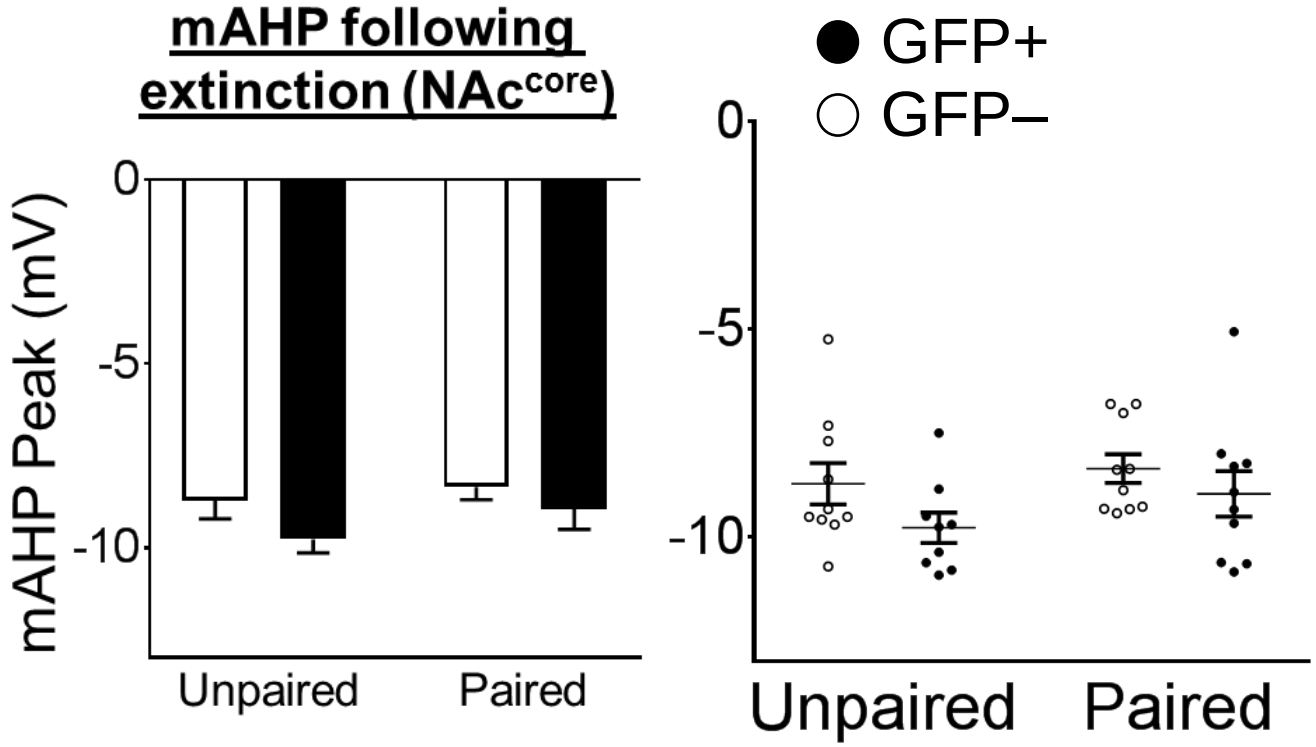
mAHP following extinction (NAc^core)
mAHP Peak (mV)
0
-5
-10
Unpaired
Paired
GFP+
GFP–
0
-5
-10
Unpaired
Paired

# Appendix B

## Animal numbers and outlier analysis

### Chapter 3.

**Histology (IHC):** Behaviour – 20 animals per group; IHC – Paired, lost 2 brains to poor perfusion. Unpaired – lost 2 brains during slicing, 1 mice excluded as staining did not work (no visible Fos anywhere). Data Analysis – Paired: 1 2 standard deviation (SD) outlier excluded (not excluded by Grubbs test). Re-run t-test including the Paired SD outlier, significant $p=0<0.05$, OFC $p<0.05$.

**Electrophysiology – Pavlovian Approach, NAc:** Behaviour - 23 mice run total – Initially 3 mice lost (1 house light broke so mouse was run in the dark for the entire experiment, 1 mis-genotype, 1 lost during slicing. Paired/Unpaired 12/8 remaining. Paired mice – 2 animals no cells retrieved due to cell death. Unpaired mice – 1 animal no cells retrieved. **OFC** Behaviour – 12 mice (6 Paired, 6 Unpaired). Paired – 1 mouse no cells retrieved, Unpaired 1 mouse no cells retrieved. Data Analysis – Paired: 1 cell excluded in data analysis (did not spike across current injections, 2SD outlier). Grubbs did not identify this as an outlier, inclusion does not change significance (negative finding initially).

**Histology (ISH):** Behaviour **– (**Paired no Extinction (EXT) /Paired EXT/ Unpaired EXT) = 12/12/8. Paired no EXT: 2 mice no staining observable, 2 mice sections lost in histological processing, Paired EXT: 1 mouse no staining observable, Unpaired EXT: 1 mouse no staining, observable, 2 mice sections lost in processing.

**Electrophysiology – Extinction, NAc**: Behaviour Paired/Unpaired = 8/8. Paired: 2 mice no cells retrieved, Unpaired: 1 mouse no cells retrieved. **OFC** Behaviour - Paired/Unpaired = 8/10. Paired: 1 brain lost in processing sections, Unpaired: 2 mice lost in processing sections.

### Chapter 4.

**Electrophysiology:** Behaviour - 12 mice Paired: 2 mice no cells retrieved during recording. 3 cells excluded as 2SD outliers (2 GFP-, 1 GFP+) in AMPA sEPSC frequency analysis which were not excluded using GRUBBS test. Pooling data across AMPA recordings and CTZ recordings (prior to CTZ application) using Grubbs test to detect outliers (1 outlier total), maintains a significant difference at $p<0.05$. Additionally, these findings have been replicated with a larger dataset by M.Sieburg in our lab (below):

Sieburg, M. C., Margetts-Smith, G., Ziminski, J., Crombag, H. S., & Koya, E. The identification of sucrose cue-evoked corticostriatal neuronal ensemble activity patterns underlying hunger states. Program No. 837.07. 2017 Neuroscience Meeting Planner. Washington, DC: Society for Neuroscience, 2017. Online.

**Chapter 5.**

**Immunohistochemistry:** Behaviour (Paired conditioned locomotion/Unpaired conditioned locomotion/ Paired extinction/Unpaired extinction) = (12/12/11/11). No mice excluded.

**Electrophysiology:** Total animals run: (Paired conditioned locomotion/Unpaired conditioned locomotion/ Paired extinction/Unpaired extinction) = (14/15/13/15). After mice lost due to slicing/ no cells retrieved total n = (12/13/12/14).